Open Research Online

The Open University's repository of research publications
and other research outputs

Functional Analysis of Transforming Growth Factor-Beta Related Molecules During Early Mouse Development

Thesis

How to cite:

Arkell, Ruth Maree (1996). Functional Analysis of Transforming Growth Factor-Beta Related Molecules During Early Mouse Development. PhD thesis The Open University.

For guidance on citations see FAQs.

© 1996 Ruth Maree Arkell

https://creativecommons.org/licenses/by-nc-nd/4.0/

Version: Version of Record

Link(s) to article on publisher's website:
http://dx.doi.org/doi:10.21954/ou.ro.0000f7b5

Copyright and Moral Rights for the articles on this site are retained by the individual authors and/or other copyright owners. For more information on Open Research Online's data policy on reuse of materials please consult the policies page.

oro.open.ac.uk

UNRESTRICTED

Functional Analysis of Transforming Growth Factor-Beta Related Molecules During Early Mouse Development

Ruth Maree Arkell
(B.Sc)

A thesis submitted for the degree of
Doctor of Philosophy
in
Developmental Biology

Laboratory of Mammalian Development,
National Institute for Medical Research
The Ridgeway, Mill Hill,
London, United
Kingdom

June 1996

Date of award: 7th October 1996

ProQuest Number: C535119

All rights reserved

INFORMATION TO ALL USERS
The quality of this reproduction is dependent upon the quality of the copy submitted.

In the unlikely event that the author did not send a complete manuscript
and there are missing pages, these will be noted. Also, if material had to be removed,
a note will indicate the deletion.

ProQuest C535119

Published by ProQuest LLC (2019). Copyright of the Dissertation is held by the Author.

All rights reserved.
This work is protected against unauthorized copying under Title 17, United States Code
Microform Edition © ProQuest LLC.

ProQuest LLC.
789 East Eisenhower Parkway
P.O. Box 1346
Ann Arbor, MI 48106 – 1346

God be with those who explore in the cause of understanding; whose search takes them far from what is familiar and comfortable and leads them into danger or terrifying loneliness. Let us try to understand their sometimes strange or difficult ways; their confronting or unusual language; the uncommon life of their emotions, for they have been affected and shaped and changed by their struggle at the frontiers of a wild darkness, just as we may be affected, shaped and changed by the insights they bring back to us.

Michael Leunig

The submitted thesis contains no material which has been presented by the candidate for the award of any other degree or diploma in any university. The results described in this thesis are from the original work of the author, and except where stated in the text, experimental work was carried out solely by the author.

ACKNOWLEDGEMENTS

Thanks are due to many people who have helped in the completion of this thesis. Work towards this thesis was begun at The Centre for Genome Research, Edinburgh University. I would like to thank Julie B. Moss for teaching me many of the necessary molecular biology techniques (including dilution of nucleotides), Penny G.A. Rashbass and Jenny F. Nichols for helpful scientific discussions. The thesis was completed at NIMR, London. I would like to thank both Mike Jones and Kathryn Anderson who provided inspiration and contributed much enthusiasm to the research presented in this thesis and I appreciate very much the continued scientific collaboration with Sally Dunwoodie.

I especially acknowledge the help of Valerie Wilson who taught me many of the embryological techniques used here and was ever ready for scientific debate. My supervisor Dr Rosa Beddington not only provided encouragement, support and astute scientific guidance but also the best possible environment for scientific training.

Michael Dobbie and Sarah MacKenzie as well as other more transient residents of "The Grove" provided help along the way and contributed much to the effort required to produce the final thesis. A special thanks must also go to Michael and my family for their understanding and tolerance of my absence from home.

ABSTRACT

Embryogenesis requires cell-cell communication in which individual cells send and receive signals that determine their final fate. The transforming growth factor-β (TGF-β) superfamily of molecules encodes secreted factors which are capable of regulating cellular growth and differentiation. Recently, members of the TGF-β superfamily have emerged as candidates for many postulated embryonic inductive interactions. As a step towards understanding such interactions, this thesis investigates the hypothesis that TGF-β superfamily molecules may act as embryonic inducing factors in the mouse. The embryonic expression of a number of *TGF-β* superfamily members and a putative inhibitor of one of these, *follistatin*, were investigated. While activin (a mesoderm inducing factor in *Xenopus* animal caps) was not expressed in the mouse embryo, *follistatin, BMP-7, BMP-2* and *Vgr-2* were expressed during gastrulation and early organogenesis. Strategies were designed to ectopically express two of these molecules, BMP-7 and Vgr-2 in embryogenesis. Firstly, embryonic stem (ES) cells were used as a vehicle to secrete Vgr-2 throughout the embryo. No effect on embryonic morphology was detected, although conditioned medium from the ES cells is capable of inducing mesoderm in *Xenopus*. Secondly, COS cells were used to deliver a localised source of BMP-7 to the cranial neural plate in cultured embryos. Such ectopic expression resulted in the induction of ectopic dorsal neural marker expression (*Msx1* and *AP-2*), the diminished expression of a ventral marker (*Shh*), and a localised expansion of neurectodermal tissue. The localisation of endogenous BMP-7 mRNA during formation and patterning of the neural axis, together with the activities shown in this assay, suggest that BMP-7 may direct one or more aspects of early central nervous system formation in the mouse.

TABLE OF CONTENTS

CHAPTER 3 ACTIVIN AND *FOLLISTATIN* MRNA LOCALISATION

CHAPTER 4 *BMP-7* AND *BMP-2* MRNA LOCALISATION

CHAPTER 5 EMBRYONIC EXPRESSION OF *VGR-2*

CHAPTER 7 ECTOPIC EXPRESSION *VIA* COS CELLS

CHAPTER 8 GENERAL DISCUSSION

LIST OF FIGURES

LIST OF TABLES

CHAPTER 1

INTRODUCTION

1.1 CELL-CELL COMMUNICATION AND EMBRYONIC DEVELOPMENT

Inductive interactions during embryogenesis

The co-ordinated programme by which the embryonic cells of multicellular organisms divide, become restricted in their potency and undergo appropriate cell movements is dependent upon cell-cell communication. The importance of this communication was first demonstrated by embryological manipulation: experiments in which transplantation of a group of cells to a new location could change the fate of the surrounding cells provided evidence of an instructive role for the transplanted cells. In this type of experiment the transplanted cells are said to have "induced" the formation of the inappropriate tissue, and the transplanted cells may be considered the "inducer" and the host tissue the "responder". A caveat of these experiments is that a lack of response from the host tissue does not necessarily mean that the transplanted cells are incapable of providing instruction. To produce an effect the host tissue must be able to respond to the inducer; it is this capability which is referred to as "competence." A tissue which has already come under the influences which restrict its developmental potential may not be competent to respond to the inducer. Hence these experiments which test the ability of tissues to send signals are at the same time a test of another tissue's ability to receive signals.

One of the most striking examples of inductive tissue interactions is that of the transplantation experiments performed by Spemann and Mangold and reviewed in Spemann (1938). In these experiments transplantation of the dorsal blastopore lip of an amphibian embryo into a ventral location in a host embryo resulted in the formation of a secondary embryo. The additional embryo contained a neural tube, otic vesicles, somites and a notochord in correct orientation with respect to themselves and parallel to the primary embryo. When these experiments were performed with marked cells so that the contribution of host and donor tissues to the second embryo could be determined, it was shown that the secondary neural plate was host derived. Thus the presence of the grafted tissue had diverted the fate of the host ectoderm and induced a secondary neural plate. In contrast to the neural tissue, the secondary notochord and somites were formed from both donor and host tissue. Therefore the blastopore lip had reorganised not only the overlying ectoderm but also the developing mesoderm on the ventral side of the host embryo. Transplantation of tissue from other regions of developing embryos did not produce a secondary embryo, consequently the amphibian dorsal blastopore lip has become known as the "organiser".

It has since been demonstrated that a structure known as Henson's node in the chick embryo shares the organiser properties of the frog dorsal blastopore lip. When this region is transplanted the graft gives rise to mesoderm structures including notochord and somites and

an ectopic neural groove may develop above the mesodermal part of the graft (Waddington, 1932). Importantly, since this thesis concerns inductive interactions in mammalian development, the node of the mouse embryo has also been shown to have similar organiser properties (Beddington, 1994). Together these experiments suggest that embryogenesis proceeds *via* a continuous process of cellular interaction, whereby cells can both influence and be influenced by their local environment. Furthermore, the continual cell movements and rearrangements during embryogenesis constantly alter a given cell's potential interactions. The fact that such interactions are fundamental to embryonic development is supported by experimental embryology in diverse organisms and organ systems (reviewed in Wessells, 1977; Jacobson and Sater, 1988). Additionally, the fact that secondary embryo formation can be demonstrated in Amphibia, Avians and Mammals highlights the possibility that the development of animals with overtly different form may utilise common interactions.

How do cells communicate?

The communication underlying the tissue interactions which occur throughout an organism's life is achieved through a variety of mechanisms. Cells in contact with one another can communicate *via* specialised membrane junctions (gap junctions) which allow exchange of small molecules or *via* plasma-membrane bound signalling molecules which can interact with adjacent cells. A more remote form of communication occurs when cells secrete signalling molecules which act either at a distant site or in the vicinity of the cell from which they were secreted. The importance of each of these forms of communication during embryogenesis will be briefly discussed.

Junctional communication and embryogenesis

Cells in most tissues are linked together *via* gap junctions (Loewenstein, 1966). These gap junctions allow the direct exchange of small molecules including ions and other second messengers (Paul, 1995). It is therefore possible that these membrane junctions play a role in cell communication during development. However, several experiments which interfere with junctional communication during embryogenesis produce surprisingly mild phenotypes. Mesoderm induction in *Xenopus* proceeds normally when an antibody directed against the major gap junction protein (connexin) is used to block junctional communication prior to gastrulation (Warner and Gurdon, 1987). If either this antibody, or a dominant negative connexin molecule, is injected into the blastomere of the *Xenopus* embryo which is the precursor of the anterior central nervous system, the resulting tadpoles display abnormalities in the brain, eye and other anterior structures (Warner et al., 1984; Paul et al., 1995). These latter experiments argue that junctional communication is required for the formation of some embryonic structures but do not provide a clear indication of the stage or process at which this requirement acts.

Similarly, a mild phenotype results when a loss of function mutation in connexin43 is introduced into the mouse embryo. Despite expression of this molecule during normal development in several regions of the developing embryo (Yancey et al., 1992), the resulting homozygous mice survive to term (Reaume et al., 1995). Putative dominant negative mutations in connexin molecules have recently been implicated in two human diseases; visceroatrial heterotaxia is associated with mutations in connexin43 (Britz-Cunningham et al., 1995), and the X-linked form of a human neuropathy, Charcot-Marie-Tooth disease is caused by mutations in connexin32 (Berghoffen et al., 1993). None of these mutations in gap junction proteins show perturbation of early embryonic development. This again argues that junctional communication is not the major form of cell-cell communication involved in embryonic induction.

Signalling molecules and embryogenesis

Chemical signalling molecules may be distinguished by the distance over which they operate; they may act systemically or locally. It has long been known that hormones, in a process termed endocrine signalling, act systemically to co-ordinate the cells of an organism in response to environmental change. Hormones are chemical agents, such as steroids, modified amino acids, peptides or proteins, which are synthesised by particular parts of the body, generally specialised ductless glands (endocrine glands). Endocrine cells secrete their hormone molecules into the extracellular fluid from where they diffuse into the bloodstream and the bloodstream carries them to another part of the body where they evoke systemic adjustments by acting on specific target tissues or organs (Turner, 1966; Gordon, 1977). The embryonic inducer molecules often act before a vascular system and blood circulation has been established in the embryo and hormones do not play a role in the local interactions utilised during embryonic induction. Another form of specialised chemical messengers are the neurotransmitters which are responsible for synaptic signalling (Keynes and Aidley, 1981). Although these chemicals act locally, synaptic signalling is confined to the specialised synaptic junctions found only in the nervous system, and this form of signalling does not participate in embryonic tissue interactions.

The overwhelming majority of molecules responsible for embryonic induction are proteins which act as local chemical mediators. These proteins may be plasma-membrane bound signalling molecules or molecules which are secreted into the extracellular environment. In some cases the same protein may exist in different forms and therefore be capable of functioning either as a cell surface bound signalling molecule or as a diffusible molecule (Rathjen et al., 1990a; Porter et al., 1995). Molecules which act locally to regulate cell behaviour have classically been said to constitute the paracrine signalling system. As more has become known about how molecules operate to produce local cell-cell signalling, the term "paracrine" has come to encompass those molecules which are secreted by one cell and act on other cells in close proximity. The additional terms, autocrine (Sporn and Todaro,

1980), juxtacrine (Massagué, 1990a) and intracrine (Re, 1989), have been proposed to define the other modes of action shown in Figure 1.1.

Just as the modes of action of these local signalling molecules are diverse, the cellular responses to these factors are varied, and the same factor may evoke different responses in different cell types (Sporn and Roberts, 1988). The first local signalling molecule to be isolated was epidermal growth factor (EGF). EGF was purified, and named, because it causes specific cells to undergo proliferation (Cohen, 1962), yet it was subsequently shown to inhibit proliferation in different cells (Panaretto et al., 1983). A large number of proteins have now been purified that function as local chemical mediators in processes which include the regulation of cell growth and also differentiation (Seyedin et al., 1986), cell-cell adhesion (Anklessaria et al., 1990), cell migration (Bhargava et al., 1992) and chemotropism (Serafini et al., 1994). All of these processes are intrinsic to embryonic development.

Cells respond to all of the chemical signalling molecules discussed in this section through receptors which bind the signalling molecule and initiate the cellular response. Certain small, hydrophobic signalling molecules, such as the steroid and thyroid hormones, pass through the plasma membrane and activate receptors inside the cell. The activated receptor hormone complexes then bind to DNA and directly influence gene transcription (King, 1988; Nunez, 1988). However, most signalling molecules are hydrophilic and activate receptors located on the surface of the target cell. In this case, binding of the signalling molecules activates the receptor which initiates an intracellular signalling cascade resulting in transduction of the appropriate signal to the nucleus.

In recent years progress has been made in identifying locally acting, signalling molecules which are capable of mimicking the interactions identified in tissue transplantation experiments. As a step towards understanding how such molecules are utilised during mouse embryogenesis, this thesis investigates the possibility that proteins implicated in inductive interactions in other organisms also act during mouse development. The proteins investigated are from the transforming growth factor-β (TGF-β) superfamily of molecules. The structure of this superfamily, as well as some biochemical aspects of the mode in which family members function, are described later in this introduction. TGF-β superfamily members have been shown to direct cell fate in both invertebrates and vertebrates. A *Drosophila* superfamily member, *decapentaplegic* (*dpp*) functions as a morphogen during early patterning of the fly embryo to direct dorsal cell fate. Because mutations have been identified in this gene and in several other genes which produce related phenotypes, *dpp* has served as a model for how superfamily members may function, More recently it has also provided tools for cloning vertebrate counterparts of genes which interact with TGF-β superfamily molecules to direct cell fate. To demonstrate the importance of TGF-β

Figure 1.1 Modes of local chemical signalling. Molecules produced by a cell (black circles) may act on the same cell that produced them (autocrine or intracrine mode), or on other cells (juxtacrine or paracrine mode). Interaction requires the presence of transmembrane receptors specific for the signalling molecule. The result of ligand/receptor interaction is shown as an arrow pointing towards the nucleus. The cellular response to the stimulus may include regulation of growth, differentiation or physical properties such as adhesion or motility. All arrows are represented by dashed lines to indicate that these actions may not be direct. Specialised chemical mediators such as hormones and neurotransmitters are not included in the diagram. Diagram adapted from McKay (1993).

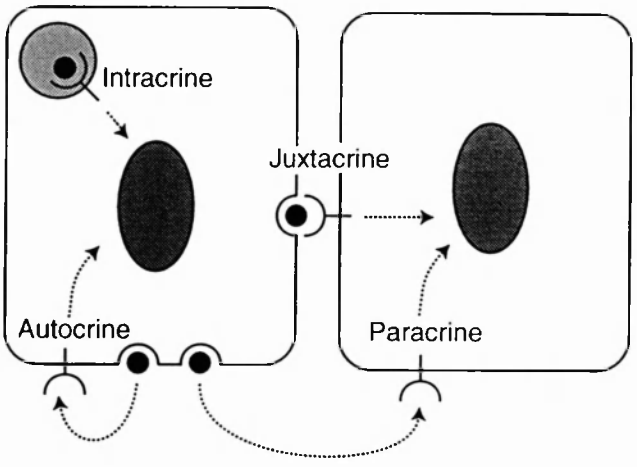
Intracrine
Juxtacrine
Autocrine
Paracrine

superfamily molecules during embryogenesis a review of the role of *dpp* in specifying dorsal cell fate is included here.

Decapentaplegic and the specification of dorsal cell fate in *Drosophila* embryogenesis

The *Drosophila dpp* gene provides an excellent example of two of the themes which will be reiterated throughout this thesis. The first is that one molecule may function in more than one aspect of embryonic development and the second is that the conservation of molecules between species potentially represents some degree of conserved function. Additionally, the methods by which *dpp* function has been investigated demonstrate the power of genetic analysis of embryonic development and this will also be discussed in this thesis. The *dpp* gene is implicated in processes as diverse as the specification of dorsal cell fates during embryogenesis (Ferguson and Anderson, 1992a; Wharton et al., 1993), gut morphogenesis (Panganiban et al., 1990), progression of the morphogenetic furrow during eye development (Heberlein et al., 1993) and appendage development (Spencer et al., 1982). Its role in establishing dorsal pattern during embryogenesis was first identified because loss of this zygotically active gene product produces embryos which lack dorsal structures (Irish and Gelbart, 1987). Of the zygotic genes which are required for the development of dorsal cell types, mutations in *dpp* produce the most severe phenotype. When *dpp* RNA is injected into mutant embryos which lack inherent dorsal-ventral polarity different amounts of RNA specify different cell fates; the highest levels of RNA define the most dorsal structures (Ferguson and Anderson, 1992a). Similarly, altering the gene dosage of *dpp* shifts cell fates along the dorsal-ventral axis (Wharton et al., 1993). Thus, during *Drosophila* embryogenesis *dpp* appears to act as a true secreted morphogen which specifies different cell fates in a dose dependent manner. Cloning of the gene responsible for the *dpp* mutation showed that it has homology to the TGF-β family (Padgett et al., 1987), although it is now known to be more closely related to other members of the superfamily.

As described later, there are two classes of receptors for TGF-β superfamily molecules, type I and type II. Three Dpp receptors have recently been identified, *thickveins* (*tkv*) and *saxophone* (*sax*) encode type I receptors and *punt* encodes a type II receptor (Childs et al., 1993; Brummel et al., 1994; Nellen et al., 1994; Okano et al., 1994; Penton et al., 1994; Letsou et al., 1995). Similar to the homologous mammalian receptors described below, it is proposed that Dpp binds to these receptors in a co-operative manner. While *tkv* is able to bind ligand on its own, co-expression of *punt* enhances ligand binding (Penton et al., 1994; Letsou et al., 1995). In the case of *sax*, co-expression of *punt* is essential for binding (Brummel et al., 1994; Letsou et al., 1995). Messenger RNA for all three receptors is provided both maternally and zygotically (Childs et al., 1993; Brummel et al., 1994; Okano et al., 1994; Penton et al., 1994). Complete loss of *tkv* or *punt* produces embryos whose phenotype is indistinguishable from one another, or from complete loss of *dpp*. This is not

due to a transcriptional dependence of one of these genes on the other; *dpp* expression is unaltered in *punt* and *tkv* mutants and transgene supplied *tkv* cannot rescue the *punt* phenotype, nor can transgene supplied *punt* rescue the *tkv* phenotype. These experiments demonstrate an absolute requirement for both *tkv* and punt during *dpp* signalling (Ruberte et al., 1995). Maternal and zygotic loss of the second type I receptor, *sax*, produces embryos which lack only the dorsal most cell type, suggesting that it is required to interpret the highest levels of Dpp (Nellen et al., 1994). RNA for *sax* is found ubiquitously, both maternally and zygotically (Brummel et al., 1994; Penton et al., 1994), yet, as described, in the absence of functional *tkv*, *sax* and *punt* are not sufficient for the development of any dorsal structures. It is not clear why *sax* appears to be able to modulate the *tkv/punt* response (to induce the most dorsal cell type) and yet cannot transduce signal in the absence of *tkv*.

Genetic analysis of the interaction between *dpp* and the six other zygotically active genes required for the development of dorsal cell types demonstrated that three (*tolloid*, *shrew* and *short gastrulation* (*sog*)) act by regulating the activity of *dpp* at a post transcriptional level (Ray et al., 1991; Ferguson and Anderson, 1992b). The dorsally transcribed gene *tolloid* (Schimmell et al., 1991) acts by elevating *dpp* activity, as does the *shrew* gene (Ferguson and Anderson, 1992b). In contrast the *sog* gene antagonises *dpp* ventrally (Ferguson and Anderson, 1992b). The sequence of *sog* (François et al., 1994) shows that it is likely to be secreted. It is expressed in an adjacent but non overlapping domain with respect to the *dpp* expression domain and it is proposed that soluble sog may diffuse into the region of *dpp* expression and antagonise its activity (François et al., 1994).

Drosophila dpp appears to have a vertebrate homologue known as *bone morphogenetic protein-4* (*BMP-4*), BMP-4 is a TGF-β superfamily molecule which can produce ectopic bone formation in rats and promote ventral mesoderm formation in *Xenopus*. *Drosophila* Dpp can induce ectopic bone formation in rats and human *BMP-4* can rescue *dpp* mutant *Drosophila* embryos, suggesting that these two molecules are functional homologues (Padgett et al., 1993; Sampath et al., 1993). Recently, a molecule has been isolated from *Xenopus*, called *chordin*, which has homology to the *Drosophila sog* gene (Sasai et al., 1994). *Xenopus chordin* is able to mimic the ability of *Drosophila sog* to promote ventral development in *Drosophila* (Holley et al., 1995). Similarly, both *chordin* and *sog* antagonise the action of BMP-4 in *Xenopus* mesoderm induction assays (Sasai et al., 1995; Schmidt et al., 1995a). The apparent, conserved interaction between Dpp/sog and BMP-4/chordin highlights the possibility that the mode of action of TGF-β superfamily molecules may be conserved from invertebrates to vertebrates. TGF-β superfamily molecules are therefore extremely good candidates for potential inducing molecules in mouse embryogenesis. Furthermore, the ability of Dpp to act as a morphogen is similar to the ability of both BMP-4 and activin, another TGF-β superfamily member, to act in a dose

Figure 1.2 The TGF-β superfamily. **(A)** Diagram showing the structure of a TGF-β superfamily molecule. TGF-β precursor proteins contain an amino-terminal signal which targets the precursor to the secretory pathway. A variable pro-domain may assist in folding, dimerisation and regulation of factor activity. The actual signalling molecule is a homo- or heterodimer of a small carboxy-terminal fragment, the mature domain. Seven characteristic cysteine residues in this region are nearly invariant between family members. aa; amino acid. **(B)** Diagram showing the similarity between the amino acid sequence, beginning with the first invariant cysteine of the mature domain, of the members of the activin and DVR subfamilies of TGF-β molecules. Human sequences are compared with the following exceptions: *dpp* and *60A* (*Drosophila*); *Vg1* (*Xenopus*); *dorsalin* (chick); *Vgr-2* and *nodal* (mouse). Both diagrams are from Kingsley (1994).

A

Leader (15-22aa) **Pro-domain** (50-375aa) **Mature domain** (110-140aa)

B

	InhβA	InhβB	nodal	BMP2	BMP4	dpp	BMP5	BMP6	BMP7	BMP8	60A	BMP3	Vg1	GDF1	Vgr2	Dorsalin
InhβA	100															
InhβB	64	100														
nodal	40	40	100													
BMP2	44	43	42	100												
BMP4	42	43	41	92	100											
dpp	39	39	42	74	76	100										
BMP5	43	40	40	61	59	57	100									
BMP6	44	40	42	61	60	59	91	100								
BMP7	43	40	41	60	58	58	88	87	100							
BMP8	41	37	45	55	55	53	74	75	74	100						
60A	37	38	40	57	54	54	74	71	69	63	100					
BMP3	34	37	42	49	48	44	44	45	43	42	42	100				
Vg1	44	39	43	58	56	48	56	58	57	55	51	50	100			
GDF1	36	35	37	45	46	42	47	47	48	48	41	43	59	100		
Vgr2	42	40	40	53	51	48	51	53	51	55	48	42	57	51	100	
Dorsalin	36	36	42	54	55	54	52	54	50	48	49	39	47	41	46	100

activin subfamily

dpp group

60A group

DVR subfamily

dependent manner in *Xenopus* mesoderm induction assays (Green and Smith, 1990; Dale et al., 1992; Ferguson and Anderson, 1992a). This has raised the issue of whether this may be a general property of the TGF-β superfamily.

1.2 THE TGF-β SUPERFAMILY OF SECRETED MOLECULES

TGF-β related molecules

TGF-β, the founding member of this superfamily, was first found in culture medium from various oncogenically transformed cell lines (Anzano et al., 1983; Massagué, 1983). Three closely related molecules, (TGF-β 1,2 and 3) now make up the mammalian TGF-β family, and many other molecules share structural homology with this family and thus are grouped together as the TGF-β superfamily. There are now at least twenty-eight molecules belonging to the TGF-β superfamily (Meno et al., 1996; reviewed by Kingsley, 1994). All of these are initially synthesised as larger precursor molecules with an amino-terminal signal sequence and a pro-domain of variable size (Figure 1.2). The pro-domain is poorly conserved between family members but appears to be necessary for the production of active protein (Thomsen and Melton, 1993). The precursor protein is cleaved to release a mature carboxy-terminal segment of 110 - 140 amino acids. This mature region may remain noncovalently associated with the pro-domain, yielding a latent complex that is unable to bind receptor but which can be activated later in the extracellular medium (Massagué et al., 1994). The active signalling molecule is made up of homo- or heterodimers of the mature region (Massagué, 1990b). The mature region is the most conserved part of the protein and it contains the seven cysteine residues which are the hallmark of the family members. Crystallography studies of TGF–β2 have shown that six of these cysteines are used to create a cysteine knot. The remaining cysteine residue is used to link two monomers into a dimer (Daopin et al., 1992; Schlunegger and Grütter, 1992). Three family members, *Vgr-2*, *GDF-9* and *lefty*, lack the cysteine involved in dimerisation and it is not clear whether these proteins function as a dimer (Jones et al., 1992a; McPherron and Lee, 1993; Meno et al., 1996).

In the same way that the TGF-β molecules may be considered a subfamily within the TGF-β superfamily, other molecules can be grouped into subfamilies based on the degree of conservation between their mature regions. This thesis concerns molecules which come from two of these subfamilies, the activin subfamily and the DVR subfamily, the structure of these subfamilies is shown in Figure 1.2. The activin subfamily contains the inhibin β_A and inhibin β_B molecules which homo- or hetero-dimerise to form activin A, activin B or activin AB. Activin was originally isolated on the basis of its ability to promote the release of follicle stimulating hormone (Ying, 1988). It is a measure of the diversity of the activity of TGF-β superfamily that the inhibin β chains can also form heterodimers with the inhibin α chain (itself a TGF-β molecule) to inhibit the release of follicle stimulating hormone (Ying,

1988). The inhibin α chain is not classified as belonging to the activin subfamily. While inhibin does not oppose the activity of activin in all assays of activin function, the ability of TGF-β superfamily molecules to form different dimers which may result in distinct activities should be kept in mind when discussing the function and regulation of this class of molecules.

The second subfamily of molecules studied in this thesis is the Dpp, Vg1 related (DVR) subfamily. This subfamily takes its name from two founding members, the first is *dpp*, the *Drosophila* gene already discussed, and the second is *Xenopus Vg1*. *Vg1* was isolated in a screen for maternal mRNAs which were unequally localised within the early *Xenopus* embryo (Rebagliati et al., 1985; Weeks and Melton, 1987). When this subfamily was described (Lyons et al., 1991) it contained fourteen molecules. Unlike either the TGF-β or the activin subfamilies, the DVR class of molecules contains invertebrate members. In fact on the basis of homology to two of the *Drosophila* homologues, this class has been further subdivided into the *dpp* subclass and the *60A* subclass. This subfamily contains many molecules which have been demonstrated to play a role in instructive interactions during early development (Ferguson and Anderson, 1992a; Basler et al., 1993; Thomsen and Melton, 1993). Many of the mammalian members of this class of molecules were purified on the basis of their ability to cause ectopic bone formation when placed subcutaneously or intramuscularly in rats, hence they are named bone morphogenetic proteins (BMP) (Lyons et al., 1991; Rosen and Thies, 1992). Although it is possible that the closely related BMP proteins hetero-dimerise, it is not clear whether they do.

Signal transduction by TGF-β superfamily members

In recent years there has been much progress made in identifying and understanding the mechanisms of action of TGF-β superfamily receptors. Not surprisingly, given the number of ligands, there are now a large number of receptor molecules identified in both invertebrate and vertebrate species. The first information came from studies on the binding properties of TGF-β1 molecules. Initial studies showed that TGF-β1 molecules bound to at least three major cell surface proteins found on many cell types, and these were designated type I, type II and type III on the basis of their size (Massagué, 1990b). The type I and type II receptors were the best candidates for the endogenous receptor because cell lines which were selected for their inability to respond to TGF-β stimulation were lacking these receptors (Laiho et al., 1990).

The expression cloning of the first type II receptor (Mathews and Vale, 1991) and the first type I receptors (Attisano et al., 1993; Ebner et al., 1993; Franzén et al., 1993) showed that both classes of molecules are serine/threonine kinases. Cloning of further receptors has allowed the general structural properties of these molecules to be identified. Both classes of receptors have a small extracellular domain, a single transmembrane spanning domain and an

intracellular kinase domain. The two classes can be distinguished on the basis of their size and the cysteine pattern in the extracellular domain and the presence of a glycine/serine rich region, the GS domain, at the amino terminus of the kinase domain (Figure 1.3) (Kingsley, 1994; Massagué et al., 1994). It appears that individual TGF-β receptors are not sufficient for signal transduction and it is believed that they function as heteromeric signalling complexes. The evidence for this is based largely on the study of the cell lines which were selected for their inability to respond to TGF-β stimulation and includes the following. In the absence of functional type I receptors, the type II receptor can bind ligand but not signal TGF-β responses (Wrana et al., 1992). The addition of functional type I receptors to this system restores TGF-β responsiveness (Franzén et al., 1993; Bassing et al., 1994; Cárcamo et al., 1995). In the absence of a functional type II receptor, a truncated type II receptor which lacks the cytoplasmic domain, binds ligand but the cells remain insensitive to TGF-β (Wieser et al., 1993). Transfection into these cells of a wild type type II receptor restores TGF-β responsiveness (Wrana et al., 1992; Inagaki et al., 1993).

Activin and BMP proteins also signal through complexes of type I and type II receptors (Attisano et al., 1993; Cárcamo et al., 1995; Liu et al., 1995). In the case of all three subfamilies the molecular basis for this interdependence is becoming clear (Figure 1.3). The activins and TGF-βs first bind to type II receptors and the receptor-ligand complex is recognised by the type I receptors which cannot bind ligand on their own (Attisano et al., 1993; Ebner et al., 1993; Franzén et al., 1993; Bassing et al., 1994). The type II receptor is a constitutively active kinase and it phosphorylates the type I receptor at the GS domain and the type I receptors propagate the signal (Wrana et al., 1994). In contrast to this, the BMP molecules are able to bind type I receptors on their own (Brummel et al., 1994; Penton et al., 1994; Suzuki et al., 1994). The cloning of the BMP and Dpp type II receptors and analysis of ligand binding demonstrated that binding of BMP molecules is co-operative between their type I and II receptors (Brummel et al., 1994; Liu et al., 1995).

Each type II receptor can interact with more than one type I receptor and some type I receptors can interact with a variety of type II receptors. In the activin and TGF-β systems, the biological response conferred by ligand binding is determined primarily by the type I receptor engaged in the complex (Attisano et al., 1993; Cárcamo et al., 1995). The existence of type I and II receptors which can bind members of both the activin and BMP subfamilies provides a mechanism of interaction between activin and BMP molecules, for example, activin can bind to its type II receptor and block BMP binding which requires interaction of both the type I and II receptor. The array of receptors so far isolated and the combinatorial nature of their function may play a large part in generating the multitude of cellular responses that various members of the TGF-β superfamily are capable of eliciting.

Figure 1.3 TGF-β superfamily receptors. **(A)** Diagram showing the general features of the TGF-β superfamily type I and type II receptors. The receptors have an extracellular domain, each with a cysteine box. Other cysteines which vary between the receptor types are also present in this region but not shown in the diagram. Both have a single transmembrane spanning domain and an intracellular serine/threonine kinase domain. Type I receptors may be distinguished by the presence of a glycine/serine rich region (GS domain) at the amino terminus of the kinase domian. **(B)** Models of ligand interaction with the heteromeric receptor complexes. BMP molecules bind co-operatively to the receptors, requiring both type I and type II receptors for efficient binding. TGF-β and activin molecules bind initially to type II receptors (1) and the type I receptor can interact with this receptor/ligand complex (2). In each case only the ligand complexed with both receptor types is capable of propagating signal. Diagrams adapted from Massagué et al. (1994) and Liu et al. (1995).

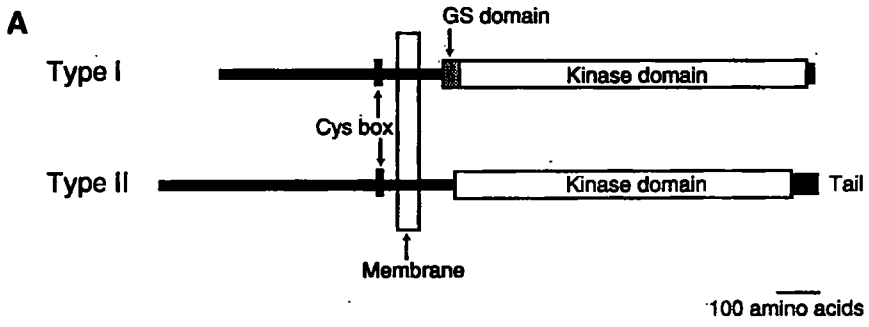
A
GS domain
Type I
Kinase domain
Cys box
Type II
Kinase domain
Tail
Membrane
100 amino acids

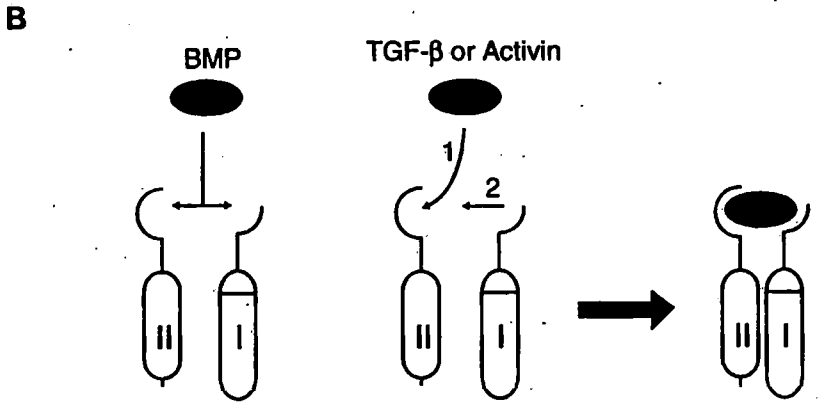
B
BMP
TGF-β or Activin
1
2
II
I
II
I
II
I

In addition to these receptors, several other TGF-β binding proteins have been isolated (Massagué, 1990b; Lin and Lodish, 1993). These include follistatin, a soluble glycoprotein made by ovaries that binds activin and blocks its effects on pituitary cells (Ying et al., 1987). Follistatin has been isolated from many vertebrates, but like activin it is not clear if it has an invertebrate counterpart. Betaglycan is also known as the TGF-β type III receptor, which may present different TGF-β isoforms to the type II receptors (Wang et al., 1991; López-Casillas et al., 1993). It is possible that this category should also include *Drosophila sog* and *Xenopus chordin*. As has already been discussed, these protein products modulate the activity of Dpp and BMP-4 respectively, yet it remains to be demonstrated that this is through direct binding. However, all of these molecules may play a part in determining the cellular response to TGF-β related molecules. Little is known about the mechanism of signal transduction between the TGF-β superfamily receptors and the nucleus. However, the recent cloning of *mothers against dpp*, a gene believed to act downstream of a *Drosophila* TGF-β as well as evidence that this molecule is conserved between *Drosophila* and *C. elegans* suggests that progress in this area will be made over the next few years (Sekelsky et al., 1995; Savage et al., 1996).

1.3 VERTEBRATE EMBRYONIC INDUCTION

The experiments so far described illustrate that cell-cell communication is indispensable during embryonic development. This communication proceeds *via* locally acting chemical signalling molecules which bind to specific receptors. The fact that members of the TGF-β superfamily are capable of acting as such signalling molecules is demonstrated both by the action of *dpp* during *Drosophila* embryogenesis and by the biochemical studies of the mode of action of these proteins. Several pieces of evidence suggest that TGF-β related molecules can function as secreted signalling factors in vertebrates, including the fact that a number of TGF-β related molecules induce ectopic bone formation when injected subcutaneously in rats (Rosen and Thies, 1992). Mutations in either of two such molecules result in skeletal defects in the mouse (Kingsley et al., 1992; Storm et al., 1994). Together, this demonstrates that these molecules can act to regulate cell fate in vertebrates.

In order to generate the tissues which form the basis of the vertebrate embryo it appears that at least two main inductions occur; mesoderm induction and neural induction. Each of these events is followed by or incorporates, a secondary process of patterning the newly formed tissues. Of all the cell-cell interactions which occur during these processes, TGF-β related molecules have most consistently been associated with mesoderm induction and patterning (for review see Smith, 1995) and with establishing dorsal-ventral axis of the neural tissue (Basler et al., 1993; Liem et al., 1995). This thesis investigates the role of TGF-β superfamily molecules in these processes during mouse embryogenesis. Therefore the rest

of this introduction summarises what is known of TGF-β superfamily molecules in these processes from other organisms and describes the development of the mouse embryo, focusing on mesoderm formation and development of the neural tissue.

Xenopus mesoderm induction

The fundamental role that TGF-β superfamily molecules play in the tissue interactions that establish the vertebrate embryo has been clearly demonstrated by experiments on *Xenopus* mesoderm induction. The phenomenon of mesoderm induction is inferred by the differences between the fate maps and specification maps of *Xenopus* development (for review see Smith, 1989). At the morula stage of development the amphibian embryo consists of two types of tissue; the animal pole cells and the vegetal pole cells. If these tissues are cultured in isolation, the animal pole will form only epidermis and the vegetal pole only endoderm (Holtfreter and Hamburger, 1955; Slack and Forman, 1980; Jones and Woodland, 1986), thus the formation of other embryonic tissues such as the mesoderm and the neurectoderm must be dependent upon subsequent embryonic interactions. Fate maps of the gastrulae show that mesoderm is formed from the equatorial region which lies at the junction of the animal and vegetal poles (the marginal zone) (Keller, 1975). When new boundaries are created between the animal pole cells and cells of the vegetal pole, either in tissue recombinants (Nieuwkoop, 1969) or *via* heterotopic grafting (Jones and Woodland, 1987), mesoderm arises from the conjugates. If these juxtaposition experiments are performed with marked tissues, it becomes clear that the mesoderm forms entirely from the animal pole in response to induction by the prospective endoderm (Nieuwkoop and Ubbels, 1972; Dale et al., 1985). Furthermore the type of mesoderm formed in animal vegetal combinations depends on the origin of the vegetal cells; cells from the dorsal vegetal region induce dorsal cell types such as notochord and muscle, and lateral and ventral vegetal blastomeres induce blood along with mesenchyme and mesothelium, i.e. ventral mesoderm (Boterenbrood and Nieuwkoop, 1973; Dale and Slack, 1987). Therefore patterning of the mesoderm occurs, at least in part, in response to information derived from the underlying vegetal blastomeres.

Additionally Slack and Forman (1980) showed that tissue from the ventral marginal zone, when juxtaposed with tissue taken from the dorsal aspect of the marginal zone (the organiser region), forms structures more dorsal than those it would form in isolation or normal development. They suggested that this was the same interaction as occurred in the ventral tissue in the organiser grafts of Spemann and Mangold. This was confirmed by repeating the original organiser grafts using cell marking techniques (Smith and Slack, 1983). This information suggested that three signals are required for mesoderm induction in the *Xenopus* embryo (Smith and Slack, 1983). The first two signals arise from the vegetal cells and are mesoderm inducing signals. The ventral vegetal signal induces ventral mesoderm while the dorsal vegetal signal induces the formation of dorsal mesoderm, or organiser region. A

third, mesoderm patterning signal subsequently emanates from the organiser to "dorsalize" adjacent ventral mesoderm, thus producing mesoderm of an intermediate character.

Mesoderm inducing factors

Many secreted factors have been proposed as candidates for molecules which instigate one or more of these interactions, as reviewed in Sive (1993); Slack (1994); Smith (1995) and several candidates come from the TGF-β superfamily. At least two family members appear to be capable of providing the signal which emanates from the vegetal region to induce dorsal mesoderm. The first of these is activin which was purified as the mesoderm inducing component of medium from a *Xenopus* cell line capable of mesoderm induction and shown to elicit the formation of dorsal mesoderm in animal caps (Smith, 1987; Smith et al., 1988; Smith et al., 1990). Activin is able to act as a morphogen in *Xenopus em*bryonic tissue: cells exposed to activin distinguish between small differences in concentration to form different types of mesoderm (Green and Smith, 1990), and a given mesodermal marker is expressed further from the source of activin as the amount of activin is increased (Gurdon et al., 1994). However, it is not clear whether activin is an endogenous inducing molecule. Overexpression of a truncated activin type II receptor blocks embryonic activin signalling and abolishes virtually all mesoderm formation (Hemmati-Brivanlou and Melton, 1992), however this truncated receptor also blocks signalling by another TGF-β related candidate mesoderm inducing molecule, Vg1 (Schulte-Merker et al., 1994; Kessler and Melton, 1995). The activin-binding protein, follistatin, which blocks the function of activin but not of Vg1 has no effect when overexpressed in whole embryos (Schulte-Merker et al., 1994). Or, if an increased amount of follistatin is injected into the embryo, results in loss of posterior structures, with relatively little effect on the dorso-anterior structures activin is supposed to promote (Kessler and Melton, 1995).

A second TGF-β superfamily member and candidate dorsal vegetal inducing factor was isolated in a screen for vegetally localised maternal RNAs and named *Vg1* (Rebagliati et al., 1985; Weeks and Melton, 1987; Vize and Thomsen, 1994). Vg1 is one of the proteins from which the previously described DVR subfamily of TGF-β related molecules takes its name. Despite the expression pattern of *Vg1* being consistent with a role in mesoderm induction injection of *Vg1* RNA into early embryos does not result in ectopic mesoderm formation (Dale et al., 1989; Tannahill and Melton, 1989; Dale et al., 1993; Thomsen and Melton, 1993). However this appears to be caused by inefficient processing of native *Vg1*: if, instead, a chimeric protein consisting of either an activin or BMP pro-domain with the Vg1 mature region is tested, it is found that this protein does have powerful mesoderm inducing properties (Dale et al., 1993; Thomsen and Melton, 1993; Kessler and Melton, 1995). It remains unclear whether processed Vg1 is produced during mesoderm induction in *Xenopus*.

Recently, three closely related molecules have been identified, two of which, like activin and *Vg1*, function as dorsal mesoderm inducers. These genes are all related to *nodal*, a murine TGF-β superfamily molecule originally identified as being the target of a retroviral insertion mutation, 413.d (Conlon et al., 1991; Zhou et al., 1993). The three *Xenopus* genes are termed *Xenopus nodal related* genes (*Xnr-1*, *Xnr-2* and *Xnr-3*). Unlike activin all three of the *Xnr* molecules can dorsalize ventral marginal zone explants and induce muscle differentiation, (Jones et al., 1995; Smith et al., 1995), thus mimicking the effect of the organiser in the recombination experiments of Slack and Forman (1980), described above. Furthermore, in the embryo these molecules are ideally placed to exert this dorsal patterning influence, since they are all expressed in presumptive mesoderm during *Xenopus* gastrulation, exhibiting highest transcript levels on the dorsal side of the embryo.

As discussed previously, the vertebrate homologue of Dpp (BMP-4) has also been implicated in mesoderm induction and patterning in *Xenopus*. BMP-4 is a good candidate for a molecule which promotes ventral mesoderm formation. Ectopic expression of BMP-4 in animal caps results in the formation of ventral mesoderm tissue, and ectopic expression in the embryo results in the formation of ventralized embryos, similar in many respects to those generated by UV irradiation (Dale et al., 1992; Jones et al., 1992b). Conversely, overexpression of a truncated BMP receptor results in embryos which lack dorsal structures (Maéno et al., 1994). BMP-4 transcripts are provided both maternally and zygotically, in the gastrula BMP-4 is present throughout the mesoderm, except in the dorsal blastopore lip (Dale et al., 1992; Fainsod et al., 1994; Schmidt et al., 1995b). It is possible that BMP-4 acts both to induce the formation of ventral mesoderm and to titrate the strength of the dorsalization signal in the prospective mesoderm so that the full range of dorsal, lateral and ventral mesodermal tissues is produced. It seems that this ability to oppose the dorsalizing signal represents a fourth signal, not predicted on the basis of the transplantation experiments, which operates during *Xenopus* mesoderm formation.

TGF-β related proteins are not the only candidates for the *Xenopus* mesoderm inducing signals. Molecules from two other families of signalling molecules, the fibroblast growth factor family and the Wnt family are also implicated in this process (for review see Sive, 1993; Slack, 1994; Smith, 1995). The *Xenopus* experiments reveal which molecules are capable of eliciting a particular response, yet the challenge is to identify the molecules responsible for these interactions *in vivo*. The inability to carry out definitive loss of function experiments in amphibians has significantly hampered progress towards identifying the endogenous inducers. The fact that the mouse is the vertebrate organism most amenable to genetic loss of function experiments means it will play a central role in identifying the endogenous molecules responsible for embryonic tissue interactions. Yet, to date, the mouse embryo has not been the organism of choice for much of the embryology on which current knowledge of these interactions is based. In order to make full use of genetic

strategies in the mouse it is important to establish the complementary isolation, recombination and overexpression systems which have proved informative in other organisms.

Mesoderm formation in the mouse embryo

In the mouse embryo mesoderm formation is concomitant with gastrulation. This section describes the formation of the embryonic germ layers focusing on mesoderm. A full description of the morphological development of the mouse embryo can be found in Snell and Stevens (1966) as well as in textbooks such as Rugh (1968); Kaufman (1992); Hogan et al. (1994) and much of the information presented here is from these sources. Throughout the thesis mouse embryos undergoing gastrulation will be staged according to Downs and Davies (1993) and for ease of reference a copy of this staging system is provided as Appendix I. Embryos of later stage will be classified according to somite number.

Prior to gastrulation the mouse embryo is a cylindrical, bilaminar structure consisting of visceral endoderm on the outside and ectoderm on the inside. As shown in Figure 1.4 the egg cylinder is surrounded by several extraembryonic membranes. The parietal endoderm which surrounds the egg cylinder is attached to the trophectoderm derived trophoblast giant cells. Between the layers of parietal endoderm and giant cells, a thin, noncellular membrane is formed (Reichert's membrane). These tissues continue to surround the embryo and separate it from the maternal decidua, in which the embryo is embedded, well into embryonic life. Before gastrulation it is apparent that the ectoderm which constitutes the inner layer of the egg cylinder is divided into two parts. The proximal ectoderm (extraembryonic ectoderm) is derived from the trophectoderm and will give rise to part of the placenta. The distal ectoderm is derived from the inner cell mass and is termed embryonic ectoderm or epiblast. The cavity in the ectoderm is known as the proamniotic cavity.

The epiblast which will give rise to all of the tissues of the embryo and to the extraembryonic mesoderm (reviewed in Beddington, 1986) is not regionalised with respect to potency (Beddington, 1983; Lawson et al., 1991; Lawson and Pedersen, 1992). The fate of epiblast cells has now been investigated by a variety of means, including single cell analysis (Lawson et al., 1991; Lawson and Pedersen, 1992), the orthotopic transplanting of groups of labelled cells (Beddington, 1981; Beddington, 1982; Tam and Beddington, 1987; Tam, 1989; Quinlan et al., 1995), or by labelling *in situ* of a group of cells (Beddington, 1994; Smith et al., 1994a). All of these studies show that the epiblast, both prior to gastrulation and during elongation of the primitive streak, is regionalised with respect to its fate. As shown in Figure 1.5, prior to gastrulation the cells which will contribute to embryonic mesoderm are located adjacent to their future site of ingression (the primitive streak) and the cells which will leave the embryo proper to form the extraembryonic mesoderm are in the posterior and proximal epiblast.

Figure 1.4 Early postimplantation mouse development. **(A)** Implantation stage blastocyst. The inner cell mass consists of the epiblast (blue) and a layer of primitive endoderm (gold). **(B)** The egg cylinder and trophoblast. The inner cell mass has grown downwards into the yolk cavity and the junction between the embryonic region (below the dotted line) and the extraembryonic region is now apparent. Two layers of endoderm are present, visceral endoderm forms the outside of the egg cylinder and parietal endoderm lines the trophectoderm which now consists of giant cells. These extraembryonic membranes are not shown in further diagrams. **(C)** Pregastrulation egg cylinder. The proamniotic cavity has developed within the ectoderm and the ectoplacental cone has formed. Only the epiblast cells will contribute to the germ layer tissues. **(D)** Early primitive streak stage embryo. The mesoderm (red) lies between the ectoderm and endoderm of both the proximal embryonic and extraembryonic region. **(E)** Mid primitive streak stage embryo. The wings of mesoderm have almost encircled the embryonic region, constricting the ectoderm at the extraembryonic/embryonic junction so that the posterior amniotic fold is visible. **(F)** Late primitive streak stage embryo. All three germ layers are present, the node and head process have formed and the definitive (gut) endoderm (yellow) has begun to displace the visceral endoderm. There are three cavities in the embryo separated by the chorion and the amnion. **(G)** Four somite stage embryo. The epiblast cells continue to invaginate through the primitive streak while rostral to the node differentiation of the germ layers into organs is beginning. The diagram is modified from Hogan et al. (1994).

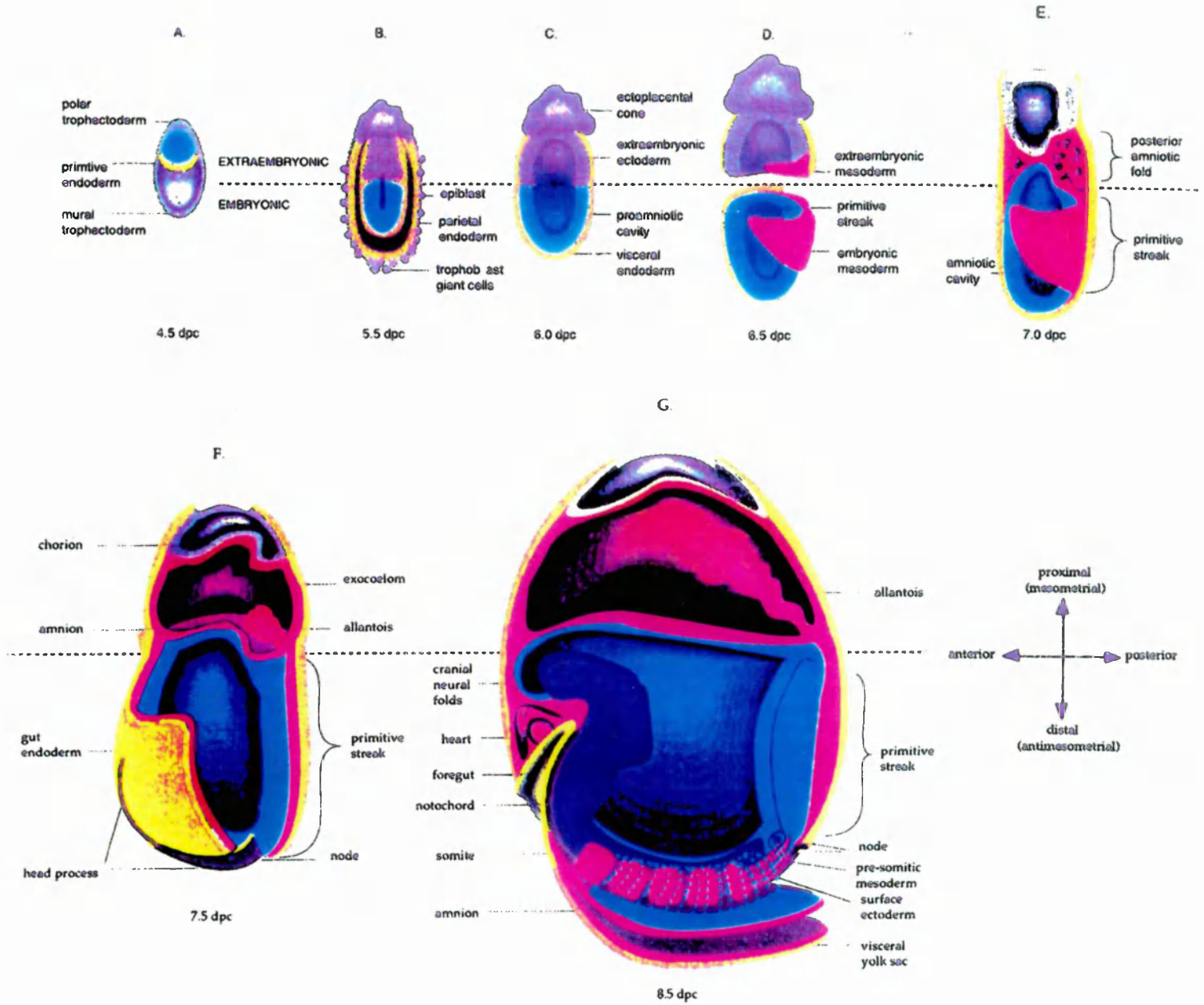
A.
B.
C.
D.
E.
polar trophectoderm
primtive endoderm
mural trophectoderm
EXTRAEMBRYONIC
EMBRYONIC
epiblast
parietal endoderm
trophob ast giant cells
ectoplacental cone
extraembryonic ectoderm
proamniotic cavity
visceral endoderm
extraembryonic mesoderm
primitive streak
embryonic mesoderm
posterior amniotic fold
primitive streak
amniotic cavity
4.5 dpc
5.5 dpc
6.0 dpc
6.5 dpc
7.0 dpc
F.
chorion
amnion
gut endoderm
head process
exocoelom
allantois
primitive streak
node
7.5 dpc
G.
cranial neural folds
heart
foregut
notochord
somite
amnion
allantois
primitive streak
node
pre-somitic mesoderm
surface ectoderm
visceral yolk sac
proximal (mesometrial)
anterior
posterior
distal (antimesometrial)
8.5 dpc

Figure 1.5 Fate maps of epiblast before and during gastrulation. (A) The prospective fate of epiblast tissue in the mouse. **(B)** A comparative representation of the fate maps of the organisms as listed. The diagram is modified from Hogan et al. (1994).

FATE MAPS OF EPIBLAST BEFORE AND DURING GASTRULATION

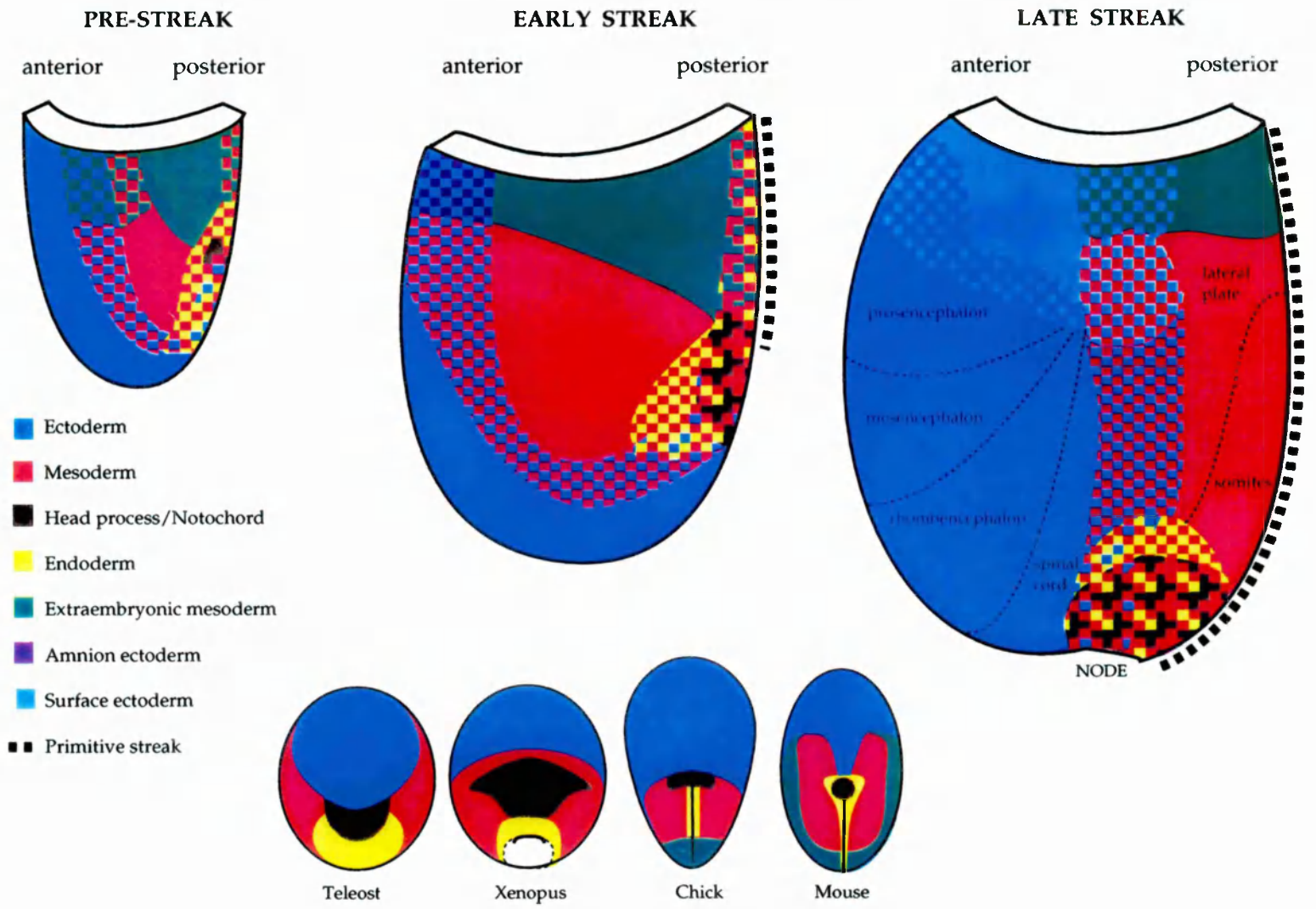

Formation of the germ layers

Gastrulation converts the relatively undifferentiated sheet of epiblast cells into the three germ layers from which the embryo is derived. The process begins when a group of epiblast cells at the junction of the embryonic and extraembryonic ectoderm delaminate and ingress through a region of the embryo known as the primitive streak. Initially the primitive streak extends approximately halfway to the distal tip of the egg cylinder (early streak stage) (Figure 1.4D). The primitive streak lies at the future posterior of the embryo, thus its appearance immediately marks an anteroposterior axis. The mesoderm cells that emerge from the primitive streak form a loose tissue which wedges its way laterally between the epiblast and the endoderm towards the anterior margin of the egg cylinder. Some mesoderm cells push their way between the extraembryonic ectoderm and the overlying endoderm, thus leaving the region of the embryo proper. These mesoderm cells will contribute to the extraembryonic tissues of amnion, visceral yolk sac, chorion and allantois. The continued formation of mesoderm causes the epiblast and extraembryonic ectoderm at the junction of the embryonic and extraembryonic regions to bulge into the amniotic cavity, this bulge is the beginning of the posterior amniotic fold (Figure 1.4E).

By 7.5 dpc the primitive streak has extended to the distal tip of the egg cylinder and the mesoderm has encircled the cylinder. At the rostral end of the primitive streak an indentation is apparent, which is known as the node, at this point there is a hiatus in the outer endoderm layer so that delaminating epiblast cells have direct access to the outer surface of the cylinder. The cells which ingress through this region of the streak form the definitive endoderm and are distributed both rostro-caudally and laterally to progressively displace most of the pre-existing visceral endoderm to extraembryonic regions (Tam and Beddington, 1992). Arising anteriorly from the node in the midline is the axial mesoderm. Initially the axial mesoderm is intercalated in a structure which is continuous with the endoderm and which will be referred to here as the notochordal plate. This structure is sometimes referred to as the head process which is how it is labelled in Figure 1.4F. The cells of the epiblast which do not move through the primitive streak differentiate to form the definitive ectoderm.

When the mesoderm reaches the anterior aspect of the egg cylinder, a small anterior proamniotic fold is formed in the ectoderm which eventually meets and fuses with the posterior amniotic fold to create the amnion. At the same time a cavity (the exocoelom) forms in the extraembryonic mesoderm separating the extraembryonic ectoderm from the epiblast. Thus three cavities are now present in the egg cylinder in place of the single proamniotic cavity. Distally the amniotic cavity is lined with epiblast and is separated by the amnion from the exocoelom which is lined with extraembryonic mesoderm. Proximally the exocoelom is separated by the chorion from the ectoplacental cavity which is lined with extraembryonic ectoderm (Figure 1.4F). Into the exocoelom grows the allantois, an

extraembryonic mesoderm structure which will fuse with the chorion to form a major component of the placenta.

The extraembryonic mesoderm is produced early in gastrulation *via* ingression of cells through the primitive streak (Lawson et al., 1991) and the movement of cells into the extraembryonic mesoderm has mostly ceased by the headfold stage of development (Tam and Beddington, 1987; Parameswaran and Tam, 1995). The embryonic mesoderm is laid down in a rostro-caudal sequence which appears to be dependent upon the time and position at which cells move through the primitive streak. The cells which move through the primitive streak first will contribute to the heart and cranial mesoderm (Lawson et al., 1991). The next cells which pass through the streak will contribute to the paraxial and lateral mesoderm of the rostral trunk, with the mesoderm of the more caudal trunk passing through the primitive streak after this (Tam and Beddington, 1987; Lawson et al., 1991; Smith et al., 1994a; Wilson and Beddington, 1996). These studies also show that the medio-lateral fate of cells is dependent on the position at which cells pass through the streak. The cells which move through the node and the most anterior streak will contribute to the notochord. In the more intermediate area of the streak are the precursors to the paraxial mesoderm and cells which move through the posterior of the streak will give rise to the lateral mesoderm. This arrangement is conserved not only during germ-layer formation but also during axis elongation and tail bud formation (Wilson and Beddington, 1996). These studies also highlight the fact that during gastrulation and axis elongation in the mouse embryo the size of the primitive streak remains the same and explicit node regression does not occur.

When heterotopic grafts of the primitive streak (late streak stage) are performed it is found that the cells take on the fate appropriate for their new location (Beddington, 1982). This demonstrates that it is unlikely that cells are committed to a particular type of mesoderm upon leaving the primitive streak. In addition, in orthotopic grafts of presomitic mesoderm, cells can contribute to both somites and lateral mesoderm (Tam and Trainor, 1994), suggesting that the cells which constitute the presomitic mesoderm are not restricted to the somitic lineage. However, because heterotopic grafts of mesoderm have yet to be performed, it is not clear when mesoderm cells do become restricted in their potential such that they can contribute to only one type of mesoderm.

Mesoderm induction in the mouse embryo

Although, as described above, it is known that in the mouse embryo mesoderm arises *de novo* from the epiblast *via* ingression through the primitive streak, there remains to date no clear evidence that this is due to an inductive event. However, when the fate maps of various vertebrates are compared (Figure 1.5) striking similarities are apparent, as discussed in Lawson et al. (1991); Beddington and Smith (1993); Tam and Quinlan, (1996). In the species compared, the cells which will form the mesoderm and endoderm are adjacent to the

region of involution, and the organiser region is associated with the involution region. The cells which will form the dorsal mesoderm (notochord and somites) are closer to this organiser region than are the precursors of the ventral mesoderm. In those animals which will produce extraembryonic mesoderm these precursors are furthest from the organiser. In all cases the cells which will form the ectoderm derivatives are separated from the site of involution by the band of mesoderm and endoderm precursors. This conservation makes it tempting to speculate that similar mechanisms do underlie events such as mesoderm formation in different vertebrates.

The vertebrate embryo in which mesoderm formation is best studied is *Xenopus* where (as discussed) mesoderm is induced in response to signals from the vegetal hemisphere. In the mouse embryo since mesoderm formation is dependent upon primitive streak formation, a mesoderm induction signal may be one which would initiate primitive streak formation in only one region of the epiblast. The potential sources of this molecule may be listed from the morphology of the pregastrulation mouse embryo. The embryo is surrounded by maternal tissue, hence the source could be the decidua, or the ectoplacental cone. It could come from a more closely apposed tissue such as the extraembryonic ectoderm, or from the primitive endoderm. Alternatively it could emanate from the site of formation of the primitive streak itself, i.e. the epiblast. If the similarities between the fate maps are taken to their logical conclusion then, the primitive endoderm in the region of the site of formation of the primitive streak must be considered the analogous tissue to the *Xenopus* vegetal pole. Interestingly, while there is no evidence that this tissue can provide the necessary signals, this endoderm remains contiguous with the primitive streak throughout germ layer formation (Tam and Beddington, 1992).

1.4 VERTEBRATE DORSAL-VENTRAL NEURECTODERM PATTERNING

The second process investigated in this thesis is patterning of the dorsal-ventral axis of the mouse neurectoderm. While a variety of embryological experiments has led to a model for how the vertebrate neural tube is patterned along the dorsal-ventral axis, few of these experiments have been performed in the mouse embryo. Many of the experiments described here have been performed in chick or amphibian embryos. From these experiments it is proposed that the dorsal-ventral fate of cells is determined *via* an interplay of signals which exert either a ventralising or dorsalizing influence on the neurepithelium. The structures which differentiate ventrally (floor plate and motor neurons) do so in response to a signal from the underlying notochord: removal of the notochord results in a failure of these cells to differentiate (Smith and Schoenwolf, 1989; Clarke et al., 1991; Hirano et al., 1991; Yamada et al., 1991), while grafting a notochord adjacent to the lateral or dorsal neural tube causes ectopic formation of a floor plate and motor neurons (van Straaten et al.,

1988; Placzek et al., 1990; Yamada et al., 1991), as does *in vitro* recombination of notochord with naive neural plate cells (Placzek et al., 1993; Yamada et al., 1993).

The discovery that *Sonic hedgehog* (*Shh*), a vertebrate homologue of the *Drosophila* segment polarity gene *hedgehog*, encodes a secreted molecule expressed in the notochord and floor plate (Echelard et al., 1993; Krauss et al., 1993; Riddle et al., 1993; Roelink et al., 1994) led to an investigation of the role of *Shh* in this process. Shh can substitute for the notochord in *in vitro* induction assays (Roelink et al., 1994) and ectopic expression of *Shh* causes activation of floor plate markers in inappropriate regions of the neurectoderm (Echelard et al., 1993; Krauss et al., 1993; Roelink et al., 1994). The Shh protein undergoes autoproteolytic cleavage to generate an amino-terminally derived (ShhN) and a carboxy-terminal portion (ShhC) (Bumcrot et al., 1995). The ShhN fragment is responsible for all of the identified activities of Shh; higher concentrations of ShhN induce floor plate markers in neural explants and lower concentrations induce motor neuron markers (Marti et al., 1995; Roelink et al., 1995) These experiments provide good evidence that Shh mediates the endogenous, notochord derived, floor plate inducing signal (for review see Ingham, 1995; Placzek, 1995).

As well as positively regulating certain genes that are normally expressed in the ventral region of the neural tube, the notochord can repress the expression of some genes which are normally restricted to the lateral or dorsal aspect of the neural tube (Darnell et al., 1992; Basler et al., 1993; Goulding et al., 1993; Liem et al., 1995) and again Shh reproduces the effect of the notochord (Liem et al., 1995). While this provides evidence that signals from the notochord may be able to regulate gene expression at all dorsal-ventral levels, the realisation that grafting a notochord adjacent to the dorsal neural tube does not prevent the differentiation of dorsal cell types (neural crest cells and commissural neurons) led to the suggestion that a positive dorsalizing signal may also exist (Artinger and Bronner-Fraser, 1992). There is now evidence that during embryonic development such a signal is provided by the surface ectoderm which abuts the dorsal neurectoderm: juxtaposition of these two tissues is sufficient to produce neural crest cells either in grafting experiments (Moury and Jacobson, 1989; Moury and Jacobson, 1990; Selleck and Bronner-Fraser, 1995) or in recombination assays (Dickinson et al., 1995; Liem et al., 1995).

In recombination assays members of the TGF-β superfamily of secreted proteins can mimic the effect of the surface ectoderm (Basler et al., 1993; Liem et al., 1995). A novel member of the TGF-β superfamily, *dorsalin-1*, was isolated by degenerate PCR from chick embryonic spinal cord. Addition of recombinant Dorsalin-1 to naive neurectoderm in culture promotes the formation of neural crest cells and inhibits the induction of motor neurons by the notochord and floorplate (Basler et al., 1993). However, *dorsalin-1* is not expressed during the period in which the proposed dorsalizing signals operate (Basler et al., 1993).

On the basis of gene expression the BMP molecules *BMP-4* and *BMP-7* are better candidates for providing such signals in the developing chick spinal cord and these molecules appear to mimic the dorsalizing activity of the surface ectoderm (Liem et al., 1995). It is proposed that *in vivo* these dorsally located proteins counteract a long-range ventralising influence of the notochord (Liem et al., 1995).

Neural development in the mouse

This section describes the origin and early differentiation events of the neurectoderm in the mouse embryo, focusing on the development of the cranial region which is the subject of experiments reported in this thesis. Because, as described above, the surface ectoderm and the axial mesoderm are believed to be crucial for patterning the dorsal-ventral axis of the neurectoderm, descriptions of the formation of these two tissues are also included here. The epiblast cells which do not move through the primitive streak differentiate to give rise to two types of ectoderm; neurectoderm and surface ectoderm. Fate maps show that before gastrulation the precursor populations of the ectoderm are localised to the anterior epiblast. The more proximal ectoderm will generate the surface ectoderm and the more distal the neurectoderm (Figure 1.5). At later stages of development, an interaction between these two epithelia generates the neural crest.

In the mouse embryo, as in other vertebrates, transplantation of the organiser region to an ectopic site is sufficient to divert the overlying ectoderm to a neural fate (Beddington, 1994) therefore formation of the neurectoderm in the mouse embryo is likely to proceed by inductive interactions. Isolation experiments show that expression of neural markers is autonomous to the anterior ectoderm in late primitive streak stage embryos, demonstrating that neural induction is underway by this stage. Molecules capable of neural induction are found in the anterior mesendoderm of early headfold stage embryos since *in vitro* recombination of this tissue with naive ectoderm induces expression of both general and region specific neural markers (Ang and Rossant, 1993).

The cranial neural plate

Shortly after the allantoic bud has been formed, the neural plate in the cranial region begins to grow rapidly, forming a large fold over the foregut invagination, thus creating the headfolds. In other vertebrates the neural plate can be subdivided into two regions: the anterior of the plate is called the prechordal plate and gives rise to the nervous system anterior to the midbrain. The rest of the neural plate is termed the epichordal plate, as it lies over the notochord. The epichordal plate will give rise to the midbrain and all of the central nervous system posterior to the midbrain (Papalopulu and Kintner, 1992). In the mouse embryo it is not known whether the forebrain does develop from a region which has never been underlain by notochordal mesoderm. However, at the headfold stage of development the notochord does not extend to the anterior of the embryo (Kaufman, 1992). Whilst not

providing evidence of lineage, the expression pattern of several genes supports the notion that at this early stage of development the rostral extent of the notochord corresponds to the future forebrain/midbrain boundary (Ang et al., 1993; Echelard et al., 1993; Echelard et al., 1994; Hermesz et al., 1996). The only other morphological landmark of the cranial neural plate at this stage of development is the preotic sulcus, which will mark the boundary between rhombomeres (r) 2 and 3 at later stages of development (Figure 1.6A). By the early somite stages several such neuromeric junctions can be distinguished and fate mapping of the cells at these divisions has shown that they do correspond to early divisions of the central nervous system as shown in Figure 1.6B (Trainor and Tam, 1995).

The development of the surface ectoderm proceeds in parallel with that of the neurectoderm. The surface ectoderm forms at the margin of the embryo between the amnion and the neural plate; in transverse section it is first seen in the rostral embryo at the late allantoic bud stage of development (Kaufman, 1992). As the yolk sac encloses the embryo the surface ectoderm grows over the mesoderm underlying the neural plate, remaining continuous with the amnion. At this early stage of development the surface ectoderm, when examined by light microscopy, is morphologically indistinguishable from the adjacent neurectoderm.

Cells from the dorsal neural tube, very close to the junction with the surface ectoderm, will give rise to the neural crest cells (Chan and Tam, 1988). In the cranial region of vertebrate embryos the neural crest provides much of the precursor population of the skeleton and connective tissue of the cranium, as well as some peripheral ganglia (Bronner-Fraser, 1993). In many vertebrates the neural crest cells migrate from the neurectoderm after the folds have fused (Tosney, 1982). However, in the cranial region of the mouse embryo, neural crest cell emigration occurs at the early somite stage and is finished by the time the neural folds have closed (Nichols, 1981; Nichols, 1986; Chan and Tam, 1988; Serbedzija et al., 1992). The first cells to emerge do so from the rostral hindbrain at the 5-somite stage and migration from this region has ceased by the 11-somite stage. Neural crest cell migration from the caudal hindbrain begins slightly later at about the 8-somite stage and finishes by the 14-somite stage. Neural crest cells arise from each of the eight rhombomeres (Serbedzija et al., 1992) and leave the neurectoderm forming three broad streams of neural crest cells which migrate subectodermally, each populating a single branchial arch.

The cranial neural tube

At the 5-somite stage of development the neural folds are still open along the entire embryonic axis. Neural tube closure is initiated at three points along the axis. The first point of closure occurs at the cervical/hindbrain boundary when the embryo has 6-7 somites. This closure then spreads in both directions. In embryos with 10- to 12-somites two sites of closure are initiated in the cranial region, one at the midbrain/hindbrain junction which is shortly followed by initiation of closure at the rostral extremity of the forebrain. Closure

Figure 1.6 Early neural development. All diagrams represent an embryo which is bisected laterally and viewed from the median. **(A)** Presomite (late headfold) stage embryo. The cranial neural plate occupies most of the neurectoderm rostral of the node. The only distinguishing features are the preotic sulcus and the anterior limit of the notochord which separates the neural plate into the prechordal and epichordal plate. **(B)** Prospective cranial region of a 5-somite embryo, prior to neural fold closure. The neuromeric junctions which divide the forebrain, midbrain and hindbrain may now be distinguished. Further segmentation of the hindbrain occurs and emigration of neural crest cells from the open neural plate begins in the hindbrain region. **(C)** Cranial region of a 19-somite embryo, after completion of cranial neural closure. The forebrain is divided into two vesicles, the telencephalon and diencephalon, and the development of 8 rhombomeres is complete (not all rhombomeres are shown). Neural crest migration from the cranial neurectoderm has ceased. F/M: forebrain/midbrain boundary, M/H: midbrain/hindbrain boundary, P: preotic sulcus, OS: otic sulcus.

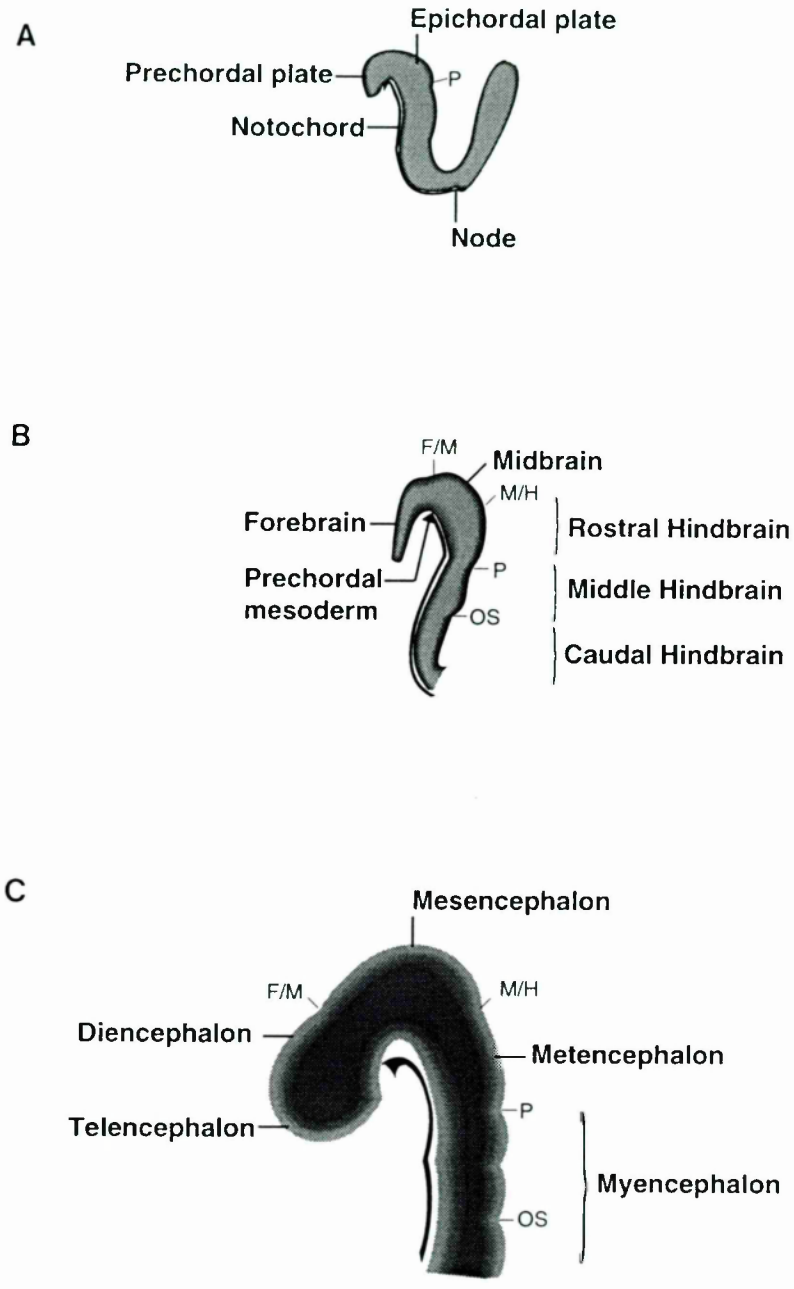
A
Epichordal plate
Prechordal plate
P
Notochord
Node
B
F/M
Midbrain
M/H
Forebrain
Rostral Hindbrain
Prechordal mesoderm
P
Middle Hindbrain
OS
Caudal Hindbrain
C
Mesencephalon
F/M
M/H
Diencephalon
Metencephalon
Telencephalon
P
Myencephalon
OS

spreads to neighbouring regions such that closure of the cranial neural folds is complete in embryos with 17- to 19-somites (Copp et al., 1994).

Once the neural folds close, the space inside enlarges so that the primary brain vesicles are formed (Figure 1.6C). During the preceding 24 hours the forebrain (prosencephalon) has enlarged considerably such that now two vesicles are recognised (rostrally the telencephalon and caudally the diencephalon). The midbrain consists of one vesicle (mesencephalon) and the hindbrain of two vesicles which are further segmented into 8 rhombomeres (metancephalon; r1 and r2, and the myelencephalon; r3 to r8). Upon closure of the neural tube, the surface ectoderm and the neurectoderm separate. Scanning electron microscopy has shown that as neurulation proceeds, the neurepithelial cells elongate while the surface ectodermal cells remain cuboidal. When the neurectoderm folds a space starts to form separating the two epithelia, this space elongates dorsally until it extends almost to the tip of the neural fold. As the neural folds fuse the interepithelial spaces in the two folds connect, thereby causing the separation of the surface ectoderm from the neurectoderm (see Figure 1.7) (Martins-Green, 1988).

The ventral neural tube

In the mouse embryo, as in other vertebrates, the cells which occupy the future floor plate do not have the same origin as cells in other regions of the neural plate. Instead, they share a common origin with the notochord cells (Figure 1.8). At the onset of gastrulation the precursor cells of the notochord and floor plate are located anterolateral to the anterior of the streak, i.e. next to the prospective organiser region, in the chick, frog and mouse (Gerhart and Keller, 1986; Jessell et al., 1989; Lawson and Pedersen, 1992). In amphibians and chick this group of cells within the developing neural plate have been termed the notoplate cells, however, the significance of these cells sharing the same origin as the notochord cells is unclear. It has been postulated that these cells undergo similar convergence and extension movements as the notochord, and therefore are important in the anteroposterior elongation of the neural plate (Keller et al., 1985). It has also been postulated that these cells may be already primed to undergo floorplate development (Jessell et al., 1989).

Upon formation of the neural groove it can be seen that the midline (future ventral) cells in the mouse neural plate have a different morphology, being wedged shape, rather than the spindle shape described for cells in the lateral region (Smith et al., 1994b). As will be shown in Chapter 4, the investigation of mRNA distribution during mouse embryogenesis is beginning to reveal restricted expression of certain genes to this region remarkably early in development. It is not clear exactly when the ventral region of the mouse neural tube acquires identified floor plate properties such as the ability to induce motor neuron differentiation, although, expression of *Shh* which is believed to mediate this function is initiated in the cranial ventral neurectoderm in embryos with 8-somites (Echelard et al.,

Figure 1.7 Neurulation in the mouse embryo. **(A)** Neural plate. The surface ectoderm and neurectoderm cells are similar in shape. Interepithelial spaces begin to form at the junction of the surface and neural ectoderm, the basal lamina (dotted line) remains continuous beneath these spaces. The notochordal plate is continuous laterally with the endoderm. **(B)** Neural fold elevation. The neurectodermal cells take on their longitiudinal shape while the surface ectoderm cells remain cuboidal, the interepithelial spaces extend dorsally. The notochord is beginning to fold off dorsally from the endoderm. **(C)** Continued fold elevation. The interepithelial spaces between the surface and the neurectoderm have created two separate epithelia, although basal lamina still does not invade these spaces. The notochord has folded off from the roof of the gut but remains in contact with the neural tube. **(D)** Neural fold fusion. The interepithelial spaces fuse, leaving two separate epithelia with the dorsal aspect of the neural tube covered by a sparse basal lamina. The notochord eventually becomes detached from the neural tube and is surrounded by a distinct basal lamina. The arrows point to the interepithelial spaces.

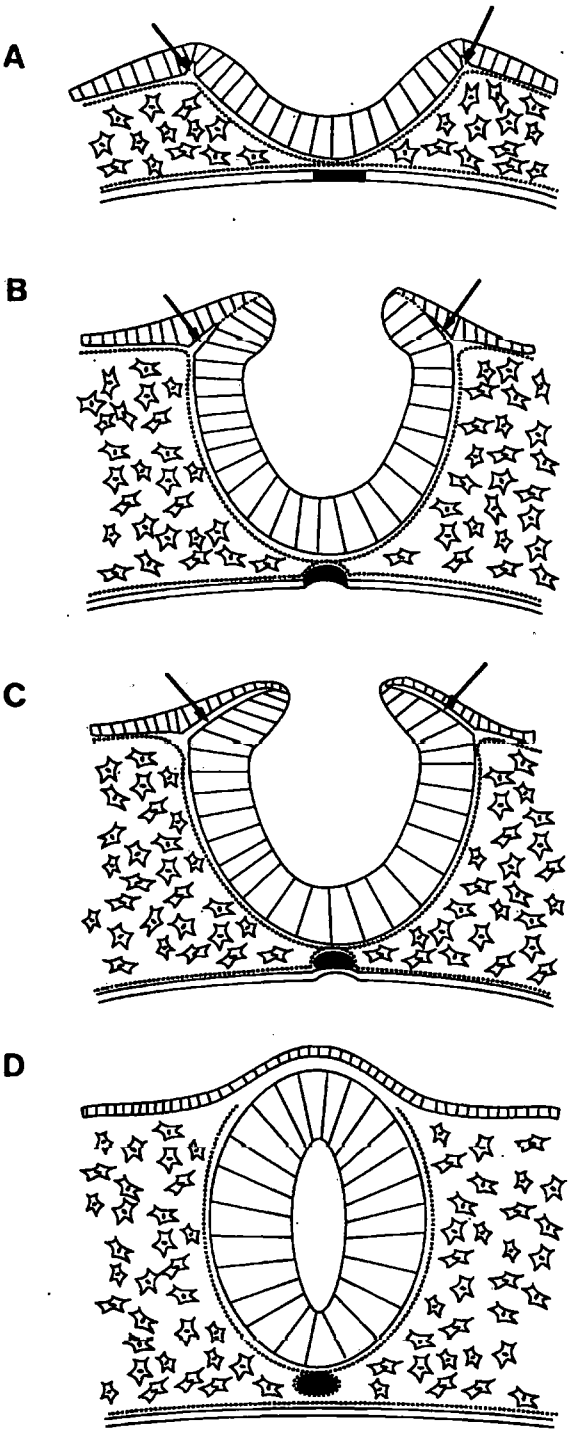
A
B
C
D

Figure 1.8 Clonal analysis of presumptive ectoderm fate between the early primitive streak and early somite stage. **(A)** Lateral view of early primitive streak stage embryo with regions which will contribute to the ectoderm identified by shading. **(B)** Lateral view of a late allantoic bud stage embryo. **(C)** Dorsal view of flattened early somite stage embryo. The extent of the primitive streak is indicated by heavy shading. ant: anterior, post: posterior. Diagram is from Lawson and Pederson (1992).

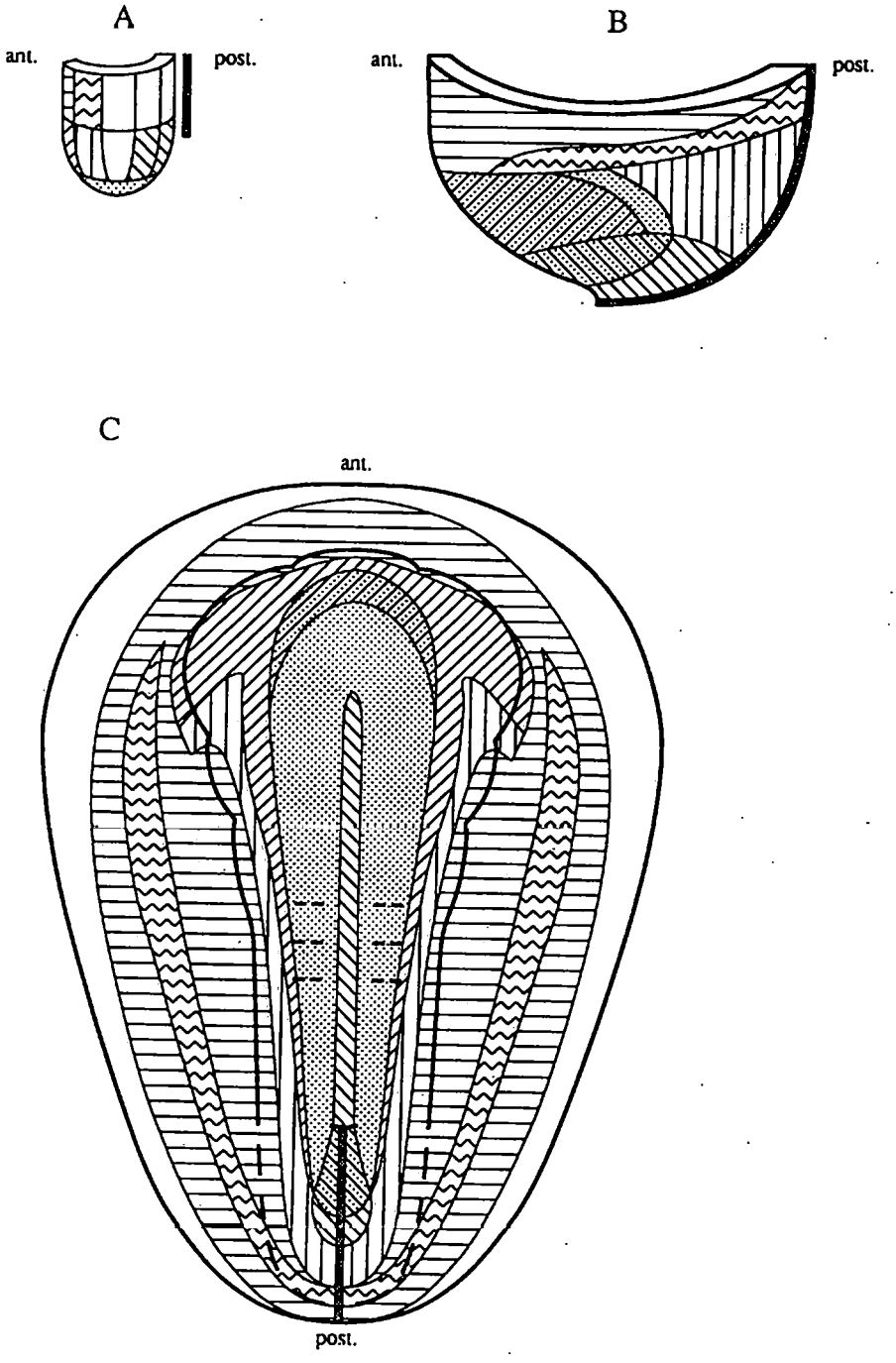
A
ant.
post.
B
ant.
post.
C
ant.
post.

1993). The first neurons to form, do so immediately lateral to the floorplate. These are the motor neurons, and *Islet1* which provides an early marker for the formation of these neurons (Ericson et al., 1992) is expressed in the cranial region of embryos which have 25-somites (Pfaff et al., 1996).

The axial mesoderm

Much confusion exists in the literature concerning nomenclature of the axial mesoderm in the mouse embryo and the following description defines the terms which will be used throughout the thesis. The node is a bilaminar structure at the anterior of the streak, the dorsal layer consists of epiblast cells and the ventral layer of a group of cells which is continuous with the axial mesendoderm. Cells which ingress through this region will give rise to the definitive endoderm and the axial mesoderm (Beddington, 1981; Tam and Beddington, 1992). It appears that the majority of cells which will contribute to the endoderm have passed through the node by the late streak stage, since labelling the ventral surface of the node later than this leads to mainly notochord labelling (Beddington, 1994; Sulik et al., 1994; Wilson and Beddington, 1996). These same labelling studies indicate that the notochord is formed not only from cells which delaminate from the epiblast, but also from a stem cell like population that resides in the node (Beddington, 1994; Wilson and Beddington, 1996).

The morphological development of the notochord has been studied by Jurand (1974), and Sulik et al (1994), and most of the information presented here is derived from these two studies. When cells of the axial mesoderm emerge from the node, they form the notochordal plate. The notochordal plate is an epithelial structure continuous laterally with the endoderm which will form the roof of the gut and is in contact dorsally with the midline neurectoderm cells. At its caudal end, adjacent to the node, it is a broad group of cells but it becomes tapered towards its rostral end. During these early stages of notochord development, the entire midline area from the prechordal plate to the node is only two cell layers thick. Sulik et al describe a morphologically distinct structure at the rostral extent of the notochordal plate, visualised by electron microscopy, which is made up of similar cells but is a broader, circular region, and is attached to the neural plate at the future forebrain level. The exact location of this structure with respect to the embryonic/extraembryonic junction in the early allantoic bud stage embryos examined is unclear and it is not known exactly what this structure corresponds to, although it is likely to be analagous to chick prechordal mesoderm.

It is not until the somite stage of development that the cells of the notochordal plate form the notochord by folding off in a dorsal direction from the roof of the gut (Figure 1.7). At this stage four regions of axial mesoderm can be distinguished. Rostrally the neurectoderm is not underlain by notochordal mesoderm, and the ectoderm in this region is called the prechordal plate; correspondingly the mesoderm of this region may be considered the

prechordal plate mesoderm. Rostral to the anterior of the notochord is a small segment of axial mesoderm which can be distinguished morphologically, and as shown in Chapter 4 can also be distinguished by gene expression, this structure will be referred to as the prechordal mesoderm. Caudally the prechordal mesoderm is continuous with the notochord, which after separation from the endoderm is rod like in shape. The notochord is continuous at its caudal extremity with the node, which will be considered the fourth region of axial mesoderm.

Dorsal-ventral patterning of mouse neurectoderm

Little is known of the interactions which establish dorsal-ventral neural pattern in the mouse neurepithelium. Again, little information has been contributed by *in vitro* isolation or recombination experiments. However, as shown in Figure 1.8, clonal analysis of the fate of cranial neurectoderm precursors shows that the dorsal-ventral pattern of cells at the early somite stage corresponds to their anterior-posterior level in the late primitive streak stage embryo (Lawson and Pedersen, 1992). The cells which at the late streak stage are located in the most proximal position (i.e. those designated as surface ectoderm/prosencephalon in the late streak fate map shown in figure 1.5) will contribute cells to the prosencephalon, but also to the surface ectoderm and dorsal most neurectoderm of all levels of the early somite stage neural plate. Correspondingly, those cells fated for the mesencephalon (Figure 1.5) will contribute to the lateral neurectoderm of more posterior regions than the midbrain and those cells fated as hindbrain will also contribute to the more medial region of the midbrain, hindbrain and spinal column. As such, the anteroposterior relationship of cells in the streak stage embryo is converted to a dorsoventral one in the hindbrain. The special origin of the ventral midline neural cells has already been described.

The available experimental evidence does suggest that some general features of dorsal-ventral neural patterning are conserved between the mouse and other organisms. In the mouse *Shh* may encode a ventral signal: the mRNA localisation of *Shh* and unusual form of autoproteolytic cleavage are conserved in the mouse (Echelard et al., 1993, Bumcrot et al., 1995) and ectopic expression of *Shh* in the dorsal neural tube induces expression of the winged helix transcription factor HNF3-β, a gene whose neurectoderm expression is usually confined to the floor plate region (Echelard et al., 1993). Furthermore, preliminary analysis of mice lacking functional *Shh* suggests these mice are lacking ventral neural structures (cited in Beddington, 1996). The possibility that the surface ectoderm may also contribute to neural pattern in the mouse is supported by analysis of mice which are homozygous for a mutation in the *Wnt-3a* gene. In these embryos the neural plate caudal of the forelimb bud exhibits additional points of contact with the surface ectoderm. The neurectoderm in these regions expresses some genes which are normally dorsally restricted (Takada et al., 1994). It is therefore likely that in the mouse, as in other vertebrates, the dorsal-ventral neural axis is patterned by the interaction of ventral and dorsal signals.

1.5: SUMMARY

Embryonic tissue diversification relies upon cell-cell interactions. These interactions are not only responsible for cellular differentiation but must stimulate appropriate growth and movement to ensure that interacting tissues are correctly juxtaposed at the appropriate developmental stage. Many of these cellular interactions are instigated by secreted signalling molecules. Members of the TGF-β superfamily of secreted molecules have been shown to function in determining cell fate in both invertebrates and vertebrates. A large number of vertebrate TGF-β superfamily molecules have so far been identified. While recent years have seen tremendous progress in understanding the potential function of many superfamily molecules, it is clear that in order to determine which of these molecules are endogenous signalling factors, genetic loss of function experiments will be required. The necessary techniques for targeted ablation of specific gene products in the mouse are now well established. However, our knowledge of embryonic tissue interactions in the mouse is quite rudimentary, for example, we do not even know whether mesoderm induction occurs. The clear indications that at least some aspects of tissues interactions and molecular interactions may be conserved across a wide range of species, from invertebrates to vertebrates, provides the incentive to begin to explore mammalian inductive interactions using knowledge from other organisms. It is hoped that such investigation will not only contribute to our understanding of gene function during mouse development, but serve as a guide for further investigation of these processes both in wildtype and mutant animals.

Objectives

The aim of this thesis is two-fold. Firstly, it aims to investigate the hypothesis that TGF-β superfamily molecules contribute to the cell-cell interactions that establish the mammalian body plan. Coupled with this is the aim to establish relatively simple gain of function assays for secreted molecules in the mouse embryo. While overexpression in the mouse may typically be achieved using transgenesis, this relies entirely on the availability of suitable, tissue-specific promoters. Two overexpression systems are presented here, both of which are independent of such promoters.

The three specific questions investigated are:

- Are TGF-β superfamily molecules expressed during early mouse development?

  The possibility that activin may function in mammalian development is explored. Despite the fact that activin appears to be produced within the maternal tissue surrounding the developing mouse embryo, as shown in Chapter 3, no evidence of activin mRNA is found within the embryo itself. Somewhat surprisingly,

follistatin, a molecule believed to bind specifically to activin, is shown to be expressed during gastrulation and early organogenesis. This finding prompted a screen to identify molecules which have structural homology to activin but which are present within the developing embryo. This resulted in the cloning of a TGF-β superfamily member, bone morphogenetic protein-7 (*BMP-7*). The mRNA localisation of *BMP-7* which is presented in Chapter 4 suggests a role in axis formation; *BMP-7* may act in conjunction with other BMP molecules in embryonic anterior-posterior axis formation, or it may be involved in establishing the dorsal-ventral axis of the neurectoderm, especially in the cranial region. Evidence from the chick embryo suggests that BMP molecules may regulate aspects of development of the dorsal-ventral neural axis and the potential role of *BMP-7* in this process in the mouse embryo was investigated.

A second TGF-β superfamily molecule implicated in *Xenopus* mesoderm formation is *Vg1*. A murine gene which has some homology to *Vg1* has previously been isolated and named *Vgr-2* (Jones et al., 1992a). Interestingly murine *Vgr-2* is capable of mesoderm induction in *Xenopus* assay systems (M. Jones, personal communication). *Vgr-2* transcripts are present in the mouse embryo at the onset of gastrulation as shown in Chapter 5.

- Does *Vgr-2* function in mesoderm formation in the mouse embryo?

To assess whether *Vgr-2* can also induce mesoderm in the mouse embryo, murine embryonic stem cells (ES cells; Robertson, 1987) overexpressing *Vgr-2* were generated and these cells secrete a factor active in *Xenopus* animal cap assays (Chapter 6). While chimeric mouse embryos generated with the *Vgr-2* overexpressing cell lines do not produce excess mesoderm, the overexpressing cells appear to preferentially colonise mesoderm derivatives. It has not been possible to demonstrate that this bias can be attributed solely to the expression of *Vgr-2* by the cell lines.

- Does BMP-7 function in establishing the mouse cranial neural plate?

To address this question a method of delivering secreted molecules to specific locations in cultured, postimplantation embryos was developed (Chapter 7). A transformed monkey kidney cell line (COS cells; Gluzman, 1981) was utilised because of its ability to drive high level expression of exogenous DNA. When COS cells transfected with *BMP-7* are grafted into the mesoderm adjacent to the developing hindbrain, several changes in the neurectoderm are elicited. These changes are consistent with *BMP-7* acting both to regulate growth and to specify

cell fate during the establishment of the dorsal-ventral axis of the mammalian cranial neural plate.

These assays represent the first demonstration that overexpression of TGF-β superfamily proteins can alter mammalian embryogenesis. They provide information about the potential function of these two molecules and establish a future framework for the study of both these and other secreted factors in mouse development.

CHAPTER 2

MATERIALS AND METHODS

2.1 MOLECULAR BIOLOGY

General materials and methods for those techniques used in more than one part of this thesis are included in this chapter. For these techniques, specific information, such as the amount of DNA used in a particular Southern analysis, will be reported in the figure legend accompanying the results of the analysis. More specialised techniques which apply to only one chapter will be described at the beginning of the appropriate chapter.

DNA isolation

Small quantities (20 μg) of plasmid DNA were isolated by alkali lysis as described in Sambrook et al. (1989). Larger quantities of plasmid DNA (150 μg) were isolated by scaled up alkali lysis and purification over QIAGEN (Hybaid) columns. Plasmid DNA to be used for COS cell transfections was further purified (after QIAGEN purification), by centrifugation over a caesium chloride gradient as described in Sambrook et al. (1989).

RNA isolation

RNA from embryonic tissue which had previously been collected and frozen in denaturing solution containing 4 M guanidinium thiocyanate, 25 mM sodium citrate, 0.5% sarcosyl and 0.01 M β-mercaptoethanol was isolated following a method modified from that of Chomczynski and Sacchi (1987). The tissue was homogenised by pipetting up and down with a Gilson P1000 tip. The volume of denaturing solution was adjusted to 500 μl for each sample, 5 μg of yeast tRNA was added to act as carrier and the following added: 0.1 volume sodium acetate, pH 4.0; 1 volume phenol and 0.2 volumes chloroform:isoamyl-alcohol (49:1). Samples were placed on ice for 15 minutes before centrifuging for 20 minutes, 10000 *g*, 4°C. The RNA-containing aqueous phase was removed and precipitated with an equal volume of isopropanol overnight at -20°C. The RNA was pelleted by centrifuging for 20 minutes, 10000 *g*, 4°C, the supernatant discarded and the RNA dissolved in 50 μl of denaturing solution. RNA was again precipitated with an equal volume of isopropanol overnight at -20°C. RNA was pelleted by centrifuging 20 minutes, 10000 *g*, 4°C. The supernatant was discarded and the pellet resuspended in 75% ethanol by vortexing and incubated for 15 minutes at room temperature. The sample was centrifuged for 5 minutes, 10000 *g*, room temperature and the supernatant discarded. The RNA pellet was air dried and dissolved in 1 μl of dH_2O per embryo and stored at -20°C. For isolation of RNA from embryonic stem (ES) cells, undifferentiated ES cells were grown to confluency on a 10 cm dish, as described in Section 2.2, and washed once with phosphate buffered saline (PBS; 10 mM phosphate buffer, 137 mM NaCl and 2.7 mM KCl), then covered with denaturing

solution and the lysed cells collected. RNA was isolated from these cells using the procedure of Chomczynski and Sacchi (1987) as described above.

Southern analysis

DNA was separated in a 1% agarose gel in TAE (0.04 M Tris-acetate, 0.001 M ethylenediaminetetra-acetic acid, disodium salt (EDTA)). After electrophoresis at 5 V cm^{-1} in TAE buffer the DNA was denatured by shaking the gel in 0.5 M NaOH, 1.5 M NaCl for 30 minutes at room temperature. The DNA was then transferred to a nylon membrane (Hybond-N, Amersham) using a dryblotting procedure as follows: the nylon membrane was placed onto the gel and two sheets of blotting paper (3Chr, Whatman) wet in the denaturing solution (0.5 M NaOH, 1.5 M NaCl) placed on top of this. Next, eight sheets of dry blotting paper were placed on top followed by a stack of paper towels, a glass plate and a 0.5 kg weight. DNA transfer continued overnight after which DNA was fixed to the membrane by exposure to UV light (1 x Autocrosslink, UV Stratalinker 1800, Stratagene) before proceeding with hybridisation as described below.

Northern analysis

RNA was denatured in 50% formamide, 1x MOPS buffer (20 mM MOPS [3(N-morpholine) propanesulfonic acid], 5 mM NaAC and 1 mM EDTA) and 6% formaldehyde by heating for 5 minutes at 65°C prior to electrophoresis. RNA was size separated in a 1% agarose in 1x MOPS and 6% formaldehyde gel electrophoresed in 1x MOPS buffer at 5 V cm^{-1}. RNA was transferred to a nylon membrane (Hybond-N) by dry blotting overnight. Dry blotting was carried out as described for Southern analysis except that the blotting paper was wet in 10x SSC (1x SSC is 0.15 M NaCl and 15 mM sodium citrate, pH 7.0) The membrane was exposed to UV light (as described for DNA) to crosslink the RNA to the filter before proceeding with hybridisation as described below.

Colony screening

Bacteria for colony screening were diluted to a volume of 4 mls in L broth (0.01% tryptone, 0.005% yeast extract (Bacto, Difco Laboratories) and 0.005% NaCl) and spread onto a nylon membrane (Biodyne A, 0.2 μm, Pall) laid on a 22 cm square plate of LB agar (0.015% Bacto-Agar (Difco Laboratories) in L broth) containing 100 μg ml^{-1} ampicillin. Bacteria were grown at 37°C until 1 mm in diameter. Colonies were transferred from this master filter to two replica nylon filters (Hybond-N) by replica plating (Sambrook et al., 1989). Colonies on the replica filters were allowed to grow for 2 hours at 37°C before colony lysis. Bacteria were lysed by placing the replica filter onto blotting paper (3Chr, Whatman) soaked in 10% sodium dodecyl sulphate (SDS) for 4 minutes. DNA was denatured by transferring the filter to blotting paper soaked in DNA denaturing solution for 5 minutes and neutralised on blotting paper soaked in 0.5 M Tris-HCl (pH 7.2), 1.5 M NaCl for 5 minutes. Bacterial debris was removed from the filter by wiping with tissues soaked in

the neutralising solution until it appeared clean. Filters were rinsed in 2x SSC and DNA fixed to the membrane by exposure to UV light. Before hybridisation, filters were prewashed twice by shaking in 50 mM Tris-HCl (pH 8.0), 1 M NaCl, 0.5 M EDTA and 0.1% SDS for 30 minutes at 42°C.

DNA probes

DNA probes for detecting mRNA transcripts and cDNA

Probes corresponding to regions of the mouse inhibin β_A and β_B subunits, *BMP-7*, *Vgr-2*, *Oct-4* and *T* cDNAs were made. All probe templates were prepared using polymerase chain reaction (PCR; see below) to amplify the region of interest. Table 2.1 describes the probes and lists the oligonucleotides used for PCR.

DNA probe for detecting rRNA transcripts

A 7.3 kilobase fragment spanning the mouse ribosomal genes was used to detect ribosomal transcripts. The fragment covers the 3' region of the 18s rRNA gene, all of the 5s rRNA gene and the 5' end of the 28s rRNA gene (Rothstein et al., 1992).

Radiolabelling DNA

All DNA probes were radiolabelled by random priming, incorporating 50 μCi α^{32}PdCTP using a Boehringer Mannheim Random Primed DNA labelling kit. Purified DNA (100 ng) was labelled, typically resulting in a specific activity of 0.7×10^8 cpm μg^{-1} DNA. Unincorporated nucleotides were removed on a Sephadex G-50 column, centrifuged at 2000 *g* for 2 minutes at room temperature.

Filter hybridisation

High stringency

Filters were prehybridised in 0.5 M phosphate buffer (Na_2HPO_4/NaH_2PO_4, pH 7.2), 7% SDS, and 1 mM EDTA (Church and Gilbert, 1984) at 65°C for 5 minutes. For hybridisation, 1×10^6 cpm of the appropriate radiolabelled probe was added per ml of hybridisation solution. Filters were hybridised for 16 hours at 65°C before washing as follows: 0.5x SSC, 0.1% SDS, two washes for 30 minutes each at 65°C; 0.2x SSC, 0.1% SDS one wash for 30 minutes at 65°C. Hybridisation signal was visualised either by exposure to Kodak X-OMAT AR or X-ograph BLUE film, or by exposure to a PhosphorImage screen and subsequent analysis with Imagequant (Molecular Dynamics).

Low stringency

Filters were prehybridised for 5 minutes and hybridised for 16 hours under the following conditions: 20% formamide, 5x SSC, 5x Denhardts (1x Denhardts is 0.1 g Ficoll, 0.1 g Polyvinylpyrolidine, 0.1 g bovine serum albumin (Fraction V) in 500 ml H_20) (Denhardt, 1966), 1% SDS and 100 μg ml^{-1} yeast RNA at 37°C. For hybridisation 1×10^6 cpm of the appropriate radiolabelled probe was added per ml of hybridisation solution. Filters were

Table 2.1 DNA probes. Probes corresponding to the regions of cDNA listed were synthesised by PCR using the primers shown. The base numbering of the cDNAs is as shown in the listed reference. The inhibin probes were provided by R. Albano and J. Smith and the Vgr-2 probe was provided by M. Jones.

Probe	Description	Oligonucleotide Sequence	Reference
Inhibin β_A	Bases 1113 - 1435 of the mouse β_A cDNA, corresponding to the mature region.	5' oligomer: GCAAGGTCAACATTTGC 3' oligomer: ACACTCCTCCACAATCAT	Albano et al. (1993)
Inhibin β_B	Bases 22 - 357 of the mouse β_B cDNA, corresponding to the mature region.	5' oligomer: GGCCTAGAGTGTGATG G 3' oligomer: ACACTCCTCCACGATCA T	Albano et al. (1993)
BMP-7	Bases 1392 - 1817 of the mouse *BMP-7* cDNA, corresponding to the 3'UTR.	5' oligomer: ACTAGCTCTTCCTGAGA 3' oligomer: CATTACAGTGGCTTCTG	Ozkaynak et al. (1991)
Vgr-2	Bases 1 - 1142 of the mouse *Vgr-2* cDNA, corresponding to full length coding sequence.	5' oligomer: ATGCAGCCTTATCAAC G 3' oligomer: CATTACAGTGGCTTCTG	Jones et al. (1992a)
Oct-4	Bases 714 - 1140 of the mouse *Oct-4* cDNA, corresponding to the last 281 bases of the coding sequence and the first 265 bases of the 3' UTR.	5' oligomer: TTCGAGTATGGTTCTGTAA CC 3' oligomer: AGGCTCCTGATCAACAGCA T	Scholer et al. (1990)
T	Bases 1213 - 1695 of the mouse *T* cDNA, corresponding to the last 207 bases of the coding sequence plus the first 275 bases of the 3' UTR.	5' oligomer: AACGGGCTGGGAGCTCAG TTCTTT 3' oligomer: GAATTCCAGGATTTCAAAG TCACA	Herrmann et al. (1990)

washed twice in 2x SSC, 0.1% SDS for 20 minutes at 37°C before exposure to Kodak X-OMAT AR film.

Ligation of DNA

Typically 50 ng of vector was ligated to a ten fold molar excess of insert in 50 mM Tris-HCl (pH 7.6), 10 mM $MgCl_2$, 1 mM ATP, 5% Poly Ethylene Glycol (PEG) 5000, 1 mM dithiothreitol (DTT) with 50 U ml^{-1} T4 DNA ligase (Gibco BRL) in a total volume of 20 µl. The ligation was incubated for 3 hours at room temperature and was then precipitated in the presence of 5 µg of carrier yeast tRNA and resuspended in 5 µl dH_2O.

Electrotransformation

Electrocompetent bacteria

A single *E. coli* colony was used to inoculate 500 ml of SOB-Mg (Hanahan et al., 1991) and grown at 37°C with shaking until the OD_{550} reached 0.75. The cells were harvested by centrifugation at 6000 *g*, 10 minutes, 0°C and washed twice by resuspension in 400 ml of 10% glycerol followed by centrifugation. The final pellet was resuspended in sufficient 10% glycerol to give an OD_{550} of 200 U ml^{-1}. The cells were snap frozen and stored at -70°C.

Transformation of E. coli

Either 10 pg of plasmid DNA or 1 µl of a ligation was added to 20 µl of electrocompetent cells and electroshocked in a 0.1 cm chamber (Bio-Rad) using a Bio-Rad genepulser under the following conditions: 1.8 kV, 25 µF and 200 W. SOC (1 ml) (Hanahan et al., 1991) was added to the cells which were transferred to a plastic tube and incubated with shaking at 37°C for 1 hour before selection on LB agar plates containing 100 µg ml^{-1} ampicillin.

Polymerase Chain Reaction

DNA was amplified in 10 mM Tris-HCl (pH 8.3, 20°C), 1.5 mM $MgCl_2$, 50 mM KCl using 50 pmoles of each oligonucleotide primer and 0.3 U Taq DNA polymerase (Perkin Elmer). DNA was denatured initially for 2 minutes at 94°C and then amplified by 30 cycles of denaturing for 20 seconds at 93°C, annealing for 30 seconds at a temperature appropriate for the melting temperature of the primer pair and DNA extension for 30 seconds at 72°C.

DNA sequencing

Double stranded DNA for sequencing was precipitated with 20% PEG-8000 in 2.5 M NaCl to remove contaminating RNA and denatured in 0.2 M NaOH. 2 µg of this DNA was resuspended in the presence of the sequencing primer and sequenced using a Sequenase version 2.O kit (USB) according to the manufacturer's instructions, incorporating α^{35}SdATP. The sequencing reactions were denatured by heating at 80°C for 2 minutes immediately before separation on a 6% Polyacrylamide, 50% Urea in TBE (0.9 M Tris-

borate, 2 mM EDTA) gel. The acrylamide gel was fixed in 5% acetic acid and 15% methanol for 15 minutes before drying and exposure to BLUE X-ray film (X-ograph).

RNA probes

Antisense riboprobes were synthesised which corresponded to specific regions of the mouse inhibin α, β_A and β_B subunit, *follistatin*, *BMP-7*, *BMP-2*, *Vgr-2*, *Pax-3*, *Shh*, *HNF3-β*, *AP-2* and *Msx1* cDNAs. Table 2.2 describes the probes. While many of the probes include regions known to be conserved between gene family members, the stringent hybridisation conditions of the whole mount *in situ* hybridisation protocol are sufficient to prevent cross hybridisation. Plasmid DNA was digested at the 5' extreme of the probe and RNA transcribed from 1-3 μg of plasmid template incorporating digoxigenin (DIG) labelled dUTP, following the protocol of the Boehringer Mannheim DIG nucleic acid labelling kit. After synthesis, probes were treated with 20 U DNase (Boehringer Mannheim) at 37°C for 20 minutes to remove the plasmid template. All probes were electrophoresed on a 1% agarose in TAE gel to check the size and integrity of the probe and the amount of DIG incorporation tested by detection of dilutions of the probe. Typically a 10^{-5} dilution of the probe could be detected after overnight incubation with the colorimetric substrate.

2.2 CELL CULTURE

COS cell culture

COS7c cells were maintained in culture at 37°C in 5% CO_2 in a humidified incubator. The cells were grown on plasticware (COSTAR) in Dulbecco's Modified Eagle's Medium (DMEM; HyClone), supplemented with 10% fetal calf serum (Advanced Protein Products) and 2 mM L-glutamine. Cells were dissociated with 0.25% trypsin, 0.5% EDTA in PBS.

ES cell culture

Germ line competent CGR8 ES cells (Mountford et al., 1994) were maintained at 37°C in 5% CO_2 in a humidified incubator, on plasticware coated with 0.1% gelatin in PBS. Cells were grown in DMEM (HyClone) with 15% fetal calf serum (Advanced Protein Products), 2 mM L-glutamine and 100 μM β-mercaptoethanol. Murine Leukemia Inhibitory Factor (LIF) was added fresh to the medium at a concentration equivalent to 1000 U ml^{-1} to prevent differentiation of the ES cells. Cells were disaggregated with 0.25% trypsin, 0.5% EDTA in PBS.

Preparation of LIF

COS cells were transfected with a LIF expression construct, pDR10 (Rathjen et al., 1990a) following the protocol described in Chapter 7. The conditioned transfection media was collected 72 hours after transfection. ES cells were grown either in dilutions of this media or

Table 2.2 RNA probes. Probes corresponding to the regions of cDNA listed were synthesised, the base numbering of the cDNAs is as shown in the listed reference. The inhibin and follistatin probes were provided by R. Albano and J. Smith, the BMP-2 and Vgr-2 probes were provided by M. Jones, the Shh probe was provided by A. McMahon, the HNF3-β probe was provided by B. Hogan and the AP-2 probe was provided by P. Mitchell.

Probe	Description and Preparation	Reference
Inhibin α	211 basepair fragment of the mouse inhibin α chain cDNA, corresponding to a region of the pro-domain. Linearised with BamHI, transcribed with T3 polymerase.	Albano et al. (1993)
Inhibin β_A	204 basepair fragment of the mouse inhibin β_A chain cDNA, corresponding to a region of the pro-domain. Linearised with EcoRI, transcribed with T7 polymerase.	Albano et al. (1993)
Inhibin β_B	245 basepair fragment of the mouse inhibin β_B chain cDNA corrsponding to a region of the 3' UTR. Linearised with PstI, transcribed with T3 polymerase.	Albano et al. (1993)
Follistatin	Bases 738-1055 of mouse *follistatin* cDNA, corresponding to the last 94 amino acids and the first 27 bases of the 3' UTR and detecting both the short and long forms of follistatin mRNA. Linearised with EcoRV, transcribed with T3 polymerase.	Albano et al. (1994)
BMP-7	Bases 1445 - 1872 of the mouse *BMP-7* cDNA, corresponding to the last 427 bases of the 3' UTR. Linearised with SalI, transcribed with SP6 polymerase.	Ozkaynak et al. (1991)
BMP-2	Bases 197-1200 of the mouse *BMP-2* cDNA, corresponding to coding sequence. Linearised with XmaIII, transribed with SP6 polymerase.	Wozney et al. (1988) Lyons et al. (1989)
Vgr-2	Bases 1 - 1142 of the mouse *Vgr-2* cDNA, corresponding to full length coding sequence. Linearised with EcoRV, transcribed with SP6 polymerase.	Jones et al. (1992a)
Shh	A 2.6kb cDNA, corresponding to the full length cDNA. Linearised with XbaI, transcribed with T7 polymerase.	Echelard et al. (1993)
HNF3-β	A 1.5kb fragment (clone c21), corresponding to coding sequence and including the forkhead domain. Linearised with BamHI, transcribed with T3 polymerase.	Sasaki and Hogan (1993)
Pax-3	Bases 1067-1586 of the mouse *Pax-3* cDNA, corresponding to coding sequence which includes the last 67 bases of the homeobox. Linearised with HindIII, transcribed with T7 polymerase.	Goulding et al. (1991)

Probe	Description and Preparation	Reference
Msx1	2 kb fragment of *Msx1* cDNA. Linearised with BsshII, transcribed with T7 polymerase.	Hill et al. (1989)
AP-2	Bases 13-255 of *AP-2* clone λ22 corresponding to coding sequence. Linearised with EcoRI, transcribed with T3 polymerase.	Mitchell et al. (1991)

in 1000 U ml^{-1} of commercially available LIF (Gibco BRL) for 7 days. The ES cells were then fixed in methanol:acetic acid (3:1) for 5 minutes, washed once with PBS and stained with 10% Giemsa (Sigma) for 5 minutes. The ES cells were scored visually for the proportion of undifferentiated and differentiated cells, and the appropriate concentration of transfection media determined.

2.3 EMBRYOLOGY

Embryo dissection

Embryos were collected from timed C57BL6 x DBA matings. Mice were maintained on a 12 hour dark: 12 hour light cycle. Noon on the day of appearance of the vaginal plug is designated 0.5 dpc. All embryos were dissected in M2 medium (Hogan et al., 1994) containing 10% fetal calf serum, instead of bovine serum albumin. Embryos for whole mount *in situ* hybridisation were dissected from maternal tissue and Reichert's membrane removed. The amnion was removed from 8.5 and 9.5 dpc embryos and holes made in regions likely to trap probe. Embryos were rinsed in PBS and transferred to 4% paraformaldehyde in PBS. Embryos for RNA isolation were dissected from maternal tissue and Reichert's membrane and ectoplacental cone removed before freezing in denaturing solution. Embryos for culture were dissected from maternal tissue and Reichert's membrane removed. Only those embryos in which the ectoplacental cone and yolk sac were fully intact were used for culture.

Whole mount *in situ* hybridisation to mouse embryos

Whole mount *in situ* hybridisation was carried out according to Wilkinson (1992) using the hybridisation conditions of Rosen and Beddington (1993). The length of proteinase K treatment varied depending on the stage of the embryos. 5.5 - 6.5 dpc embryos were incubated for 5 minutes, 7.0 - 8.5 dpc embryos for 10 minutes and 9.0 dpc and older embryos for 15 minutes. After completion of the *in situ* procedure, embryos were destained in PBT (PBS with 0.1% Tween 20: polyoxyethylene sorbitan monolaurate; Sigma) for 48 hours and post-fixed in 4% paraformaldehyde, 0.1% glutaraldehyde in PBS for 1 hour at room temperature.

Sectioning of mouse embryos

Embryos were processed for paraffin sectioning by dehydration through an ethanol series (50%,70%, 80%, 87%, 90%, 95%, 100%, 10 minutes each), clearing in Histoclear (National Diagnostics) and embedding in paraffin wax (Histoplast, m.p. 56°C). Sections (7 μm) were cut using a Bright microtome. Sections were dewaxed in Histoclear (5 minutes) and mounted under coverslips in DPX mountant (BDH). Embryos were prepared for cryosectioning by equilibration in OCT cryoembedding solution (BDH) for 30 minutes at

4°C. The specimens were then frozen in fresh OCT and stored at -70°C. Frozen sections (10 μm) were cut using a Bright cryostat and mounted under coverslips in either Mowiol (for non-fluorescent specimens; Heimer and Taylor, 1974) or glycerol (4% PFA in PBS (1:1), for fluorescent specimens).

Dissection of neurectoderm from embryos

Embryos were placed in a drop of Aquamount (BDH) on a glass microscope slide and the surface ectoderm, endoderm and paraxial and lateral mesoderm removed using tungsten needles under the high power objective of a dissecting microscope. The neurectoderm was transferred to another microscope slide, a fresh drop of aquamount added and the neurectoderm bisected along the dorsal aspect of the neural tube. The neurectoderm was flattened and a glass cover slip supported by dabs of silicon grease placed over the specimen. The cover slip was gently pushed down until the tissue was held flat.

Embryo culture

All embryos were cultured using the conditions described by Beddington (1987). Briefly, up to 4 embryos were placed in a universal (Nunc) containing 2.5 ml of culture media (DMEM; HyClone, containing 50% rat serum and 2 mM L-glutamine). The medium was equilibrated in 6% CO_2 in a humidified incubator, at 37°C for 20 minutes, after which the universal was sealed with silicon grease. The embryos were allowed to develop in roller culture at 37°C for 24 hours.

Photography

Low power (up to 7.5 x) bright field and dark field colour photographs were taken using tungsten film (Kodak 64T) with a dissecting microscope (Nikon) using a 35 mm camera attachment. Higher power (10-40 x) colour photographs were taken in a compound microscope (Zeiss Axiophot) with a 35 mm camera attached. Colour photos taken using bright field or Nomarski optics used tungsten film (Kodak 64T), while Kodak p1600 film was used for fluorescence photography or fluorescence/Nomarski double exposures. A variety of background substrates (glass microscope slide, shallow cavity slide, 0.5% agarose in PBS) and photography media (PBT, 4% PFA in PBT, Aquamount) were used in a variety of combinations, depending on the specimen to be photographed. Black and white photographs were taken with 400 ASA film (Ilford).

CHAPTER 3

ACTIVIN AND *FOLLISTATIN* MRNA LOCALISATION

3.1 INTRODUCTION

As described in Chapter 1, mesoderm formation in amphibian embryos occurs as the result of an inductive interaction in which cells of the vegetal pole act on the overlying equatorial cells. Activin is one of the several TGF-β superfamily molecules which are candidate mesoderm inducing factors, for review see Smith (1995). In *Xenopus*, activin is capable of acting as a morphogen. It is able to act over a distance of at least ten cell diameters to specify mesoderm cell fates in a graded manner; dorsal mesoderm is induced in response to high concentrations of activin whereas more ventral mesoderm results from exposure to lower concentrations (Green and Smith, 1990; Gurdon et al., 1994). However, little or no activin is found in the early amphibian embryo. Messenger RNA encoding activins A and B are present in *Xenopus* oocytes and early embryos at levels so low that they can barely be detected by polymerase chain reaction (Dohrmann et al., 1993; Rebagliati and Dawid, 1993).

In order to assess the contribution of activin to embryonic development inhibition experiments have been attempted in *Xenopus*. Overexpression of a truncated activin type II receptor, predicted to behave in a dominant negative manner, ablates the mesoderm inducing activity of activin in animal cap assays. Blocking embryonic activin signalling with this construct produces embryos which are deficient in mesodermal and axial development (Hemmati-Brivanlou and Melton, 1992). However, this construct also blocks signalling by other TGF-β related proteins, such as Vg1 (Schulte-Merker et al., 1994; Kessler and Melton, 1995) and these experiments can not be used to analyse embryonic activin function. In contrast, the activin-binding protein, follistatin, blocks activin function but does not inhibit Vg1 function (Nakamura et al., 1990; Asashima et al., 1991; Schulte-Merker et al., 1994). Overexpression of follistatin in the whole embryo produces either no effect on mesoderm formation (Schulte-Merker et al., 1994), or if larger amounts of follistatin are injected, the development of postero-ventral structures is compromised, but the development of dorso-anterior structures is relatively unaffected (Kessler and Melton, 1995). This is opposite to the phenotype predicted on the basis of the activity identified for activin in the mesoderm induction assays. Although follistatin does not block the activity of Vg1 its ability to interact with other TGF-β superfamily molecules has not been systematically tested.

Despite the lack of mesoderm induction assays, the mouse provides the opportunity to unequivocally inactivate different isoforms of activin, making it important to begin to investigate the potential role of activin in mesoderm formation in the mouse embryo. Activins are homo- or heterodimers of the β_A or β_B subunits of inhibin. Inhibin itself is a heterodimer consisting of one of the β subunits with an α inhibin subunit (Ying, 1988). Therefore probes to all three subunits are required to determine if activin is present. cDNAs

encoding each of the three inhibin subunits have been cloned from the mouse (Albano et al., 1993) and it is clear, on the basis of sequence analysis, that these cDNAs represent homologues of the *Xenopus* genes. In preimplantation mouse embryos activin is present in all cells of the morula, it becomes restricted to the inner cell mass of the blastocyst at 3.5 dpc, but by 4.5 dpc expression has become confined to the trophectoderm (Albano et al., 1993).

Studies of postimplantation embryos, using RNase protection assays and sectioned radioactive *in situ* hybridisation analysis have demonstrated that activin is expressed in the maternal tissue immediately surrounding the embryo at 5.0 to 8.0 dpc (Manova et al., 1992; Albano et al., 1994). The maternal tissue may supply activin to the embryo during mesoderm formation but because in the decidua, activin is expressed uniformly around the embryo it is not clear how mesoderm formation might be initiated at only one site. One possibility is that the effects of activin may be modulated in particular regions by activin-binding proteins such as follistatin (Nakamura et al., 1990), which inhibits the mesoderm inducing activity of activin (Asashima et al., 1991). In the experiments detailed in this chapter, using whole mount *in situ* hybridisation, it was confirmed that inhibin subunit mRNA is not present in the embryo proper during gastrulation and the pattern of *follistatin* mRNA distribution was determined. *Follistatin* is expressed in the primitive streak, and at later stages of development, transcripts accumulate in the somites and hindbrain. The results argue against a function for these activin isoforms in mesoderm formation and suggest that follistatin may have function(s) beyond the inhibition of activin activity.

3.2 RESULTS

Embryonic expression of the inhibin subunits

Whole mount *in situ* analysis of full length primitive streak stage to 30-somite embryos confirmed that the α subunit, diagnostic of the presence of inhibin, is not detected in the embryo at any stages studied (data not shown). The inhibin chains are expressed in adult ovaries (Meunier et al., 1988) and strong hybridisation was seen with all probes to mouse ovaries indicating that the whole mount *in situ* hybridisation procedure had worked. Transcripts encoding the β subunit are not detected in the embryo until at least the 6-somite stage when there appears to be expression in the heart of both β_A (Figure 3.1) and β_B (data not shown) transcripts. This hybridisation signal is weak and it is not possible, from this whole mount *in situ* hybridisation analysis, to distinguish between low level expression of the β inhibin subunits and trapping of the colorimetric product in the heart.

Embryonic expression of *follistatin*

Through RNase protection and sectioned radioactive *in situ* hybridisation analysis *follistatin*

Figure 3.1 Inhibin β_A mRNA localisation. Top row, left to right: full length primitive streak stage, 4-somite embryo and 8-somite embryo. Bottom row, left to right: 2 embryos with 12 - 14-somites, adult ovary. There is weak signal in the heart of embryos with 8 somites or more (arrowheads). Strong hybridisation was seen in the follicle cells of the ovary. Scale bar, 480 μm.

was known to be expressed at high levels within the embryo itself during the stages of primitive streak formation (Albano et al., 1994). To more precisely determine the sites of embryonic expression of *follistatin* whole mount *in situ* hybridisation was carried out on embryos of pregastrulation stage to 30-somites (Figure 3.2). *Follistatin* expression is first detected in the parietal endoderm surrounding the embryo. Expression in the embryo proper begins at the early primitive streak stage when *follistatin* transcripts accumulate in the cells of the primitive streak. Sections of full length primitive streak stage embryos show hybridisation in both the ectodermal and mesodermal germ layers in the vicinity of the streak; this expression extends laterally to approximately halfway around the cylinder. At the early headfold stage, strong expression continues in the primitive streak and in a spur of paraxial mesoderm underlying the cranial neural folds (Figure 3.2C). The ventral population of cells in the node of early headfold stage embryos do not appear to contain *follistatin* mRNA.

Transcripts decline in the primitive streak around the 4- to 5-somite stage and by the 8- to 10-somite stage no signal is detected in this region. High transcript levels are, however, evident in the somites and paraxial mesoderm of the cranial region and low levels of mRNA can be detected in the presomitic mesoderm. In addition, by the 5-somite stage two prominent stripes of expression can be distinguished in the developing hindbrain. In turned embryos it is clear that the neurectodermal expression is limited to rhombomeres 1, 2, 4 and 6, although transcripts are absent in the ventral midline of the hindbrain (data not shown). Expression is still evident in the cranial paraxial mesoderm of embryos with 30-somites, up to the forebrain/midbrain junction as well as in all mature somites. Caudally a graded hybridisation signal is apparent in the presomitic mesoderm; the levels of mRNA increase towards its rostral aspect. However, *follistatin* transcripts remain undetectable in the most rostral presomitic cells (those about to undergo segmentation) and in the most recently formed somite, although there is a narrow trail of positively stained cells, of unknown character, immediately ventrolateral to the somites in this region (Figure 3.2E).

3.3 DISCUSSION

Activin and early mouse development

The majority of the evidence which implicates activin in early embryonic processes comes from the study of *Xenopus* embryos where treatment of prospective ectodermal cells with activin causes ectopic mesoderm formation (Green et al., 1990). In the mouse embryo, the apparent lack of inhibin subunit expression at the stages studied here, argues that activin is not involved in mesoderm formation. However, inhibin β_A and β_B transcripts are present in the maternal tissue immediately surrounding the embryo at the time of mesoderm formation and are down-regulated beyond this stage and the inhibin α chain is not detected in the maternal tissue (Manova et al., 1992; Albano et al., 1994). It is possible that decidual

Figure 3.2 ***Follistatin*** **mRNA localisation.** **(A)** Lateral view of pregastrulation and early primitive streak stage embryos, the youngest embryo is on the left. Expression is first detected in the parietal endoderm surrounding the embryo, which is not fully dissected away from the two left hand embryos and is seen as dots of expression (arrowhead). The first embryonic expression of *follistatin* at the onset of gastrulation is restricted to the primitive streak. **(B)** Lateral view of 7.5 dpc embryos. *Follistatin* transcripts are localised to the primitive streak and adjacent mesoderm and ectoderm. **(C)** Lateral view of headfold-stage embryos. Expression persists in the streak and *follistatin* mRNA is also detected in paraxial mesoderm (arrowhead) but is absent from the ventral node. **(D)** Dorsal view of 8.5 dpc early somite stage embryos. The youngest embryo is on the right. Transcript levels decline in the primitive streak region and cannot be detected by the 10-somite stage (left embryo). Strong expression is evident in the paraxial mesoderm and two stripes are present in the hindbrain corresponding to rhombomeres 1 and 2, and 4 of the hindbrain neurectoderm. **(E)** Lateral view of 14 - 17-somite embryos. Three stripes of expression are apparent in the hindbrain neurectoderm corresponding to rhombomeres 1 and 2, 4, and 6. Transcripts are evident in all mature somites and in the cranial paraxial mesoderm extending rostrally to the midbrain/forebrain junction (embryo on left). Expression is detectable in presomitic mesoderm but is absent in the most recently formed somite and in the most rostral aspect of the presomitic mesoderm. There is a narrow trail of ventrolateral cells expressing *follistatin* in this region (arrowhead). **(F)** Expression in the paraxial mesoderm of an 18-somite stage embryo. Transcript levels increase in a graded manner from caudal to rostral in the presomitic mesoderm and, except for the most recently formed somite and for mesoderm in the process of segmenting (arrowhead), they remain high in the somites. **(G)** Dorsal view of the hindbrain region of an 18-somite stage embryo, showing the alternating pattern of rhombomeric expression and the presence of transcripts in the cranial paraxial mesoderm (arrowhead). Scale bar, 250 μm (A); 200 μm (B,C,F); 300 μm (D,G); 400 μm (E).

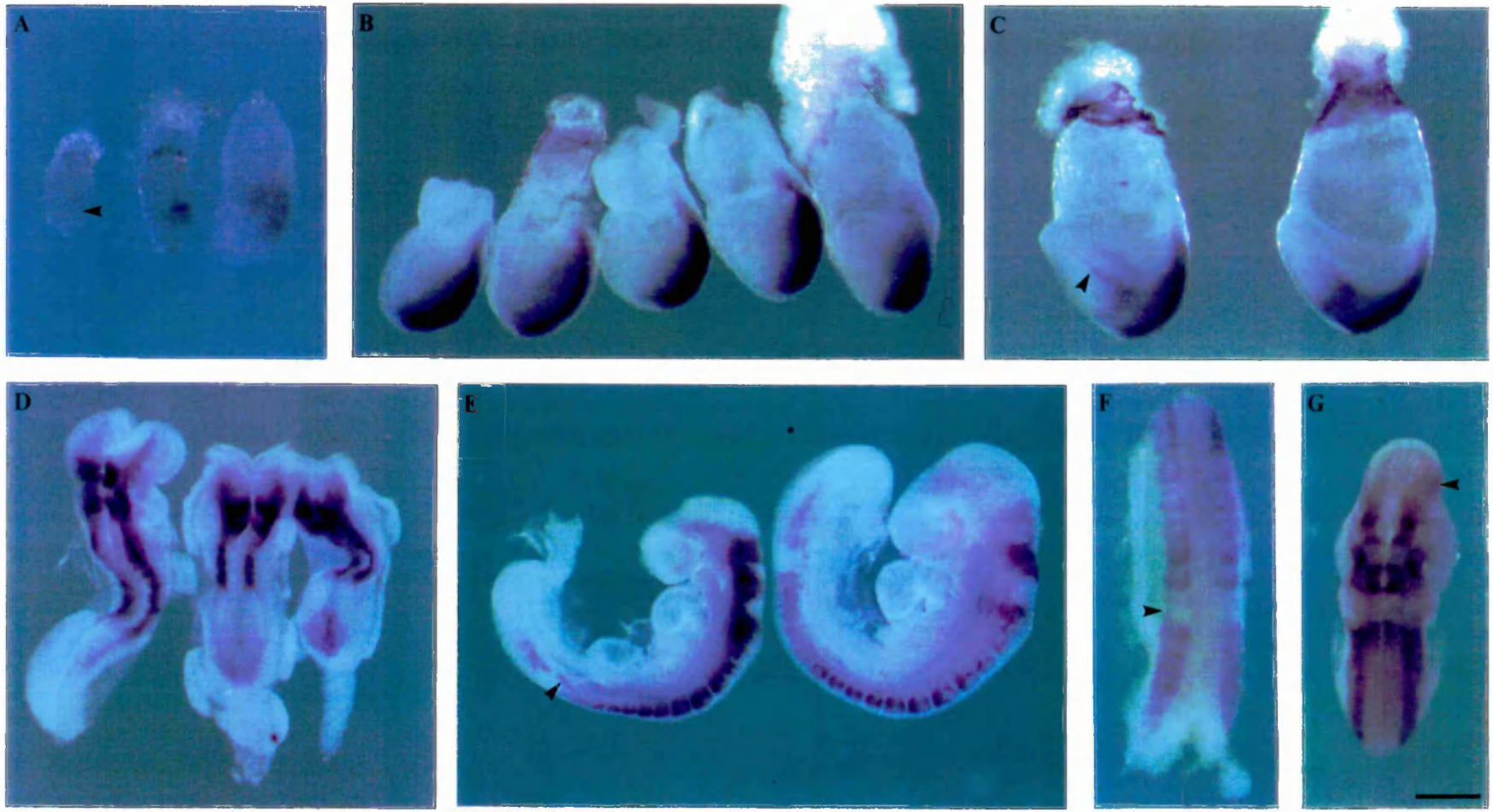
A
B
C
D
E
F
G

activin acts as an embryonic mesoderm inducer, although it is not clear whether proteins from the decidua can act on the embryo. The demonstration that maternal TGF-β1 can rescue embryos lacking TGF-β1 (Letterio et al., 1994) shows that during at least some stages of embryonic development, TGF-β1 can be passed from the mother to the embryo. *TGF-β1* mRNA is first detected in the endocardial cells of embryos with 5-7 somites (Ackhurst et al., 1990). Therefore the experiments which demonstrate maternal rescue by TGF-β1 do not constitute evidence of mother-to-embryo transfer of proteins at the onset of gastrulation. Additionally, at the stage at which activin subunit mRNA is found immediately adjacent to the embryo, the parietal endoderm which surrounds the embryo expresses *follistatin*. In *Xenopus* mesoderm induction assays follistatin inhibits the activity of activin, (Asashima et al., 1991) thus in the mouse embryo decidually provided activin may be inactivated by the follistatin localised to the parietal endoderm. However, on the basis of the expression data presented in this chapter, the possibility that maternally provided activin is important for mesoderm formation cannot be ruled out.

Direct evidence that mesoderm formation is not dependent on activin B transported from the decidua is provided by mice deficient in the inhibin β_B subunit. The mice exhibit eyelid defects and homozygous mutant females do not rear their young normally. Yet, homozygous mutant females give birth to pups, demonstrating that embryos form mesoderm in the absence of either maternal activin B or AB (Vassalli et al., 1994). The test of requirement for decidual activin A cannot be addressed in the same manner since mice deficient for the inhibin β_A chain die within 24 hours of birth, presumably as a consequence of not being able to feed (Matzuk et al., 1995a). Additionally, mice which lack both the inhibin β_A and β_B chains survive to birth, showing only the additive defects of the individual mutants, providing clear evidence that mesoderm formation occurs in the absence of any zygotic activin, and that one activin subunit does not compensate for the absence of the other (Matzuk et al., 1995a). Unless decidually provided activin A does function in the embryo then the lack of embryonic expression of activin and the analysis of the mutant mice argue that these isoforms of activin are not one of the endogenous mesoderm inducers in the mouse embryo.

The recent isolation of novel activin isoforms from the human, mouse and *Xenopus* raises the question of whether these molecules function during embryogenesis. *Xenopus* activin D is present in the early embryo and exhibits mesoderm inducing activity, although this activity is weaker than that of the activins A and B (Oda et al., 1995). A novel human activin isoform was recently isolated and named activin C (Hötten et al., 1995). The mouse homologue of this gene has been cloned but RNase protection analysis of total RNA isolated from whole embryos failed to detect expression before embryonic day 14 (Schmidt et al., 1996). The relevance of these isoforms to embryonic development remains to be tested.

Follistatin and early mouse development

The expression of follistatin could serve to localise the activity of decidually derived activin. However, *follistatin* is expressed strongly at the site of mesoderm formation and in the cells of the epiblast fated to form mesoderm. Since follistatin is known to inhibit the mesoderm inducing activity of activin (Asashima et al., 1991) this seems an unlikely localisation for *follistatin* mRNA and raises the question of whether follistatin has a function, distinct from activin binding, in the mouse embryo.

Follistatin binds to both activin and inhibin, although this interaction is achieved through their common beta subunit (Shimonaka et al., 1991). *In vitro* binding studies have shown that TGF-β1 does not compete for the binding of activin to follistatin (Nakamura et al., 1990), however it is possible that follistatin is capable of binding to other members of the TGF-β family. Additionally, while there is evidence that follistatin is an inhibitor of activin both in mesoderm induction (Asashima et al., 1991) and in stimulating release of follicle stimulating hormone from the pituitary (Robertson et al., 1987; Ying et al., 1987), it is not clear that this is always the case. Follistatin can bind heparan sulfate proteoglycans (Nakamura et al., 1991) and it has been proposed that follistatin may present activin to its receptor(s) (Matzuk et al., 1995b). The phenotype of mice which lack follistatin shares some features with that of activin A deficient mice (Matzuk et al., 1995b) suggesting that in some circumstances follistatin *is* used co-operatively with activin. The follistatin deficient mice are growth retarded and fail to develop fully functioning intercostal and diaphragm muscles, leading to post-natal lethality. The mice also exhibit various skin and bone deformations. Skeletal defects are also observed in two mouse mutants, both of which have recently been attributed to mutations in TGF-β related molecules. A deletion in *BMP-5* is responsible for the *short ear* mutant (Kingsley et al., 1992), and the recently cloned *GDF-5* is responsible for the *brachypodism* mutant (Storm et al., 1994). It remains possible that in the absence of activin, follistatin may bind other proteins and such interactions may be inhibitory or stimulatory.

The survival to birth of follistatin deficient mice suggests that if *follistatin* does play an important role during early embryogenesis, other molecules must be capable of fulfilling its function. A follistatin related protein has been isolated on the basis of its induction in response to treatment of osteoblasts with TGF-β1 (Shibanuma et al., 1993). Hence, follistatin may actually belong to a class of molecules which have diverse effects when combined with various TGF-β family members. Cloning of this TGF-β1 responsive molecule has revealed a follistatin-like motif which may now be used to search for similar molecules and it would be of interest to determine if other family members are also expressed during mouse development.

Follistatin and neural development

Somewhat surprisingly, *Xenopus follistatin* is expressed in the organiser region of the gastrula and expression continues in the prechordal mesoderm and notochord (Hemmati-Brivanlou et al., 1994). Overexpression of follistatin in *Xenopus* animal pole tissue has either a weak (Schulte-Merker et al., 1994) or a strong (Hemmati-Brivanlou et al., 1994) neural inducing effect. This could occur because of inhibition of activin, or follistatin may function independently of activin in this assay. In either case, it seems unlikely that follistatin functions to promote neural development in the mouse embryo. The cells of the ventral node, or presumptive organiser region, do not express *follistatin* transcripts and mice homozygous for a mutation in *follistatin* do not have neural defects (Matzuk et al., 1995b). Analysis of the distribution of follistatin protein in these organisms, together with further information on potential follistatin isoforms, may resolve this discrepancy.

While the embryonic function of follistatin remains unclear, its presence during gastrulation in the apparent absence of activin raises the question of whether activin-related molecules are present at this stage of development. In an attempt to identify molecules expressed during mouse gastrulation which have homology to activin, low stringency screening of embryonic cDNA libraries was carried out. Although screening of mouse embryonic libraries for TGF–β superfamily molecules had previously been carried out (Jones et al., 1991; Jones et al., 1992a), the construction of libraries from specific regions of the gastrulation stage mouse embryo provided a new, enriched substrate for screening (Harrison et al., 1995). The results of this screen, in which a cDNA homologous to murine *bone morphogenetic protein-7* (*BMP-7*) was isolated, are presented in the following chapter.

CHAPTER 4

BMP-7 AND *BMP-2* MRNA LOCALISATION

4.1 INTRODUCTION

The term "bone morphogenetic protein" (BMP) was originally used to describe an activity, noticed in several substances such as demineralized bone, or extracts isolated from osteosarcomas and certain epithelia. These substances all had the ability to direct new cartilage and bone formation when placed subcutaneously or intramuscularly in rats (Urist, 1965; Hall and van Exan, 1982; Takaoka, 1989). The subsequent purification of the proteins responsible for this activity has led to the isolation of a family of proteins, often named osteogenic proteins, or bone morphogenetic proteins (reviewed by Rosen and Thies, 1992). The cloning of the relevant genes has shown that they are expressed at sites of chondrogenesis and more recently mutations in two of these genes have been shown to be responsible for mouse mutants which exhibit skeletal defects. A deletion in *BMP-5* is responsible for the *short ear* mutant (Kingsley et al., 1992) and the recently cloned *growth and differentiation factor-5 (GDF-5)* is responsible for the *brachypodism* mutant (Storm et al., 1994).

The realisation that these genes are closely related to the *Drosophila dpp* gene suggested that BMP molecules may be involved, not only in bone formation, but also in regulation of cell fate during early vertebrate embryogenesis. This assumption is now backed up by evidence that BMP-4, which appears to be the vertebrate homologue of dpp, is utilised during early embryogenesis in both *Xenopus* and the mouse. In *Xenopus*, BMP-4 is expressed maternally and zygotically and BMP-4 can induce the formation of ventral mesoderm and act to oppose the putative dorsalizing signal to maintain the fate of ventral mesoderm (Dale et al., 1992; Jones et al., 1992b; Fainsod et al., 1994; Schmidt et al., 1995b). In the mouse embryo, BMP-4 is expressed in the posterior primitive streak during gastrulation and targeted ablation of the BMP-4 gene product suggests one role of BMP-4 may be to stimulate growth of the epiblast prior to gastrulation (Jones et al., 1991; Winnier et al., 1995).

The cloning of BMP-7 from gastrulation stage mouse cDNA libraries reported here, suggests that it too may be utilised during the processes of axis formation and tissue specification. In other studies BMP-7 was isolated by screening human genomic libraries with a consensus probe for TGF-β family members and named *osteogenic protein-1* (*OP-1*) (Ozkaynak et al., 1990) and the mouse cDNA was cloned by homology to the human sequence (Ozkaynak et al., 1991). The cDNA was also independently isolated from human osteosarcoma cell libraries and named *BMP-7* (Celeste et al., 1990). More recently *BMP-7* was isolated from mouse embryonic cDNA libraries (Lyons et al., 1995).

This chapter reports the cloning of BMP-7 and describes the mRNA localisation of BMP-7 during early mouse development. Additionally, the expression of other previously cloned family members, including *BMP-5*, *BMP-6*, *GDF-5*, *GDF-9* and *BMP-2* was investigated. Of these, *BMP-2* was the only one which showed a restricted expression pattern during gastrulation and as such its expression pattern is also reported here. Interestingly *BMP-2* and *BMP-7* share some sites of expression at these stages of development. The possibility that BMP molecules may function during mouse embryogenesis in axis determination, heart development and early development of the central nervous system is discussed, based on this expression data.

4.2 RESULTS

cDNA cloning of *BMP-7*

In an attempt to identify molecules with homology to activin, which are expressed in the gastrulating mouse embryo, plasmid libraries constructed from undifferentiated embryonic stem (ES) cells, 7.5 dpc embryonic region, embryonic ectoderm, embryonic endoderm, mesoderm and primitive streak (Harrison et al., 1995) were screened for the presence of inhibin β subunits and related clones. Probes corresponding to the mature region of inhibin β_A and β_B subunits were hybridised to a Southern filter of the cDNA inserts from each of these libraries. High stringency hybridisation failed to detect inhibin β clones in any of the libraries. Low stringency hybridisation of the β_A probe detected two bands in the primitive streak library (Figure 4.1). The 2.2 kb band was gel purified and recloned into the original library vector to construct a mini-library. Six thousand unamplified clones were screened and two positively hybridising clones selected. Each of these was plated onto bacterial plates and six single colonies from each plate rescreened by Southern analysis and low stringency hybridisation to the β_A probe. The hybridising clones were sequenced and found to be identical. Data base searches with the 3' sequence showed 100% homology to murine *BMP-7*. However, initial sequence obtained from the 5' end of the clone did not match the 5' end of mouse *BMP-7*. The size of the cDNA obtained from the primitive streak library suggested that it may be longer than the published cDNA and further sequencing from the 5' end did coincide with the already published cDNA sequence. Figure 4.2 shows the sequence obtained from one primitive streak clone (PS1) and the regions of corresponding *BMP-7* sequence. Although the primitive streak clone was not sequenced in its entirety, the position of the open reading frame was known in mouse *BMP-7* and thus the cDNA obtained from the primitive streak library was known to contain all of the open reading frame, in addition it has a further 200 bases of 5' UTR compared to the published *BMP-7* cDNA.

Figure 4.1 Low stringency screening of the primitive streak cDNA library with inhibin βA. 5 μg of library plasmid DNA was digested with Not I and Sal I to release the cDNA inserts and analysed by Southern for the presence of clones related to inhibin βA. The size of the DNA (basepairs) is indicated on the left. Two strongly hybridising bands were detected in the primitive streak 1 DNA preparation; one of these (arrow) was also detectable in an independent DNA preparation, primitive streak 2. The hybridising material of size 3 kb - 5 kb represents the plasmid backbone of the library. The plasmid lane contained 100 ng of a *NotI* and *SalI* digest of a cDNA cloned into the same vector as the libraries, and served as a control for cross hybridisation of the probe fragment to the vector backbone. The probe used for screening and the inhibin βA plasmid serve as positive controls. The filter was exposed to Kodak X-AR film, -70°C for two weeks.

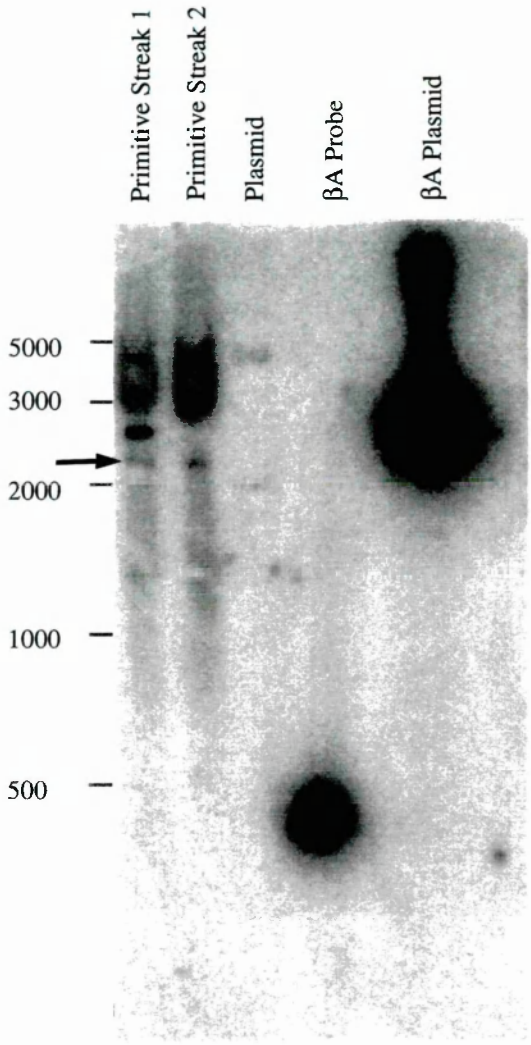
Primitive Streak 1
Primitive Streak 2
Plasmid
βA Probe
βA Plasmid
5000
3000
2000
1000
500

Figure 4.2 Sequence of the PS1 clone and homology to published *BMP-7* sequence. The sequence obtained from the 5' and 3' ends of the PS1 clone is aligned with published sequence for mouse *BMP-7* (*OP-1*). The full published sequence (accession number X56906) is not shown and the omitted sequence is represented with a dotted line. Identical bases are shown with a vertical line. The transcription start site (ATG) and stop site (TAG) are underlined.

```
PS1       CCACGCGTCCGCGACTTGTAGGTCTGCAAGCTGCTGCTCCTCCCACCCCG 50

PS1       GCNCGCCTCCTCRCTCTCTTGCTCGCTCTCTGGAGTTGCTGTGCTAGCCT 100

PS1       TGCCGTGCGTCCTGGCGAGTGCGGGCCGAGGGGCCGGGCAGAACTGAGTA 150

PS1       AAGGACAGGGGCGTCCCGGGCAAAGCGCACGCGGCCGGGGAGTGGCCATG 200

PS1       TGTGTGGCGAGGCCGCCTTGAAGCTCGCCTGCAGCAAGTGACCTCGGGTC 250
                                    ||||||||||||||||||||||
BMP-7                               CTGCAGCAAGTGACCTCGGGTC

PS1       GTGGACCGCTGCCCT
          |||||||||||||||
BMP-7     GTGGACCGCTGCCCTGCCCCCTCCGCTGCCACCTGGGGCGGCGCGGGCCC

BMP-7     GGTGCCCCGGATCGCGCGTAGAGCCGGCGCGATGCACGTGCGCTCGCTGC

BMP-7     GCGCTGCGGCGCCACACAGCTTCGTGGCGCTCTGGGCGCCTCTGTTCTTG

BMP-7     CTGCGCTCCGCCCTGGCCGATTTCAGCC.....................

BMP-7     .............................................GAA

BMP-7     GAAGTACAGAAACATGGTGGTCCGGGCCTGTGGCTGCCACTAGCTCTTCC

BMP-7     TGAGACCCTGACCTTTGCGGGGCCACACCTTTCCAAATCTTCGATGTCTC

BMP-7     ACCATCTAAGTCTCTCACTGCCCACCTTGGCGAGGAGCCAACAGACCAAC

BMP-7     CTCTCCTGAGCCTTCCCCTCACCTCCCCAACCGGAAGCATGTAAGGGTTC

BMP-7     CAGAAACCTGAGCGTGCAGGCAGCTGATGAGCGCCCTTTCCTTCTGGCAC

BMP-7     GTGACGGACAAGATCCTACCAGCTACCACAGCAAACGCCTAAGAGCAGGA

PS1                    CAGGAAAGTGTCCATTGGCCACATGGCCCCTGGCGCTCT 2025
                       |||||||||||||||||||||||||||||||||||||||
BMP-7     AAAATGTCTGCCAGGAAAGTGTCCATTGGCCACATGGCCCCTGGCGCTCT

PS1       GAGTCTTTGAGGAGTAATCGCAAGCCTCGTTCAGCTGCAGCAGAAGGAAG 2075
          ||||||||||||||||||||||||||||||||||||||||||||||||||
BMP-7     GAGTCTTTGAGGAGTAATCGCAAGCCTCGTTCAGCTGCAGCAGAAGGAAG

PS1       GGCTTAGCCAGGGTGGGCGCTGGCGTCTGTGTTGAAGGGAAACCAAGCAG 2125
          ||||||||||||||||||||||||||||||||||||||||||||||||||
BMP-7     GGCTTAGCCAGGGTGGGCGCTGGCGTCTGTGTTGAAGGGAAACCAAGCAG

PS1       AAGCCACTGTAATGATATGTCACAATAAAACCCATGAATGAAA 2175
          |||||||||||||||||||||||||||||||||||||||||||
BMP-7     AAGCCACTGTAATGATATGTCACAATAAAACCCATGAATGAAA
```

Northern analysis has previously been carried out with the mouse *BMP-7* cDNA (Ozkaynak et al., 1991). Using probes specific for *BMP-7*, four transcripts were detected in mRNA isolated from 17 dpc mouse embryos. The transcripts were 1.9 kb, 2.2 kb, 2.4 kb and 4 kb in length. The published cDNA is 1.9 kb and it is likely that the 2.2 kb transcript is the one recovered from the primitive streak library. The only difference between these two transcripts is in their 5' UTR and it is likely that the other clones may also have additional UTR sequences. The significance of the differently sized transcripts is unknown and probes which include the 3' portion of the 2.2 kb transcript will detect all four transcripts.

Embryonic expression of *BMP-7*

Murine *BMP-7* is expressed in adult tissues including kidneys, bladder, adrenal tissue and brain but is not detected in heart and liver (Ozkaynak et al., 1991). Hybridisation of a probe specific for *BMP-7* to cDNA from the embryonic libraries showed that *BMP-7* clones were present in the ectoderm, mesoderm, endoderm and primitive streak libraries (data not shown), suggesting it was widely expressed during gastrulation. Whole mount *in situ* hybridisation and subsequent dissection or sectioning of the embryos was undertaken to determine the spatial pattern of *BMP-7* mRNA localisation. *BMP-7* expression can be divided into two phases; during germ layer formation *BMP-7* mRNA is found almost exclusively in the mesoderm components of the embryo, however once the processes of organogenesis begin in the anterior of the embryo, *BMP-7* transcripts are detected in derivatives of all three germ layers. The expression of *BMP-7* in the neurectoderm changes considerably during development and is described in more detail in a separate section.

BMP-7 mRNA localisation during germ layer formation

As shown in Figure 4.3, shortly after the onset of gastrulation, at the early streak stage, *BMP-7* is detected at the anterior of the primitive streak. Staining is also seen in the extraembryonic ectoderm, however further analysis of pre-gastrulation stage embryos is necessary to determine whether this represents true hybridisation signal. By the late streak stage it is apparent that *BMP-7* is localised to the anterior third of the primitive streak, the node and to the axial mesendoderm emanating from the node. Transverse sections of the distal third of these embryos show hybridisation in the delaminating mesoderm of the primitive streak, the lateral mesoderm and in axial mesendoderm. As the allantoic bud forms, mRNA accumulates within the allantois and cells in the lateral wings of mesoderm in the distal two-thirds of the embryonic region show hybridisation signal (Figure 4.3C), however in transverse sections it is apparent that there are no transcripts in the primitive streak. Longitudinal sections of this stage embryo (Figure 4.3E) confirmed that there are no transcripts in the epiblast, except in the region overlying the node. By the early headfold stage it is apparent that the non-axial mesoderm which contains *BMP-7* transcripts corresponds to the prospective heart and cranial paraxial mesoderm (Figure 4.3D). Strikingly, the primitive streak does not contain *BMP-7* transcripts by this stage.

Figure 4.3 ***BMP-7*** **mRNA localisation during germ layer formation.** In all photographs the anterior of the embryo is to the left. **(A)** Lateral view of an early streak stage embryo, *BMP-7* transcripts are seen at the anterior of the primitive streak in the node, transcripts are also detected in the extraembryonic ectoderm (arrowhead). **(B)** Lateral view of a late streak embryo. Expression continues in the anterior of the primitive streak and is now seen in the anterior axial mesendoderm and in the extraembryonic mesoderm. **(C)** Lateral view of an early allantoic bud embryo. *BMP-7* expression in the primitive streak has declined but transcripts are detected in the lateral mesoderm of the distal two thirds of the embryonic region. The highest transcript levels are seen in the node and axial mesendoderm. Expression is now clearly seen in the allantois. **(D)** Lateral view of an early headfold embryo. *BMP-7* transcripts are absent from the primitive streak, but the expression in node and axial mesendoderm persists. Transcripts are seen in the anterior paraxial and lateral mesoderm and in the allantois. **(E)** Longitudinal section through an early allantoic bud stage embryo, such as the one shown in (C). *BMP-7* mRNA is seen in the mesoderm surrounding the embryonic ectoderm, although it is excluded from the mesoderm closest to the extraembryonic region. The only epiblast expression is at the distal tip, in the region of the node. **(F)** Transverse section through the distal embryonic region of a late streak embryo as shown in (B). *BMP-7* mRNA accumulates in the primitive streak in the lateral mesoderm and in the axial mesendoderm. **(G)** Transverse section through the distal embryonic region of an early allantoic bud embryo as shown in (C). Transcripts are absent from the primitive streak but are seen in both the mesoderm and axial mesendoderm. **(H)** Longitudinal section through an early headfold embryo, at a similar stage to that shown in (D). Signal is seen in the ventral node and the axial mesendoderm. al: allantois, e: epiblast, em: extraembryonic mesoderm, m: mesoderm, p: primitive streak, vn: ventral node. Scale bar 200 μm (A,B,C,D); 100 μm (E); 50 μm (F,G,H).

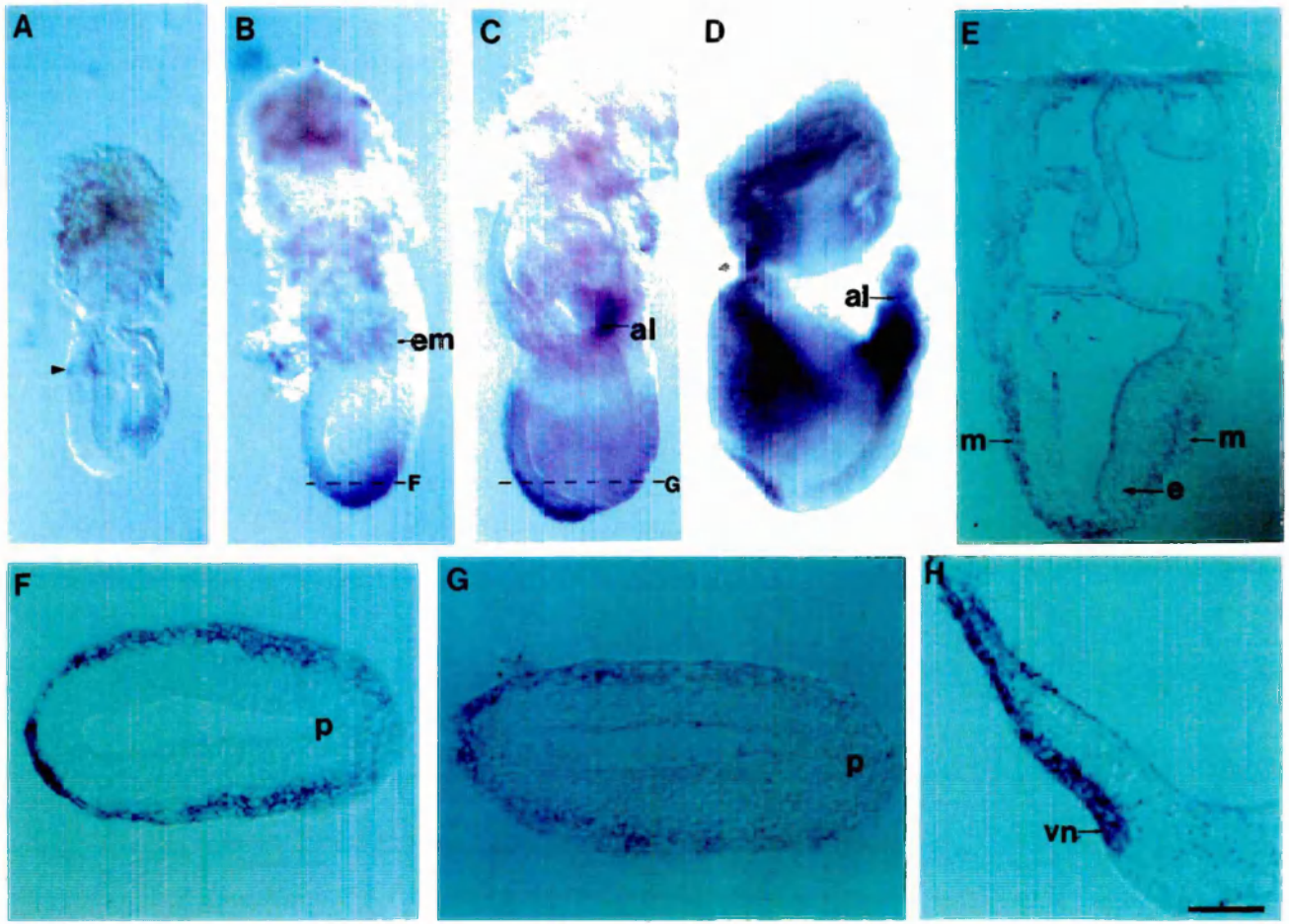
A
B
em
F
C
al
G
D
al
E
m
m
e
F
p
G
p
H
vn

Longitudinal sections of a headfold embryo revealed that the expression in the node is restricted to the ventral cells; this section also showed transcripts in the axial mesendoderm (Figure 4.3H).

BMP-7 mRNA localisation during early organogenesis

At the late headfold stage, as organogenesis begins, *BMP-7* transcripts are detected in all germ layers. As shown in Figure 4.4A and B, in embryos with a foregut pocket but no somites, expression is seen in derivatives of the previously expressing tissues. In all embryos examined, the myocardium of the developing heart continues to be a site of strong expression of *BMP-7*. However, as organogenesis proceeds the pattern of mRNA localisation in other regions of the mesoderm changes. The expression in the cranial paraxial mesoderm declines; in 6-somite embryos *BMP-7* transcripts are detected only in the paraxial mesoderm adjacent to the forebrain and midbrain. This expression becomes further restricted to more rostral regions as somitogenesis continues. In 8-somite embryos only the mesoderm around the optic cup expresses *BMP-7*. This expression then becomes very strong as can be seen in Figure 4.4G and I, but has declined in the 30-somite embryo where it is localised to the nasal placode region (Figure 4.4J). Transcripts are never detected in the trunk paraxial mesoderm. The axial mesoderm continues to express *BMP-7*, although it is not expressed uniformly along the whole axis. Expression in this mesoderm is described more fully in the section on neural expression. In the allantois, transcripts gradually become restricted to the junction with the embryonic tissue, such that in embryos with 13 or more somites no mRNA is detected in the allantois (Figure 4.4I). As expression in these regions is declining, transcription is initiated in other regions of the mesoderm. *BMP-7* transcripts accumulate in the lateral mesoderm anterior to the node (Figure 4.4D), in the developing mesonephros (Figure 4.4J) and limb bud.

At the headfold presomite stage of development *BMP-7* transcription is initiated in gut endoderm, and upon foregut formation, all of the gut endoderm in the region of the closed gut contains *BMP-7* mRNA (Figure 4.4B). In the early somite embryo *BMP-7* transcripts are detected in the definitive endoderm along the length of the axis. In 6-somite embryos mRNA is localised both to the endoderm of the foregut and hindgut pockets and in the prospective midgut (Figure 4.4F). Expression in gut endoderm persists in the 30-somite embryo.

While at all stages of development the undifferentiated ectoderm over the primitive streak remains devoid of transcripts, at the headfold presomite stage expression is detected in both types of differentiated ectoderm. *BMP-7* mRNA is localised to the ventral neurectoderm (Figure 4.4B and C) in a region which does not extend the full anterior-posterior length of the neural groove. The extent of this expression is described more fully in the section on neural development. At this late headfold stage the first transcripts in the surface ectoderm

Figure 4.4 *BMP-7* mRNA localisation during early organogenesis. (A) Lateral view of 2 headfold presomite embryos and a 2-somite embryo (right). In this view expression can be seen in the cranial paraxial mesoderm and heart mesoderm, the node and notochord and the allantois. **(B)** A section through the headfold presomite embryo as labelled in (A); only the anterior portion of the section is shown. In addition to the paraxial and lateral mesoderm and cardiogenic plate expression, *BMP-7* transcripts are detected in the surface ectoderm and in the midline neurectoderm. **(C)** A section caudal to the foregut pocket through the headfold, presomite embryo as labelled in (A). *BMP-7* mRNA localisation is similar to the more rostral section shown in (B), however, the endoderm expression is confined to the axial mesendoderm. **(D)** Dorsal view of a 6-somite embryo. There are now *BMP-7* transcripts in all of the surface ectoderm. The node and lateral mesoderm anterior to the node show *BMP-7* expression, as does the yolk sac mesoderm. Expression has begun to recede from the distal part of the allantois, although the ectoderm at the base of the allantois shows elevated levels of signal (arrowhead). **(E)** Ventral view of the 6-somite embryo shown in (B). From this view it can be seen that the dense staining in the cranial region is due to a combination of signal from the heart mesoderm, foregut pocket, paraxial mesoderm and surface ectoderm. While the majority of the neurectoderm does not express BMP-7, the floor plate staining in the cranial region can be seen in this view. **(F)** Transverse section through the posterior region of a 6-somite embryo. The approximate level of the section is shown in (D). *BMP-7* transcripts are detected in all of the surface ectoderm, including the junction with the neurectoderm, and in the endoderm. **(G)** Lateral view of an 11-somite embryo. *BMP-7* continues to be expressed in the mesoderm: the heart, the lateral mesoderm, the node and emergent notochord and the yolk sac mesoderm all contain transcripts. *BMP-7* expression is seen in all of the surface ectoderm and is elevated in particular regions of the surface ectoderm. The ectoderm which covers the frontal placodes, the otic vesicles, the branchial arch and the base of the allantois all show stronger levels of signal. **(H)** Transverse section through the hindbrain and the heart of a 10-somite embryo. *BMP-7* is expressed in all of the heart mesoderm, gut endoderm and surface ectoderm. **(I)** Lateral view of a 13-somite embryo. The beginning of the roof plate expression is seen in the anterior of the embryo and the gut expression is clearly seen at the posterior of the embryo. The elevated expression in the ectoderm covering the forelimb bud is just visible (arrowhead). Expression is no longer seen in the allantois. **(J)** Lateral view of a 30-somite embryo. Transcripts are seen in the optic lens placode and expression continues in the otic vesicle. The expression in the roof plate now extends to the posterior of the neural tube. The forelimb bud expression is now more obvious and mRNA accumulates in the newly formed mesonephros (arrowhead). **(K)** Dorsal view of the embryo shown in (J), showing expression in the roof plate, the otic vesicle and the forelimb bud. am: axial mesendoderm, f: floor plate, fg: foregut, hg: hindgut, m: mesonephros, n: node, r: roof plate, se: surface ectoderm, y: yolk sac. Scale bar 400 μm (A,J,K); 350 μm (D,E,G,I); 50 μm (B,C,F,H).

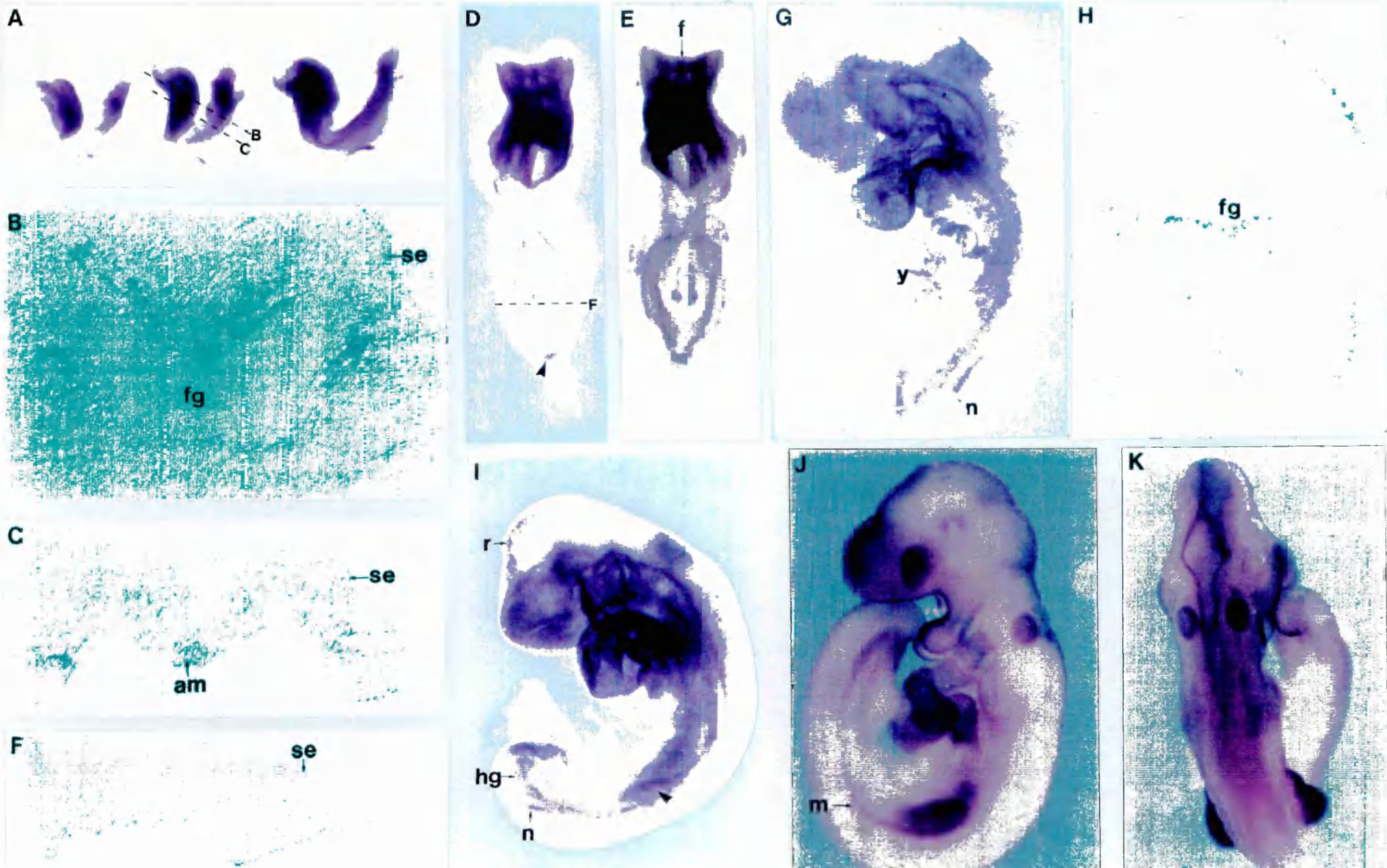
A
B
C
D
E
f
G
y
n
H
fg
B
se
fg
C
se
am
F
se
I
r
hg
n
J
m
K

are also detected. Both the surface ectoderm in the anterior regions (Figure 4.4B and C) and the posterior regions (not shown) of the embryo show accumulation of *BMP-7* transcripts. The expression in the surface ectoderm continues and as many epithelial structures begin to differentiate, elevated levels of *BMP-7* transcripts are found at the site of differentiation. Often transcripts are detected in these structures at the earliest stages of their formation. An example is the formation of the otic placodes. These first become evident as circular regions of columnar epithelium located on either side of the hindbrain in embryos with 9-11 pairs of somites. Figure 4.4G shows an 11-somite embryo in which an elevated level of *BMP-7* signal is seen at the site of formation of the otic placode. As development proceeds the placode deepens to form the otic pit (embryos with 13-20 pairs of somites) and finally closes and becomes separated from the surface ectoderm (embryos with 25-30 pairs of somites) to form the otic vesicle. *BMP-7* transcripts are detected in both the otic pit and otic vesicle. Similarly, from the time that the branchial arches first become apparent (embryos with 6-7 pairs of somites), the surface ectoderm over the arches shows strong expression of *BMP-7*, and transcripts are still prominent in this region in the latest embryos examined (30-somite). The surface ectoderm over the forebrain contains high levels of *BMP-7* transcripts and when the lens placodes form (embryos with 20-25 pairs of somites), they too contain transcripts (Figure 4.4J). The surface ectoderm at the site of the future forelimb bud (somites 8-12) also shows elevated levels of *BMP-7* transcripts in embryos with 13 or more somites. The first evidence of the raised ridge of tissue that will form the forelimb bud is not seen until embryos have 15-18 pairs of somites. The surface ectoderm expression at the base of the allantois shows elevated expression from the 6-somite stage embryo onwards. All of the sites of elevated surface ectoderm expression are tissues thought to be instructive with respect to the adjacent mesoderm (O'Rahilly and Müller, 1985).

BMP-7 mRNA localisation during neural development

This section describes the expression of BMP-7 in the neurectoderm and in the axial mesendoderm. As described above, from the early stages of gastrulation, *BMP-7* transcripts are detected in the node and in the cells which emanate from it to form the notochord. As developmental stage increases, *BMP-7* expression disappears from most of the notochord but transcription continues at its anterior and posterior. Immediately anterior of the rod-like notochord is a cone shaped region of cells, the prechordal mesoderm. *BMP-7* mRNA accumulates in this tissue from headfold, pre-somite stages and is still detected in the oldest embryos examined (18-somite). Immediately posterior to this the signal declines during early somite stages: in transverse sections of a 6-somite embryo, *BMP-7* signal is detected in sections up to 105 μm behind the rostral extent of the prechordal mesoderm and in transverse sections of a 12-somite embryo, *BMP-7* signal is detected in sections up to 140 μm behind the rostral extent of the prechordal mesoderm. In both of these cases this expression includes some notochord tissue. However, in axial mesendoderm dissected from a 18-somite embryo, *BMP-7* transcripts are not detected posterior of the prechordal mesoderm.

The node at the posterior of the notochord contains mRNA for *BMP-7* at all stages examined. Additionally, the notochord immediately anterior to the node continues to express *BMP-7*, in an 18-somite embryo expression rostral of the node continues for 450 μm.

BMP-7 transcripts are detected in the ventral midline of the cranial neurectoderm, however, appreciable levels of signal are not detected in the ventral trunk neurectoderm. The hybridisation signal is first detected in the ventral midline of the neural groove (prospective floor plate region) of embryos in which the headfolds are forming, but before the onset of somitogenesis. Even at this stage, transcripts are not seen along the full length of the ventral neural groove. As development proceeds appreciable levels of hybridisation signal become restricted to the ventral midline of the midbrain. As seen in Figure 4.4B, in 6-somite embryos, transcripts are detected in the midline of the neural plate in two regions: a region of higher signal extends from the anterior limit of the midbrain to the preotic sulcus which corresponds to the future posterior limit of rhombomere 2 (Trainor and Tam, 1995); a lower level of signal extends from the preotic sulcus to the otic sulcus which corresponds to the future posterior limit of rhombomere 4 (Trainor and Tam, 1995). In embryos with 10 somites (Figure 4.4C) mRNA is essentially only detected in the ventral midline of the midbrain but, in a 16-somite embryo it is apparent that the transcripts are also located ventrally in the rostral diencephalon. This expression is transient; by the 18-somite stage the diencephalic expression disappears (Figure 4.4D and F). The forebrain is the only region in which transcripts are seen in lateral neurectoderm. In the 10- to 12-somite embryo transcripts are localised to the neurectoderm which lines the optic pit. The remains of this expression can be seen in Figure 4.5H.

BMP-7 transcripts are also detected at the dorsal aspect of the neurectoderm. Initially mRNA is localised to the surface ectoderm which abuts the dorsal neural folds. As described above this expression is first detected in embryos with headfolds prior to the onset of somitogenesis. *BMP-7* transcripts continue to be detected at this junction up until neural tube closure, at which point the expression continues in all of the surface ectoderm including that which covers the dorsal aspect of the neural tube. Additionally *BMP-7* transcripts begin to accumulate in the dorsal-most neural tissue: sections of the anterior region of a 14-somite embryo revealed hybridisation to the prospective roof plate of the neural tube; this expression progresses caudally such that in embryos with 30 somites, *BMP-7* mRNA is localised to this region along the full antero-posterior length of the neural tube (Figure 4.5D,F and H).

Sectioning of embryos after whole mount *in situ* hybridisation showed that *BMP-7* mRNA is also localised to some neural crest tissue. Transcripts are not detected in the crest cells as they emerge from the dorsal neural tube, rather in some cells which are already undergoing migration. Examples of neural crest populations in which transcripts are detected are the

Figure 4.5 *BMP-7* mRNA localisation during early neural development. (A) Lateral view of two headfold, pre-somite stage embryos. The extent of the ventral neurectoderm expression is estimated for the lefthand embryo. **(B)** Cranial neurectoderm from a 6-somite embryo. The dorsal staining is a result of some surface ectoderm remaining attached. **(C)** Cranial neurectoderm from a 10-somite embryo. Some mesoderm remains in the forebrain region and some surface ectoderm remains in the hindbrain region. **(D)** Cranial neurectoderm from a 16-somite embryo, with mesoderm remaining around the telencephalon. *BMP-7* is detected in the dorsal midline of the neural tube (roof plate) and the ventral midline of the mesencephalon and the rostral diencephalon. Transcripts are also seen in the prechordal mesoderm. **(E)** Anterior region of the notochord removed from a 15 somite embryo showing that transcripts are not seen caudal to the prechordal mesoderm. **(F)** The neurectoderm and axial mesoderm from an 18-somite embryo. Some mesoderm remains at the anterior and posterior of the neurectoderm. Transcripts are seen in the roof plate of the cranial region and the ventral region the mesencephalon. The prechordal mesoderm is obscured by some remaining endoderm. **(G)** An enlargement of the boxed area in (F). The node and the axial mesoderm immediately rostral to it express *BMP-7*. **(H)** Transverse section through the forebrain and the hindbrain of a 25-somite embryo. Transcripts are seen in the surface ectoderm, the roof plate and the optic cup (arrowhead). fb: forebrain, hb: hindbrain, n: node, pc: prechordal mesoderm, os: otic sulcus, pos: preotic sulcus, r: roof plate. Scale bar, 450 μm (B,C); 400 μm (A,F); 200 μm (D,E); 100 μm (G,H).

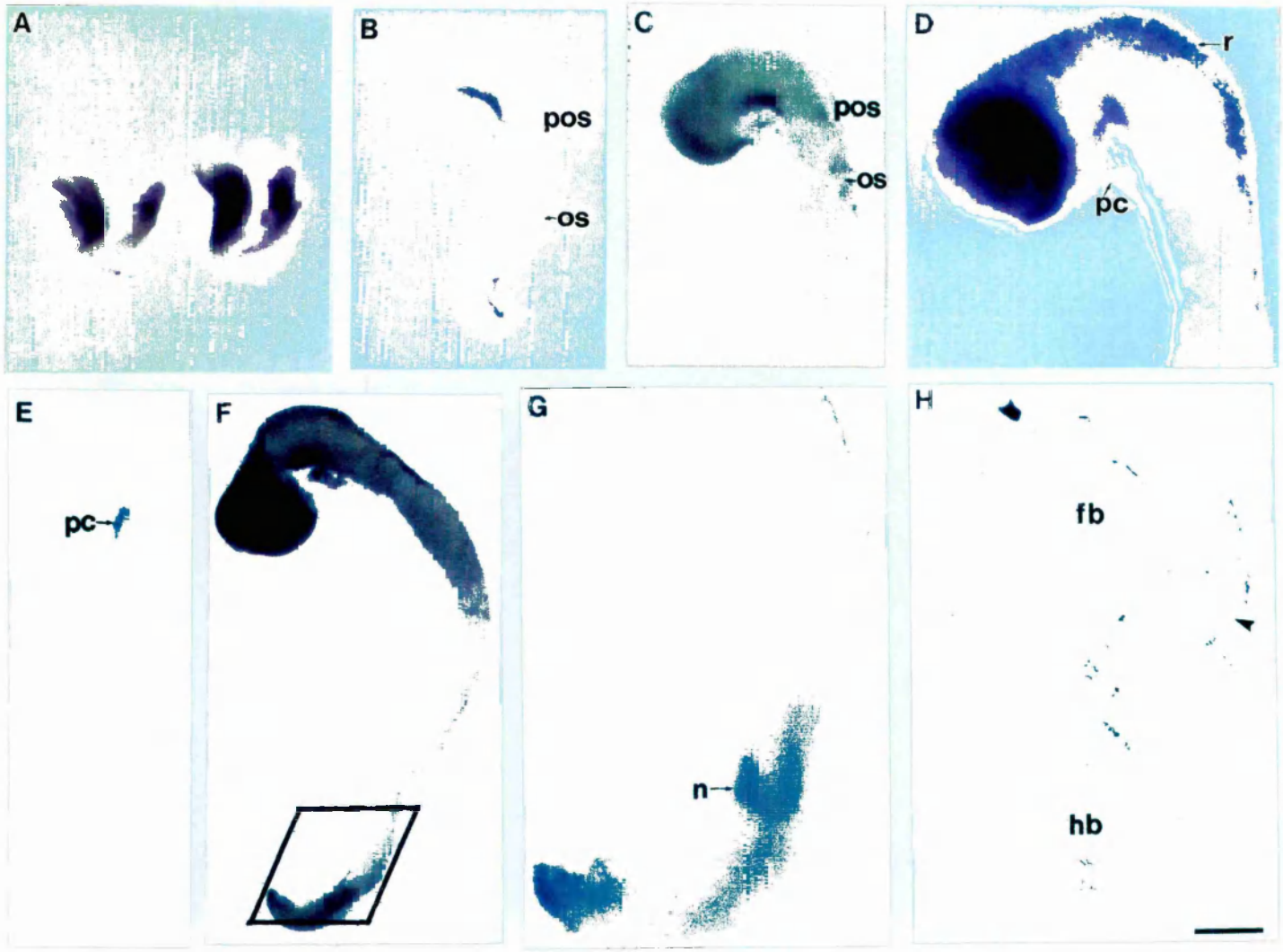
A
B
pos
os
C
pos
os
D
r
pc
E
pc
F
G
n
H
fb
hb

facial crest of 10-12 somite embryos and in the 25-30 somite embryo it is seen in perioptic crest and facio-acoustic crest (data not shown).

Co-expression of *BMP-7* and *BMP-2* during gastrulation

Whole mount *in situ* hybridisation to *BMP-2* was undertaken to determine whether it was also expressed during gastrulation. This analysis revealed that *BMP-2* is expressed during gastrulation and that there are regions of overlapping expression of *BMP-2* and *BMP-7*.

BMP-2 mRNA localisation during germ layer formation

As shown in Figure 4.6, in the early primitive streak stage embryo *BMP-2* transcripts are detected in the anterior cells of the primitive streak (the node) and in the endoderm overlying the most anterior aspect of the embryo. By the full streak stage expression is more widespread: transcripts are seen not only in the node and anterior endoderm, but also in the notochord. Thus a line of signal is seen between the two earlier sites of expression. A transverse section of a mid streak stage embryo revealed that *BMP-2* transcripts are also in the most anterior mesoderm of the embryonic region, underlying the endoderm expression (Figure 4.6G). At early allantoic bud stages of development endoderm expression is seen in a ring around the extraembryonic and embryonic junction (Figure 4.6D). Additionally, the newly formed amnion and distal extraembryonic mesoderm express *BMP-2*. In embryos between the onset of gastrulation and full streak stage, unilateral staining is seen in the extraembryonic endoderm underneath the ectoplacental cone. An example of this type of signal is shown in Figure 4.6F. The identity of these cells is unknown. During headfold stages the node and anterior axial expression declines and at the headfold pre-somite stage, very little evidence is seen of transcripts in the embryonic region. However at the junction of the embryonic and extraembryonic regions transcripts are still detected in the most anterior embryonic mesoderm (Figure 4.6I). The extraembryonic mesoderm components of the amnion and yolk sac express *BMP-2* as does the allantois. No expression in any embryonic ectoderm derivatives is seen up to and including the pre-somite embryo.

BMP-2 mRNA localisation during early organogenesis

By the 3-somite stage, no endoderm expression of *BMP-2* remains and the major embryonic site of expression is the surface ectoderm. The ectoderm at the junction of the neural and surface ectoderm in the cranial region of the embryo is the first ectoderm to express *BMP-2* (Figure 4.7). By the 5-somite stage both the cranial surface ectoderm and the ectoderm over the trunk neural tube are sites of *BMP-2* expression. The allantois now expresses *BMP-2* strongly and the amniotic expression continues but *BMP-2* is not detected in the yolk sac. This pattern of expression continues such that in the 8-somite embryo there is expression in all of the surface ectoderm, but it is elevated at the site of contact with the neural ectoderm. The extraembryonic tissues of allantois and amnion continue to express *BMP-2*. By the 12-somite embryo, transcripts are only detected in the surface ectoderm of the anterior embryo,

Figure 4.6 *BMP-2* mRNA localisation during germ layer formation. The anterior of the embryo is towards the left in all cases, except (I) where anterior is towards the bottom. **(A)** Lateral view of an early primitive streak stage embryo. *BMP-2* transcripts are detected in the node (arrowhead) and at the most anterior aspect of the embryonic region (arrow). **(B)** Anterior view of a mid primitive streak stage embryo. *BMP-2* transcripts in the anterior of the embryo are localised to a crescent shaped region. **(C)** Lateral view of a full length streak stage embryo. Expression persists in the node and the anterior of the embryo and expression is initiated in the axial mesendoderm. **(D)** Lateral view of a full length primitive streak stage embryo. The signal in the node is beginning to recede but the axial mesendoderm signal is now more obvious. Expression in the extraembryonic mesoderm, including the allantoic bud is evident as is signal in the amnion. **(E)** Lateral view of an early headfold stage embryo. Transcripts decline in the embryonic region; the only signal found in the embryonic region at this stage is shown in figure (I). However, expression in the extraembryonic mesoderm persists. **(F)** Sagittal section through a mid primitive streak stage embryo. Transcripts are seen in the node and anterior axial mesendoderm cells. One region of the extraembryonic endoderm underlying the ectoplacental cone also shows hybridisation signal (arrowhead). **(G)** Transverse section through a full length primitive streak stage embryo, slightly distal to the embryonic/extraembryonic junction, as marked on the embryo in (C). The anterior endoderm and some of the mesoderm cells in this region show hybridisation signal. **(H)** Transverse section through a full length primitive streak stage embryo, as shown in (D). The section shows the neural folds at the anterior and the allantois at the posterior. Transcripts are seen in the yolk sac mesoderm, the allantois and the amnion. **(I)** Transverse section through an early headfold stage embryo, as shown in (E). Transcripts are seen in the endoderm and mesoderm at the anterior of the embryo and in the yolk sac mesoderm. al: allantois, an: amnion, m: mesoderm, n: node, y: yolk sac mesoderm. Scale bar 300μm (A,B,C,D,E); 100μm (H); 50μm (G,I).

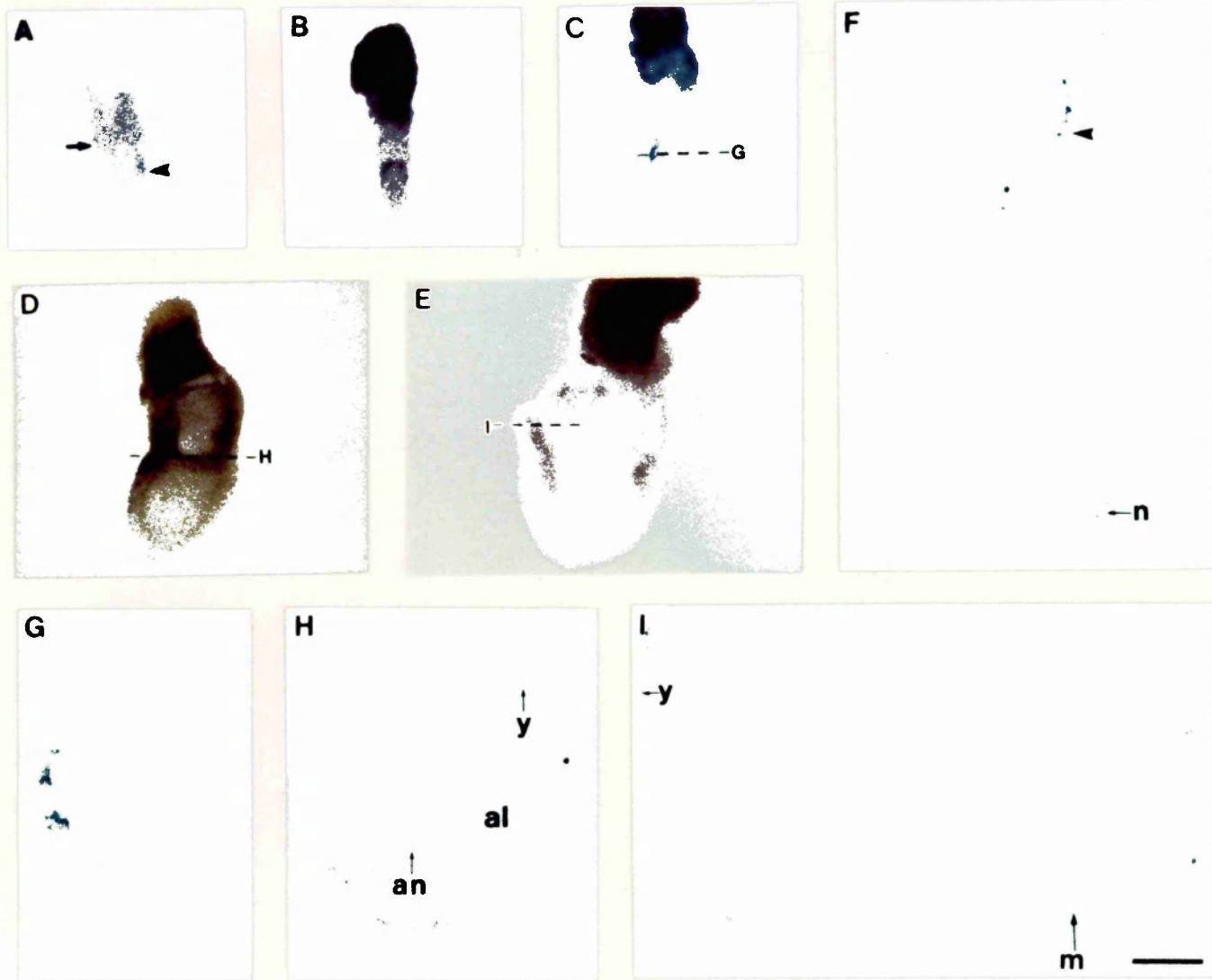
A
B
C
G
F
n
D
H
E
I
G
H
y
al
an
I
y
m

Figure 4.7 ***BMP-2*** **mRNA localisation during early organogenesis.** In all of the wholemount figures the anterior of the embryo is towards the left. **(A)** Antero-lateral view of a 3-somite embryo, the first stage at which transcripts were detected in the surface ectoderm. The transcripts initially accumulated in the surface ectoderm of the cranial region, and transcripts are seen in the yolk sac mesoderm. **(B)** Lateral view of a 5-somite embryo showing that *BMP-2* transcripts are now detected in the surface ectoderm along the whole embryo. Expression persists in the allantois. **(C)** Dorsal view of an 8-somite embryo. *BMP-2* is expressed in the surface ectoderm surrounding all of the embryo. Expression in the yolk sac is now absent but continues in the extraembryonic tissues of amnion and allantois. **(D)** An outline drawing of an 8-somite embryo showing the plane of the sections through the embryo in (C) and shown in (G) and (H). **(E)** Lateral view of a 12-somite embryo. Much of the extraembryonic tissue has been dissected away, however it can be seen that expression of *BMP-2* in the allantois has decreased but is continued in the amnion. The only embryonic site of expression is the surface ectoderm. **(F)** Coronal section through the 5-somite embryo shown in (B). *BMP-2* is expressed in the surface ectoderm and yolk sac. **(G)** Transverse section through the cranial region of the 8-somite embryo shown in (C) with the forebrain towards the top of the photo. Transcripts are restricted to the surface ectoderm. **(H)** Transverse section through the 8-somite embryo shown in (C). Expression is seen in the surface ectoderm over the dorsal aspect of the neural tube and in the amnion. al: allantois, an: amnion, se: surface ectoderm, y: yolk sac. Scale bar 300μm (A,B,C,E); 100μm (F,G,H).

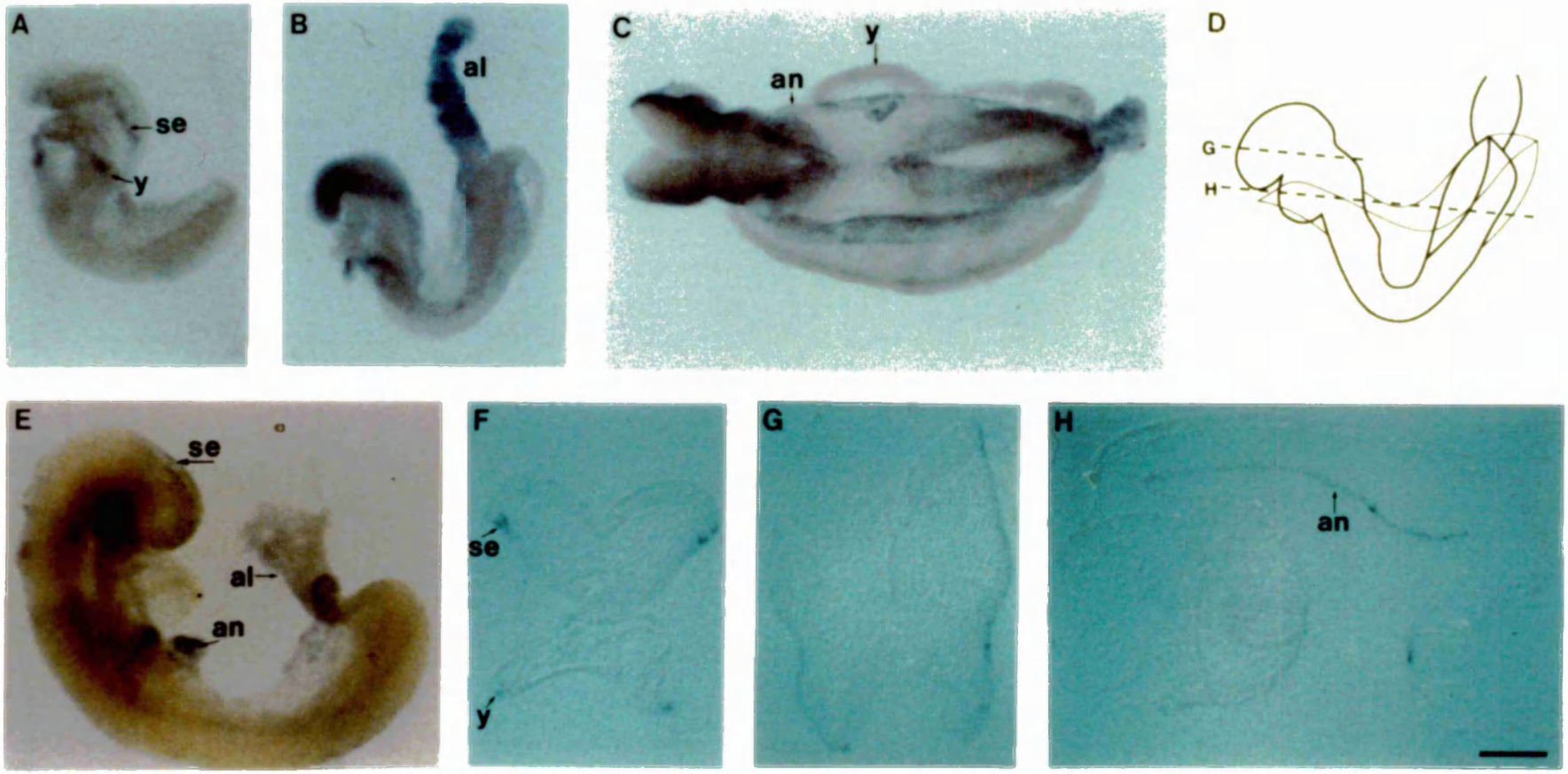
A
se
y
B
al
C
y
an
D
G
H
E
se
al
an
F
se
y
G
H
an

and the allantois. Due to problems with distinguishing between low level expression of *BMP-2* and trapping of the *in situ* substrate which often occurs in later stage mouse embryos, the analysis was not carried out on older embryos.

4.3 DISCUSSION

BMP molecules and axis specification

Because BMP molecules are likely to function as secreted signalling molecules it is possible that they regulate processes such as the growth and/or differentiation of either the cells in which they are transcribed or the surrounding cells. Although mRNA localisation is not evidence of either cell lineage or gene function, knowledge of the normal fate of expressing cells does allow the identification of processes in which the gene may be involved.

The expression data presented in this chapter suggests that BMPs may, as in other organisms, be involved in axis development. In the mouse embryo the first overt sign of axis formation is the appearance of the primitive streak. From the earliest stage of primitive streak formation at least three *BMP*s are expressed in restricted patterns in the mouse embryo: *BMP-4* (Jones et al., 1991), *BMP-2* and *BMP-7* (Figure 4.8A). *BMP-2* is localised to the endoderm of the most anterior aspect of the embryo and to the anterior of the primitive streak. *BMP-7* and *BMP-2* are co-expressed only in the anterior of the primitive streak and *BMP-4* is expressed at the most posterior of the primitive streak. By the full length streak stage these regions of expression have continued and in some cases expanded such that the situation shown in Figure 4.8B arises. Along the antero-posterior axis there are now three regions in which one *BMP* gene is expressed and a fourth region in which *BMP-2* and *BMP-7* are co-expressed. If BMP-2 and BMP-7 are capable of forming a heterodimer then overlapping expression could provide a fourth, perhaps distinct, signal. Figure 4.8 also shows that none of the *BMP*s so far examined are restricted to the mid-portion of the primitive streak.

At the anterior of the embryo, it is possible that BMP-2 expression in the endoderm exerts an effect on the overlying ectoderm. During the early stages of gastrulation, the ectoderm in this region will participate in the formation of the amnion and *BMP-2* appears to be expressed in the amnion when it first forms, but not at later stages of development. Alternatively, BMP-2 could exert an effect on the newly formed mesoderm. It may be involved in directing the movement of the mesoderm which quickly encircles the proximal embryo, or it could pattern the mesoderm once it arrives at this location. As the mesoderm in this region will contribute to the heart, this predicts a role for BMP-2 in the earliest stages of heart development. A targeted mutation has now been generated in the *BMP-2* locus. Homozygous null embryos die soon after the onset of gastrulation and consequently the

Figure 4.8 Diagram of BMP expression during germ layer formation. (A) Early primitive streak stage embryo showing three distinct antero-posterior regions of expression of BMP molecules. **(B)** Full length primitive streak stage embryo showing a fourth region of BMP molecule expression. In each diagram, anterior is to the left.

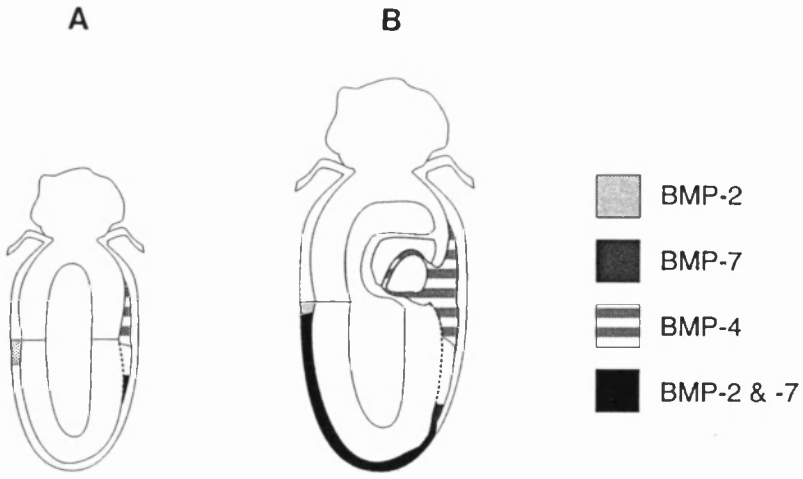
A
B
BMP-2
BMP-7
BMP-4
BMP-2 & -7

phenotype is difficult to analyse, although it has been suggested that death is caused by lack of amnion formation (cited in Hogan, 1995). Unfortunately, this makes the role of BMP-2 in heart development and the potential function of the later surface ectoderm expression impossible to assess in these mutants.

More caudally, in the region of the node and primitive streak, BMP molecules may affect the cells which involute through the regions expressing the particular BMP. Different outcomes of such an interaction can be imagined. For example, cells passing through the primitive streak at different rostro-caudal levels will be exposed to different BMP molecules, and this may be sufficient to elicit distinct differentiation programmes in these cells. In this case the BMP molecules are implicated in the primary embryonic patterning which occurs during germ layer formation. Alternatively, the cells which pass through a particular region of the primitive streak may inherit the ability to express the *BMP* gene and therefore gain the capacity to carry out secondary patterning processes. This second possibility is interesting in view of the expression patterns of *BMP-4* and *BMP-7*. *BMP-7* continues to be expressed in the axial mesendoderm and the cranial mesoderm; derivatives of the node and anterior primitive streak. Hence, is *BMP-7* expression in the node and anterior primitive streak important for the differentiation of the axial mesendoderm and cranial mesoderm, or does it simply serve as a convenient place for eliciting *BMP-7* expression in these cells which will subsequently signal to the overlying ectoderm? Similarly, since *BMP-4* is expressed in the extraembryonic mesoderm, which is an early derivative of the posterior streak, an equivalent question may be posed with respect to the function of BMP-4.

The majority of mice homozygous for a mutation in the *BMP-4* gene die during early gastrulation stages. It has been suggested that the primary defect in these embryos may be a lack of cell proliferation prior to gastrulation. However, some *BMP-4* mutant embryos survive beyond the onset of gastrulation. These embryos show apparently normal production of anterior primitive streak derivatives, but are deficient in tissues derived from the posterior primitive streak (Winnier et al., 1995). It is not clear whether this deficit is due to a requirement for BMP-4 during proliferation of the newly formed posterior mesoderm cells or during differentiation of the mesoderm. The experiment supports the notion that in mammals as in other organisms, BMPs are involved in axis specification. Null mutations have also been introduced into the *BMP-7* locus (Dudley et al., 1995; Luo et al., 1995) and the phenotype of these mice will be discussed in Chapter 7 in light of the ectopic expression data presented in that chapter.

Interestingly, BMP-7 has now been shown to bind to the previously identified activin type II receptor, ActRII and this receptor ligand combination forms a functional signalling complex with various type I receptors. Furthermore, in these assays follistatin can neutralise the activity of BMP-7, albeit at higher concentrations than required for inhibition of activin

(Yamashita et al., 1995). These data show that follistatin possesses the potential to modulate the activity of molecules other than activin. The expression of *follistatin* in the primitive streak may serve to inhibit BMP molecules until the *BMP* expressing cells have moved away from the primitive streak and are in the correct location to interact with appropriate target tissues. If follistatin is able to bind various BMPs with different kinetics, or to only some BMPs, this may introduce further variation in the cellular responses elicited by BMPs in different regions of the primitive streak.

BMP-7 and neural development

At the early headfold stage of development *BMP-7* is expressed in almost all of the mesoderm anterior to the node (see Figure 4.3D), corresponding to prospective heart mesoderm and cranial paraxial mesoderm. When anterior mesendoderm from embryos of this stage is recombined with naive ectoderm, the mesendoderm is found to be capable of inducing the expression of both a general neural marker and an anterior neural marker. If naive ectoderm is recombined with posterior mesendoderm only expression of the general neural marker is activated (Ang and Rossant, 1993). At this early stage of development, *BMP-7* is therefore expressed in the manner consistent with a molecule which may induce anterior neural structures. However, at this stage of development *BMP-7* also begins to be expressed in a manner consistent with a molecule which influences dorsal-ventral pattern of the neurectoderm. As described in the Introduction, two tissues believed to be important in defining initial dorsal-ventral neural pattern are the axial mesendoderm and the surface ectoderm, and later these tissues may confer patterning ability on the floor plate and roof plate of the neural tube, respectively. In the cranial region of the mouse embryo, *BMP-7* is expressed in all of these tissues at some stage during the period in which neural cell fate is acquired. Figure 4.9 summarises the expression of *BMP-7* in the developing hindbrain, which is the embryonic region in which the function of BMP-7 is investigated in the experiments presented in Chapter 7.

The data presented in this chapter suggests that BMP molecules may have diverse roles during germ layer formation and early organogenesis in the mouse embryo. It therefore provides a guide for further experiments which test gene function. Of the two molecules whose expression is reported in this chapter, BMP-7 appeared to be the better molecule with which to try to establish overexpression assays. Its expression pattern is restricted enough to permit ectopic expression studies, yet it is implicated in a range of processes spanning the time during which recombination assays and embryo culture are possible. In particular, it is likely that BMP-7 functions in one or more of the aspects of early development and patterning of the neurepithelium.

Figure 4.9 Diagram of *BMP-7* expression during hindbrain development. **(A)** Prior to the formation of the foregut pocket *BMP-7* is localised to the axial mesendoderm and overlying neurectoderm. The paraxial mesoderm expresses *BMP-7* as does the surface ectoderm. **(B)** During early somite stages of development, the paraxial mesoderm expression decreases and has disappeared from the hindbrain region in 6-somite embryos. The midline neurectoderm expression and the expression in the forming notochord also declines. Endoderm expression spreads to all regions of the foregut and the surface ectoderm expression persists. **(C)** By the 10-somite stage only the surface ectoderm and gut endoderm expression continues. **(D)** After neural tube closure, the separated surface ectoderm continues to express *BMP-7* and expression is initiated in the roof plate of the neural tube. The endoderm expression continues.

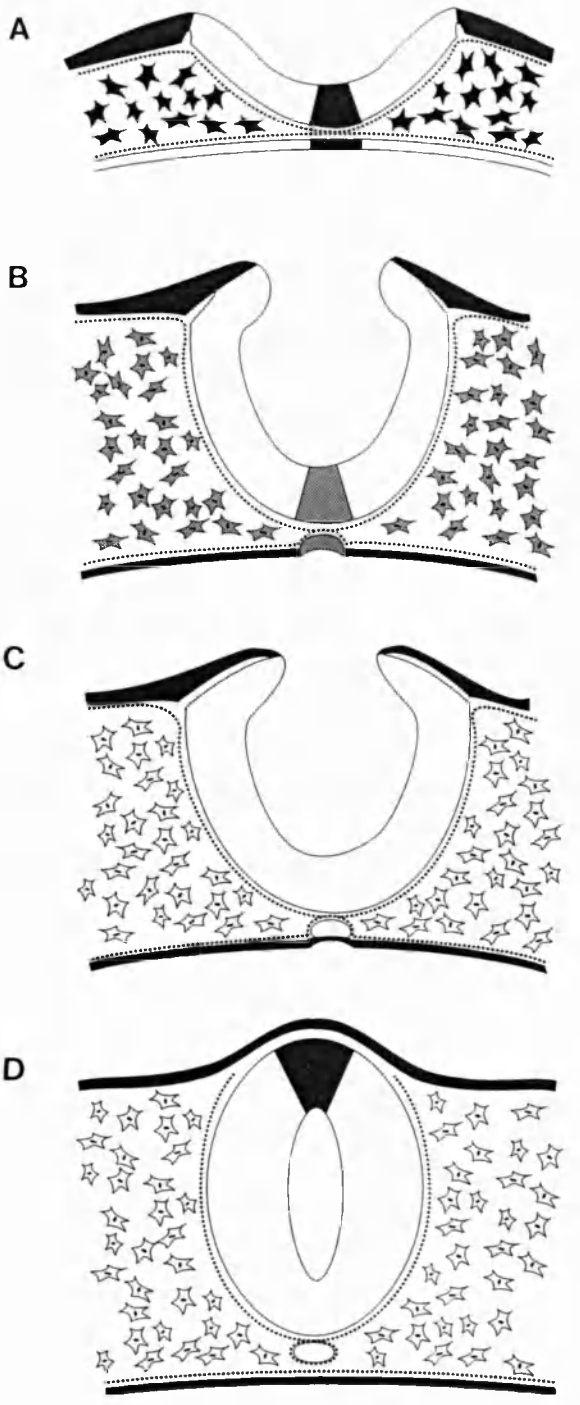
A
B
C
D

CHAPTER 5

EMBRYONIC EXPRESSION OF *VGR-2*

5.1 INTRODUCTION

The second TGF-β superfamily molecule which served as a starting point for experiments reported in this thesis is *Xenopus Vg1*. As described in the Introduction, *Vg1* was isolated in a screen for vegetally localised maternal RNAs (Rebagliati et al., 1985; Weeks and Melton, 1987; Vize and Thomsen, 1994) and is one of the proteins from which the previously described DVR subfamily of TGF-β related molecules takes its name. *Vg1* is a strong candidate for a molecule which imparts a dorsal mesoderm inducing signal resulting in formation of the organiser region during *Xenopus* development. Not only is the pattern of *Vg1* distribution consistent with this, but the mature form of Vg1 causes prospective ectoderm tissue to form dorsal mesoderm (Dale et al., 1989; Dale et al., 1993; Thomsen and Melton, 1993). Furthermore, it appears that the ability of a truncated activin receptor to block mesoderm formation may be due to interference with *Vg1* signalling (Schulte-Merker et al., 1994; Kessler and Melton, 1995).

Attempts have previously been made to identify mouse homologues of *Vg1*, and screening of a mouse 6.5 dpc embryonic cDNA library with a probe encoding the C-terminal portion of *Xenopus Vg1* resulted in the cloning of *Vgr-2* (Jones et al., 1992b). An identical molecule was subsequently identified by PCR amplification of mouse genomic DNA using degenerate oligonucleotides and named *growth and differentiation factor-3* (*GDF-3*) (McPherron and Lee, 1993). While *Vgr-2* is more closely related to *Vg1* than any other member of the TGF-β superfamily, unlike *Vg1*, *Vgr-2* lacks one of the conserved cysteines of the mature region. On the basis of sequence similarity *Vgr-2* appears to belong to a separate subfamily and is not necessarily the murine homologue of *Vg1*. Despite having been isolated from a 6.5 dpc embryonic library, RNase protection analysis and sectioned radioactive *in situ* hybridisation analysis failed to detect embryonic transcription of *Vgr-2* before 10.5 dpc (Jones et al., 1992b).

If RNA for murine *Vgr-2* is injected into *Xenopus* embryos and animal caps isolated from the injected embryos, the animal caps are induced to form mesoderm. In this autoinduction assay, the *Vgr-2* injected animal caps elongate and analysis by RNase protection of the type of mesoderm formed suggests that *Vgr-2* behaves like activin or *Vg1*, inducing dorsal mesoderm (M. Jones, personal communication). Because of the mesoderm inducing ability of this murine TGF-β superfamily member it was decided to investigate further its expression during the early stages of mouse embryogenesis. This chapter reports *Vgr-2* expression in embryonic stem (ES) cells and gastrulating embryos, making it a good candidate to test for mesoderm inducing activity in the mouse embryo.

5.2 MATERIALS AND METHODS

Whole mount *in situ* hybridisation to ES cells

ES cells were maintained as described in Chapter 2. For whole mount *in situ* hybridisation $1.5x10^4$ ES cells were plated per well of a 4-well plate (Nunc), resulting in a density of $5x10^3$ cells cm^{-2}. Undifferentiated cells were fixed as soon as they became adherent, about 6 hours after plating. Differentiated ES cells were obtained by growing for 72 hours in the absence of LIF prior to fixation. All cells were fixed in 4% paraformaldehyde (PFA) in PBS for 20 minutes and whole mount *in situ* hybridisation performed following the protocol of Rosen and Beddington (1993).

cDNA synthesis

Total RNA prepared as described in Chapter 2, to be used in Reverse Transcription-Polymerase Chain Reaction (RT-PCR) was subjected to treatment with RNase free DNase (1 U DNase μg^{-1} RNA) to remove contaminating genomic DNA and then treated with 0.1 mg ml^{-1} proteinase K. This was followed by a phenol/chloroform extraction and 2 rounds of high salt precipitation (3M NaAC) with ethanol. Under these conditions RNA will precipitate but DNA will remain soluble. For cDNA synthesis 100 ng of total RNA was added to dH_2O in the presence of 50 pmoles of oligonucleotide (dT)17 and heated at 70°C for 10 minutes and cooled on ice. Reaction components were then added to give a final composition of 50 mM Tris-HCl (pH 8.3, room temperature), 75 mM KCl, 3 mM $MgCl_2$, 10 mM DTT, 10 mM each dNTP and 200 U of RNase H free reverse transcriptase (Superscript, Gibco BRL). The reaction was incubated at 37°C for 40 minutes. The entire cDNA reaction was then placed onto a filter (Millipore, type VS, 0.025 μm) floating in a dish of 0.5x TE (1x: 10 mM Tris-HCl, pH 7.5, 1 mM EDTA) and allowed to dialyse for 6 hours to remove unincorporated nucleotides and oligonucleotide primer.

RT-PCR

In each RT-PCR reaction one tenth of the cDNA (made as described in Chapter 2) was amplified using the PCR conditions described above. The following oligonucleotide primers and annealing temperatures were used:

T	5'	AACGGGCTGGGAGCTCAGTTCTTT	68°C
	3'	GAATTCCAGGATTTCAAAGTCACA	
Oct-4	5'	TTCGAGTATGGTTCTGTAACC	62°C
	3'	AGGCTCCTGATCAACAGCAT	
Vgr-2	5'	ACTTCTGCCACGGTCAT	57°C
	3'	CGACTACCATGTCTTCA	

RT-PCR products were subcloned using the TA cloning kit (Novagen).

5.3 RESULTS

Detection of *Vgr-2* transcripts in embryonic stem cells

In order to investigate the expression of *Vgr-2* at early stages of mouse development, cDNA libraries constructed from undifferentiated ES cells and fractions of the 7.5 dpc mouse embryo (Harrison et al., 1995) were screened by Southern analysis. Figure 5.1 shows that hybridising cDNAs were detected in the ES cell library but not in any of the embryonic libraries. This result was confirmed by PCR from each of the libraries in which *Vgr-2* could only be amplified from the ES cell library (data not shown).

The full length *Vgr-2* transcript is 1181 bp in length (Jones et al., 1992a). The Southern analysis (Figure 5.1) detected strongly hybridising cDNA clones of approximately 1200 bp, indicating the presence of full length clones in the ES cell library. Weaker signal was also detected from cDNAs of size 900 bp and 2000 bp. The 900 bp clone may represent a cDNA which is not full length. The presence of signal which appears to represent a larger clone is puzzling as *Vgr-2* transcript size has been determined on the basis of Northern analysis of ES cell RNA (see Figure 6.3) and genomic sequencing (Jones et al., 1992a). Attempts to clone a longer *Vgr-2* cDNA from the ES cell library using a PCR based strategy did not yield a larger cDNA. This signal may be due to cross hybridisation of the probe to denatured plasmid backbone DNA, or to the presence of a chimeric clone in the cDNA library.

The expression of *Vgr-2* in ES cells was also analysed by whole mount *in situ* hybridisation to both undifferentiated ES cells and to ES cells which had been allowed to differentiate for 72 hours in monolayer. ES cells can be maintained in an undifferentiated state by continuous culture in leukemia inhibitory factor (LIF) containing media (Rathjen et al., 1990b). When LIF is withdrawn from ES cells they differentiate and give rise to a variety of cell types. As shown in Figure 5.2 a large proportion of the cells in a plate of undifferentiated ES cells contain *Vgr-2* transcript. When *Vgr-2* transcription was examined in ES cells grown in the absence of LIF for 72 hours, despite an increase in cell number, very few cells exhibited hybridisation signal. Thus, it appears that during differentiation of embryonic stem cells *Vgr-2* expression is downregulated. It is possible that the staining detected after 72 hours of differentiation represents undifferentiated ES cells which are present even after LIF withdrawal. This would be consistent with the observation that a few cells still express *Oct-4*, a marker of undifferentiated ES cells, 72 hours after the withdrawal of LIF.

Detection of embryonic *Vgr-2* transcripts by RT-PCR

To investigate whether *Vgr-2* is expressed during the early stages of embryonic differentiation whole mount *in situ* hybridisation of *Vgr-2* to 5.5 dpc and 6.5 dpc embryos

Figure 5.1 *Vgr-2* transcripts are present in an ES cell cDNA library. 5 μg of library total insert DNA was analysed by Southern hybridisation for the presence of *Vgr-2* clones. The six libraries analysed were constructed from either undifferentiated ES cells or fractions of the 7.5 dpc mouse embryo (embryonic region, ectoderm, mesoderm, endoderm and primitive streak: Harrison et al., 1995). The two primitive streak library samples represent individual DNA preparations from the same library. The plasmid lane contained 250 ng of a *NotI* and *SalI* digest of a cDNA cloned into the same vector as the libraries, and served as a control for cross hybridisation of the probe fragment to the vector backbone. The *Vgr-2* cDNA lane contained 250 pg of the *Vgr-2* cDNA and served as a positive control for the blotting and hybridisation procedures. The size of the DNA (basepairs) is indicated on the left. *Vgr-2* cDNAs were detected only in the ES cell library. The faintly hybridising material of size 3 kb - 5 kb represents the plasmid backbone of the library. The filter was exposed to a phosphorimage screen for 60 hours.

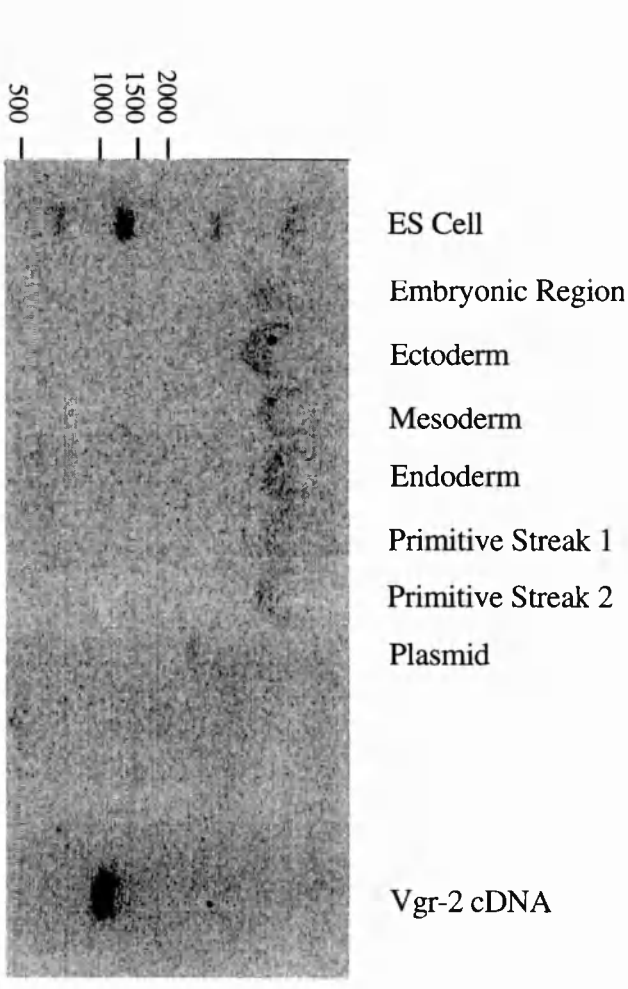
500
1000
1500
2000
ES Cell
Embryonic Region
Ectoderm
Mesoderm
Endoderm
Primitive Streak 1
Primitive Streak 2
Plasmid
Vgr-2 cDNA

Figure 5.2 Production of *Vgr-2* transcripts is downregulated upon differentiation in ES cells. Whole mount in situ hybridisation to *Vgr-2* in CGR8 ES cells. **(A)** Phase contrast view of undifferentiated ES cells. The cells are sparsely plated and grow in small colonies. **(B)** Bright field view of the same field shown in (A), showing the hybridisation signal to *Vgr-2*. **(C)** Phase contrast view of a duplicate plate of ES cells after 72 hours of growth in the absence of LIF. The density of the cells has increased, and differentiated cell types are present. **(D)** Bright field view of the same field shown in (C). Scale bar, 200 μm.

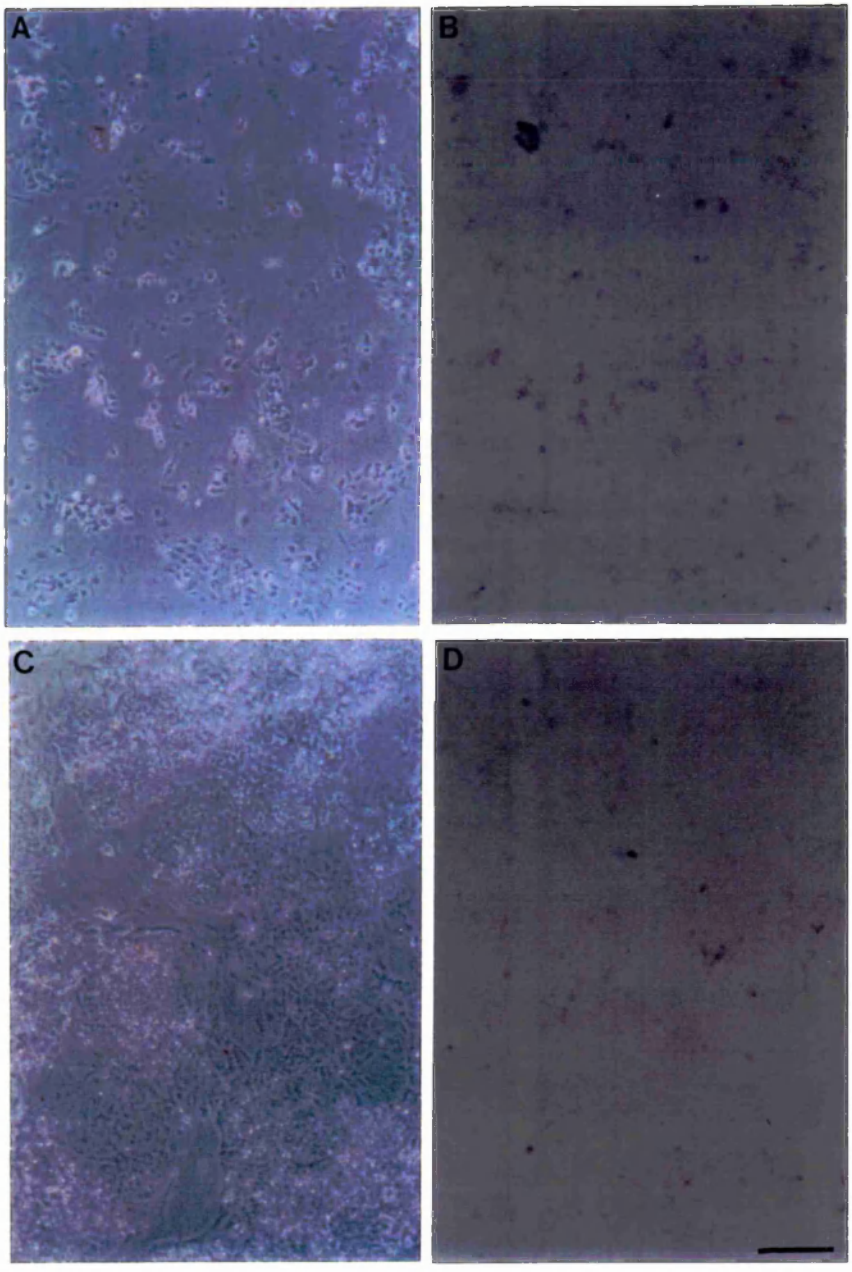
A
B
C
D

was carried out. This analysis failed to detect any localised signal (data not shown) using the same hybridisation conditions as those which detected *Vgr-2* transcripts in ES cells. To determine whether there is low level expression of *Vgr-2*, RT-PCR was utilised. Embryonic tissue was collected from 30 x 5.5 dpc and 25 x 6.5 dpc embryos and total RNA isolated. Due to the small amount of starting material it was necessary to use Northern analysis to quantitate and check the integrity of the RNA. The embryonic RNA was analysed alongside a dilution series of mouse liver RNA of known concentration. The Northern blot was hybridised to a probe which spans a region of the mouse ribosomal gene cluster and so recognises 28s rRNA, 18s rRNA and a variety of small rRNAs (Rothstein et al., 1992). This analysis demonstrated that the RNA was intact and that approximately 1250 ng of total RNA was obtained from the 5.5 dpc embryos and 2500 ng total RNA from the 6.5 dpc embryos.

First strand cDNA was synthesised from this RNA and from undifferentiated ES cell RNA. PCR using cDNA specific primers was carried out from this cDNA in order to determine whether *Vgr-2* transcripts were present in these samples. The *Oct-4* gene was used as a positive control for the RT-PCR analysis. Since *Oct-4* is expressed at high levels in undifferentiated ES cells and throughout the pregastrulation and early gastrulation epiblast, (Rosner et al., 1990) it should be possible to amplify it from all of the tissues used in this analysis. As shown in Figure 5.3, *Oct-4* transcript could be amplified from all three RNA samples as expected. The *Brachyury* (T) gene is expressed at low levels in undifferentiated ES cells (Rosen and Beddington, 1993) and expression begins in the primitive streak at the onset of gastrulation at 6.5 dpc (Wilkinson et al., 1990). Hence its absence from the 5.5 dpc RNA demonstrates that this tissue was collected from pre-gastrula stage embryos. *Vgr-2* transcripts could be amplified from all samples indicating that it is expressed within the embryo prior to and at the beginning of gastrulation. The PCR products were hybridised to probes for the respective cDNAs to verify the identity of the PCR products (Figure 5.3) and RT-PCR products from the *Vgr-2* amplification of 6.5 dpc RNA were cloned and sequenced and found to correspond to *Vgr-2* sequence (not shown).

5.4 DISCUSSION

The inability to determine the exact location of *Vgr-2* mRNA makes it difficult to speculate about the potential function of this molecule. It may be possible to obtain more information on the spatial pattern of *Vgr-2* expression by direct incorporation of a *lac Z* reporter gene into the *Vgr-2* locus. This method has proved successful in reporting the tissue specific localisation of the *nodal* gene. Nodal mRNA is difficult to detect by *in situ* hybridisation but transcripts have been detected in the posterior region of the early gastrulation egg cylinder

Figure 5.3 Temporal expression pattern of *Vgr-2* during early mouse development. RNA was reverse transcribed and cDNAs amplified by PCR. The PCR products were analysed by southern hybridisation to specific probes. **(A)** PCR amplification using *T* primers and hybridisation to the *T* probe. **(B)** PCR amplification using *Oct-4* primers and hybridisation to the *Oct-4* probe. **(C)** PCR amplification using *Vgr-2* primers and hybridisation to the *Vgr-2* probe. The size of the DNA (basepairs) is indicated on the left. 5.5 dpc: amplified products from cDNA of pooled 5.5 dpc embryos. 6.5 dpc: amplified products from cDNA of pooled 6.5 dpc embryos. ES Cell: amplified products from cDNA of undifferentiated CGR8 ES cells. No RNA: amplified products from a cDNA reaction with no RNA. No cDNA: no cDNA placed in the PCR reaction.

A
5.5dpc
6.5dpc
ES Cell
No RNA
No cDNA
1000
500
300
200
B
5.5dpc
6.5dpc
ES Cell
No RNA
No cDNA
1000
500
300
200
C
5.5dpc
6.5dpc
ES Cell
No RNA
No cDNA
1000
500
300
200

(Conlon et al., 1994). Incorporation of the *lac Z* reporter gene into the endogenous *nodal* locus revealed transcription of this gene in all of the primitive streak and the anterior endoderm (Collignon et al., 1996a). This strategy was not adopted here because another laboratory (B. Hogan, personal communication) was including a *lac Z* reporter gene in a construct designed to specifically disrupt the *Vgr-2* gene. However, to date, no further information is available on the expression pattern of *Vgr-2*.

Even in the absence of information on the exact spatial distribution of expression, three pieces of evidence support the idea that *Vgr-2* may function in mesoderm formation. *Vgr-2* is expressed in undifferentiated ES cells but is downregulated upon differentiation, consistent with a role during early development. *Vgr-2* mRNA is also detected in the mouse embryo immediately prior to, and at the onset of, mesoderm formation. Most intriguingly, murine *Vgr-2* induces mesoderm in the *Xenopus* autoinduction assay. This not only serves as incentive to test whether *Vgr-2* functions in mesoderm formation in the mouse embryo but also provides an assay for the production of active Vgr-2 protein. Because of the lack of information on the exact localisation of *Vgr-2* a system which would allow widespread overexpression of this molecule was used. The result of an experiment based on constitutive expression of secreted molecules by ES cells is presented in the following chapter.

CHAPTER 6

OVEREXPRESSION *VIA* EMBRYONIC STEM CELLS

6.1 INTRODUCTION

Mouse ES cells are pluripotent, inner cell mass derived lines which may be grown continuously in culture and re-introduced into blastocysts. There, they contribute to all tissues of the embryo, including the germ line (Robertson, 1987). As such ES cells provide a unique opportunity to genetically manipulate cells in culture and introduce the altered cells into the embryo. While the use of ES cells to generate mice which lack a specific gene product has been widely reported (Brandon et al., 1995a; Brandon et al., 1995b; Brandon et al., 1995c), only a few examples exist of ES cells being utilised for embryonic gain of function approaches. This strategy has been used to investigate the function of the ES cell differentiation inhibitor, LIF (Conquet et al., 1992) and the membrane bound protein neuropilin (Kitsukawa et al., 1995) demonstrating that such an approach is feasible. One reason for the paucity of ES cell based embryonic overexpression experiments may be that such approaches usually require the coexpression of a selectable marker. Neither methods involving co-transfection with two independent constructs or transfection with one vector containing two discrete expression cassettes have proved entirely satisfactory (Mountford and Smith, 1995).

The unusual method of translation initiation by certain viruses has been proposed as a way of circumventing these problems. These viruses produce non-capped transcripts, the translational efficiency of which is dependent upon the presence of specific sequences within the 5' UTR called internal ribosomal entry sites (IRES) (Pelletier and Sonenberg, 1988; Molla et al., 1992). Because the function of the IRES is not dependent on viral gene products but relies on interaction with normal cellular products (Macejak and Sarnow, 1991) it is likely that these elements can be adapted for use in mammalian expression systems. Incorporation of an IRES into an expression construct should allow a single transcription unit to provide efficient production of both the protein of interest and a selectable marker (Kaufman et al., 1991). Single cell analysis of coexpression mediated by an IRES in Quail QT6 cells *in vitro* showed that more than 90% of cells expressed both the selectable marker and the linked reporter (Ghattas et al., 1991). The IRES sequence has also been shown to direct translation of a reporter gene in ES cells and mouse embryos (Mountford et al., 1994).

Here a dicistronic expression vector in which an IRES element is used to mediate expression of the putative inducer and a reporter gene is utilised. ES cell populations transfected with this vector coexpressed the desired molecules. Unfortunately, overexpression of *BMP-7* appeared to be lost with continuous culture. In contrast, marked ES cell lines which expressed *Vgr-2* transcript and secreted active Vgr-2 were obtained. These cells were introduced into the embryo and alterations in mesoderm production assessed by

immunohistochemical detection of *Brachyury* (T) protein. In addition, β-galactosidase activity was used to monitor the colonisation pattern of *Vgr-2* expressing cells. Although this indicated that they preferentially colonise mesoderm tissues, this apparent bias was not borne out by an independent isoenzyme measure of chimerism. The experiments presented in this chapter were carried out in collaboration with V. Wilson and M. Jones who were responsible for blastocyst injection and the animal cap assays, respectively.

6.2 MATERIALS AND METHODS

ES cell transfection

CGR8 ES cells were transfected using Lipofectamine (Gibco BRL) according to the manufacturers instructions. Briefly, 1 μg of QIAGEN prepared plasmid DNA was allowed to form a complex with liposomes (14 μg Lipofectamine) for 30 minutes at room temperature. The lipo-complexes were then added to $2x10^5$ ES cells in serum free medium (Opti-MEM, Gibco BRL) and LIF. After growth for 4 hours at 37°C in 5% CO_2 and humidified air, Opti-MEM containing fetal calf serum was added to give a final concentration of 15%. Fresh ES cell medium replaced the transfection medium 24 hours after the start of the transfection. For transient transfection assays, the ES cells were allowed to grow for a further 24 hours before removing one tenth of the transfected cells for detection of β-galactosidase activity. The efficiency of transfection was compared to that achieved with pBβ-geopA, which contains the β-geo reporter gene under the control of the human β-actin promoter. To generate stable transfectants, ES cells were selected for ten days in 350 μg ml^{-1} G418 (Gibco BRL). Since preliminary experiments showed that expression of the exogenous DNA was lost upon continual culture, ES cell clones of interest were routinely cultured in selective media. Two to three days prior to blastocyst injection cells were removed from selection to restore maximal growth and eliminate traces of G418 from media in contact with the blastocysts.

Detection of β-galactosidase activity

Samples were fixed in 0.2% glutaraldehyde, 0.1 M phosphate buffer (Na_2HPO_4/NaH_2PO_4, pH 7.2), 2 mM $MgCl_2$ and 5 mM ethylene glycol tetra-acetic acid (EGTA) for either 10 minutes (ES cells and embryos without closed cranial neural folds) or 20 minutes (embryos with closed neural folds and older) at 4°C before washing in 0.1 M phosphate buffer, 2 mM $MgCl_2$, 0.1% sodium deoxycholate, 0.02% Nonidet P40 and 0.05% bovine serum albumin three times for 30 seconds each at room temperature. β-galactosidase activity was then detected in 1 mg ml^{-1} X-gal (5-bromo-4-chloro-3-indolyl β-D-galactopyranoside; Sigma), 0.2 mg ml^{-1} spermidine, 5 mM $K_3Fe(CN)_6$, 5 mM $K_4Fe(CN)_6$ and 0.2 mM NaCl at 37°C overnight.

ES cell chimeras, generation and analysis

ES cell chimeras were generated via blastocyst injection and transfer of embryos to pseudopregnant females as described in Bradley (1987). Potential chimeras were dissected from the uterus 4-7 days after transfer.

Detection of β-galactosidase activity and T protein in mouse embryos

Embryos were fixed in 4% PFA in PBS for 1 hour at 4°C, and then washed and X-gal stained as described above for up to eight hours. The embryos were postfixed in 4% PFA in PBS, 4°C overnight and dehydrated through a methanol in PBS series (25%, 50%, 75%, 100%, 5 minutes each) and stored in 100% methanol 4°C for 1 hour. The embryos were then processed as described in Kispert and Herrmann (1994) using an antiserum directed against amino-acid residues 1-123 of the T protein (Kispert and Herrmann, 1993).

Detection of glucose phosphate isomerase isozymes in tissue samples

To separate somitic and lateral mesoderm from neurectoderm, the unseparated trunk sample was incubated in 0.5% trypsin/2.5% pancreatin in PBS (Svajger and Levak-Svajger, 1975) for 15 - 20 minutes at 4°C, then replaced in M2 medium (Hogan et al., 1994). The tissues were gently separated using forceps. All tissues samples were washed once in PBS and transferred to microwell dishes in a minimum volume of PBS. The samples were frozen at -20°C, until analysis. The dish was thawed and refrozen twice to fracture tissues and release GPI enzyme. The GPI assay was performed as described in Rashbass et al. (1991) and the ratio of GPI-A:GPI-B was estimated by eye. To assist quantitation, a 50:50 mixture of blood from Gpi-1^a/Gpi-1^a and Gpi-1^b/Gpi-1^b mice was run in parallel with the embryonic tissue fractions. Each sample was assessed by two observers and the resulting estimates did not vary by more than 10% for a given sample. It can therefore be assumed that this method of quantitation is accurate to at least 10 percentage points.

Animal cap assay

Medium which had been in contact with ES cells for 48 hours was removed, centrifuged at 100 *g* for 5 minutes to remove any cells and used in the following animal cap assay. *Xenopus* embryos were obtained by artificial fertilisation as described by Smith and Slack (1983) and staged according to Nieuwkoop and Faber (1994). They were cultured in 75% NAM (Slack, 1984) and dejellied with 2% cysteine hydrochloride (pH 7.8). Animal caps were dissected at mid-blastula stage and cultured for 4 hours in conditioned medium before transfer to 75% NAM until sibling embryos had reached at least stage 35 (swimming tadpole stage). The embryos were fixed and processed for histological examination using the procedure described for generating paraffin sections of mouse embryos (Chapter 2). Sections were stained by the Feulgen/Light Green/Orange G technique of Cooke (1979).

6.3 RESULTS

Generation of stably transfected ES cell lines

In order to generate ES cells that contained a reporter gene and produced a secreted protein, an expression vector which would create a dicistronic message was utilised. The cDNAs were cloned into the kFGF/PGK-IRES-β-geo-BS vector. This vector (Figure 6.1) contained the full length coding sequence of either *Vgr-2* or *BMP-7* downstream of the kFGF enhancer element and PGK promoter. The kFGF enhancer is a 316 bp sequence from the 3' UTR of the murine *kFGF* (also known as *FGF-4* or *hst*) gene (Curatola and Basilico, 1990). This enhancer increases expression of heterologous sequences in embryonic stem cells (Ma et al., 1992). The PGK promoter should drive high level expression in ES cells and in all tissues of the mouse embryo (Adra et al., 1987). Immediately downstream of the *Vgr-2* cDNA is the Encephalomyocarditis Virus internal ribosomal entry site (EMCV IRES) sequence. The IRES is a 594 bp sequence from the 5' UTR of the EMCV mRNA which has been modified by mutagenesis of the native initiation codon such that translation is initiated at an ATG codon which lies 9 bp 3' of the normal start site (Ghattas et al., 1991). This sequence allows cap independent translation of the downstream β-geo sequence. β-geo is an in frame fusion transcript which encodes a protein which has both β-galactosidase (β-gal) reporter activity and neomycin activity for drug selection (Friedrich and Soriano, 1991). The β-geo sequence is followed by a β-globin intron sequence and the SV40 polyadenylation signal. The vector should therefore drive co-ordinated expression of both the introduced cDNA and the *lac Z* gene in the same cells, allowing the location of the overexpressing cells to be followed in chimeric embryos.

BMP-7 expression cell lines

The full length *BMP-7* cDNA was cloned into the kFGF/PGK-IRES-βGeo-BS vector and transfected into CGR8 ES cells. A total of 1.8×10^6 cells were transfected and after 10 days of growth under selection, 32 colonies were picked into 48-well plates. These colonies were grown for three days without selection and a proportion of the cells from each clone were passaged onto 24-well plates, grown overnight and stained with X-gal to test for β-gal activity. Of the clones tested in this manner, 16 exhibited some β-gal activity and were expanded and frozen for further analysis. Subsequently, X-gal staining of these cell lines demonstrated that β-gal activity was rapidly lost during culture. While this effect was noted to some degree with the *Vgr-2* expression lines (see below), it was more extreme in the *BMP-7* transfected cell lines, such that within 2-3 passages after expansion, β-gal activity was barely detectable in these cell lines. While the proportion of X-gal positive cells could be increased again with growth under selection (Figure 6.2), it was decided not to use these cell lines in further experiments as an assay for active BMP-7 protein was not available and therefore it could not be demonstrated that the ES cells were secreting active BMP-7.

Figure 6.1 FPIG expression construct for transfection into ES cells. The *Vgr-2* cDNA was cloned by blunt end ligation into the FPIG construct at the site shown. For the *Vgr-2* cDNA the box region represents the coding sequence; leader sequence (black), pro-domain (grey), and mature domain (white) and the line represents untranslated regions. The FPIG vector is constructed in pSport (Gibco BRL). Scale bar, 300 basepairs.

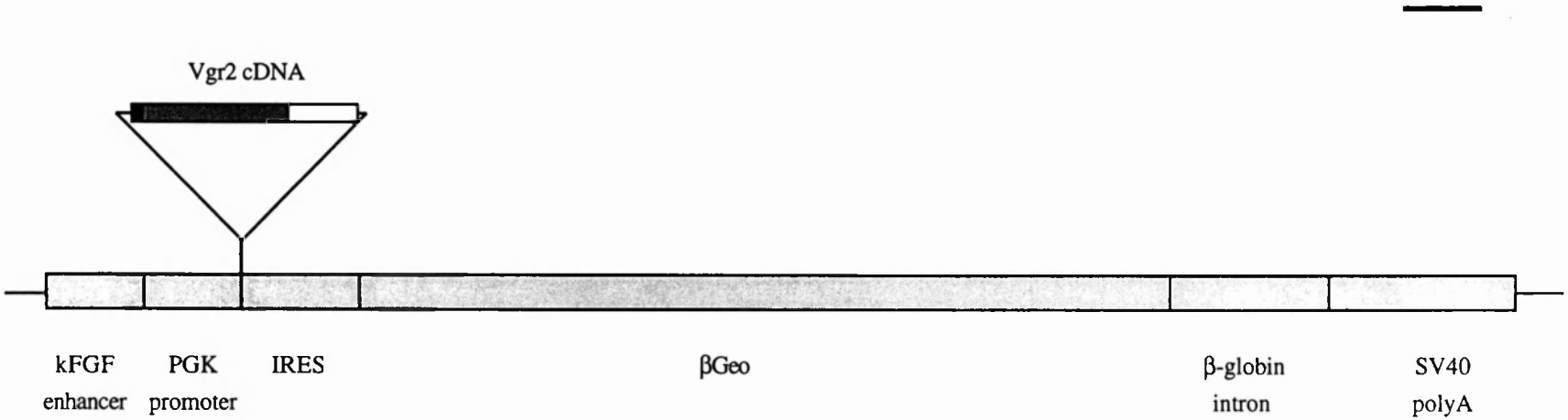
Vgr2 cDNA
kFGF
enhancer
PGK
promoter
IRES
βGeo
β-globin
intron
SV40
polyA

Figure 6.2 Loss and recovery of β-gal activity in a BMP-7 expression ES cell line. X-gal staining of BMP-7 expression line 1. **(A)** Stained cells after selection and initial expansion; passage 5. **(B)** X-gal staining at passage 16, cells were grown without selection. **(C)** X-gal staining at passage 17, after growth under selection conditions.

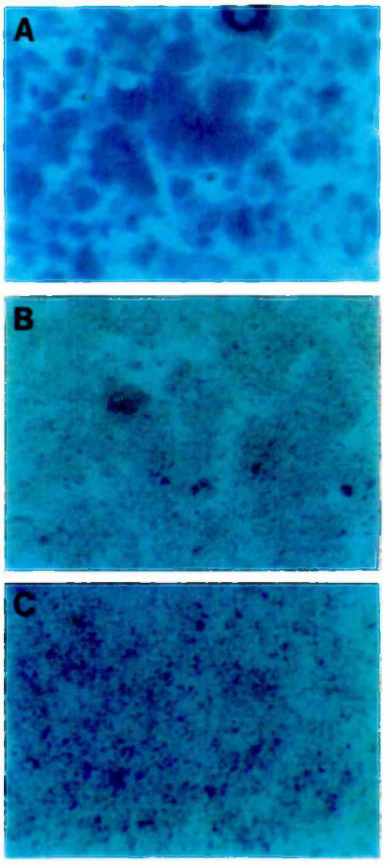
A
B
C

Vgr-2 expression cell lines

The *Vgr-2* cDNA was cloned into the kFGF/PGK-IRES-βGeo-BS vector and transfected into CGR8 ES cells. A total of $1.6x10^6$ cells were transfected and after 10 days of growth under selection a total of 10 resistant colonies were picked into 48-well plates. These colonies were grown for three days without selection and a proportion of the cells from each clone were passaged onto 24-well plates, grown overnight and stained with X-gal to test for β-gal activity. Of the *Vgr-2* expression clones tested in this manner, 4 were found to exhibit high levels of β-gal activity. The two clones which stained blue within three hours at 37°C were used in subsequent analysis and designated VE1 and VE2. The vectors used to generate both the *BMP-7* and *Vgr-2* expressing cell lines were found to be at least 100 fold less efficient in transient transfection assays when compared to the same reporter gene (β-geo) under the control of the β-actin promoter.

Transcription of the dicistronic message

To assess whether the ES cell lines which exhibited high levels of X-gal activity also expressed the introduced fusion transcript, RNA was isolated from the expression ES cell lines and from the parental CGR8 ES cells. In the transfected cells the endogenous *Vgr-2* transcript can be distinguished from the introduced transcript on the basis of size since the introduced transcript will be fused to the IRES and β-geo transcript. The endogenous *Vgr-2* transcript is approximately 1.2 kb in length (Jones et al., 1992a) and the introduced transcript should be approximately 7.5 kb in length. Northern analysis of total RNA isolated from the ES cell lines (Figure 6.3) showed that the VE2 cells were expressing the fusion transcript and the endogenous transcript. Expression was evident at both passage 5 and at passage 10. Cells from passage 10 were used for the initial chimeric analysis. In the parent cells, and the mock transfected cells, only the endogenous *Vgr-2* transcript was detected. In this analysis a fusion transcript was not detected in the VE1 cell line. However, this analysis examined total RNA and a long exposure time of the hybridised filter to the PhosphorImage screen was necessary to detect any signal. It is possible that Northern analysis of polyA selected mRNA might detect the fusion transcript in the VE1 cell line.

Production of Vgr-2 protein

If the ES cell lines are producing and secreting active Vgr-2, then conditioned media from these cells may be expected to induce mesoderm formation in the *Xenopus* animal cap assay. This assay differs from the autoinduction assay described in chapter 5 which utilises injection of *in vitro* transcribed mRNA for the test molecule. In the animal cap assay naive ectoderm is removed from the animal pole of pre-gastrulation *Xenopus* embryos. A simple salt solution supports growth of these animal pole cells and they round up to form a sphere of epidermis. If, however, proteins capable of inducing mesoderm formation are present in the culture media, then the ectoderm differentiates into a range of mesoderm types and often this differentiation is associated with elongation of the animal caps. The mesoderm

Figure 6.3 mRNA production from the exogenous DNA in stably transfected ES cell lines. The production of a fusion transcript from the introduced plasmid was monitored by northern analysis of 10μg of total RNA isolated from the ES cell lines and hybridisation to the *Vgr-2* probe. RNA from the cell lines transfected with the *Vgr-2* expression construct (VE1 and VE2) at passage 5 (p5) and 10 (p10) was analysed alongside RNA from CGR8 ES cells (Parent cells) and from an ES cell line transfected with an FPIG expression construct which did not contain the Vgr-2 cDNA (Mock transfected). The size of the RNA (basepairs) is indicated on the left. The hybridised filter was exposed to a phosphorimage screen for 10 days.

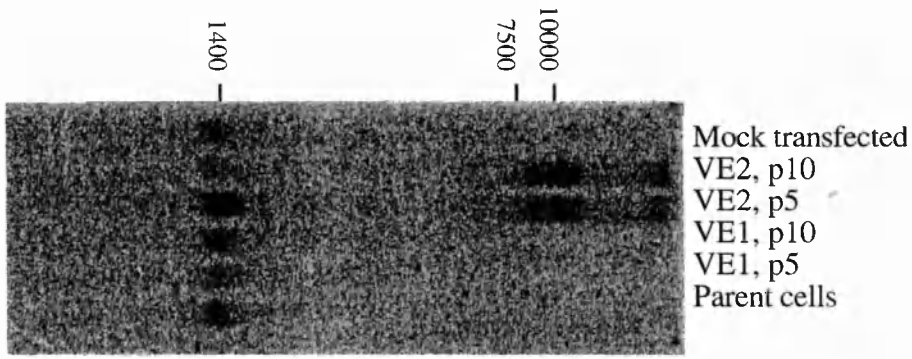
1400
7500
10000
Mock transfected
VE2, p10
VE2, p5
VE1, p10
VE1, p5
Parent cells

produced in both of these assays varies with the inducing molecule and concentration of the inducer. Thus, on the basis of the autoinduction assay, conditioned media from the ES cell lines is expected to cause mesoderm formation in the animal cap assay, although it is not possible to predict what type of mesoderm should be induced.

Conditioned media was obtained from the parental ES cell line (CGR8) and from both the VE1 and VE2 cell lines. Animal caps were exposed to this media and assayed for mesoderm induction. Figure 6.4 shows that while animal caps cultured in media from the CGR8 cells remained spherical, the animal caps cultured in media from the transfected cell lines showed slight elongation. This elongation suggests that the animal caps have undergone mesoderm formation. This was confirmed by histological analysis which demonstrated the presence of mesothelium and muscle in experimental animal caps and atypical epidermis in control animal caps. The animal cap assay provides good evidence that both of these cell lines secrete active Vgr-2 protein, despite not detecting the fusion transcript in Northern analysis of total RNA from the VE1 cell line.

Overexpression of *Vgr-2* in the mouse embryo

To determine whether these cell lines could also induce mesoderm formation in the mouse embryo, chimeric embryos consisting of *Vgr-2* expressing cells and wild-type cells (VE↔+/+) were generated from ES cells which were concurrently assayed for Vgr-2 activity as shown in Figure 6.5. In initial experiments, potential chimeras were dissected at 6.5 dpc and stained with X-gal to distinguish the chimeras. Examination of the chimeras in whole mount did not detect any gross morphological abnormalities. However, overnight staining of these embryos resulted in only very low level β-gal signal. This was surprising as the cell line used (VE1) had previously shown high level β-gal signal after three hours. Further X-gal staining of the cells maintained in culture, suggested that the cells were exhibiting decreased β-gal activity with increased passage number. However, if the cells were maintained in selection conditions, then higher levels of β-gal activity were recovered.

Morphological analysis of VE chimeras

Further chimeras were constructed using VE1 and VE2 cells maintained under selection. The potential chimeras were dissected at stages equivalent to 8.0 - 10.0 dpc and assayed for β-gal activity. X-gal staining was carried out for between eight to twenty four hours and the level of staining obtained was sufficient to identify chimeric embryos. Whole mount examination of chimeras generated from either the VE1 or VE2 cell lines detected no gross morphological defects. To confirm that embryonic tissue arrangement was not altered in chimeric embryos, six embryos of stages ranging from headfold to 25-somites were sectioned. No changes in the proportion of the mesoderm component of these embryos relative to other tissues was noted. The mesoderm distribution was also studied in headfold embryos by detection of T protein. T, the mouse counterpart of *Xbra*, is found in the

Figure 6.4 Mesoderm induction by marked ES cell lines secreting Vgr-2 protein. **(A)** Animal caps incubated in media conditioned by the parental ES cell line (CGR8). **(B)** VE1 ES cells stained for β-gal activity. **(C)** Animal caps incubated in conditioned media from the VE1 cell line. **(D)** VE2 ES cells stained for β-gal activity. **(E)** Animal caps incubated in conditioned media from the VE2 cell line. **(F)** Section through animal caps incubated in control CGR8 conditioned media. **(G)** Section through animal caps incubated in VE1 conditioned media. **(H)** Section through animal caps incubated in VE2 conditioned media. ep: atypical epidermis, m: muscle, my: mesenchyme. Scale bar 600 μm (A,C,E); 100 μm (B,D,F,G,H).

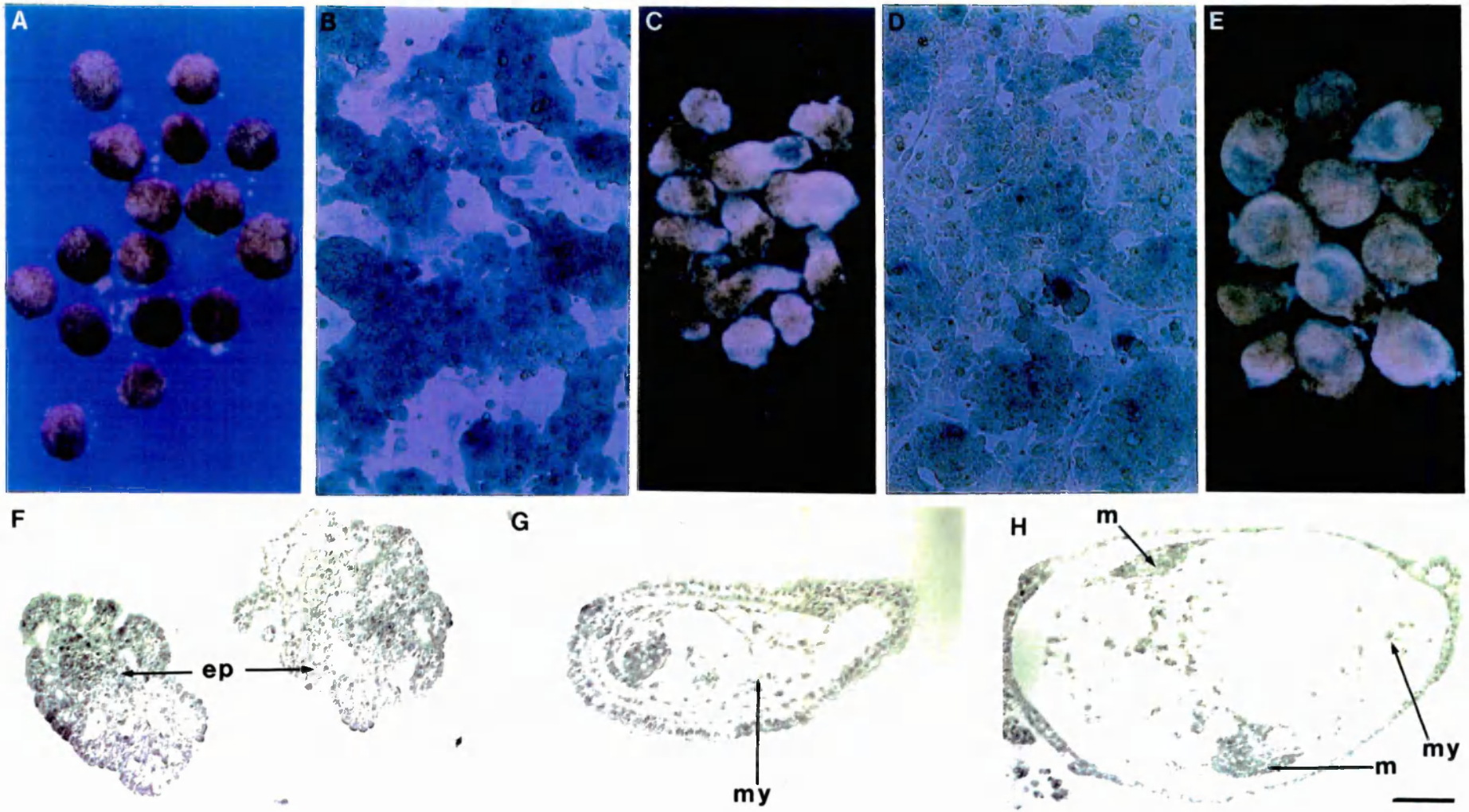
A
B
C
D
E
F
ep
G
my
H
m
m
my

Figure 6.5 : Strategy for overexpressing *Vgr-2* in the mouse embryo. ES cells are transfected with the FPIG vector and G418 resistant clones selected. These are assayed for ß-gal activity, and supernatant from clones with highest expression assayed for mesoderm induction activity in the *Xenopus* animal cap assay. The cells are injected into blastocysts, transferred to pseudopregnant recipient females and recovered at 7.5-9.5 dpc. Embryos are processed through a variety of treatments including X-gal staining, T antibody immunohistochemistry, and GPI isoenzyme analysis.

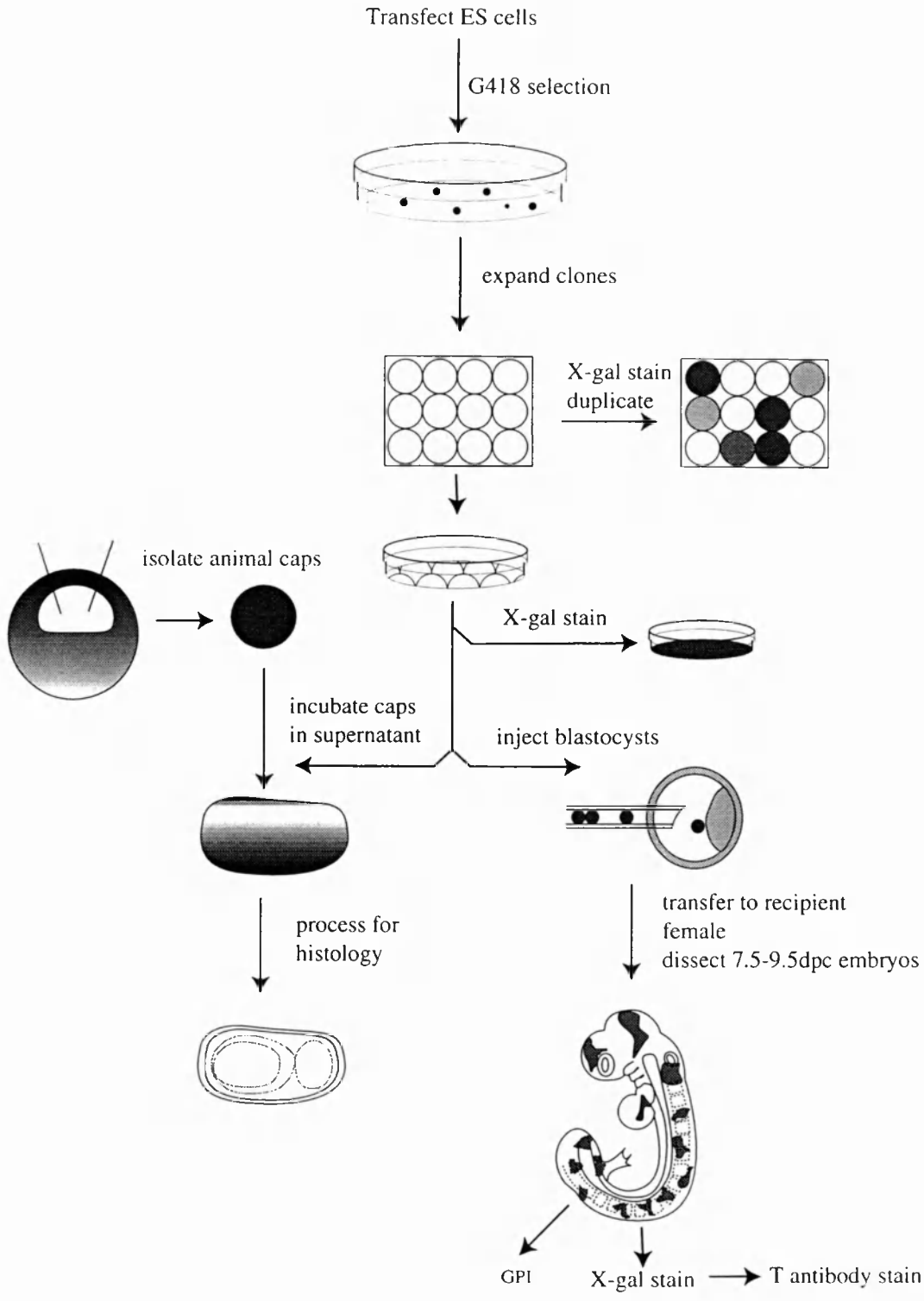
Transfect ES cells
G418 selection
expand clones
X-gal stain
duplicate
isolate animal caps
X-gal stain
incubate caps
in supernatant
inject blastocysts
process for
histology
transfer to recipient
female
dissect 7.5-9.5dpc embryos
GPI
X-gal stain
T antibody stain

primitive streak, the node and developing notochord of headfold stage mouse embryos (Wilkinson et al., 1990; Kispert and Herrmann, 1994). In all chimeras examined, the distribution of T protein was normal; it was not ectopically expressed, nor were any of the structures which normally express T expanded, as shown in Figure 6.6.

Analysis of colonisation of VE cells

From the examination of intact, X-gal stained, chimeric embryos it appeared there was a high level of contribution of VE1 and VE2 cells to extraembryonic mesoderm. This was noticeable because in what appeared (on the basis of β-gal positive cells) to be relatively low level chimeras, a high proportion of stained cells were usually found in the yolk sac mesoderm (particularly the blood islands) and often also the allantois (Figure 6.7). Additionally, in chimeras where stained cells were seen in the embryo proper these too appeared to contribute preferentially to mesoderm tissues. For example, when such embryos were viewed from the dorsal aspect, the neurectoderm appeared devoid of stained cells relative to the mesoderm components of the embryo. A nonquantitative analysis of sectioned chimeras supported the notion of a preferential colonisation of mesoderm by β-gal positive cells.

Before attempting to quantify this difference on the basis of the distribution of X-gal positive cells, an independent measure of tissue distribution of the ES cell progeny was employed. The method used relies on the fact that the ES cells express a different GPI isozyme than the host blastocyst. These two isozymes can be electrophoretically separated and a colorimetric reaction used to visualise the relative proportions of the isozymes in a given tissue sample. Potential chimeras were dissected into several components as shown in Figure 6.8. Half of the yolk sac and a portion of the embryo was X-gal stained to determine if the embryo was chimeric. The remainder of the yolk sac was kept for GPI analysis, along with other tissues. Part of the embryo was separated into mesoderm and ectoderm components to allow direct comparison of germ layer contribution. Table 6.1 shows that in the five embryos analysed in this manner, the distribution of ES cells is in fact very even. This is best demonstrated by the results from the germ layer fractions; in all embryos the proportion of ES cell progeny in the ectoderm is the same as that in the mesoderm. The yolk sac fraction invariably showed lower contribution than the other tissues, but this is most likely due to the fact that this fraction consists of both extraembryonic mesoderm and visceral yolk sac endoderm. This endoderm is rarely colonised by ES cells (Beddington and Robertson, 1989) and so the contribution of the ES cells is diluted by the endoderm population.

Figure 6.6 T protein distribution in VE1↔+/+ chimeras. **(A)** Non-chimeric littermate, showing T protein localised to the primitive streak and node. **(B)** The extraembryonic region of a chimeric embryo showing localisation of β-gal activity to the blood islands and no ectopic T protein. **(C)** The embryonic region of the chimeric embryo shown in (B). T protein distribution is the same as in the non-chimeric embryo in (A), the node is out of focus in this picture. p: primitive streak. Scale bar, 200 μm (A); 100 μm (B,C).

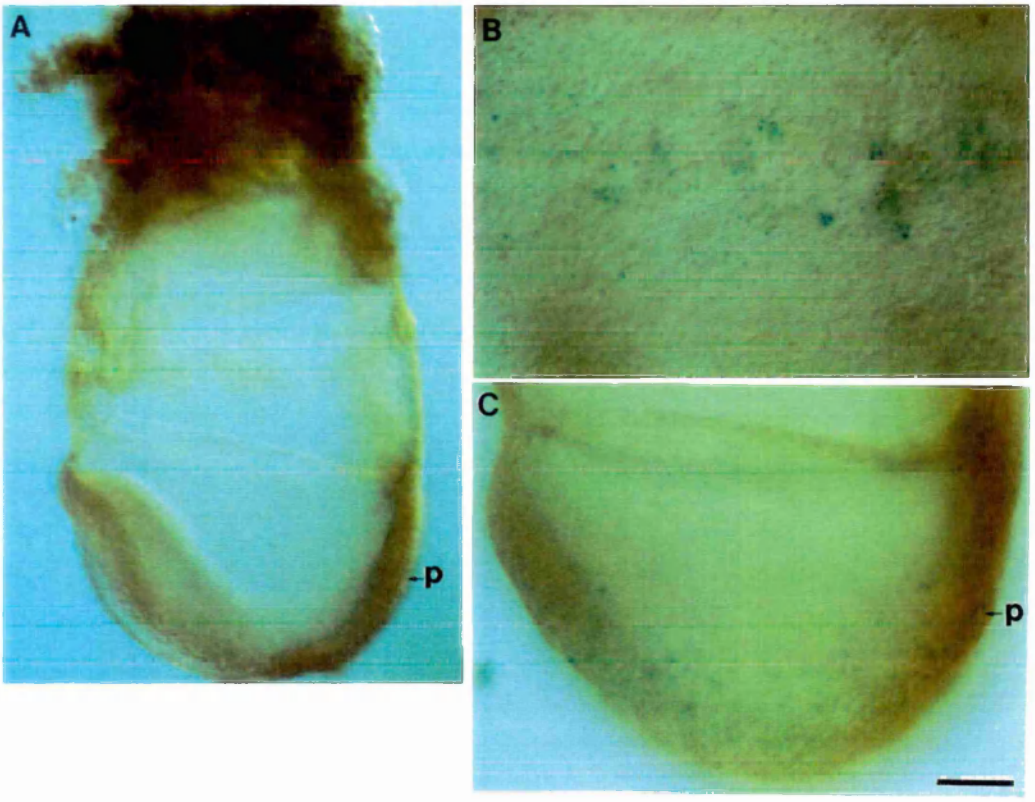
A
B
C
p
p

Figure 6.7 Chimeric embryos consisting of VE2 and wildtype cells stained for β-gal activity. **(A)** Four headfold stage embryos showing contribution to embryonic tissues and extraembryonic mesoderm (blood islands). **(B)** 8-somite embryo; much of the yolk sac has been removed. **(C)** A 16-somite and 14-somite embryo, both with extraembryonic tissues removed. **(D)** 12-somite embryo with the yolk sac still attached. **(E)** Section through the posterior of an 8.5 dpc embryo (~ 8 somites) showing β-gal positive cells in all germlayers. al: allantois, b: blood, bi: blood islands, hg: hindgut, n: neurectoderm, y: yolk sac. Scale bar, 800 μm (A); 700 μm (C,D); 400 μm (B); 200 μm (E).

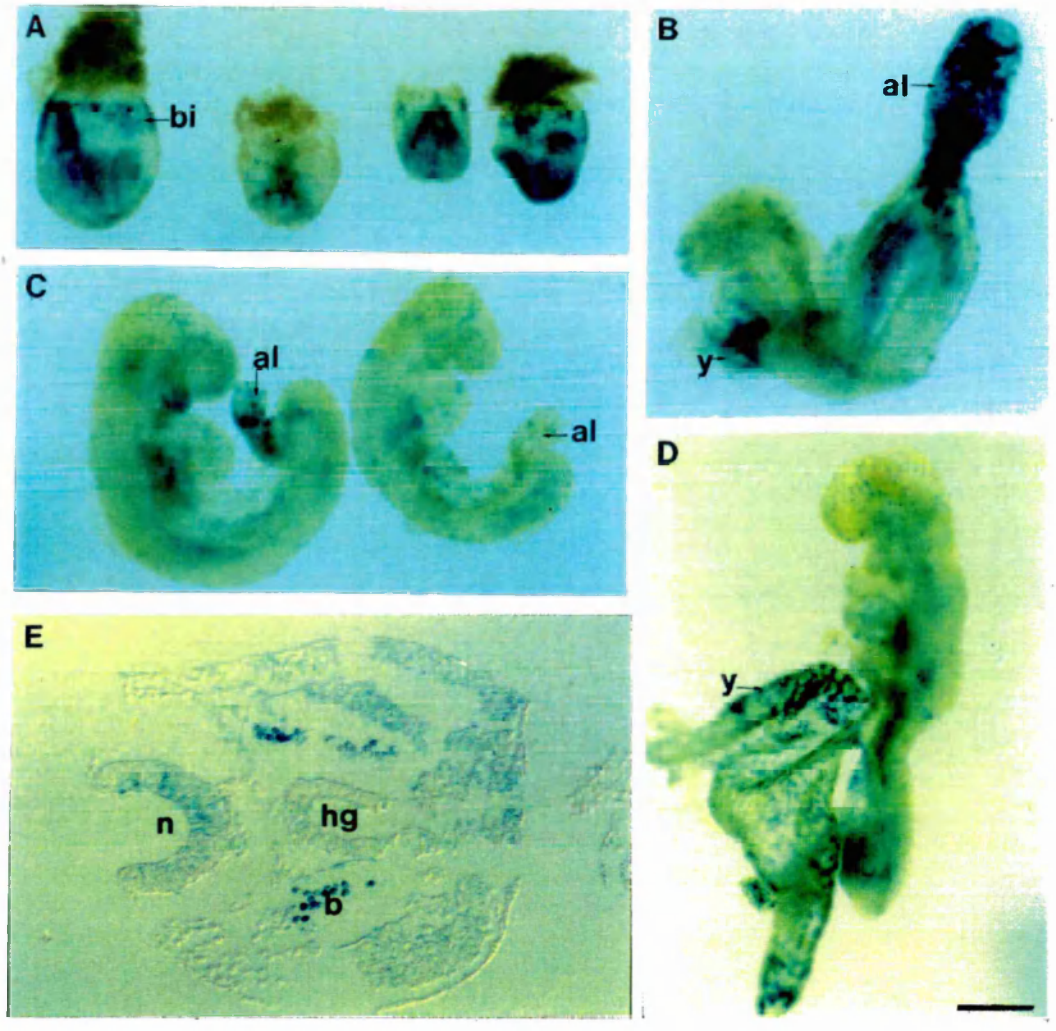
A
bi
B
al
y
C
al
al
D
y
E
n
hg
b

Figure 6.8 Collection of tissues for GPI analysis.

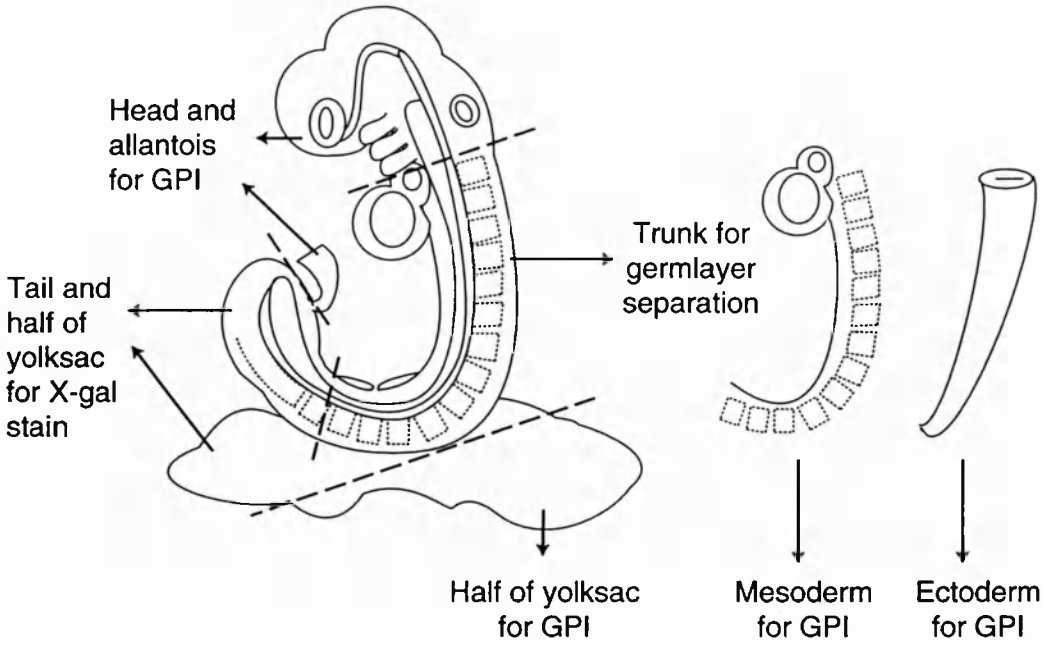
Head and
allantois
for GPI
Tail and
half of
yolksac
for X-gal
stain
Trunk for
germlayer
separation
Half of yolksac
for GPI
Mesoderm
for GPI
Ectoderm
for GPI

Table 6.1 Distribution of VE cells in VE1↔+/+ chimeras. The percentages denote the contribution made by the VE1 ES cells to the dissected tissues as determined by GPI analysis.

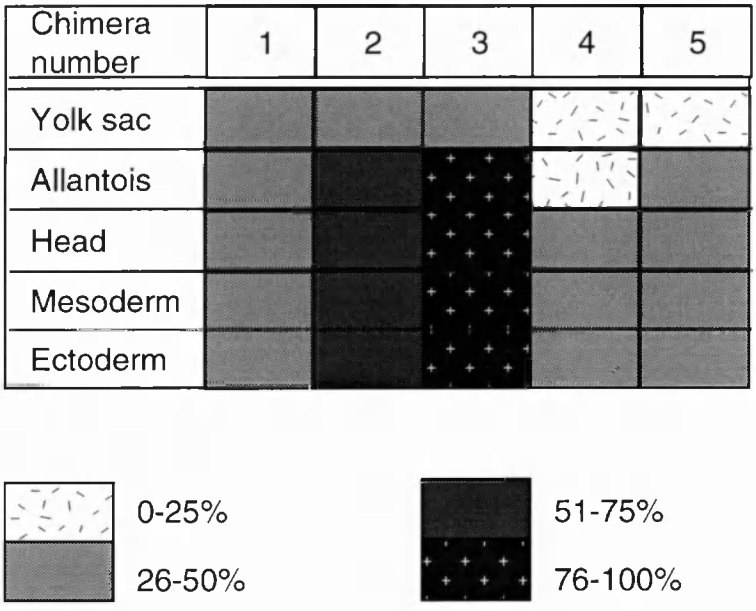
Chimera number
1
2
3
4
5
Yolk sac
Allantois
Head
Mesoderm
Ectoderm
0-25%
26-50%
51-75%
76-100%

6.4 DISCUSSION

When murine Vgr-2 is overexpressed in *Xenopus* it diverts the fate of prospective ectodermal cells to mesoderm, as evidenced by the induction of *Xbra* expression (M. Jones, personal communication). In the experiments reported here, despite the fact that conditioned media from the ES cells overexpressing Vgr-2 is able to induce mesoderm in *Xenopus* animal caps, no evidence that overexpression of *Vgr-2* in the mouse embryo reproduces this effect was found. Chimeric embryos were inspected at stages ranging from the early headfold stage to 10.5 days of development. No change in the relative proportion of mesoderm to ectoderm tissues were detected either in whole mount or section analysis and no change in the tissue distribution of T protein could be discerned. Interestingly, no definitive examples of increased mesoderm production in the mouse embryo are reported. Mutants which appear to be defective in the formation of the primitive streak and therefore lack embryonic and extraembryonic mesoderm exist (Conlon et al., 1991; Iannaccone et al., 1992; Holdener et al., 1994; Winnier et al., 1995) and in mice homozygous for a mutation in the *eed* gene, production of embryonic mesoderm is severely impaired whilst extraembryonic mesoderm production proceeds as usual (Faust et al., 1995). It remains to be demonstrated that the phenotype of overproduction of mesoderm can be generated in the mouse embryo.

Analysis of chimeric embryos constructed from ES cells secreting Vgr-2 suggested that the majority of *lac Z* expressing cells colonised mesoderm tissues. *lac Z* transcription in this assay is dependent upon *Vgr-2* transcription and thus β-gal positive cells represent *Vgr-2* expressing cells. This apparent bias in tissue distribution is unusual because ES cells can contribute to all embryonic tissues and to extraembryonic mesoderm (Beddington and Robertson, 1989; Nagy et al., 1990). Even when embryonic tissues are separated and GPI analysis carried out on the individual tissues, it is found that in general, within a given chimera, ES cells contribute equally to tissues of different germ layer origin (Wilson et al., 1993). In contrast to the β-gal results, when the VE↔+/+ chimeric embryos were assayed by GPI analysis it was found that the contribution of ES cell progeny to all tissues was approximately equivalent.

There are several possible explanations for these apparently contradictory results. The GPI assay illustrates that the parental ES cells used in this experiment are not inherently biased in their contribution to embryonic tissues. It is possible that there is selection against *Vgr-2* expression (and therefore *lac Z* expression) in ectoderm and endoderm Alternatively, given that expression is mosaic in the ES cell population (Figure 6.4), it is possible that some form of cell sorting occurs such that *Vgr-2* expressing (and hence *lac Z* expressing) cells

preferentially colonise mesoderm tissues. Therefore, descendants of ES cells which do not express the construct may comprise a large portion of the other tissues. However, the results could also be explained by some form of differential regulation of the introduced expression construct such that higher levels of active β-gal are present in mesoderm tissues. Since two independent cell lines yield indistinguishable results this is not likely to be caused by position effects due to the integration site of the vector. A similar dicistronic construct which consists of PGK promoter/neo/EMCV IRES/lac Z has previously been characterised in chimeric mouse embryos (Kim et al., 1992). This construct shows strong expression in the embryonic portion of the embryo at full length primitive streak stages and no obvious bias towards mesoderm colonisation of the ES cells at any stages examined (up to 11.5 dpc), demonstrating that neither the PGK promoter or the IRES usually produce such differential expression of β-gal activity.

The *kFGF* enhancer has been extensively studied *in vitro*, where it is responsible for the expression of *kFGF* in undifferentiated EC and ES cells (Curatola and Basilico, 1990; Ma et al., 1992). In EC cells, enhancer activity requires the synergistic action of the Sox-2 and Oct-4 transcription factors (Schoorlemmer and Kruijer, 1991; Yuan et al., 1995). Between 7.5 and 10 dpc *Sox-2* and *Oct-4* show restricted embryonic patterns of expression, both being predominantly expressed in ectoderm or primordial germ cells (Rosner et al., 1990; Collignon et al., 1996b). The expression pattern of these two genes is distinct from that of *kFGF* at these stages. Hence it is unlikely that during this stage of development the activity of the *kFGF* enhancer is dependent upon the interaction identified in EC cells. The endogenous pattern of *kFGF* expression is perhaps the best guide to potential tissue specific *kFGF* enhancer effects. The distribution of β-gal positive cells does not resemble the embryonic expression pattern of *kFGF* during the stages at which the VE chimeric mice are analysed (Drucker and Goldfarb, 1993).

These results raise the problem of the regulation of heterologous promoters in ES cells, which will be discussed in the general conclusions. The strategy for overexpression of secreted molecules used in these experiments, while initially seeming worthwhile, proved to be unreliable. It appears the secretion of particular molecules may be strongly selected against in ES cell populations. For example, when the identical strategy was attempted with *BMP-7*, *lac Z* activity could not be maintained. In this case it is likely that expression of *BMP-7* is incompatible with the maintenance of ES cell properties, as has been described for the effects of BMP-7 on EC cells (Andrews et al., 1994). Additionally, it appears that differences may exist between the regulation of exogenous DNA during ES cell culture and embryonic development. As such, a second method for overexpression of secreted molecules in the mouse embryo was developed. This method, and the results of overexpression of BMP-7 are the subject of the next chapter.

CHAPTER 7

ECTOPIC EXPRESSION *VIA* COS CELLS

7.1 INTRODUCTION

As an alternative to stably expressing ES cell lines the COS cell overexpression system was utilised. The COS cell line is a monkey kidney cell line transformed by an origin-defective mutant of the SV40 virus (Gluzman, 1981). Since the cell line expresses the wildtype large T antigen the cells will replicate introduced plasmids which contain the SV40 origin of replication to high copy number. COS cells have been used to overexpress secreted molecules in a variety of recombination assays (Basler et al., 1993; Fan and Tessier-Lavigne, 1994; Kennedy et al., 1994; Roelink et al., 1994; Liem et al., 1995) and in many of these cases the reported activity of the secreted molecule is duplicated by recombinant protein. For example, COS cells transfected with *Shh* exhibit floor plate and motor neuron inducing activity, as does purified Shh (Roelink et al., 1994), It therefore seemed likely that COS cells could act as an inert source of secreted molecules.

The ability to deliver COS cells to specific locations in cultured postimplantation embryos renders this strategy particularly suitable for molecules whose function during the optimal culture period is predicted by their restricted expression pattern. The distribution of *BMP-7* transcripts suggests that it may play one or more roles during anterior-posterior axis formation or dorsal-ventral neural patterning (Chapter 4) and as such *BMP-7* is a better candidate for such studies than *Vgr-2*. Unfortunately, to date, no true homologues of *BMP-7* have been isolated from *Xenopus* and mammalian BMP-7 produces no effect in *Xenopus* overexpression assays (Yamashita et al., 1995) so that its function is unknown from the study of *Xenopus* embryos. However, in the chick embryo, TGF-β superfamily molecules, including *BMP-7*, have been shown to promote the differentiation of cells derived from the dorsal neurectoderm and to inhibit the induction of ventrally located motor neurons by signals from the notochord and floor plate (Basler et al., 1993; Liem et al., 1995).

As described in the Introduction the dorsal-ventral fate of neurectoderm cells is believed to result from an interplay of signals which are initially derived from the notochord and the surface ectoderm, at later stages the patterning ability may be passed to the midline floor plate and roof plate structures, respectively. *Shh* is believed to mediate the notochord and floor plate inducing properties, and it is proposed that the role of dorsally located TGF-β related molecules is to oppose a long range *Shh* signal and in doing so promote differentiation of dorsal structures such as the neural crest (for review see Placzek, 1995). While few of the experiments which have led to this model have been performed in the mouse embryo, ectopic expression of *Shh* in the mouse embryo (Echelard et al., 1993) and analysis of mice in which additional neurectoderm comes in contact with the surface

ectoderm (Takada et al., 1994) suggest that the tissue interactions identified in other vertebrates are also utilised in patterning the mammalian neural plate.

As described in Chapter 4, BMP-7 is expressed in the surface ectoderm of the developing mouse embryo from the late gastrulation stage of development. Expression of *BMP-7* adjacent to the dorsal aspect of the neural tube is initiated some twelve hours before the first overt sign of dorsal differentiation occurs with neural crest emigration (5-somite stage; Serbedzija et al., 1992). Thus *BMP-7* is expressed in the temporal-spatial manner expected of a dorsal signalling molecule. Paradoxically, at the same stage of development *BMP-7* transcripts in the developing cranial region are found in all of the paraxial mesoderm, the axial mesendoderm and the ventral midline neurectoderm itself. Beyond this stage of development all but the surface ectoderm expression of *BMP-7* progressively recedes from the hindbrain region. To assess whether *BMP-7* may participate in patterning the hindbrain neural plate COS cells were used to extend the duration of ventro-lateral BMP-7 expression. Such ectopic expression interferes with endogenous ventral signals and elicits expression of a subset of dorsally restricted genes in ventro-lateral neurectoderm. Additionally, BMP-7 causes expansion of the neurectoderm due to a localised increase in cell number.

7.2 MATERIALS AND METHODS

Expression constructs

Shh expression constructs were supplied by A. McMahon and D. Bumcrot. Plasmid phykmShh encodes the full length mouse Shh protein and phykmShh/198 encodes amino acids 1-198 of mouse Shh, which corresponds to the amino peptide generated by Shh auotcleavage (Bumcrot et al., 1995). In both cases *Shh* is expressed under the control of the adenovirus major late promoter. The full length coding sequence of human *BMP-7* cloned into pcDNA1/Amp (Invitrogen) was provided by A. Furley and M. Jones.

COS cell transfection

COS cells were grown to 70% confluency in a 75 cm^2 flask, the cells trypsinized and pelleted in a universal by centrifuging at 100 g for 5 minutes and washed with PBS. Cells were resuspended in 500 µl of PBS and 5 µg of plasmid DNA (purified on a caesium chloride gradient) added to the cells and incubated for 10 minutes at 4°C. The cells were electroshocked in a 0.5 cm chamber (Bio-Rad) using a Bio-Rad genepulser under the following conditions: 0.45 kV, 250 µF. Cells were incubated at 4°C for a further 10 minutes before plating on a 75 cm^2 flask. Fresh COS cell media was added 24 hours after the transfection.

COS cell grafts

48 hours after transfection, cells from a 75 cm^2 flask were detached using enzyme free cell dissociation buffer (GIBCO BRL) and collected by centrifugation (100 g, 5 minutes). The cells were resuspended in 600 µl of COS cell medium and placed in 10 µl hanging drops. The drops were incubated at 37°C in 5% O_2, 6% CO_2 and humidified air for 2 hours or until they had formed an adherent sheet of cells. A sheet of COS cells was labelled with the fluorescent dye DiI (1,1'-dioctadecyl-3,3,3',3'-tetramethyl indocarbocyanine perchlorate; Molecular Probes) by placing in 10 µl of a 0.3 M sucrose solution containing 0.05% DiI in ethanol (Serbedzija et al., 1990) for 30 seconds. The labelled COS cells were transferred to M2 medium to remove excess DiI. They were again transferred to fresh M2 medium and broken into suitable size clumps for grafting by pipetting up and down with a fine, hand-pulled, glass pipette with an internal diameter of 50-100 µm. COS cells were drawn into a glass micropipette of internal diameter 30-40 µm made as described in Beddington (1987). An embryo was gently held at the ectoplacental cone using a pair of watchmaker's forceps (Number 5) and the pipette containing the COS cells was placed into the mesoderm adjacent to the prospective hindbrain neurectoderm on the left side of the embryo. The COS cells were expelled into the mesoderm by aspiration. Typically 10-20 clumps, of 5-10 COS cells each, were expelled into the embryo.

Analysis of grafted embryos

At the end of the culture period embryos were dissected from the yolk sac and amnion and fixed in 4% PFA in PBS, overnight at 4°C. Embryos were placed under a coverslip in a shallow cavity slide (Fisons) and the location of the COS cells visualised with rhodamine filter epifluorescence optics (Zeiss filter set 48 79 15) in a compound microscope (Axiophot, Zeiss), and recorded on film. Those embryos found to have COS cells in the mesoderm adjacent to the hindbrain neurectoderm were numbered and stored individually in 4% PFA in PBS at 4°C in the dark for further analysis. The fluorescent label used to mark the COS cells is unstable through *in situ* hybridisation, therefore after photographically recording the location of the COS cells the embryos were processed individually.

Calculation of relative mitotic frequency

Measurement of mitotic rate using BrdU labelling is hindered by the extremely inefficient uptake of BrdU during culture of intact mammalian embryos (Copp, 1990). Therefore the nuclear stain DAPI was used to score the proportion of neurectoderm cells in mitosis. Paraffin sections (7 µm) were prepared from embryos. The sections were dewaxed in Histoclear and rehydrated through an ethanol series and washed twice in PBS. The sections were incubated in 2 µg ml^{-1} DAPI (4', 6-diamidin-2-phenylindol-dihydrochlorid; Boehringer Mannheim) in PBS for 5 minutes and washed twice in PBS (15 minutes each), before mounting under coverslips in Vectashield (Vector Laboratories). The sections were examined with epifluorescence optics as described above and the sections scored using a 40x

objective. The cell density was estimated by counting nuclei in a 2000 μm^2 area. The number of mitotic cells in the left and right sides of the neurectoderm in a given section was counted. An image of each scored section captured onto computer using a video camera (SONY) fitted to the microscope and Improvision software, which was then used to determine the area of the neurectoderm. The relative mitotic frequency was calculated as the number of mitotic cells per volume of neurectoderm.

7.3 RESULTS OF PRELIMINARY EXPERIMENTS

Strategy for overexpression of secreted molecules in the 8.5 dpc mouse embryo

Preliminary experiments were carried out to determine if it was possible to graft COS cells into specific sites in the post-implantation mouse embryo without adverse developmental consequences caused by either the grafting procedure, or the presence of the grafted cells. In all experiments the introduced COS cells were located by labelling cells before grafting with the lipophillic fluorescent dye, DiI. The efficacy of labelling and viability of labelled COS cells was checked by growing labelled cells on tissue culture surfaces in the same culture conditions as embryos for 24 hours. Examination of these cultured cells under phase contrast and fluorescent optics showed that the cells were living and all were fluorescently labelled, demonstrating that the labelling procedure was both efficient and non-toxic.

Table 7.1 illustrates the preliminary experiments carried out with nontransfected COS cells. From these experiments it was noted that if the COS cells were not placed into the embryonic tissue but expelled into the amniotic cavity, the cells would aggregate and attach as a ball of cells to either the neurectoderm or amnion, or in older embryos become enclosed within the developing neural tube. No morphological effect of such cells was observed. Thus subsequent experiments were aimed at attempting to graft the COS cells into the embryonic mesoderm. As shown in Table 7.1 it was possible to graft the COS cells into mesoderm and in embryos which had already formed somites at the time of grafting it was possible to place the cells accurately adjacent to the prospective hindbrain. In all cases where nontransfected COS cells were grafted into the mesoderm, there appeared to be no gross morphological effect on the embryos. The presence of cells in the foregut pocket is due to the method of grafting; the pipette is placed inside the foregut pocket up to the level of the prospective hindbrain, and then into the mesoderm next to the foregut endoderm. When removing the pipette cells will often be left behind in the foregut. No effect of these trapped COS cells on normal development was noted in any of the experiments carried out to date. Similarly, this method of grafting also results in some cases of cells being enclosed within the neural lumen or attached to the neurectoderm, this occurs when during the grafting procedure cells are

Table 7.1 Preliminary COS cell experiments. Fluorescently labelled COS cells were placed into embryos either via injection into the amniotic cavity, or via grafting into mesoderm. After culture for 24 hours the location of the COS cells was recorded for each embryo. A summary of the location of the COS cells in each category of experiments is reported. In many cases an individual embryo had cells at more than one location.

Method of COS cell incorporation	Number of somites before culture	Number of embryos treated	Number with incorporated cells	Location of incorporated cells
Amniotic cavity injection	pre-somite	14	5	Attached to neurectoderm Attached to amnion Enclosed in neural lumen
	1-5	10	7	Attached to neurectoderm Attached to amnion Enclosed in neural lumen
	6-10	5	3	Attached to neurectoderm Attached to amnion Enclosed in neural lumen
Tissue graft	pre-somite	6	4	Mesoderm adjacent to forebrain Foregut pocket Lateral mesoderm adjacent to heart
	1-5	5	5	Mesoderm adjacent to hindbrain Foregut pocket Enclosed in neural lumen
	6-10	5	4	Mesoderm adjacent to hindbrain Attached to neurectoderm

expelled into the amniotic cavity. Such COS cells have no developmental consequence. It appeared that it would be possible to use this grafting procedure to develop an efficient and reproducible method of introducing secreted molecules into ectopic locations within the developing embryo. The experimental strategy that was developed is shown in Figure 7.1.

Shh transfected COS cells induce ectopic *HNF3-β* expression

It has previously been reported that misexpression of *Shh* in the dorsal neural tube, driven by the *Wnt-1* promoter in transgenic mice, leads to ectopic expression of the floor plate marker *HNF3-β* (Echelard et al., 1993). To ascertain whether the experimental system utilised here can deliver sufficient active protein to cause changes in gene expression COS cells transfected with *Shh* were grafted into the mesoderm adjacent to the hindbrain neurectoderm. The COS cells were transfected either with an expression vector designed to express the first 198 amino acids of the Shh protein, or with a vector designed to express the full length protein. As shown in Table 7.2 and Figure 7.2 COS cells transfected with either construct were capable of inducing additional *HNF3-β* expression.

Table 7.2 shows the results of experiments in which COS cells transfected with *Shh* were grafted into embryos and after 24 hours of *in vitro* development the embryos were analysed for additional *HNF3-β* mRNA. COS cells transfected with the full length construct were grafted into 12 embryos, and after culture 7 embryos were found to contain no COS cells, or cells only in the foregut pocket or attached to the neurectoderm. In none of these embryos was ectopic *HNF3-β* expression detected. Of the 5 embryos in which COS cells had been grafted into the mesoderm in 4 cases the cells were found adjacent to the ventral neurectoderm (the normal source of Shh protein). This did not result in additional *HNF3-β* expression. However, in the one embryo in which this graft was large and thus extended into the region adjacent to more dorsal neurectoderm, an expanded domain of *HNF3-β* expression occurred, as shown in Figure 7.2. In a second experiment COS cells were transfected with the construct coding for the first 198 amino acids of the shh protein. Table 7.2 shows that in this experiment, of the 9 embryos treated, 6 contained no cells or had cells attached to the neurectoderm. After culture, 2 embryos were found to have cells grafted into the ventral mesoderm and again this failed to elicit additional *HNF3-β* expression. In this experiment, 1 embryo had COS cells grafted into the dorsal neurectoderm itself (rather than the underlying mesoderm). This type of graft occurs only rarely as it is much more usual for the COS cells to incorporate into a mesh of mesoderm rather than into an epithelium. In this embryo, ectopic *HNF3-β* expression was detected in the neurepithelium in a ring around the grafted COS cells, as shown in Figure 7.2.

The rather low proportion of embryos ectopically expressing *HNF3-β* may therefore result from the low proportion of dorsally located cells. Experiments in which COS cells were specifically placed adjacent to the dorsal neurectoderm did not increase the number of

Figure 7.1 Strategy for misexpression in the 8.5 dpc embryo. **(A)** COS cells were transiently transfected with an expression construct. **(B)** 48 hours after transfection the COS cells were collected and placed in hanging drop culture. **(C)** After 2 hours the COS cells had formed a coherent sheet of cells which could be DiI labelled and broken into suitable size groups of cells for grafting. The labelled COS cells were grafted into mesoderm adjacent to the prospective hindbrain. **(D)** Embryos into which cells were grafted were allowed to develop in culture for 24 hours and then dissected free of the extraembryonic membranes and fixed. Embryos were examined under fluorescent optics and the location of incorporated cells recorded. **(E)** Embryos in which cells were incorporated were examined further, for example by whole mount in situ hybridisation (WMISH) to determine if changes in gene expression had occurred.

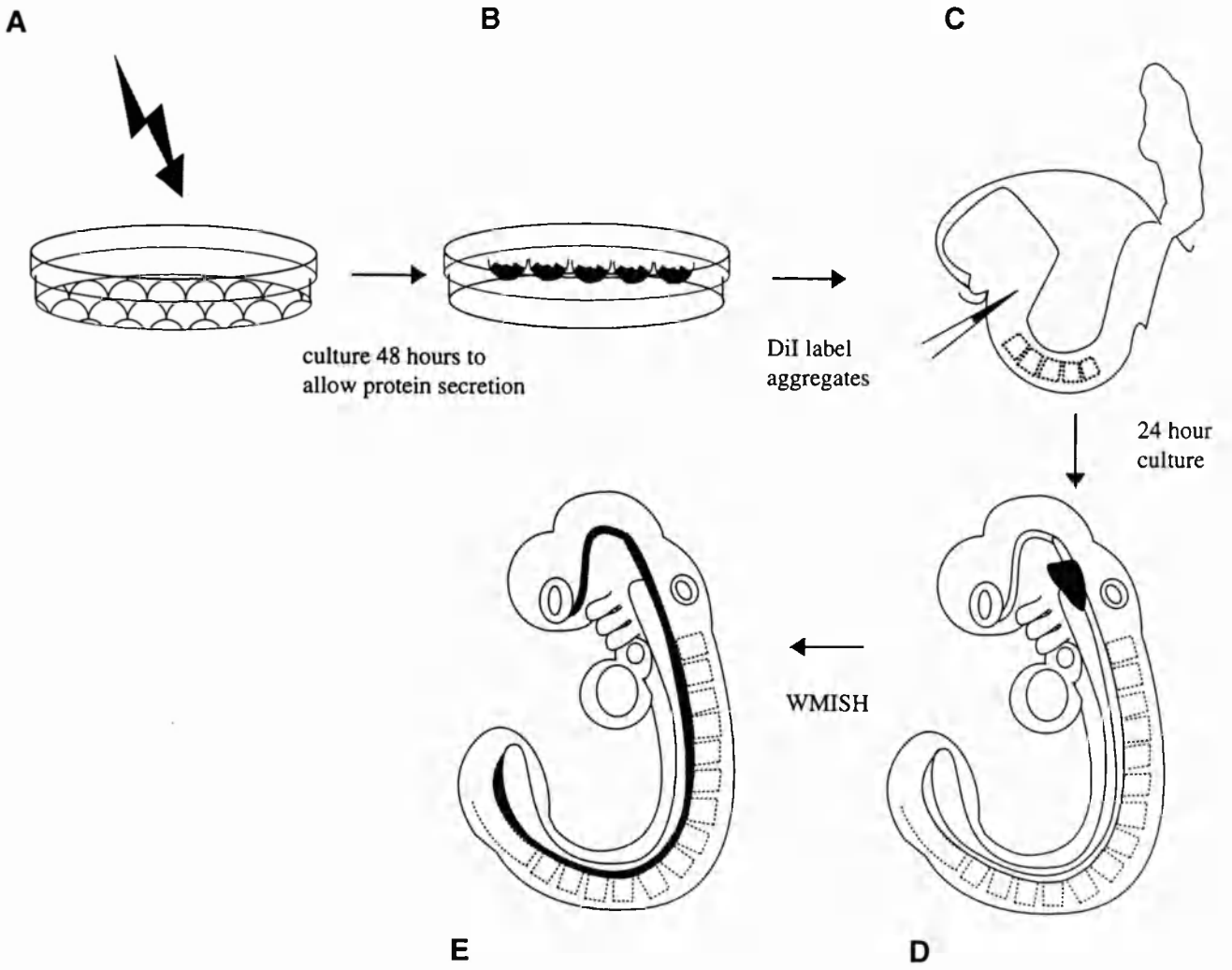
A
B
C
culture 48 hours to
allow protein secretion
DiI label
aggregates
24 hour
culture
WMISH
D
E

Table 7.2 Overexpression of *Shh* in the 8.0 dpc embryo. COS cells were grafted into cranial mesoderm and after recording the location of the grafted cells *HNF3-β* mRNA localisation was examined. Changes in mRNA localisation were only seen when cells were grafted into dorsal mesoderm or into the dorsal neurectoderm itself. The numbers in brackets show the number of embryos in each category for the location of the COS cells after culture.

Expression construct	Number of somites before culture	Number of embryos treated	Location of cells after culture	Ectopic expression of *HNF3-β*
shh full length	Pre-somite	12	No cells (1) Attached to ectoderm, either surface or neural (3) Foregut (3) Foregut and grafted into ventral mesoderm (4) Grafted into mesoderm adjacent to midbrain, both ventral and dorsal mesoderm (1)	Yes
shh 198 aa	Pre-somite	9	No cells (5) Attached to neurectoderm (1) Grafted into ventral mesoderm (2) Grafted into dorsal neurectoderm (1)	Yes

Figure 7.2 Ectopic expression of *HNF3-β* induced by *Shh* misexpression. **(A)** Lateral view of an embryo showing the location of grafted COS cells after 24 hours of culture. Labelled COS cells were grafted into the mesoderm and extend to underlie both ventral and dorsal mesoderm. **(B)** Dark field picture of 2 embryos, viewed from the anterior, after whole mount in situ hybridisation to *HNF3-β* mRNA. The embryo on the left shows the normal distribution of transcripts while the embryo on the right shows a dorsally expanded domain of expression (arrowhead). The embryo on the right is the same as that shown in (A). **(C)** Dorsal view of 2 embryos showing *HNF3-β* mRNA localisation. The embryo on the right has COS cells located within the dorsal neurectoderm and these are surrounded by ectopic *HNF3-β* transcripts (arrowhead). **(D)** A lateral view of an embryo which contained COS cells but did not show ectopic expression of *HNF3-β*. COS cells are located at three sites: (a) grafted into ventral mesoderm; (b) the foregut, and; (c) attached to the surface ectoderm. Scale bar, 300 μm (B,C); 200 μm (A,D).

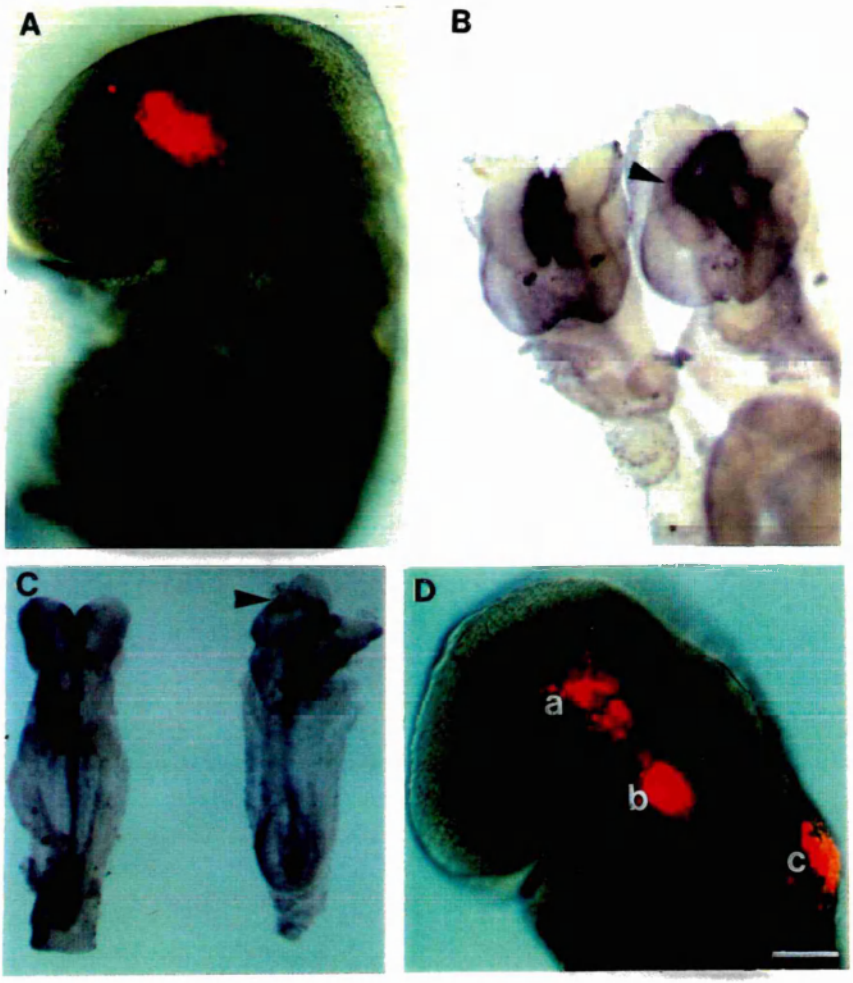
A
B
C
D
a
b
c

embryos in which COS cells were located dorsally after culture. However, the results presented here suggest that transfected COS cells can be used to deliver secreted proteins within the mouse embryo and that gene expression can be altered in a manner consistent with that obtained from misexpression via transgenesis.

7.4 RESULTS OF ECTOPIC EXPRESSION OF BMP-7

Location of COS cell grafts

In all of the experiments reported here COS cells were grafted into the cranial mesoderm of embryos with 3- to 8-somites. Since the region between the preotic and the otic sulcus corresponds to the future location of rhombomeres 3 and 4 (Trainor and Tam, 1995), these two indentations were used as a guide to ensure grafts were placed in the vicinity of prospective hindbrain. Six embryos which had received grafts were fixed immediately and the location of the cells determined. As shown in Figure 7.3 the COS cells were placed into the mesoderm adjacent to the neurectoderm of the developing hindbrain.

Morphology of the grafted embryos

In all experiments some embryos received grafts of COS cells which had been transfected with *BMP-7* while control embryos received nontransfected COS cells. In total, nontransfected COS cells were grafted into 51 embryos which had between 3 and 8 somites at the time of grafting. After 24 hours *in vitro* these embryos were dissected, fixed and examined for morphological abnormalities. The embryos developed normally in culture as judged by axis elongation, somite number, and the presence of a beating heart and other organ rudiments. None of the grafted embryos showed gross morphological abnormalities in the cranial region when viewed from either the lateral or dorsal aspect. When these embryos were viewed under fluorescent optics, 38 were found to contain COS cells adjacent to the hindbrain neurectoderm. Two embryos were cryosectioned and the neurectoderm in the region of the COS cells found to be morphologically normal (Figure 7.4).

When COS cells transfected with an expression construct for *BMP-7* were grafted into the mesoderm underlying the developing hindbrain, changes in the neurectoderm occurred. While the embryos developed essentially normally in culture, it was apparent that in a large proportion of embryos the neurectoderm on the grafted side of the hindbrain was distorted, often appearing highly convoluted (Figure 7.4C). The 47 embryos which had received an experimental graft were viewed under fluorescent optics and all embryos that showed overt deformity (38) had COS cells within the adjacent mesoderm. Two embryos were cryosectioned and the neurectoderm in the region of the COS cells found to be kinked in a manner consistent with an overproduction of neurectoderm (Figure 7.4D).

Figure 7.3 Location of grafted cells. **(A)** The grafting procedure. An embryo is held using a pair of forceps and the COS cells micropipetted into the mesoderm as close as possible to the neurectoderm. **(B)** A 4-somite embryo. Immediately after grafting the fluorescent COS cells the embryo was fixed, and yolksac and amnion removed so that the position of the incorporated cells could be determined. The cells are located between the preotic sulcus and the otic sulcus. **(C)** A transverse section through a 6-somite embryo which was fixed immediately after the grafting procedure. The fluorescent COS cells are located in the mesoderm underlying the hindbrain neurectoderm. pos: preotic sulcus, os: otic sulcus. Scale bar 200 μm (B); 100 μm (C).

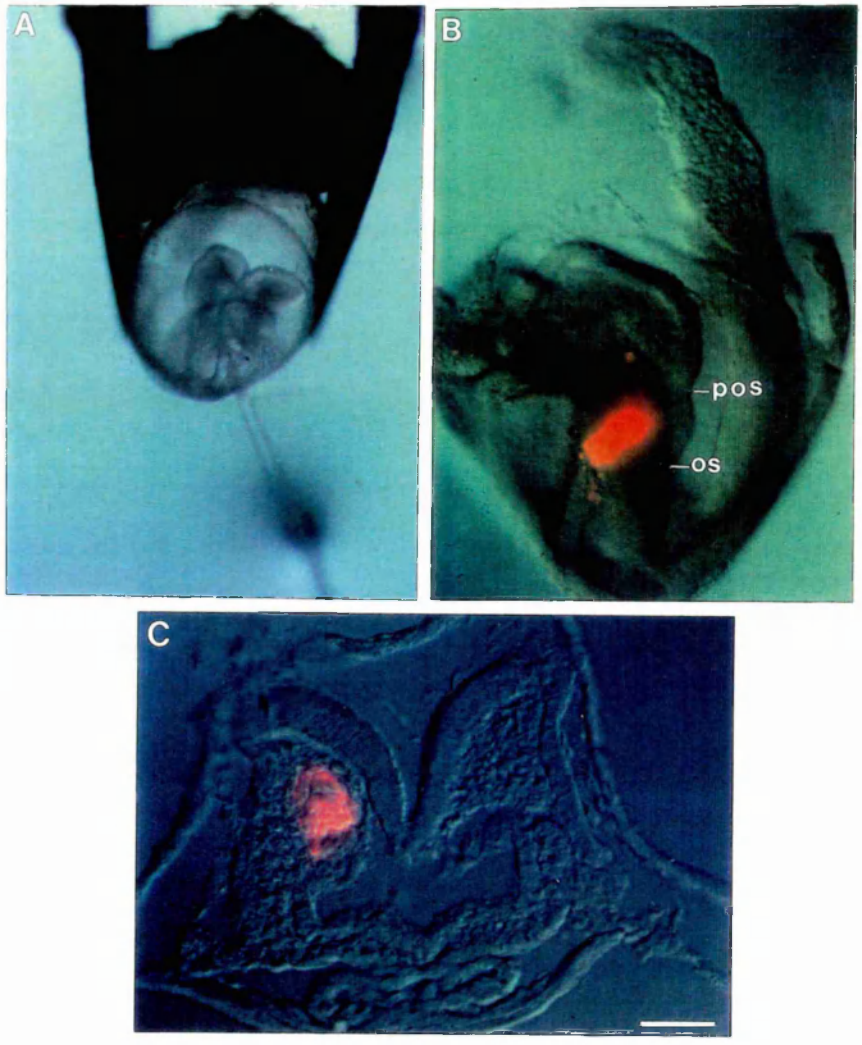
A
B
pos
os
C

Figure 7.4 Morphology of grafted embryos. (A) Embryo which received a control graft, after 24 hours culture. **(B)** Transverse section through the region of grafted nontransfected COS cells. **(C)** Embryo which received a graft of BMP-7 transfected COS cells, after 24 hours culture. The deformity, adjacent to the COS cells is marked with an arrow. **(D)** Transverse section through the hindbrain in the region of grafted BMP-7 transfected COS cells. Scale bar 400 μm (A,C); 100 μm (D); 75 μm (B).

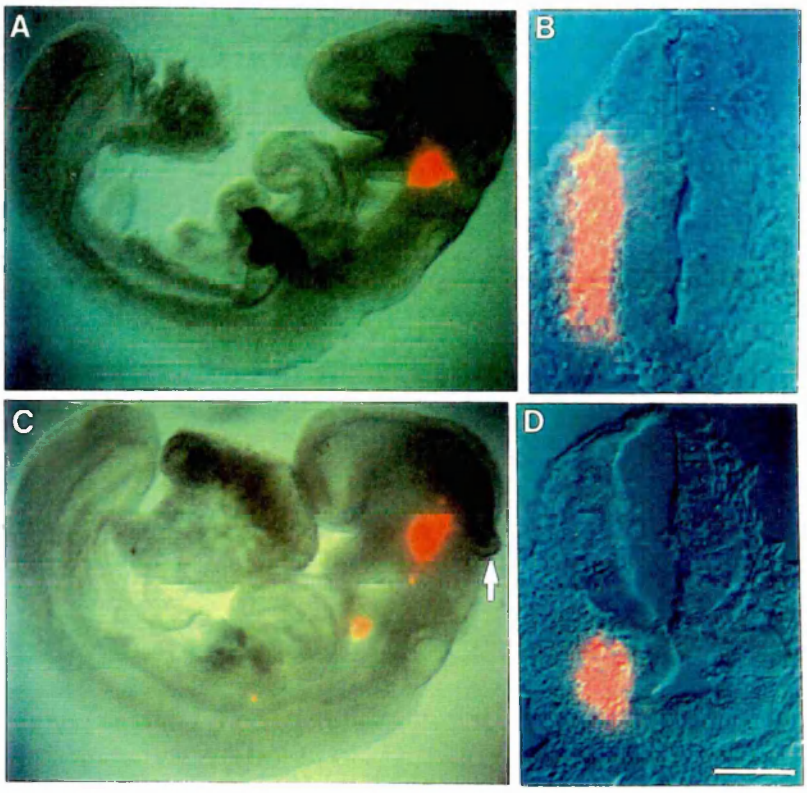
A
B
C
D

Dorsal-ventral pattern in the neurectoderm adjacent to the COS cells

To determine whether dorsal-ventral pattern in the grafted embryos was altered they were examined using whole mount *in situ* hybridisation to a variety of genes which show restricted expression patterns in the developing neural plate. While the expression pattern of potential markers has previously been reported, in many cases detailed information about expression of these molecules in the hindbrain region of 3- to 20-somite embryos is not available. Thus *in situ* hybridisation to a variety of mRNAs was undertaken and *Shh*, *Pax-3*, *Msx1* and *AP-2* chosen as suitable markers. The details of the mRNA distribution of these genes is not the subject of this chapter, however, some of the information obtained from the whole mount *in situ* analysis is not published elsewhere, and for ease of reference, a summary of the expression of these genes is provided in Appendix II.

Expression of dorsal markers in the ventro-lateral neurectoderm

BMP molecules have previously been implicated in the differentiation of dorsal neurectoderm structures (Liem et al., 1995), therefore *Msx1*, which in 8.5 dpc wildtype embryos is known to be expressed in a narrow domain within the dorsal neural tube (Hill et al., 1989), was chosen as a marker. The analysis of the wildtype expression pattern of *Msx1* showed that in the mouse neural plate *Msx1* transcription is initiated in a narrow lateral domain during headfold stages of development and upon neural tube closure transcripts are seen in the roof plate of the neural tube. During normal development *Msx1* transcripts never cross the ventral midline of the cranial neurectoderm, as shown in Appendix II.

The localisation of *Msx1* mRNA was examined in embryos which received a graft of nontransfected COS cells. Embryos in which the cranial neural folds were still open were examined in wholemount and flatmount to determine that the dorsal restriction of *Msx1* was maintained. Sectioning of embryos in which closure of the cranial neural folds was more advanced was used to ascertain that *Msx1* expression in the roof plate was maintained. In all 11 embryos analysed, no differences were noted in any features of *Msx1* expression (Figure 7.5 and Table 7.3). In contrast to this in all embryos analysed which had received a graft of *BMP-7* transfected COS cells there was an enlargement in the amount of tissue which expressed *Msx1* (Figure 7.5C). In mildly affected embryos this was seen as a shift of the *Msx1* hybridisation signal to a more ventral level. In the embryos which appeared very distorted not only was this shift in expression seen but additional neural tissue was present which invariably expressed *Msx1*. In all of the embryos examined ectopic expression of *Msx1* was either confined to the neurectoderm on the grafted side or was markedly more extensive on this side. The variation in the extent of the phenotype presumably reflects differences in the exact size and/or location of the graft. Figure 7.5D shows a flat mount preparation of an embryo in which the grafted side shows additional neural tissue and in rhombomere 3 there is a ventral shift in the expression domain of *Msx1* on both sides of the neurectoderm.

Figure 7.5 *Msx1* and *AP-2* mRNA localisation. **(A)** Dorsal view of an embryo which received a graft of nontransfected COS cells, to the left side, showing *Msx1* mRNA localisation. *Msx1* transcripts are confined to the dorsal neurectoderm and rhombomeres 3 and 5 exhibit increased transcript levels. **(B)** Lateral view of the embryo in (C), showing the location of the *BMP-7* transfected COS cells. **(C)** Dorsal view of the embryo in (B) showing the expanded expression domain of *Msx1* on the grafted (left) side. **(D)** Flat mount of hindbrain neurectoderm of an embryo which received a graft of BMP-7 transfected COS cells to the left side. The *Msx1* expression domain expands ventrally in rhombomere 3 on both the grafted and non grafted sides. On the grafted side there is additional neural tissue which also expresses *Msx1* (arrow). **(E)** Transverse section through the hindbrain of an embryo which received a BMP-7 graft (left side) showing the ventral shift of the *Msx1* expression domain and additional neural tissue expressing *Msx1*. **(F)** Lateral view of an embryo showing the location of nontransfected COS cells. **(G)** Transverse section through the grafted region of the embryo in (F) showing *AP-2* expression. **(H)** Lateral view of an embryo showing the location of the *BMP-7* transfected COS cells. **(I)** Transverse section through the grafted region of the embryo in (H) showing ventral *AP-2* expression and *AP-2* positive cells exiting the neurectoderm at two sites on the left side of the neural tube. r: rhombomere. Scale bar 450 μm (A,C); 300 μm (B,F,H); 150 μm (D); 100 μm (G,I); 75 μm (E).

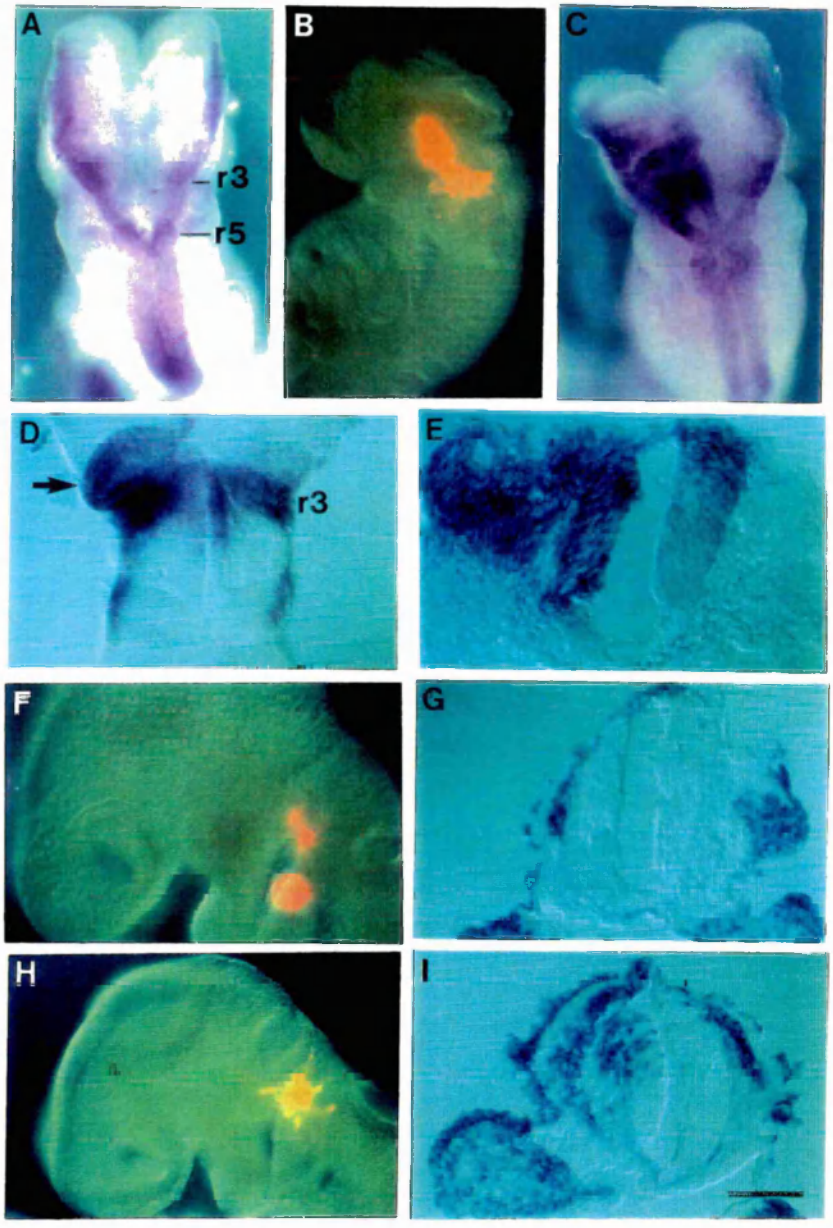
A
r3
r5
B
C
D
r3
E
F
G
H
I

Table 7.3 Ectopic expression of *BMP-7* in the 8.5 dpc embryo. COS cells were grafted into hindbrain mesoderm and after recording the location of the grafted cells mRNA localisation of the marker genes listed was examined. **(1)** In general all embryos examined in whole mount were subsequently examined in either flat mount or section however in the case of *Msx1*, all necessary information could be collected from whole mount specimens of younger embryos. Thus some embryos (6 which had received nontransfected COS cells and 2 which had received BMP-7 transfected COS cells) were examined only in whole mount. **(2)** The neural folds of this embryo were damaged slightly during whole mount in situ hybridisation, it is most likely that absence of Pax-3 expression in this region is due to physical loss of the tissue.

Grafted Cells	Marker gene	Number of embryos examined: Wholemount	Flatmount	Section	Abnormalities detected
Non-transfected	*Msx1*	11	1[(1)]	4	None (11)
	Pax-3	8	5	3	None (8)
	Shh	3	0	3	None (3)
	AP-2	4	0	4	None (4)
BMP-7 transfected	*Msx1*	6	1[(1)]	3	Ventralised Msx-1 expression only (2) Ventralised expression + extra tissue (4) Expanded branchial arch expression (5)
	Pax-3	8	5	3	None (7) Loss of expression in rostral hindbrain (1)[(2)]
	Shh	4	1	3	Decreased floor plate expression (4)
	AP-2	4	0	4	Ventralised AP-2 expression only (2) Ventralised expression + ventral neural crest (2)

The analysis of *Msx1* expression in the neurectoderm suggests that the ventro-lateral neurectoderm has taken on characteristics normally associated with the dorsal aspect of the neurectoderm. Cells in the dorsal region of the neural tube give rise not only to dorsal neural tube cells but also to the neural crest population (Chan and Tam, 1988). Therefore, the pattern of mRNA accumulation of two genes expressed in different subsets of the neural crest was examined. In wildtype embryos *Msx1* expression is seen in the post-migratory neural crest cells that populate the branchial arches and the dorsal limit of this expression is never more dorsal than the base of each arch. Grafts of nontransfected COS cells did not result in any alteration in *Msx1* transcript accumulation in the branchial arches. However, in 5 of the 6 embryos in which *BMP-7* transfected COS cells were grafted and *Msx1* mRNA localisation examined, the domain of *Msx1* expression in the branchial arches extended more dorsally on the grafted side than on the non grafted side, suggesting increased production of neural crest cells (Table 7.3). The sixth embryo was developmentally less advanced, having only 10 somites after culture, and no hybridisation signal was evident in the branchial arches on either the grafted or nongrafted side.

To further examine neural crest production at the site of the graft, *AP-2* expression was examined. The AP-2 transcription factor is expressed in the surface ectoderm and in the dorsal neurectoderm from early neural plate stages and when at the 5-somite stage neural crest begins to emigrate from the hindbrain region it is expressed in the migratory cells (Mitchell et al., 1991). In embryos which had received a graft of nontransfected COS cells no ventral shift in *AP-2* expression was seen. In contrast, as shown in Table 7.3, of the 4 embryos which received a graft of *BMP-7* transfected COS cells all showed ectopic expression of *AP-2*. In all cases *AP-2* was expressed in a more ventral location in the neurectoderm than in unoperated embryos. In the 2 embryos in which this was most pronounced *AP-2* expressing crest was located adjacent to ventro-lateral neurectoderm (Figure 7.5). Taken together with the *Msx1* expression it appears that a sustained ventro-lateral source of BMP-7 has caused the overlying neurectoderm to adopt dorsal characteristics.

Decreased expression of ventral markers in the midline neurectoderm

Experiments in chick embryos have shown that when an ectopic notochord is grafted to a dorsal site, activation of ventral markers is induced (Yamada et al., 1991). However, expression of dorsal markers persist (Artinger and Bronner-Fraser, 1992). Since the graft of *BMP-7* transfected COS cells appeared to have enlarged the dorsal domain, it was important to ascertain whether ventral markers were affected. *Shh*, which is believed to be essential for development of the floor plate, is expressed in the developing notochord from the early headfold stage of development and expression in the floor plate is initiated in the midbrain region of embryos with 8-somites. This floor plate expression quickly spreads along the axis such that by 10 somites the ventral midline of the hindbrain neurectoderm is

expressing *Shh* (Echelard et al., 1993). Of the 3 embryos examined for the expression of *Shh* after grafting nontransfected COS cells, no alterations were noted in the localisation of *Shh* (Figure 7.6 and Table 7.3). In contrast, in all 4 of the embryos which had received grafts of *BMP-7* transfected COS cells it was evident that normal levels of expression of *Shh* in the notochord were maintained, but in the floor plate adjacent to the graft expression was greatly diminished.

Pax-3 expression is unaffected by ectopic expression of BMP-7

Pax-3 is expressed in the dorsal half of the neural tube in both the mouse and the chick (Goulding et al., 1991; Goulding et al., 1993), and experiments in the chick have identified *Pax-3* as a gene whose dorsal restriction may be primarily regulated by the notochord expression of *Shh* (Goulding et al., 1993; Liem et al., 1995). However, it has also been shown that BMP molecules can upregulate expression of *Pax-3* in chick spinal cord which is already expressing low levels of *Pax-3* (Liem et al., 1995). Unlike the chick, at no level of the mouse cranial or spinal neurectoderm does *Pax-3* expression cross the ventral midline in embryos between the onset of *Pax-3* transcription and the 20-somite stage (Appendix II). This provides the opportunity to ask whether BMP-7 is capable of eliciting *Pax-3* expression in neurectoderm which otherwise would not express *Pax-3*, but which is competent to express other dorsal markers. In all embryos which had received grafts of either nontransfected or *BMP-7* transfected COS cells, *Pax-3* expression in the hindbrain region remained unaltered on the grafted side compared to the non grafted side (Figure 7.7 and Table 7.3). Interestingly, the whole mount *in situ* hybridisation analysis of *Pax-3* expression in the developing hindbrain region showed that *Pax-3* is not expressed in the roof plate at all levels of the hindbrain (see Figure 7.7) although it is detected throughout the roof plate at other rostro-caudal levels.

Increased area of the neurectoderm

From analysis of the experimental embryos it was obvious that the volume of the neurepithelium is increased in the region of the graft. The increase in size may result from an increase in the volume of the individual cells, or from an increased number of cells. A nuclear stain was used to distinguish between these possibilities: if cell volume increases, the density of nuclei will decrease. The nuclear density was sampled at 4 sites in each embryo: on both halves of the neurectoderm adjacent to the COS cells, and on both halves of the neurectoderm at a site distant from the graft. In each embryo 3-8 sections were scored at each site. The mean nuclear density of the neurectoderm adjacent to the graft was compared to that at each of the 3 other sites. For each comparison the significance of difference was determined by Student's *t*-test. Table 7.4 shows that the mean nuclear density adjacent to the graft was not significantly different from that at any of the 3 other sites. Thus the neurectoderm expansion results from an increase in cell number. The nuclear stain used in these experiments (DAPI) also allows identification of both mitotic cells and apoptotic cells.

Figure 7.6 *Shh* mRNA localisation. **(A)** Lateral view of the embryo in (B), showing the location of the nontransfected COS cells. **(B)** Lateral view of the embryo in (A) showing that the expression of *Shh* remains unaltered in the region of the graft. **(C)** Transverse section through the hindbrain region of an embryo with a control graft showing *Shh* expression in the notochord and floor plate. **(D)** Lateral view of the embryo in (E), showing the location of the *BMP-7* transfected COS cells. **(E)** Lateral view of the embryo in (D), *Shh* expression is maintained in the hindbrain notochord but is depleted in the floor plate in the region of the graft (arrow). **(F)** Transverse section through the hindbrain of an embryo which received a graft of *BMP-7* transfected COS cells to the left side showing diminished floor plate expression of *Shh*. Scale bar 450 μm (B,E); 300 μm (A,D); 75 μm (C,F).

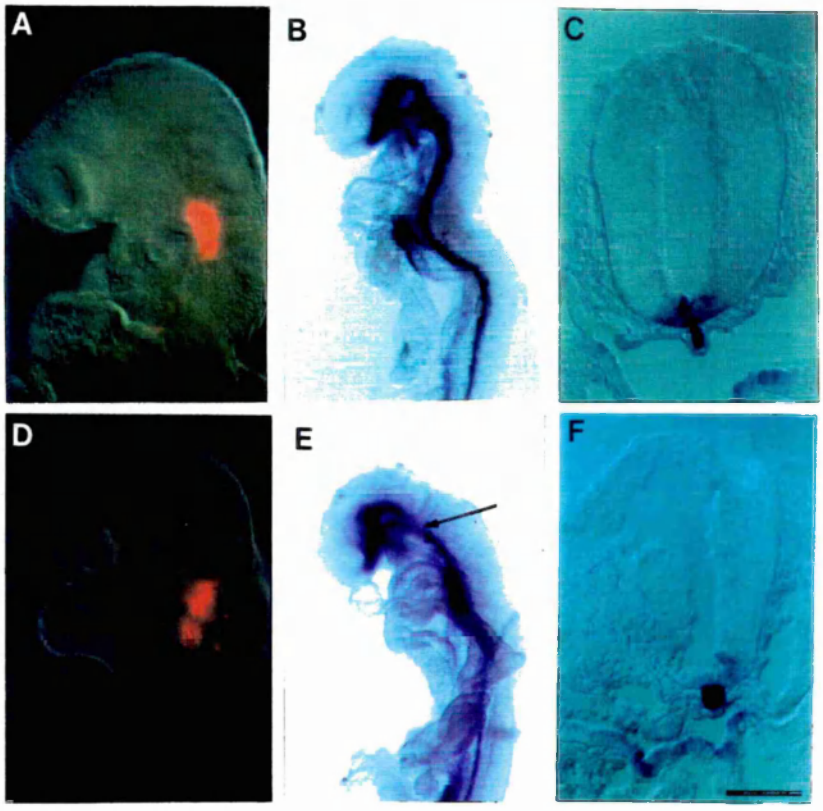
A
B
C
D
E
F

Figure 7.7 ***Pax-3*** **mRNA localisation.** **(A)** Transverse section through the hindbrain of a wildtype embryo showing lack of *Pax-3* transcripts in the roof plate. **(B)** Dorsal view of an embryo which received a graft of nontransfected COS cells, to the left side, showing *Pax-3* expression. **(C)** Dorsal view of an embryo which received a graft of *BMP-7* transfected COS cells to the left side showing *Pax-3* expression. The neurectoderm is expanded in the region of rhombomere 2. **(D)** Flatmount of the embryo shown in (B), the expression domain of *Pax-3* is unaltered in the region of the graft (arrow) relative to the non grafted side. r: rhombomere. Scale bar 450 μm (B,C,D); 50 μm (A).

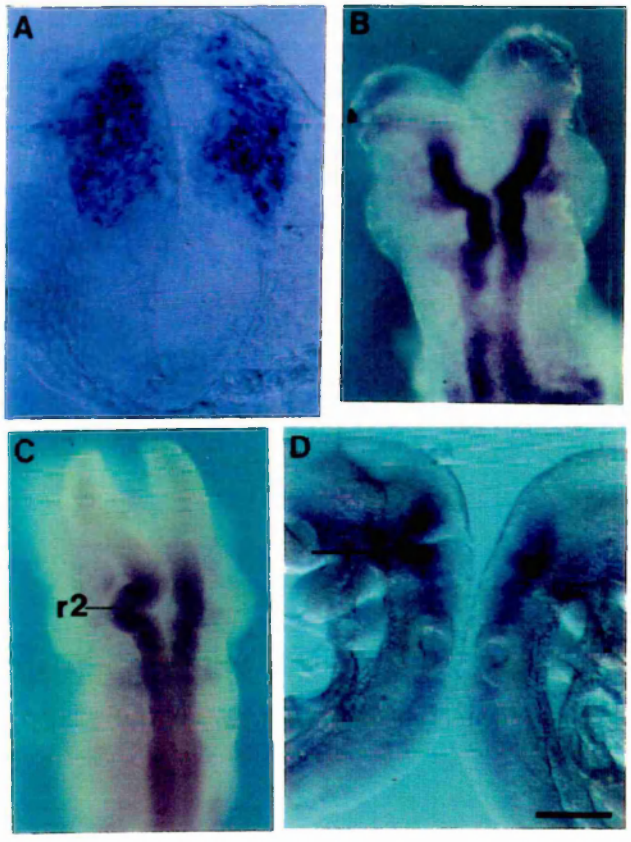
A
B
C
r2
D

Table 7.4 Neurectoderm mean nuclear density. Values are presented as the means of the nuclear density at each of the sites listed, ± s.e.m. Student's *t*-test was performed to compare the mean nuclear density at sites adjacent to the graft (bold lettering) with that on the nongrafted side and distant from the graft. (1): $p > 0.05$; (2): $p > 0.1$.

Table 7.5 Neurectoderm relative mitotic frequency. Values are presented as the ratio of the relative mitotic frequency on the grafted side of the neurectoderm, to the relative mitotic frequency on the nongrafted side, ± s.e.m. Student's *t*-test was performed to compare the relative mitotic frequency adjacent to the graft with the corresponding frequency distant from the graft. (1): $p < 0.01$.

Location	Grafted side	Nongrafted side
Nontransfected		
Distant from graft	32.7±0.7(1)	33.5±0.8(2)
Adjacent to graft	**34.5±0.6**	34.2±0.7(2)
BMP-7 transfected		
Distant from graft	32.9±0.8(2)	33.7±0.9(2)
Adjacent to graft	**33.6±1.5**	31.4±0.4(2)

Grafted Cells	Neurectoderm adjacent to graft	Neurectoderm adjacent to the otic vesicle
Nontransfected	1.16 ± 0.18	1.05 ± 0.143
	1.65 ± 0.56	0.94 ± 0.19
	0.88 ± 0.09	1.44 ± 0.32
BMP-7 transfected	2.16 ± 0.18(1)	1.35 ± 0.28
	2.47 ± 0.68(1)	1.34 ± 0.23
	2.66 ± 0.54(1)	1.23 ± 0.19

From the analysis of the DAPI stained sections no alteration in the proportion of apoptotic cells was noted. However in the region of BMP-7 transfected COS cells an abundance of mitotic figures was apparent on the ventricular surface.

To quantify this, the relative mitotic frequency was determined as described in materials and methods. When this was measured at 30 μm intervals along the hindbrain (data not shown) it was found to vary in a manner consistent with that reported for chick neurectoderm (Guthrie et al., 1991). This indicated that centres of increased proliferation, corresponding to the rhombomeres, are probably also found in the mouse. Despite this variation along the axis, at any one point the relative mitotic frequency on both sides of the neurectoderm should be the same. Therefore to determine whether there are more mitotic figures adjacent to the *BMP-7* transfected COS cells, a ratio of the relative mitotic frequency on the grafted side to that on the nongrafted side was calculated. For each embryo this ratio was calculated for 8-10 sections corresponding to the region of the grafted COS cells and for 8-10 sections at the level of the otic vesicle. For each set of data the significance of difference was determined by Student's *t* -test. Table 7.5 shows that in embryos in which nontransfected COS cells were grafted there was no difference between the grafted and nongrafted side of the neurectoderm either at the site of the graft or remote from the graft. In contrast to this, relative mitotic frequency increased by more than two-fold in the vicinity of grafted *BMP-7* transfected COS cells, whereas outside of the region of the graft the relative mitotic frequency did not increase. These data taken together with the increase in cell number are consistent with BMP-7 causing increased proliferation of the neurectoderm.

7.5 DISCUSSION

This study shows for the first time that the activity of secreted molecules can be examined in the early mouse embryo by the precise grafting of cells expressing the desired molecule. The ectopic expression study identifies three distinct activities of BMP-7 in the mammalian hindbrain. Firstly BMP-7 promotes dorsal cell fate and in general this is consistent with the activity identified for BMP-7 using *in vitro* assays of chick spinal cord development (Liem et al., 1995). The two other, previously unidentified activities, are interference with accumulation of *Shh* transcripts in the floor plate and an ability to increase cell number in the neurectoderm. When these data are combined with the expression information presented in Chapter 4, several functions are suggested for BMP-7 during the early establishment of the central nervous system.

Dorsal differentiation of the cranial neurectoderm

In vertebrates the first differentiated cell population to arise from the lateral neurectoderm is the neural crest population (Nichols, 1981; Tosney, 1982; Sadaghiani and Thiébaud, 1987),

which in most vertebrates emerges shortly after closure of the neural tube. In the mouse embryo, the cranial neural crest is formed unusually early: the first crest emigrates from the hindbrain region in the 5-somite embryo and all of the neural crest cells have left the hindbrain neurectoderm by the time the neural folds fuse to form the neural tube (Serbedzija et al., 1992). Thus the influences which promote dorsal differentiation in this region must operate in concert with, or very soon after, the signals which induce the anterior epiblast to adopt a neural fate. The acquisition of dorsal neurectoderm fate has previously been studied in the chick spinal cord. It is proposed that two mechanisms interact to generate dorsal restriction of gene products: the expression of early patterning genes is regulated primarily by ventral repression, mediated by notochord derived Shh and later, positive signals possibly mediated by surface ectoderm derived BMP molecules promote the differentiation of definitive dorsal cell types such as neural crest cells (Liem et al., 1995).

During the earliest stages of mouse cranial neurectoderm development, ventral repression of dorsally restricted genes does not appear to be necessary. *Msx1* and *AP-2* transcripts are first localised to the lateral edge (future dorsal) of the cranial neural plate at the headfold stage of development. At this stage of development neither gene is expressed in the midline neurectoderm above the node (Appendix II) and their transcripts are never seen in the midline neurectoderm of the cranial neural plate. Moreover, it is clear that ectopic expression of BMP-7 is sufficient to elicit the expression of both *Msx1* and *AP-2* in neural tissue which otherwise would never express these genes. Furthermore this occurs in the presence of a notochord expressing *Shh*. These data argue that in the mouse cranial neurectoderm, notochord derived Shh is not the major factor regulating *Msx1* expression as has been proposed for the chick spinal cord (Liem et al., 1995). Possibly, differentiation of the cranial neural crest population is initiated before ventral repression is in operation: both *Msx1* and *AP-2* expression begin either before, or concomitant with, the notochord expression of *Shh* (Echelard et al., 1993). The early acquisition of dorsal cell fate which occurs in the cranial region may be more dependent upon a BMP mediated signal and certainly the early onset of *BMP-7* expression in the surface ectoderm is consistent with it playing such a role.

BMP-7 is not sufficient to elicit the expression of all genes which show a dorsal restriction during normal development. The dorsal-ventral domain of *Pax-3*, a gene whose expression in the mouse embryo is initiated later than that of *Msx1* and *AP-2*, is not altered in response to BMP-7. However the possibility that the *level* of *Pax-3* expression may be altered by BMP-7 as it can be in the chick spinal cord (Liem et al., 1995) cannot be ruled out. The dorsal restriction of *Pax-3* appears to be primarily regulated via negative signals which derive from the notochord in both the chick (Goulding et al., 1993; Liem et al., 1995) and the mouse spinal cord (Ang and Rossant, 1994; Rashbass et al., 1994). It is likely that in the cranial region of the mouse embryo *Pax-3* expression is also repressed by the notochord

and that BMP-7 cannot interfere with this interaction. In the chick spinal cord, Shh can mimic the ability of the notochord to decrease the level of Pax-3 expression in dorsal neurectoderm explants (Liem et al., 1995). The assay presented here suggests that ventral repression of *Pax-3* expression continues in the absence of high levels of floor plate expression of *Shh*.

Timing of cranial floor plate induction

BMP-7 is expressed in axial mesendoderm and the midline neurectoderm at a stage when the neurectoderm should still be labile with respect to dorsoventral pattern. What is the function of a midline 'dorsalising' signal? One possible function is suggested by the overexpression of *Shh* and *HNF3-β* in *Xenopus* embryos which demonstrates that *in vivo* mechanisms exist which restrict the timing of floor plate induction (Ruiz i Altaba et al., 1995a). It is possible that BMP-7 regulates the timing of floor plate induction in the hindbrain region. It is believed that the initiation of floor plate development occurs in response to a contact dependent signal emanating from the notochord (Placzek et al., 1993), and that Shh mediates this (Echelard et al., 1993; Roelink et al., 1994). An immediate early response to induction is expression of the winged helix transcription factor *HNF3-β* (Ruiz i Altaba et al., 1995b) which, in turn, is sufficient for the activation of *Shh* floor plate expression (Ruiz i Altaba et al., 1993; Sasaki and Hogan, 1994; Ruiz i Altaba et al., 1995a). In the cranial region of the mouse embryo there is a considerable time-lag between the notochord expression of *Shh* and the onset of floor plate expression of *Shh*. For example in the developing hindbrain region *Shh* first appears in the notochord some fifteen hours before the onset of floor plate expression of *Shh*, and *HNF3-β* is present in the floor plate for some twelve hours before *Shh* is expressed (Echelard et al., 1993). Once *Shh* floor plate expression is initiated, it spreads quickly along the axis, so that in the posterior of the embryo there is much less delay between the notochord and floor plate expression of *Shh*. The data presented here show that the disappearance of *BMP-7* from the ventral hindbrain precedes the appearance of *Shh* in this region, and that BMP-7 is capable of interfering with *Shh* expression in the floor plate. The midline expression of *BMP-7* may delay initiation of cranial floor plate development until a sufficient proportion of the embryonic axis has been generated to allow relatively synchronous ventral differentiation.

Growth of the cranial neurectoderm

Cell culture studies carried out with recombinant BMP-7 have shown that this molecule inhibits proliferation of embryonal carcinoma cells (Andrews et al., 1994) but stimulates the proliferation of osteoblasts (Knutsen et al., 1993; Chen et al., 1995). However little is known about the ability of BMP molecules to regulate cell growth during embryogenesis. Mice lacking either functional BMP-4 or a BMP type I receptor fail to undergo gastrulation. In each case the primary defect may be decreased proliferation of the pre-gastrulation epiblast, suggesting that *in vivo* a BMP signalling pathways may mediate cell growth

(Mishina et al., 1995; Winnier et al., 1995). At later stages of development, BMP-4 has been shown to stimulate apoptosis in prospective neural crest cells in odd numbered rhombomeres during the establishment of the chick hindbrain (Graham et al., 1994). Because BMP-4 is not expressed in the mouse hindbrain (Winnier et al., 1995), the relevance of this observation to the development of the mammalian cranial neurectoderm development is not clear. The assay reported here provides the first evidence that BMP molecules may stimulate growth of the neurectoderm, although from this assay it is impossible to distinguish whether this effect is specific to all neurectoderm or only to dorsal neurectoderm. However, the finding that BMP-7 causes expansion of the neurectoderm, combined with its expression surrounding the cranial neural plate during the headfold stage of development makes it tempting to speculate that BMP-7 could be involved in the differential growth of the headfold neurectoderm relative to the trunk neurectoderm during the early stages of neural development.

Recently two laboratories reported the production of mice which carry null alleles of BMP-7. While mice homozygous for the mutations appear to have defects consistent with BMP-7 participating in cell growth and/or survival during embryogenesis, the abnormalities observed are limited to limb, eye and kidney development. The mice do not have defects consistent with an absolute requirement for BMP-7 during establishment of the central neural system (Dudley et al., 1995; Luo et al., 1995). The conflict between these findings and the data presented here highlights the difficulties of experimental analysis of single members of multigene families. It is known, for example that BMP-2 is localised to the surface ectoderm in a manner which overlaps with BMP-7 (Chapter 4; Lyons et al., 1995). It is possible that embryos lacking both these gene products may exhibit dorsal neural tube defects. However, since embryos lacking BMP-2 fail to develop beyond gastrulation (cited in Hogan, 1995), such an effect will have to await the construction of a conditional BMP-2 mutation, unless a haploinsufficiency of BMP-2 can be observed in BMP-7$^{-/-}$ embryos.

The studies presented here identify several potential functions for the signalling molecule, BMP-7, during early neural development and highlight differences between the establishment of the cranial and spinal neurectoderm. The initial restriction of expression of *BMP-7* to the anterior region of the developing embryo may be relevant to several features which are unique to cranial development. These features include the rapid growth of the headfolds, the early generation of the neural crest from this region, and the delay in the transfer of expression of the *Shh* signalling molecule between the notochord and the floor plate. The establishment of an assay with which the function of secreted factors may be tested in different locations in the mouse embryo will contribute to the understanding of the roles of such molecules.

Chapter 8

General Discussion

8.1 SUMMARY OF RESULTS

The general aims of this thesis were to investigate the hypothesis that TGF-β superfamily molecules function during mouse embryogenesis and to establish relatively simple gain of function assays of secreted molecules in the mouse embryo. The first part of the experimental work demonstrates that several TGF-β superfamily members are expressed during mouse embryogenesis. In the second part of the thesis the potential function of two of these molecules is investigated using different overexpression assays. One of these assays did not prove to be a reliable strategy for the investigation of *Vgr-2* function. However, the experiments presented in this section do provide a framework for establishing a feasible gain of function approach which capitalises on the unique ability of murine ES cells to contribute to normal embryonic development after continuous culture, as will be discussed below. The second strategy proved to be more useful and thus has revealed information about the potential mechanisms by which the mammalian cranial neural plate develops. The major experimental findings and perspectives are summarised below.

Activin, *follistatin* and mouse embryogenesis

Surprisingly, given the strong case that activin acts as a morphogen to direct mesoderm fate in *Xenopus*, activin transcripts are not detected in the mouse embryo during gastrulation (Chapter 3). Furthermore, other laboratories have generated targeted mutations in the inhibin subunit genes and analysis of the mice has not uncovered a requirement for activin A,B or AB during embryogenesis (Vassalli et al., 1994; Matzuk et al., 1995a). However, the activin-binding protein, *follistatin*, is highly expressed during germ layer formation and early organogenesis in the mouse embryo. This finding prompted the search for activin related molecules which *are* expressed during gastrulation which led to the isolation of a cDNA for *BMP-7*. Interestingly, at the early headfold stage of development *follistatin* and *BMP-7* have complementary embryonic expression patterns (compare Figure 4.3D and Figure 3.2C). Furthermore it is now known that follistatin can antagonise BMP-7 function (Yamashita et al., 1995). This situation is reminiscent of the *Drosophila dpp/sog* interaction reviewed in the Introduction. In either case an inducing molecule (*dpp* or *BMP-7*) and an antagonist (*sog/follistatin*) are expressed in adjacent but nonoverlapping domains. An experimental system similar to the one reported in Chapter 7, may now be used to investigate whether *follistatin* can neutralise the effects of *BMP-7* during mouse embryogenesis.

Vgr-2 and mouse embryogenesis

The second candidate mesoderm inducing factor investigated in this thesis was *Vgr-2*. *Vgr-2* is expressed at the onset of mesoderm formation in the mouse embryo and ES cells which overexpress *Vgr-2* secrete a mesoderm inducing factor, presumably Vgr-2. Yet when these

cells are introduced into the mouse embryo no ectopic mesoderm formation is detected. It may be that some form of selection for *Vgr-2* expression occurs, which results in *Vgr-2* expressing cells preferentially colonising mesoderm tissues. However, the interpretation of this experiment is hampered by the uncertain behaviour of heterologous regulatory elements in the vector, both in ES cells and in the embryo.

While gain of function assays in the mouse embryo have so far failed to identify mesoderm inducing factors, if stable gene expression could be achieved in ES cells, the approach used here could prove extremely fruitful. The use of endogenous promoters would circumvent these problems. The targeted replacement of a ubiquitously expressed gene, with a cDNA coding for the putative inducing molecule should generate the appropriate constitutively expressing ES cell lines. Provided that loss of one copy of the targeted gene is known to be developmentally neutral, such cell lines could then be used for embryonic overexpression studies.

BMP molecules and mouse embryogenesis

A large body of experimental data, from *Drosophila, Xenopus*, chick and mouse suggests that BMP molecules act as endogenous embryonic inducing factors. The expression studies presented in Chapter 4, in combination with the expression pattern of BMP-4 (Jones et al., 1991; Winnier et al., 1995), suggest that BMP molecules may contribute to the formation of vertebrate embryonic axes. This is supported by the findings presented in Chapter 7. Ectopic expression of BMP-7 induces expression of dorsal markers in ventro-lateral neurectoderm and interferes with the endogenous ventral signals. BMP molecules in the mouse embryo may therefore promote dorsal neural differentiation by the opposition of a ventral inducing signal as has been proposed in the chick (Liem et al., 1995). The work presented here may be used to design experiments which further investigate the function of *BMP-7* . For example, the finding that *BMP-7* interferes with ventral signalling pathways could be pursued using a transgenic approach to maintain floor plate expression of *BMP-7*. This would allow the ventral inhibition properties of *BMP-7* to be tested at additional rostro-caudal levels. Moreover, the ability of TGF-β superfamily molecules to interfere with the differentiation of motor neurons has been inferred from *in vitro* studies in the chick (Basler et al., 1993). The earliest marker of motor neuron formation (Islet1) is first expressed some twelve hours after the end point of the experiments presented here (Pfaff et al., 1996) but a transgenic approach, (or a further 24 hours of culture) would allow the study of later differentiation events.

In addition, the method for overexpression of secreted molecules described in this thesis may be used to investigate the function of other BMP molecules during embryogenesis. One hypothesis identified by the expression studies in Chapter 4 is that BMP-2 may be important in patterning the anterior mesoderm which will form the heart. This can now be tested using

the COS cell overexpression system and early markers of heart development such as the homeobox containing gene Nkx2.5 (Lints et al., 1993).

8.2 ANALYSIS OF GENE FUNCTION IN VERTEBRATE EMBRYOS

The work presented here provides examples of several features which are intrinsic to the analysis of gene function in vertebrates. Current investigations of gene function in a variety of organisms continue to uncover evidence of conserved tissue interactions between vertebrates, as well as molecular interactions which are conserved throughout invertebrates and vertebrates. This has led to the realisation that information obtained from the study of the molecular interactions which result in cytodifferentiation can be applied to vertebrates. However, it is also obvious that although the study of *Drosophila* and *C. elegans* provide clues with which to approach vertebrate embryogenesis, additional interactions and molecular pathways will also be involved. The multigene nature of the vertebrate TGF-β superfamily compared to that of *Drosophila* (discussed in the Introduction), provides a good example of such molecular diversification. Additionally, the difference between the loss of function studies reported for BMP-7 in the mouse embryo (Dudley et al., 1995; Luo et al., 1995) and the results of the overexpression study presented in Chapter 7 highlight the difficulties of analysis of vertebrate gene function.

Of the vertebrate organisms most studied by developmental biologists, the amphibian and chick embryos provide excellent tools for the analysis of tissue interactions through gain of function approaches. However, for these organisms no definitive loss of function approaches are feasible. The use of naturally occurring or synthetic antagonists, dominant negative forms of the protein, antisense RNA and antibody blockades all require extensive prior knowledge of the target protein. Moreover, in each of these strategies, interpretation of the experimental results is hampered by the difficulty of establishing that the function of only the test molecule has been inhibited.

The mouse is the only vertebrate organism in which definitive loss of function experiments can be performed. In order to investigate gene function in vertebrates it is therefore imperative to establish the complementary gain of function approaches in the mouse embryo. While such experiments have previously been performed using transgenic approaches, these rely on the availability of appropriate tissue specific promoters. This thesis demonstrates that the perceived difficulties of manipulating the postimplantation mouse embryo can be overcome and that convenient gain of function assays for secreted molecules can be performed. The method presented in Chapter 7 requires only the cDNA of the putative inducer and is aided by knowledge of the endogenous expression pattern of the test molecule. Therefore, one of the most important aspects of the work presented in this thesis

is that it provides a method with which to continue to investigate the function of secreted molecules. Moreover, the activities so far identified can now be used to establish *in vitro* recombination assays. Together these would provide a range of gain of function approaches with which to assay those factors proposed to act as the local chemical mediators of embryonic inductive interactions. In combination with the powerful molecular genetic approaches already available in the mouse embryo, such studies will enhance our understanding of the mechanisms by which embryonic cells differentiate to generate the complex adult form of vertebrates.

Reference List

REFERENCE LIST

Ackhurst, R.J., Lehnert, S.A., Faissner, A. and Duffie, E. (1990). TGFβ in murine morphogenetic processes: the early embryo and cardiogenesis. *Development* **108**, 645-656.

Adra, C.N., Boer, P.H. and McBurney, M.W. (1987). Cloning and expression of the mouse *pgk-1* gene and the nucleotide sequence of its promoter. *Gene* **60**, 65-74.

Albano, R.M., Arkell, R., Beddington, R.S.P. and Smith, J.C. (1994). Expression of inhibin subunits and follistatin during postimplantation mouse development: decidual expression of activin and expression of follistatin in primitive streak, somites and hindbrain. *Development* **120**, 803-813.

Albano, R.M., Groome, N. and Smith, J.C. (1993). Activins are expressed in preimplantation mouse embryos and in ES and EC cells and are regulated on their differentiation. *Development* **117**, 711-723.

Andrews, P.W., Damjanov, I., Berends, J., Kumpf, S., Zappavigna, V., Mavilio, F. and Sampath, K. (1994). Inhibition of proliferation and induction of differentiation of pluripotent human embryonal carcinoma cells by osteogenic protein-1 (or bone morphogenetic protein-7). *Lab. Invest.* **71**, 243-251.

Ang, S.-L. and Rossant, J. (1993). Anterior mesendoderm induces mouse *Engrailed* genes in explant culture. *Development* **118**, 139-149.

Ang, S.-L. and Rossant, J. (1994). *HNF-3β* is essential for node and notochord formation in mouse development. *Cell* **78**, 561-574.

Ang, S.-L., Wierda, A., Wong, D., Stevens, K.A., Cascio, S., Rossant, J. and Zaret, K.S. (1993). The formation and maintenance of the definitive endoderm lineage in the mouse: involvement of HNF3/*forkhead* proteins. *Development* **119**, 1301-1315.

Anklessaria, P., Teixidó, J., Laiho, M., Pierce, J.H., Greenberger, J.S. and Massagué, J. (1990). Cell-cell adhesion mediated by binding of membrane-anchored transforming growth factor α to epidermal growth factor receptors promotes cell proliferation. *Proc. Natl. Acad. Sci. USA* **87**, 3289-3293.

Anzano, M.A., Roberts, A.B., Smith, J.M., Sporn, M.B. and De Larco, J.E. (1983). Sarcoma growth factor from conditioned medium of virally transformed cells is composed of both type α and type β transforming growth factors. *Proc. Natl. Acad. Sci. USA* **80**, 6264-6268.

Artinger, K.B. and Bronner-Fraser, M. (1992). Notochord grafts do not suppress formation of neural crest cells or commissural neurons. *Development* **116**, 877-886.

Asashima, M., Nakano, H., Uchiyama, H., Sugino, H., Nakamura, T., Eto, Y., Ejima, D., Davids, M., Plessow, S., Cichocka, I. and Kinoshita, K. (1991). Follistatin inhibits the mesoderm-inducing activity of activin A and the vegetalizing factor from chicken embryo. *Roux's Arch. Dev. Biol.* **200**, 4-7.

Attisano, L., Cárcamo, J., Ventura, F., Weis, F.M.B., Massagué, J. and Wrana, J. (1993). Identification of human activin and TGFβ type I receptors that form heteromeric kinase complexes with type II receptors. *Cell* **75**, 671-680.

Basler, K., Edlund, T., Jessell, T.M. and Yamada, T. (1993). Control of cell pattern in the neural tube: regulation of cell differentiation by *dorsalin-1*, a novel TGFß family member. *Cell* **73**, 687-702.

Bassing, C.H., Yingling, J.M., Howe, D.J., Wang, T., He, W.W., Gustafson, M.L., Shah, P., Donahoe, P.K. and Wang, X.-F. (1994). A transforming growth factor β type I receptor that signals to activate gene expression. *Science* **263**, 87-89.

Beddington, R. (1986). Analysis of tissue fate and prospective potency in the egg cylinder. In *Experimental Approaches to Mammalian Embryonic Development.* (eds. J. Rossant and R.A. Pederson), pp121-147. New York, Cambridge University Press.

Beddington, R.S.P. (1981). An autoradiographic analysis of the potency of embryonic ectoderm in the 8th day postimplantation mouse embryo. *J. Embryol. exp. Morph.* **64**, 87-104.

Beddington, R.S.P. (1982). An autoradiographic analysis of tissue potency in different regions of the embryonic ectoderm during gastrulation in the mouse. *J. Embryol. exp. Morph.* **69**, 265-285.

Beddington, R.S.P. (1983). Histogenic and neoplastic potential of different regions of the mouse embryonic egg cylinder. *J. Embryol. exp. Morph.* **75**, 189-204.

Beddington, R.S.P. (1987). Isolation, culture and manipulation of post-implantation mouse embryos. In *Mammalian Development: a practical approach.* (ed. M. Monk), pp43-69. Oxford, IRL Press.

Beddington, R.S.P. (1994). Induction of a second neural axis by the mouse node. *Development* **120**, 613-620.

Beddington, R.S.P. (1996). Seaside signal success. *Trends Genet.* **12**, 237.

Beddington, R.S.P. and Robertson, E.J. (1989). An assessment of the developmental potential of embryonic stem cells in the midgestation mouse embryo. *Development* **105**, 733-737.

Beddington, R.S.P. and Smith, J.C. (1993). Control of vertebrate gastrulation: inducing signals and responding genes. *Curr. Opin. Genet. Dev.* **3**, 655-661.

Berghoffen, J., Scherer, S.S., Wang, S., Oronzi Scott, M., Bone, L.J., Paul, D.L., Chen, K., Lensch, M.W., Chance, P.F. and Fischbeck, K.H. (1993). Connexin mutations in X-linked Charcot-Marie-Tooth disease. *Science* **262**, 2039-2042.

Bhargava, M., Joseph, A., Knesal, J., Halahan, R., Li, Y., Pang, S., Goldberg, I., Setter, E., Donovan, M.A., Zarnegar, R., Michalopoulous, G.A., Nakamura, T., Faletto, D. and Rosen, E.M. (1992). Scatter factor and hepatocyte growth factor: activities, properties, and mechanism. *Cell Growth Differ.* **3**, 11-20.

Boterenbrood, E.C. and Nieuwkoop, P.D. (1973). The formation of the mesoderm in urodelean amphibians. V. Its regional induction by the endoderm. *Wilhelm Roux's Arch. Dev. Biol.* **173**, 319-332.

Bradley, A. (1987). Production and analysis of chimeric mice. In *Teratocarcinomas and embryonic stem cells: a practical approach.* (ed. E.J. Robertson), pp113-151. Oxford, IRL Press.

Brandon, E.P., Idzerda, R.L. and McKnight, B.S. (1995). Targeting the mouse genome: a compendium of knockouts. Part 1. *Curr. Biol.* **5**, 625-634.

Brandon, E.P., Idzerda, R.L. and McKnight, B.S. (1995). Targeting the mouse genome: a compendium of knockouts. Part 2. *Curr. Biol.* **5**, 758-765.

Brandon, E.P., Idzerda, R.L. and McKnight, B.S. (1995). Targeting the mouse genome: a compendium of knockouts. Part 3. *Curr. Biol.* **5**, 873-881.

Britz-Cunningham, S.H., Shah, M.M., Zuppan, C.W. and Fletcher, W.H. (1995). Mutations of the *connexin43* gap-junction gene in patients with heart malformations and defects of laterality. *N Engl. J Med.* **332**, 1323-1329.

Bronner-Fraser, M. (1993). Neural crest cell migration in the developing embryo. *Trends Cell Biol.* **3**, 392-397.

Brummel, T.J., Twombly, V., Marques, G., Wrana, J.L., Newfeld, S.J., Attisano, L., Massague, J., O'Connor, M.B. and Gelbart, W.M. (1994). Characterization and relationship of Dpp receptors encoded by the *saxophone* and *thick veins* genes in Drosophila. *Cell* **78**, 251-261.

Bumcrot, D.A., Takada, R. and McMahon, A.P. (1995). Proteolytic processing yields two secreted forms of sonic hedgehog. *Mol. Cell Biol.* **15**, 2294-2303.

Cárcamo, J., Zentella, A. and Massagué, J. (1995). Disruption of transforming growth factor β signalling by a mutation that prevents transphosphorylation within the receptor complex. *Mol. Cell. Biol.* **15**, 1573-1581.

Celeste, A.J., Iannazzi, J.A., Taylor, R.C., Hewick, R.M., Rosen, V., Wang, E.A. and Wozney, J.M. (1990). Identification of transforming growth factor β family members present in bone-inductive protein purified from bovine bone. *Proc. Natl. Acad. Sci. U S A* **87**, 9843-9847.

Chan, W.Y. and Tam, P.P.L. (1988). A morphological and experimental study of the mesencephalic neural crest cells in the mouse embryo using wheat germ agglutinin-gold conjugate as the cell marker. *Development* **102**, 427-442.

Chen, P., Vukicevic, S., Sampath, T.K. and Luyten, F.P. (1995). Osteogenic protein-1 promotes growth and maturation of chick sternal chondrocytes in serum-free cultures. *J. Cell Sci.* **108**, 105-114.

Childs, S.R., Wrana, J.L., Arora, K., Attisano, L., O'Connor, M.B. and Massagué, J. (1993). Identification of a *Drosophila* activin receptor. *Proc. Natl. Acad. Sci. USA* **90**, 9475-9479.

Chomczynski, P. and Sacchi, N. (1987). Single step method of RNA isolation by guanidinium thiocyanate-phenol-chloroform extraction. *Analyt. Biochem.* **162**, 156-159.

Church, G.M. and Gilbert, W. (1984). Genomic sequencing. *Proc. Natl. Acad. Sci. USA* **81**, 1991-1995.

Clarke, J.D.W., Holder, N., Soffe, S.R. and Storm-Mathisen, J. (1991). Neuroanatomical and functional analysis of neural tube formation in notochordless *Xenopus* embryos; laterality of the ventral spinal cord is lost. *Development* **112**, 499-516.

Cohen, S. (1962). Isolation of a mouse submaxilliary gland protein accelerating incisor eruption and eyelid opening in the new-born animal. *J. Biol. Chem.* **237**, 1555-1562.

Collignon, J., Sockanathan, S., Hacker, A., Cohen-Tannoudji, M., Norris, D., Rastan, S., Stevanovic, M., Goodfellow, P.N. and Lovell-Badge, R. (1996b). A comparison of the properties of *Sox-3* with *Sry* and two related genes, *Sox-1* and *Sox-2*. *Development* **122**, 509-520.

Collignon, J., Varlet, I. and Robertson, E.J. (1996a). Relationship between asymmetric *nodal* expression and the direction of embryonic turning. *Nature* **381**, 155-158.

Conlon, F.L., Barth, K.S. and Robertson, E.J. (1991). A novel retrovirally induced embryonic lethal mutaton in the mouse: assessment of the developmental fate of embryonic stem cells homozygous for the 413.d proviral integration. *Development* **111**, 969-981.

Conlon, F.L., Lyons, K.M., Takaesu, N., Barth, K.S., Kispert, A., Herrmann, B. and Robertson, E.J. (1994). A primary requirement for *nodal* in the formation and maintenance of the primitive streak in the mouse. *Development* **120**, 1919 - 1928.

Conquet, F., Peyriéras, N., Tiret, L. and Brûlet, P. (1992). Inhibited gastrulation in mouse embryos everexpressing the leukemia inhibitory factor. *Proc. Natl. Acad. Sci., USA* **89**, 8195-8199.

Cooke, J. (1979). Cell number in relation to primary pattern formation in the embryo of *Xenopus laevis*. I. The cell cycle during new pattern formation in response to implanted organisers. *J. Embryol. exp. Morph.* **51**, 165-182.

Copp, A.J. (1990). Studying developmental mechanisms in intact embryos. In *Postimplantation mammalian embryos*. (eds. A.J. Copp and D.L. Cockroft), pp293-326. Oxford, IRL Press.

Copp, A.J., Checiu, I. and Henson, J.N. (1994). Developmental basis of severe neural tube defects in the *loop-tail* (*Lp*) mutant mouse: use of microsatellite DNA markers to identify embryonic genotype. *Dev. Biol.* **165**, 20-29.

Curatola, A.M. and Basilico, C. (1990). Expression of the K-*fgf* proto-oncogene is controlled by 3' regulatory elements which are specified for embryonal carcinoma cells. *Mol. Cell. Biol.* **10**, 2475-2484.

Dale, L., Howes, G., Price, B.M.J. and Smith, J.C. (1992). Bone morphogenetic protein 4: a ventralizing factor in early *Xenopus* development. *Development* **115**, 573-585.

Dale, L., Matthews, G. and Colman, A. (1993). Secretion and mesoderm-inducing activity of the TGF-β-related domain of *Xenopus* Vg1. *EMBO J.* **12**, 4471-4480.

Dale, L., Matthews, G., Tabe, L. and Colman, A. (1989). Developmental expression of the protein product of Vg1, a localized maternal mRNA in the frog *Xenopus laevis*. *EMBO J.* **8**, 1057-1065.

Dale, L. and Slack, J.M.W. (1987). Regional specification within the mesoderm of early embryos of *Xenopus laevis*. *Development* **100**, 279-295.

Dale, L., Smith, J.C. and Slack, J.M.W. (1985). Mesoderm induction in *Xenopus laevis*: a quantitiative study using a cell lineage label and tissue-specific antibodies. *J. Embryol. exp. Morph.* **89**, 289-312.

Daopin, S., Piez, K.A., Ogawa, Y. and Davies, D.R. (1992). Crystal structuré of transforming growth factor-β2: An unusual fold for the superfamily. *Science* **257**, 369-373.

Darnell, D.K., Schoenwolf, G.C. and Ordahl, C.P. (1992). Changes in dorsoventral but not rostrocaudal regionalization of the chick neural tube in the absence of cranial notochord, as revealed by expression of *Engrailed-2*. *Dev. Dyn.* **193**, 389-396.

Denhardt, D.T. (1966). A membrane filter technique for the detection of complementary DNA. *Biochem. Biophys. Res. Commun.* **23**, 641-646.

Dickinson, M.E., Selleck, M.A.J., McMahon, A.P. and Bronner-Fraser, M. (1995). Dorsalization of the neural tube by the non-neural ectoderm. *Development* **121**, 2099-2106.

Dohrmann, C.E., Hemmati-Brivanlou, A., Thomsen, G.H., Fields, A., Woolf, T.M. and Melton, D.A. (1993). Expression of activin mRNA during early development in *Xenopus laevis*. *Dev. Biol.* **157**, 474-483.

Downs, K.M. and Davies, T. (1993). Staging of gastrulating mouse embryos by morphological landmarks in the dissecting microscope. *Development* **118**, 1255-1266.

Drucker, B.J. and Goldfarb, M. (1993). Murine FGF-4 gene expression is spatially restricted within embryonic skeletal muscle and other tissues. *Mech. Dev.* **40**, 155-163.

Dudley, A.T., Lyons, K.M. and Robertson, E.J. (1995). A requirement for bone morphogenetic protein-7 during development of the mammalian kidney and eye. *Genes Dev.* **9**, 2795-2807.

Ebner, R., Chen, R.-H., Shum, L., Lawler, S., Zioncheck, T.F., Lee, A., Lopez, A.R. and Derynck, R. (1993). Cloning of a type I TGF-β receptor and its effect on TGF-β binding to the type II receptor. *Science* **260**, 1344-1348.

Echelard, Y., Epstein, D.J., St-Jacques, B., Shen, L., Mohler, J., McMahon, J.A. and McMahon, A.P. (1993). Sonic hedgehog, a member of a family of putative signaling molecules, is implicated in the regulation of CNS polarity. *Cell* **75**, 1417-1430.

Echelard, Y., Vassileva, G. and McMahon, A.P. (1994). *Cis*-acting regulatory sequences governing *Wnt-1* expression in the developing mouse CNS. *Development* **120**, 2213-2224.

Ericson, J., Thor, S., Edlund, T., Jessell, T.M. and Yamada, T. (1992). Early stages of motor neuron differentiation revealed by expression of homeobox gene *Islet-1*. *Science* **256**, 1555-1560.

Fainsod, A., Steinbeisser, H. and De Robertis, E.M. (1994). On the function of *BMP-4* in patterning the marginal zone of the *Xenopus* embryo. *EMBO J.* **13**, 5015-5025.

Fan, C.-M. and Tessier-Lavigne, M. (1994). Patterning of mammalian somites by surface ectoderm and notochord: evidence for sclerotome induction by a hedgehog homolog. *Cell* **79**, 1175-1186.

Faust, C., Schumacher, A., Holdener, B. and Magnuson, T. (1995). The *eed* mutation disrupts anterior mesoderm production in mice. *Development* **121**, 273-285.

Ferguson, E.L. and Anderson, K.V. (1992a). *decapentaplegic* acts as a morphogen to organize dorsal-ventral pattern in the Drosophila embryo. *Cell* **71**, 451-461.

Ferguson, E.L. and Anderson, K.V. (1992b). Localized enhancement and repression of the activity of the TGF-β family member, *decapentaplegic*, is necessary for dorsal-ventral pattern formation in the *Drosophila* embryo. *Development* **114**, 583-597.

François, V., Solloway, M., O'Neill, J.W., Emery, J. and Bier, E. (1994). Dorsal-ventral patterning of the *Drosophila* embryo depends on a putative negative growth factor encoded by the *short gastrulation* gene. *Genes Dev.* **8**, 2602-2616.

Franzén, P., ten Dijke, P., Ichijo, H., Yamashita, H., Schulz, P., Heldin, C.-H. and Miyazono, K. (1993). Cloning of a TGFβ type I receptor that forms a heteromeric complex with the TGFβ type II receptor. *Cell* **75**, 681-692.

Friedrich, G. and Soriano, P. (1991). Promoter traps in embryonic stem cells: a genetic screen to identify and mutate developmental genes in mice. *Genes Dev.* **5**, 1513-1523.

Gerhart, J. and Keller, R. (1986). Region-specific cell activities in amphibian gastrulation. *Ann. Rev. Cell Biol.* **2**, 201-229.

Ghattas, I.R., Sanes, J.R. and Majors, J.E. (1991). The encephalomyocarditis virus internal ribosome entry site allows efficient coexpression of two genes from a recombinant provirus in cultured cells and in embryos. *Mol. Cell. Biol.* **11**, 5848-5859.

Gluzman, Y. (1981). SV40-tansformed simian cells support the replication of early SV40 mutants. *Cell* **23**, 175-182.

Gordon, M.S. (1977). *Animal physiology: principles and adaptations.* London, Collier Macmillan Publishers.

Goulding, M.D., Chalepakis, G., Deutsch, U., Erselius, J.R. and Gruss, P. (1991). Pax-3, a novel murine DNA binding protein expressed during early neurogenesis. *EMBO J.* **10**, 1135-1147.

Goulding, M.D., Lumsden, A. and Gruss, P. (1993). Signals from the notochord and floor plate regulate the region-specific expression of two Pax genes in the developing spinal cord. *Development* **117**, 1001-1016.

Graham, A., Francis-West, P., Brickell, P. and Lumsden, A. (1994). The signalling molecule BMP4 mediates apoptosis in the rhombencephalic neural crest. *Nature* **372**, 684-686.

Green, J.B.A., Howes, G., Symes, K., Cooke, J. and Smith, J.C. (1990). The biological effects of XTC-MIF: quantitative comparison with *Xenopus* bFGF. *Development* **108**, 173-183.

Green, J.B.A. and Smith, J.C. (1990). Graded changes in dose of a *Xenopus* activin A homologue elicit stepwise transitions in embryonic cell fate. *Nature* **347**, 391-394.

Gurdon, J.B., Harger, P., Mitchell, A. and Lemaire, P. (1994). Activin signalling and response to a morphogen gradient. *Nature* **371**, 487-492.

Guthrie, S., Butcher, M. and Lumsden, A. (1991). Patterns of cell division and interkinetic nuclear migration in the chick embryo hindbrain. *J. Neurobiol.* **22**, 742-754.

Hall, B.K. and van Exan, R.J. (1982). Induction of bone by epithelial cell products. *J. Embryol. exp. Morph.* **69**, 37-46.

Hanahan, D., Jesse, J. and Bloom, F.R. (1991). Plasmid transformation of *Escherichia coli* and other bacteria. *Methods Enzymol.* **204**, 63-113.

Harrison, S.M., Dunwoodie, S.L., Arkell, R.M., Lehrach, H. and Beddington, R.S.P. (1995). Isolation of novel tissue-specific genes from cDNA libraries representing the individual tissue constituents of the gastrulating mouse embryo. *Development* **121**, 2479-2489.

Heberlein, U., Wolff, T. and Rubin, G.M. (1993). The TGFβ homolog *dpp* and the segment polarity gene *hedgehog* are required for propagation of a morphogenetic wave in the Drosophila retina. *Cell* **75**, 913-926.

Heimer, G.V. and Taylor, C.E.D. (1974). Improved mountant for immunofluorescence preparations. *J. Clin. Pathol.* **27**, 254-256.

Hemmati-Brivanlou, A., Kelly, O.G. and Melton, D.A. (1994). Follistatin, an antagonist of activin, is expressed in the Spemann organizer and displays direct neuralizing activity. *Cell* **77**, 283-295.

Hemmati-Brivanlou, A. and Melton, D.A. (1992). A trunctated activin receptor inhibits mesoderm induction and formation of axial structures in *Xenopus* embryos. *Nature* **359**, 609-614.

Hermesz, E., Mackem, S. and Mahon, K.A. (1996). *Rpx*: a novel anterior-restricted homeobox gene progressively activated in the prechordal plate, anterior neural plate and Rathke's pouch of the mouse embryo. *Development* **122**, 41-52.

Herrmann, B.G., Labeit, S., Poustka, A., King, T.R. and Lehrach, H. (1990). Cloning of the *T* gene required in mesoderm formation in the mouse. *Nature* **343**, 617-622.

Hill, R.E., Jones, P.F., Rees, A.R., Sime, C.M., Justice, M.J., Copeland, N.G., Jenkins, N.A., Graham, E. and Davidson, D.R. (1989). A new family of

mouse homeo box-containing genes: molecular structure, chromosomal location and developmental expression of *Hox-7.1*. *Genes Dev.* **3**, 26-37.

Hirano, S., Fuse, S. and Sohal, G.S. (1991). The effect of floor plate on pattern and polarity in the developing central nervous system. *Science* **251**, 310-313.

Hogan, B., Beddington, R., Constantini, F. and Lacy, E. (1994). *Manipulating the mouse embryo: a laboratory manual.* Cold Spring Harbour, Cold Spring Harbour Laboratory Press.

Hogan, B.L.M. (1995). Upside-down ideas vindicated. *Nature* **376**, 210-211.

Holdener, B.C., Faust, C., Rosenthal, N.S. and Magnuson, T. (1994). *msd* is required for mesoderm induction in mice. *Development* **120**, 1335-1346.

Holley, S.A., Jackson, P.D., Sasai, Y., Lu, B., De Robertis, E.M., Hoffmann, F.M. and Ferguson, E.L. (1995). A conserved system for dorsal-ventral patterning in insects and vertebrates involving *sog* and *chordin*. *Nature* **376**, 249-253.

Holtfreter, J. and Hamburger, V. (1955). Embryogenesis: progressive differentiation. In *Analysis of Development*. pp230-296. New York, Saunders. 230-296.

Hötten, G., Neidhardt, H., Schneider, C. and Pohl, J. (1995). Cloning of a new member of the TGF-β family: a putative new activin β_C chain. *Biochem. Biophys. Res. Commun.* **206**, 608-613.

Iannaccone, P.M., Zhou, X., Khokha, M., Boucher, D. and Kuehn, M.R. (1992). Insertional mutation of a gene involved in growth regulation of the early mouse embryo. *Dev. Dyn.* **194**, 198-208.

Inagaki, M., Moustakas, A., Lin, H.Y., Lodish, H.F. and Carr, B.I. (1993). Growth inhibition by transforming growth factor β (TGF-β) type I is restored in TGF-β-resistant hepatoma cells after expression of TGF-β receptor type II cDNA. *Proc. Natl. Acad. Sci. USA* **90**, 5359-5363.

Ingham, P.W. (1995). Signalling by hedgehog family proteins in *Drosophila* and vertebrate development. *Curr. Opin. Genet. Dev.* **5**, 492-498.

Irish, V.F. and Gelbart, W.M. (1987). The decapentaplegic gene is required for dorsal-ventral patterning of the *Drosophila* embryo. *Genes Dev.* **1**, 868-879.

Jacobson, A.G. and Sater, A.K. (1988). Features of embryonic induction. *Development* **104**, 341-359.

Jessell, T.J., Bovolenta, P., Placzek, M., Tessier-Lavigne, M. and Dodd, J. (1989). Polarity and patterning in the neural tube: the origin and function of the floor plate. In *Cellular basis of morphogenesis (Ciba Foundation Symposium, 144)*. pp 225-280. Chichester, Wiley.

Jones, C.M., Kuehn, M.R., Hogan, B.L.M., Smith, J.C. and Wright, C.V.E. (1995). Nodal-related signals induce axial mesoderm and dorsalize mesoderm during gastrulation. *Development* **121**, 3651-3662.

Jones, C.M., Lyons, K.M. and Hogan, B.L. (1991). Involvement of *Bone Morphogenetic Protein-4* (BMP-4) and *Vgr-1* in morphogenesis and neurogenesis in the mouse. *Development* **111**, 531-542.

Jones, C.M., Lyons, K.M., Lapan, P.M., Wright, C.V. and Hogan, B.L. (1992a). DVR-4 (bone morphogenetic protein-4) as a posterior-ventralizing factor in *Xenopus* mesoderm induction. *Development* **115**, 639-647.

Jones, C.M., Simon-Chazottes, D., Guenet, J.L. and Hogan, B.L. (1992b). Isolation of*Vgr-2*, a novel member of the transforming growth factor-β-related gene family. *Mol. Endocrinol.* **6**, 1961-1968.

Jones, E.A. and Woodland, H.R. (1986). Development of the ectoderm in Xenopus tissue specification and the role of cell association and division. *Cell* **44**, 345-355.

Jones, E.A. and Woodland, H.R. (1987). The development of animal cap cells in *Xenopus*: the effects of environment on the differentiation and the migration of grafted ectodermal cells. *Development* **101**, 23-32.

Jurand, A. (1974). Some aspects of the development of the notochord in mouse embryos. *J. Embryol. exp. Morph.* **32**, 1-33.

Kaufman, M.H. (1992). *The atlas of mouse development*. London, Academic Press.

Kaufman, R.J., Davies, M.V., Wasley, L.C. and Michnick, D. (1991). Improved vectors for stable expression of foreign genes in mammalian cells by use of the untranslated leader sequence from EMC virus. *Nucleic Acids Res.* **19**, 4485-4490.

Keller, R.E. (1975). Vital dye mapping of the gastrula and neurula of *Xenopus laevis* I. Prospective areas and morphogenetic movements of the superficial layer. *Dev. Biol.* **42**, 222-241.

Keller, R.E., Danilchik, M., Gimlich, R. and Shih, J. (1985). The function and mechanism of convergent extension during gastrulation of *Xenopus laevis*. *J. Embryol. exp. Morph.* **89 (Supplement)**, 185-209.

Kennedy, T.E., Serafini, T., de la Torre, J.R. and Tessier-Lavigne, M. (1994). Netrins are diffusible chemotropic factors for commissural axons in the embryonic spinal cord. *Cell* **78**, 425-435.

Kessler, D.S. and Melton, D.A. (1995). Induction of dorsal mesoderm by soluble, mature Vg1 protein. *Development* **121**, 2155-2164.

Keynes, R.D. and Aidley, D.J. (1981). *Nerve and Muscle*. Cambridge, Cambridge University Press.

Kim, D.G., Kang, H.M., Jang, S.K. and Shin, H.-S. (1992). Construction of a bifunctional mRNA in the mouse by using the internal ribosomal entry site of the encephalomyocarditis virus [published erratum appears in Mol. Cell. Biol. 1992 Oct;12(10):4807]. *Mol. Cell. Biol.* **12**, 3636-3643.

King, R.J.B. (1988). An overview of molecular aspects of steroid hormone action. In *Hormones and their actions. Part I.* Oxford, Elsevier. 29-38.

Kingsley, D.M. (1994). The TGF-β superfamily: new members, new receptors, and new genetic tests of function in different organisms. *Genes Dev.* **8**, 133-146.

Kingsley, D.M., Bland, A.E., Grubber, J.M., Marker, P.C., Russell, L.B., Copeland, N.G. and Jenkins, N.A. (1992). The mouse *short ear* skeletal morphogenesis locus is associated with defects in a bone morphogenetic member of the TGFβ superfamily. *Cell* **71**, 399-410.

Kispert, A. and Herrmann, B.G. (1993). The *Brachyury* gene encodes a novel DNA binding protein. *EMBO J.* **12**, 3211-3220.

Kispert, A. and Herrmann, B.G. (1994). Immunohistochemical analysis of the *Brachyury* protein in wild-type and mutant mouse embryos. *Dev. Biol.* **161**, 179-193.

Kitsukawa, T., Shimono, A., Kawakami, A., Kondoh, H. and Fujisawa, H. (1995). Overexpression of a membrane protein, neuropilin, in chimeric mice causes anomalies in the cardiovascular system, nervous system and limbs. *Development* **121**, 4309-4318.

Knutsen, R., Wergedal, J.E., Sampath, T.K., Baylink, D.J. and Mohan, S. (1993). Osteogenic protein-1 stimulates proliferation and differentiation of human bone cells in vitro. *Biochem. Biophys. Res. Commun.* **194**, 1352-1358.

Krauss, S., Concordet, J.P. and Ingham, P.W. (1993). A functionally conserved homolog of the Drosophila segment polarity gene *hh* is expressed in tissues with polarizing activity in zebrafish embryos. *Cell* **75**, 1431-1444.

Laiho, M., Weis, F.M.B. and Massagué, J. (1990). Concomitant loss of transforming growth factor (TGF)-β receptor types I and II in TGF-β-resistant cell mutants implicates both receptor types in signal transduction. *J. Biol. Chem.* **265**, 18518-18524.

Lawson, K.A., Meneses, J.J. and Pedersen, R.A. (1991). Clonal analysis of epiblast fate during germ layer formation in the mouse embryo. *Development* **113**, 891-911.

Lawson, K.A. and Pedersen, R.A. (1992). Clonal analysis of cell fate during gastrulation and early neurulation in the mouse. In *Postimplantation development in the mouse*. (eds. D.J. Chadwick and J. Marsh), pp3-26. Chichester, John Wiley & sons.

Letsou, A., Arora, K., Wrana, J.L., Simin, K., Twombly, V., Jamal, J., Staehling-Hampton, K., Hoffmann, F.M., Gelbart, W.M., Massagué, J. and O'Connor, M.B. (1995). Drosophila dpp signaling is mediated by the *punt* gene product: a dual ligand-binding type II receptor of the TGFβ receptor family. *Cell* **80**, 899-908.

Letterio, J.J., Geiser, A.G., Kulkarni, A.B., Roche, N.S., Sporn, M.B. and Roberts, A.B. (1994). Maternal rescue of transforming growth factor-β1 null mice. *Science* **264**, 1936-1938.

Liem, K.F.J., Tremml, G., Roelink, H. and Jessell, T.M. (1995). Dorsal differentiation of neural plate cells induced by BMP-mediated signals from epidermal ectoderm. *Cell* **82**, 969-979.

Lin, H.Y. and Lodish, H.F. (1993). Receptors for the TGF-β superfamily: multiple polypeptides and serine/threonine kinases. *Trends Cell Biol.* **3**, 14-19.

Lints, T.J., Parsons, L.M., Hartley, L., Lyons, I. and Harvey, R.P. (1993). Nkx-2.5: a novel murine homeobox gene expressed in early heart progenitor cells and their myogenic descendants. *Development* **119**, 419-431.

Liu, F., Ventura, F., Doody, J. and Massagué, J. (1995). Human type II receptor for bone morphogenic proteins (BMPs): extension of the two-kinase receptor model to the BMPs. *Mol. Cell. Biol.* **15**, 3479-3486.

Loewenstein, W.R. (1966). Permeability of membrane junctions. *Ann. N.Y. Acad. Sci.* **137**, 441-472.

López-Casillas, F., Wrana, J.L. and Massagué, J. (1993). Betaglycan presents ligand to the TGFβ signaling receptor. *Cell* **73**, 1435-1444.

Luo, G., Hofmann, C., Bronckers, A.L.J.J., Sohocki, M., Bradley, A. and Karsenty, G. (1995). BMP-7 is an inducer of nephrogenesis, and is also required for eye development and skeletal patterning. *Genes Dev.* **9**, 2808-2820.

Lyons, K.M., Hogan, B.L.M. and Robertson, E.J. (1995). Colocalization of BMP 7 and BMP 2 RNAs suggests that these factors cooperatively mediate tissue interactions during murine development. *Mech. Dev.* **50**, 71-83.

Lyons, K.M., Jones, C.M. and Hogan, B.L. (1991). The DVR gene family in embryonic development. *Trends Genet.* **7**, 408-412.

Lyons, K.M., Pelton, R.W. and Hogan, B.L.M. (1989). Patterns of expression of murine Vgr-1 and BMP-2a RNA suggest that transforming growth factor-β-like genes coordinately regulate aspects of embryonic development. *Genes Dev.* **3**, 1657-1668.

Ma, Y.-G., Rosfjord, E., Huebert, C., Wilder, P., Tiesman, J., Kelly, D. and Rizzino, A. (1992). Transcriptional regulation of the murine k-FGF gene in embryonic cell lines. *Dev. Biol.* **154**, 45-54.

Macejak, D.G. and Sarnow, P. (1991). Internal initiation of translation mediated by the 5' leader of a cellular mRNA. *Nature* **353**, 90-94.

Maéno, M., Ong, R.C., Suzuki, A., Ueno, N. and Kung, H.-F. (1994). A truncated bone morphogenetic protein 4 receptor alters the fate of ventral mesoderm to dorsal mesoderm: roles of animal pole tissue in the development of ventral mesoderm. *Proc. Natl. Acad. Sci. USA* **91**, 10260-10264.

Manova, K., Paynton, B.V. and Bachvarova, R.F. (1992). Expression of activins and TGFβ1 and β2 RNAs in early postimplantation mouse embryos and uterine decidua. *Mech. Dev.* **36**, 141-152.

Marti, E., Bumcrot, D.A., Takada, R. and McMahon, A.P. (1995). Requirement of 19K form of Sonic hedgehog for induction of distinct ventral cell types in CNS explants. *Nature* **375**, 322-325.

Martins-Green, M. (1988). Origin of the dorsal surface of the neural tube by progressive delamination of epidermal ectoderm and neuroepithelium: implications for neurulation and neural tube defects. *Development* **103**, 687-706.

Massagué, J. (1983). Epidermal growth factor-like transforming growth factor. *J. Biol. Chem.* **258**, 13606-13613.

Massagué, J. (1990a). Transforming growth factor-α. *J. Biol. Chem.* **265**, 21393-21396.

Massagué, J. (1990b). The transforming growth factor-β family. *Annu. Rev. Cell Biol.* **6**, 597-641.

Massagué, J., Attisano, L. and Wrana, J.L. (1994). The TGF-β family and its composite receptors. *Trends Cell Biol.* **4**, 172-178.

Mathews, L.S. and Vale, W.W. (1991). Expression cloning of an activin receptor, a predicted transmembrane serine kinase. *Cell* **65**, 973-982.

Matzuk, M.M., Kumar, T.R., Vassalli, A., Bickenbach, J.R., Roop, D.R., Jaenisch, R. and Bradley, A. (1995a). Functional analysis of activins during mammalian development. *Nature* **374**, 354-356.

Matzuk, M.M., Lu, N., Vogel, H., Sellheyer, K., Roop, D.R. and Bradley, A. (1995b). Multiple defects and perinatal death in mice deficient in follistatin. *Nature* **374**, 360-363.

McPherron, A.C. and Lee, S.-J. (1993). GDF-3 and GDF-9: Two new members of the transforming growth factor-β superfamily containing a novel pattern of cysteines. *J. Biol. Chem.* **268**, 3444-3449.

McKay, I.A., Ed. (1993). Types of growth factor activity: detection and characterization of new growth factor activities. In *Growth factors: A practical approach.* (eds. I McKay and I. Leigh), pp1-11. Oxford, Oxford University Press.

Meno, C., Saijoh, Y., Fujii, H., Masako, I., Yokoyama, T., Yokoyama, M., Toyoda, Y. and Hamada, H. (1996). Left-right asymetric expression of the TGFβ-family member *lefty* in mouse embryos. *Nature* **381**, 151-155.

Meunier, H., Rivier, C., Evans, R. and Vale, W. (1988). Gonadal and extragonadal expression of inhibin α, βA, and βB subunits in various tissues predicts diverse functions. *Proc. Natl. Acad. Sci. USA* **85**, 247-251.

Mishina, Y., Suzuki, A., Ueno, N. and Behringer, R.R. (1995). *Bmpr* encodes a type I bone morphogenetic protein receptor that is essential for gastrulation during mouse embryogenesis. *Genes Dev.* **9**, 3027-3037.

Mitchell, P.J., Timmons, P.M., Hébert, J.M., Rigby, P.W.J. and Tjian, R. (1991). Transcription factor AP-2 is expressed in neural crest cell lineages during mouse embryogenesis. *Genes Dev.* **5**, 105-119.

Molla, A., Jang, S.K., Paul, A.V., Reuer, Q. and Wimmer, E. (1992). Cardioviral internal ribosomal entry site is functional in a genetically engineered dicistronic poliovirus. *Nature* **356**, 255-257.

Mountford, P., Zevnik, B., Duwel, A., Nichols, J., Li, M., Dani, C., Robertson, M., Chambers, I. and Smith, A. (1994). Dicistronic targeting constructs: reporters and modifiers of mammalian gene expression. *Proc. Natl. Acad. Sci. USA* **91**, 4303-4307.

Mountford, P.S. and Smith, A.G. (1995). Internal ribosome entry sites and dicistronic RNAs in mammalian transgenesis. *Trends Genet.* **11**, 179-184.

Moury, J.D. and Jacobson, A.G. (1989). Neural fold formation at newly created boundaries between neural plate and epidermis in the axolotl. *Dev. Biol.* **133**, 44-57.

Moury, J.D. and Jacobson, A.G. (1990). The origins of neural crest in the axolotl. *Dev. Biol.* **141**, 243-253.

Nagy, A., Gócza, E., Diaz, M.E., Prideaux, V., Iványi, E., Markkula, M. and Rossant, J. (1990). Embryonic stem cells alone are able to support fetal development in the mouse. *Development* **110**, 815-821.

Nakamura, T., Sugino, K., Titani, K. and Sugino, H. (1991). Follistatin, an activin-binding protein, associates with heparan sulfate chains of proteoglycans on follicular granulosa cells. *J. Biol. Chem.* **266**, 19432-19437.

Nakamura, T., Takio, K., Eto, Y., Shibai, H., Titani, K. and Sugino, H. (1990). Activin-binding protein from rat ovary is follistatin. *Science* **247**, 836-838.

Nellen, D., Affolter, M. and Basler, K. (1994). Receptor serine/threonine kinases implicated in the control of Drosophila body pattern by *decapentaplegic*. *Cell* **78**, 225-237.

Nichols, D.H. (1981). Neural crest formation in the head of the mouse embryo as observed using a new histological technique. *J. Embryol. exp. Morph.* **64**, 105-120.

Nichols, D.H. (1986). Formation and distribution of neural crest mesenchyme to the first pharyngeal arch region of the mouse embryo. *Am. J. Anat.* **176**, 221-231.

Nieuwkoop, P.D. (1969). The formation of the mesoderm in the Urodelean amphibians. I. Induction by the endoderm. *Wilhelm Roux's Arch. Entwmech. Org.* **162**, 341-373.

Nieuwkoop, P.D. and Faber, J. (1994). *Normal Table of Xenopus laevis (Daudin).* Amsterdam, North Holland.

Nieuwkoop, P.D. and Ubbels, G.A. (1972). The formation of mesoderm in Urodelean amphibians. IV. Quantitative evidence for the purely "ectodermal" origin of the entire mesoderm and of the pharyngeal endoderm. *Wilhelm Roux's Arch. Entwmech. Org.* **169**, 185-199.

Nunez, J. (1988). Mechanism of action of thyroid hormone. In *Hormones and their actions. Part I.* Oxford, Elsevier. 61-80.

O'Rahilly, R. and Müller, F. (1985). The origin of the ectodermal ring in staged human embryos of the first five weeks. *Acta. Anat.* **122**, 145-157.

Oda, S., Nishimatsu, S.-I., Murakami, K. and Ueno, N. (1995). Molecular cloning and functional analysis of a new activin β subunit: a dorsal mesoderm-inducing activity in *Xenopus*. *Biochem. Biophys. Res. Commun.* **210**, 581-588.

Okano, H., Yoshikawa, S., Suzuki, A., Ueno, N., Kaizu, M., Okabe, M., Takahashi, T., Matsumoto, M., Sawamoto, K. and Mikoshiba, K. (1994). Cloning of a *Drosophila melanogaster* homologue of the mouse type-I bone morphogenetic proteins-2/-4 receptor: a potential decapentaplegic receptor. *Gene* **148**, 203-209.

Ozkaynak, E., Rueger, D.C., Drier, E.A., Corbett, C., Ridge, R.J., Sampath, T.K. and Oppermann, H. (1990). OP-1 cDNA encodes an osteogenic protein in the TGF-β family. *EMBO J.* **9**, 2085-2093.

Ozkaynak, E., Schnegelsberg, P.N. and Oppermann, H. (1991). Murine osteogenic protein (OP-1): high levels of mRNA in kidney. *Biochem. Biophys. Res. Commun.* **179**, 116-123.

Padgett, R.W., St. Johnston, R.D. and Gelbart, W.M. (1987). A transcript from a *Drosophila* pattern gene predicts a protein homologous to the transforming growth factor-β family. *Nature* **325**, 81-84.

Padgett, R.W., Wozney, J.M. and Gelbart, W.M. (1993). Human BMP sequences can confer normal dorsal-ventral patterning in the *Drosophila* embryo. *Proc. Natl. Acad. Sci. USA* **90**, 2905-2909.

Panaretto, B.A., Leish, Z., Moore, G.P.M. and Robertson, D.M. (1983). Inhibition of DNA synthesis in dermal tissue of Merino sheep treated with depilatory doses of mouse epidermal growth factor. *J. Endocrinology* **100**, 25-31.

Panganiban, G.E.F., Reuter, R., Scott, M.P. and Hoffmann, F.M. (1990). A *Drosophila* growth factor homologue, *decapentaplegic*, regulates homeotic gene expression within and across germ layers during midgut morphogenesis. *Development* **110**, 1041-1050.

Papalopulu, N. and Kintner, C. (1992). Induction and patterning of the neural plate. *Sem. Neurosci.* **4**, 295-306.

Parameswaran, M. and Tam, P.P.L. (1995). Regionalisation of cell fate and morphogenetic movement of the mesoderm during mouse gastrulation. *Dev. Genet.* **17**, 16-28.

Paul, D.L. (1995). New functions for gap junctions. *Curr. Op. Cell Biol.* **7**, 665-672.

Paul, D.L., Yu, K., Bruzzone, R., Gimlich, R.L. and Goodenough, D.A. (1995). Expression of a dominant negative inhibitor of intercellular communication in the early *Xenopus* embryo causes delamination and extrusion of cells. *Development* **121**, 371-381.

Pelletier, J. and Sonenberg, N. (1988). Internal initiation of translation of eukaryotic mRNA directed by a sequence derived from poliovirus RNA. *Nature* **334**, 320-325.

Penton, A., Chen, Y., Staehling, H.K., Wrana, J.L., Attisano, L., Szidonya, J., Cassill, J.A., Massagué, J. and Hoffmann, F.M. (1994). Identification of two bone morphogenetic protein type I receptors in Drosophila and evidence that Brk25D is a *decapentaplegic* receptor. *Cell* **78**, 239-250.

Pfaff, S.L., Mendelsohn, M., Stewart, C.L., Edlund, T. and Jessell, T.M. (1996). Requirement for LIM homeobox gene *Isl1* in motor neuron generation reveals a motor neuron-dependent step in interneuron differentiation. *Cell* **84**, 309-320.

Placzek, M. (1995). The role of the notochord and floor plate in inductive interactions. *Curr. Opin. Genet. Dev.* **5**, 499-506.

Placzek, M., Jessell, T.M. and Dodd, J. (1993). Induction of floor plate differentiation by contact-dependent, homeogenetic signals. *Development* **117**, 205-218.

Placzek, M., Tessier-Lavigne, M., Yamada, T., Jessell, T. and Dodd, J. (1990). Mesodermal control of neural cell identity: floor plate induction by the notochord. *Science* **250**, 985-988.

Porter, J.A., von Kessler, D.P., Ekker, S.C., Young, K.E., Lee, J.J., Moses, K. and Beachy, P.A. (1995). The product of *hedgehog* autoproteolytic cleavage active in local and long-range signalling. *Nature* **374**, 363-366.

Quinlan, G.A., Williams, E.A., Tan, S.-S. and Tam, P.P.L. (1995). Neurectodermal fate of epiblast cells in the distal region of the mouse egg cylinder: implication for body plan organization during early embryogenesis. *Development* **121**, 87-98.

Rashbass, P., Cooke, L.A., Herrmann, B.G. and Beddington, R.S.P. (1991). A cell autonomous function of *Brachyury* in *T/T* embryonic stem cell chimaeras. *Nature* **353**, 348-351.

Rashbass, P., Wilson, V., Rosen, B. and Beddington, R.S.P. (1994). Alterations in gene expression during mesoderm formation and axial patterning in *Brachyury* (*T*) embryos. *Int. J. Dev. Biol.* **38**, 35-44.

Rathjen, P.D., Nichols, J., Toth, S., Edwards, D.P., Heath, J.K. and Smith, A.G. (1990b). Developmentally programmed induction of differentiation inhibiting activity and the control of stem cell populations. *Genes Dev.* **4**, 2308-2318.

Rathjen, P.D., Toth, S., Willis, A., Heath, J.K. and Smith, A.G. (1990a). Differentiation inhibiting activity is produced in matrix-associated and diffusible forms that are generated by alternative promoter usage. *Cell* **62**, 1105-1114.

Ray, R.P., Arora, K., Nüsslein-Volhard, C. and Gelbart, W.M. (1991). The control of cell fate along the dorsal-ventral axis of the *Drosophila* embryo. *Development* **113**, 35-54.

Re, R.N. (1989). The cellular biology of angiotensin: paracrine, autocrine and intracrine actions in cardiovascular tissues. *J. Mol. Cell. Cardiol.* **21**, 63-69.

Reaume, A.G., de Sousa, P.A., Kulkarni, S., Langille, B.L., Zhu, D., Davies, T.C., Juneja, S.C., Kidder, G.M. and Rossant, J. (1995). Cardiac malformation in neonatal mice lacking connexin43. *Science* **267**, 1831-1834.

Rebagliati, M.R. and Dawid, I.B. (1993). Expression of activin transcripts in follicle cells and oocytes of *Xenopus laevis*. *Dev. Biol.* **159**, 574-580.

Rebagliati, M.R., Weeks, D.L., Harvey, R.P. and Melton, D.A. (1985). Identification and cloning of localized maternal RNAs from Xenopus eggs. *Cell* **42**, 769-777.

Riddle, R.D., Johnson, R.L., Laufer, E. and Tabin, C. (1993). *Sonic hedgehog* mediates the polarizing activity of the ZPA. *Cell* **75**, 1401-1416.

Robertson, D.M., Klein, R., de Vos, F.L., McLachlan, R.I., Wettenhall, R.E.H., Hearn, M.T.W., Burger, H.G. and de Kretser, D.M. (1987). The isolation of polypeptides with FSH suppressing activity from bovine follicular fluid which are structurally different to inhibin. *Biochem. Biophys. Res. Commun.* **149**, 744-749.

Robertson, E.J. (1987). Embryo-derived stem cell lines. In *Teratocarcinomas and Embryonic Stem Cells: A Practival Approach.*(ed. E.J. Robertson), pp71-112. Oxford, IRL Press.

Roelink, H., Augsburger, A., Heemskerk, J., Korzh, V., Norlin, S., Ruiz i Altaba, A., Tanabe, Y., Placzek, M., Edlund, T., Jessell, T.M. and Dodd, J. (1994). Floor plate and motor neuron induction by *vhh-1*, a vertebrate homolog of *hedgehog* expressed by the notochord. *Cell* **76**, 761-775.

Roelink, H., Porter, J.A., Chiang, C., Tanabe, Y., Chang, D.T., Beachy, P.A. and Jessell, T.M. (1995). Floor plate and motor neuron induction by different concentrations of the amino-terminal cleavage product of sonic hedgehog autoproteolysis. *Cell* **81**, 445-455.

Rosen, B. and Beddington, R.S.P. (1993). Whole-mount *in situ* hybridization in the mouse embryo: gene expression in three dimensions. *Trends Genet.* **9**, 162-167.

Rosen, V. and Thies, R.S. (1992). The BMP proteins in bone formation and repair. *Trends Genet.* **8**, 97-102.

Rosner, M.H., Vigano, M.A., Ozato, K., Timmons, P.M., Poirier, F., Rigby, P.W.J. and Staudt, L.M. (1990). A POU-domain transcription factor in early stem cells and germ cells of the mammalian embryo. *Nature* **345**, 686-692.

Rothstein, J.L., Johnson, D., DeLoia, J.A., Skowronski, J., Solter, D. and Knowles, B. (1992). Gene expression during preimplantation mouse development. *Genes Dev.* **6**, 1190-1201.

Ruberte, E., Marty, T., Nellen, D., Affolter, M. and Basler, K. (1995). An absolute requirement for both the type II and type I receptors, punt and thick veins, for dpp signaling in vivo. *Cell* **80**, 889-897.

Rugh, R. (1968). *The Mouse*. Minneapolis, Burgess.

Ruiz i Altaba, A., Cox, C., Jessell, T.M. and Klar, A. (1993). Ectopic neural expression of a floor plate marker in frog embryos injected with the midline transcription factor Pintallavis. *Proc. Natl. Acad. Sci. USA* **90**, 8268-8272.

Ruiz i Altaba, A., Jessell, T.M. and Roelink, H. (1995a). Restrictions to floor plate induction by *hedgehog* and winged-helix genes in the neural tube of frog embryos. *Mol. Cell. Neurosci.* **6**, 106-121.

Ruiz i Altaba, A., Placzek, M., Baldassare, M., Dodd, J. and Jessell, T.M. (1995b). Early stages of notochord and floor plate development in the chick embryo defined by normal and induced expression of HNF-3β. *Dev. Biol.* **170**, 299-313.

Sadaghiani, B. and Thiébaud, C.H. (1987). Neural crest development in the *Xenopus laevis* embryo, studied by interspecific transplantation and scanning electron microscopy. *Dev. Biol.* **124**, 91-110.

Sambrook, J., Fritsch, E.F. and Maniatis, T. (1989). *Molecular Cloning: A Laboratory Manual*. Cold Spring Harbour, Cold Spring Harbor Laboratory Press.

Sampath, T.K., Rashka, K.E., Doctor, J.S., Tucker, R.F. and Hoffmann, F.M. (1993). *Drosophila* transforming growth factor β superfamily proteins induce endochondral bone formation in mammals. *Proc. Natl. Acad. Sci. USA* **90**, 6004-6008.

Sasai, Y., Lu, B., Steinbeisser, H. and De Robertis, E. (1995). Regulation of neural induction by the Chd and Bmp-4 antagonistic patterning signals in *Xenopus*. *Nature* **376**, 333-336.

Sasai, Y., Lu, B., Steinbeisser, H., Geissert, D., Gont, L.K. and De Robertis, E.M. (1994). Xenopus *chordin*: a novel dorsalizing factor activated by organizer-specific homeobox genes. *Cell* **79**, 779-790.

Sasaki, H. and Hogan, B.L.M. (1993). Differential expression of multiple fork head related genes during gastrulation and axial pattern formation in the mouse embryo. *Development* **118**, 47-59.

Sasaki, H. and Hogan, B.L.M. (1994). *HNF-3β* as a regulator of floor plate development. *Cell* **76**, 103-115.

Savage, C., Das, P., Finelli, A.L., Townsend, S.R., Sun, C.-Y., Baird, S.E. and Padgett, R.W. (1996). *Caenorhabditis elegans* genes *sma-2*, *sma-3*, and *sma-4* define a conserved family of transforming growth factor β pathway components. *Proc. Natl. Acad. Sci. USA* **93**, 790-794.

Schimmell, M.J., Ferguson, E.L., Childs, S.R. and O'Connor, M.B. (1991). The Drosophila dorsal-ventral patterning gene tolloid is related to human bone morphogenetic protein-1. *Cell* **67**, 469-481.

Schlunegger, M.P. and Grütter, M.G. (1992). An unusual feature revealed by the crystal structure at 2.2 Angstrom resolution of human transforming growth factor-β2. *Nature* **358**, 430-434.

Schmidt, J., Francois, V., Bier, E. and Kimelman, D. (1995a). *Drosophila short gastrulation* induces an ectopic axis in *Xenopus*: evidence for conserved mechanisms of dorsal-ventral patterning. *Development* **121**, 4319-4328.

Schmidt, J., Hötten, G., Jenkins, N.A., Gilbert, D.J., Copeland, N.G., Pohl, J. and Schrewe, H. (1996). Structure, chromosomal location, and expression analysis of the mouse inhibin/activin β_C (Inhbc) gene. *Genomics* **32**, 358-366.

Schmidt, J.E., Suzuki, A., Ueno, N. and Kimelman, D. (1995b). Localized BMP-4 mediates dorsal/ventral patterning in the early Xenopus embryo. *Dev. Biol.* **169**, 37-50.

Scholer, H., Ruppert, S., Suzuki, N., Chowdhury, K. and Gruss, P. (1990). New type of POU domain in germ line-specific protein Oct-4. *Nature* **344**, 435-439.

Schoorlemmer, J. and Kruijer, W. (1991). Octamer-dependent regulation of the kFGF gene in embryonal carcinoma and embryonic stem cells. *Mech. Devel.* **36**, 75-86.

Schulte-Merker, S., Smith, J.C. and Dale, L. (1994). Effects of truncated activin and FGF receptors and of follistatin on the inducing activities of BVg1 and activin: does activin play a role in mesoderm induction. *EMBO J.* **13**, 3533-3541.

Sekelsky, J.J., Newfeld, S.J., Raftery, L.A., Chartoff, E.H. and Gelbart, W.M. (1995). Genetic characterization and cloning of *Mothers against dpp*, a gene required for *decapentaplegic* function in *Drosophila melanogaster*. *Genetics* **139**, 1347-1358.

Selleck, M.A.J. and Bronner-Fraser, M. (1995). Origins of the avian neural crest: the role of neural plate-epidermal interactions. *Development* **121**, 525-538.

Serafini, T., Kennedy, T.E., Galko, M.J., Mirzayan, C., Jessell, T.M. and Tessier-Lavigne, M. (1994). The netrins define a family of axon outgrowth-promoting proteins homologous to C. elegans UNC-6. *Cell* **78**, 409-424.

Serbedzija, G.N., Bronner-Fraser, M. and Fraser, S.E. (1992). Vital dye analysis of cranial neural crest cell migration in the mouse embryo. *Development* **116**, 297-307.

Serbedzija, G.N., Fraser, S.E. and Bronner-Fraser, M. (1990). Pathways of trunk neural crest cell migration in the mouse embryo as revealed by vital dye labelling. *Development* **108**, 605-612.

Seyedin, S.M., Thompson, A.Y., Bentz, H., Rosen, D.M., McPherson, J.M., Conti, A., Siege, N.R., Galluppi, G.R. and Piez, K.A. (1986). Cartilage-inducing Factor-A. *J. Biol. Chem.* **261**, 5693-5695.

Shibanuma, M., Mashimo, J., Mita, A., Kuroki, T. and Nose, K. (1993). Cloning from a mouse osteoblastic cell line of a set of transforming-growth-factor-β 1-regulated genes, one of which seems to encode a follistatin-related polypeptide. *Eur. J. Biochem.* **217**, 13-19.

Shimonaka, M., Inouye, S., Shimasaki, S. and Ling, N. (1991). Follistatin binds to both activin and inhibin through the common beta-subunit. *Endocrinology* **128**, 3313-3315.

Sive, H.L. (1993). The frog prince-ss: A molecular formula for dorsoventral patterning in *Xenopus*. *Genes Dev.* **7**, 1-12.

Slack, J.M.W. (1984). Regional biosynthetic markers in the early amphibian embryo. *J. Embryol. exp. Morph.* **80**, 289-319.

Slack, J.M.W. (1994). Inducing factors in *Xenopus* early embryos. *Curr. Biol.* **4**, 116-126.

Slack, J.M.W. and Forman, D. (1980). An interaction between dorsal and ventral regions of the marginal zone in early amphibian embryos. *J. Embryol. exp. Morph.* **56**, 283-299.

Smith, J.C. (1987). A mesoderm inducing factor is produced by a *Xenopus* cell line. *Development* **99**, 3-14.

Smith, J.C. (1989). Mesoderm induction and mesoderm-inducing factors in early amphibian development. *Development* **105**, 665-677.

Smith, J.C. (1995). Mesoderm-inducing factors and mesodermal patterning. *Curr. Opin. Cell Biol.* **7**, 856-861.

Smith, J.C., Price, B.M.J., Van Nimmen, K. and Huylebroeck, D. (1990). Identification of a potent *Xenopus* mesoderm-inducing factor as a homologue of activin A. *Nature* **345**, 729-731.

Smith, J.C. and Slack, J.M.W. (1983). Dorsalization and neural induction: properties of the organizer in *Xenopus laevis*. *J. Embryol. exp. Morph.* **78**, 299-317.

Smith, J.C., Yaqoob, M. and Symes, K. (1988). Purification, partial characterization and biological effects of the XTC mesoderm-inducing factor. *Development* **103**, 591-600.

Smith, J.L., Gesteland, K.M. and Schoenwolf, G.C. (1994a). Prospective fate map of the mouse primitive streak at 7.5 days of gestation. *Dev. Dyn.* **201**, 279-289.

Smith, J.L. and Schoenwolf, G.C. (1989). Notochordal induction of cell wedging in the chick neural plate and its role in neural tube formation. *J. exp. Zool.* **250**, 49-62.

Smith, J.L., Schoenwolf, G.C. and Quan, J. (1994b). Quantitative analyses of neuroepithelial cell shapes during bending of the mouse neural plate. *J. Comp. Neurol.* **342**, 144-151.

Smith, W.C., McKendry, R., Ribisi, S.J. and Harland, R.M. (1995). A *nodal*-related gene defines a physical and functional domain within the Spemann organizer. *Cell* **82**, 37-46.

Snell, G.D. and Stevens, L.C. (1966). Early embryology. In *Biology of the Laboratory Mouse*. (ed. E.L. Green), pp205-245. New York, McGraw-Hill.

Spemann, H. (1938). *Embryonic Development and Induction*. New Haven, Yale University Press.

Spencer, F.A., Hoffmann, F.M. and Gelbart, W.M. (1982). Decapentaplegic: a gene complex affecting morphogenesis in Drosphila melanogaster. *Cell* **28**, 451-461.

Sporn, M.B. and Roberts, A.B. (1988). Peptide growth factors are multifunctional. *Nature* **332**, 217-219.

Sporn, M.B. and Todaro, G.J. (1980). Autocrine secretion and malignant transformation of cells. *N. Engl. J. Med.* **303**, 878-880.

Storm, E.E., Huynh, T.V., Copeland, N.G., Jenkins, N.A., Kingsley, D.M. and Lee, S.J. (1994). Limb alterations in *brachypodism* mice due to mutations in a new member of the TGF β-superfamily. *Nature* **368**, 639-643.

Sulik, K., Dehart, D.B., Inagaki, T., Carson, J.L., Vrablic, T., Gesteland, K. and Schoenwolf, G.C. (1994). Morphogenesis of the murine node and notochordal plate. *Dev. Dyn.* **201**, 260-278.

Suzuki, A., Thies, R.S., Yamaji, N., Song, J.J., Wozney, J.M., Murakami, K. and Ueno, N. (1994). A truncated bone morphogenetic protein receptor affects dorsal-ventral patterning in the early *Xenopus* embryo. *Proc. Natl. Acad. Sci. U S A* **91**, 10255-10259.

Svajger, A. and Levak-Svajger, B. (1975). Technique of separation of germ layers in rat embryonic shields. *Wilhelm Roux Arch. Dev. Biol.* **178**, 303-308.

Takada, S., Stark, K.L., Shea, M.J., Vassileva, G., McMahon, J.A. and McMahon, A.P. (1994). *Wnt-3a* regulates somite and tailbud formation in the mouse embryo. *Genes Dev.* **8**, 174-189.

Takaoka, K. (1989). Establishment of a cell line producing bone morphogeneteic protein from a human osteosarcoma cell line. *Clin. Orthop. Rel. Res.* **244**, 258-264.

Tam, P.P.L. (1989). Regionalisation of the mouse embryonic ectoderm: allocation of prospective ectodermal tissues during gastrulation. *Development* **107**, 55-67.

Tam, P.P.L. and Beddington, R.S.P. (1987). The formation of mesodermal tissues in the mouse embryo during gastrualtion and early organogenesis. *Development* **99**, 109-126.

Tam, P.P.L. and Beddington, R.S.P. (1992). Establishment and organization of germ layers in the gastrulating mouse embryo. In *Postimplantation development in the mouse*. (eds. D.J. Chadwick and J. Marsh), pp27-41. Chichester, John Wiley & sons.

Tam, P.P.L. and Quinlan, G.A. (1996). Mapping vertebrate embryos. *Curr. Biol.* **6**, 104-106.

Tam, P.P.L. and Trainor, P.A. (1994). Specification and segmentation of the paraxial mesoderm. *Anat. Embryol.* **189**, 275-305.

Tannahill, D. and Melton, D.A. (1989). Localized synthesis of the Vg1 protein during early *Xenopus* development. *Development* **106**, 775-785.

Thomsen, G.H. and Melton, D.A. (1993). Processed Vg1 protein is an axial mesoderm inducer in Xenopus. *Cell* **74**, 433-441.

Tosney, K.W. (1982). The segregation and early migration of cranial neural crest cells in the avian embryo. *Dev. Biol.* **89**, 13-24.

Trainor, P.A. and Tam, P.P.L. (1995). Cranial paraxial mesoderm and neural crest cells of the mouse embryo: co-distribution in the craniofacial mesenchyme but distinct segregation in branchial arches. *Development* **121**, 2569-2582.

Turner, C.D. (1966). *General endocrinology*. London, W.B. Saunders Company.

Urist, M.R. (1965). Bone: formation by autoinduction. *Science* **150**, 893-899.

van Straaten, H.W.M., Hekking, J.W.M., Wiertz-Hoessels, E.J.L.M., Thors, F. and Drukker, J. (1988). Effect of the notochord on the differentiation of a floor plate area in the neural tube of the chick embryo. *Anat. Embryol.* **177**, 317-324.

Vassalli, A., Matzuk, M.M., Gardner, H.A.R., Lee, K.-F. and Jaenisch, R. (1994). Activin/inhibin β B subunit gene disruption leads to defects in eyelid development and female reproduction. *Genes Dev.* **8**, 414-427.

Vize, P.D. and Thomsen, G.H. (1994). Vg1 and regional specification in vertebrates: a new role for an old molecule. *Trends Genet.* **10**, 371-376.

Waddington, C.H. (1932). Experiments on the development of chick and duck embryos, cultivated *in vitro*. *Phil. Trans. R. Soc. Lond. (B)* **211**, 179-230.

Wang, X.-F., Lin, H.Y., Ng-Eaton, E., Downward, J., Lodish, H.F. and Weinberg, R.A. (1991). Expression cloning and characterisation of the TGF-β type III receptor. *Cell* **67**, 797-805.

Warner, A. and Gurdon, J.B. (1987). Functional gap junctions are not required for muscle gene activation by induction in *Xenopus* embryos. *J. Cell Biol.* **104**, 557-564.

Warner, A.E., Guthrie, S.C. and Gilula, N.B. (1984). Antibodies to gap-junctional protein selectively disrupt junctional communication in the early amphibian embryo. *Nature* **311**, 127-131.

Weeks, D.L. and Melton, D.A. (1987). A maternal mRNA localized to the vegetal hemisphere in Xenopus eggs codes for a growth factor related to TGF-β. *Cell* **51**, 861-867.

Wessells, N.K. (1977). *Tissue interactions and development*. London, W.A. Benjamin, Inc.

Wharton, K.A., Ray, R.P. and Gelbart, W.M. (1993). An activity gradient of *decapentaplegic* is necessary for the specification of dorsal pattern elements in the *Drosophila* embryo. *Development* **117**, 807-822.

Wieser, R., Attisano, L., Wrana, J.L. and Massagué, J. (1993). Signalling activity of transforming growth factor β type II receptors lacking specific domains in the cytoplasmic region. *Mol. Cell. Biol.* **13**, 7239-7247.

Wilkinson, D.G. (1992). Whole mount in situ hybridisation of vertebrate embryos. In *In situ hybridisation*. Oxford, IRL Press. 75-83.

Wilkinson, D.G., Bhatt, S. and Herrmann, B.G. (1990). Expression pattern of the mouse *T* gene and its role in mesoderm formation. *Nature* **343**, 657-659.

Wilson, V. and Beddington, R.S.P. (1996). Cell fate and morphogenetic movement in the late mouse primitive streak. *Mech. Dev.* **55**, 1-11.

Wilson, V., Rashbass, P. and Beddington, R.S.P. (1993). Chimeric analysis of *T* (*Brachyury*) gene function. *Development* **117**, 1321-1331.

Winnier, G., Blessing, M., Labosky, P.A. and Hogan, B.L.M. (1995). Bone morphogenetic protein-4 is required for mesoderm formation and patterning in the mouse. *Genes Dev.* **9**, 2105-2116.

Wozney, J.M., Rosen, V., Celeste, A.J., Mitsock, L.M., Whitters, M.J., Kriz, R.W., Hewick, R.M. and Wang, E.A. (1988). Novel regulators of bone formation: molecular clones and activities. *Science* **242**, 1528-1534.

Wrana, J.L., Attisano, L., Cárcamo, J., Zentella, A., Doody, J., Laiho, M., Wang, X.-F. and Massagué, J. (1992). TGFβ signals through a heteromeric protein kinase receptor complex. *Cell* **71**, 1003-1014.

Wrana, J.L., Attisano, L., Wieser, R., Ventura, F. and Massagué, J. (1994). Mechanism of activation of the TGF-β receptor. *Nature* **370**, 341-347.

Yamada, T., Pfaff, S.L., Edlund, T. and Jessell, T.M. (1993). Control of cell pattern in the neural tube: motor neuron induction by diffusible factors from notochord and floor plate. *Cell* **73**, 673-686.

Yamada, T., Placzek, M., Tanaka, H., Dodd, J. and Jessell, T.M. (1991). Control of cell pattern in the developing nervous system: polarizing activity of the floor plate and notochord. *Cell* **64**, 635-647.

Yamashita, H., ten Dijke, P., Huylebroeck, D., Sampath, T.K., Andries, M., Smith, J.C., Heldin, C.-H. and Miyazono, K. (1995). Osteogenic protein-1 binds to activin type II receptors and induces certain activin-like effects. *J. Cell Biol.* **130**, 217-226.

Yancey, S.B., Biswal, S. and Revel, J.-P. (1992). Spatial and temporal patterns of distribution of the gap junction protein connexin43 during mouse gastrulation and organogenesis. *Development* **114**, 203-212.

Ying, S.-Y. (1988). Inhibins, activins, and follistatins: gonadal proteins modulating the secretion of follicle-stimulating hormone. *Endocrine Reviews* **9**, 267-293.

Ying, S.-Y., Becker, A., Swanson, G., Tan, P., Ling, N., Esch, F., Ueno, N., Shimasaki, S. and Guillemin, R. (1987). Follistatin specifically inhibits pituitary follicle stimulating hormone release *in vitro*. *Biochem. Biophys. Res. Commun.* **49**, 133-139.

Yuan, H., Corbi, N., Basilico, C. and Dailey, L. (1995). Developmental-specific activity of the FGF-4 enhancer requires the synergistic action of Sox2 and Oct-3. *Genes Dev.* **9**, 2635-2645.

Zhou, X., Sasaki, H., Lowe, L., Hogan, B.L.M. and Kuehn, M.R. (1993). *Nodal* is a novel TGF-β-like gene expressed in the mouse node during gastrulation. *Nature* **361**, 543-547.

APPENDICES

APPENDIX I

STAGING OF GASTRULATING MOUSE EMBRYOS

Diagram of staging system of Downs and Davies (1993), (the anterior of the embryo in all diagrams is on the left) showing the following stages:

PS	Pre Streak Stage
ES	Early Streak Stage
MS	Mid Streak Stage
LS	Late Streak Stage
OB	No Bud Stage
EB	Early Bud Stage
LB	Late Bud Stage
EHF	Early Headfold Stage
LHF	Late Headfold stage

Abbreviations: ab: allantoic bud, al: allantois, am: amnion, clf: cranial limiting furrow, e: embryonic portion of the egg cylinder, ec: ectoplacental cone, etc: ectoplacental cavity, fg: foregut, hf: headfolds, hp: head process, m: embryonic mesoderm, n: node, nec: neurectoderm, ng: neural groove, np, neural plate, paf: posterior amniotic fold, x: extraembryonic portion of the egg cylinder, xc: exocoelemic cavity.

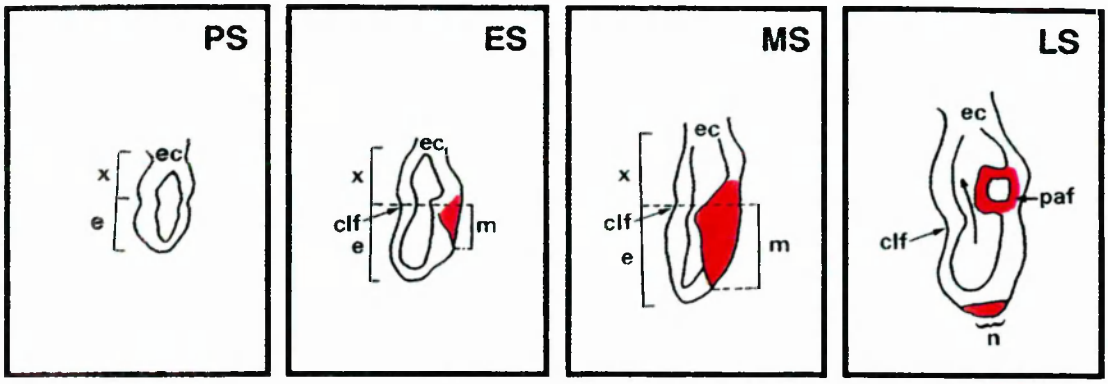

Neural Plate Stages

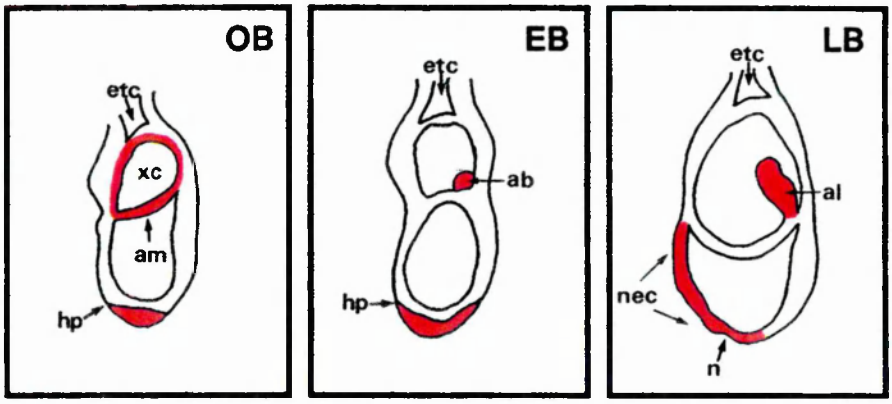

Headfold Stages

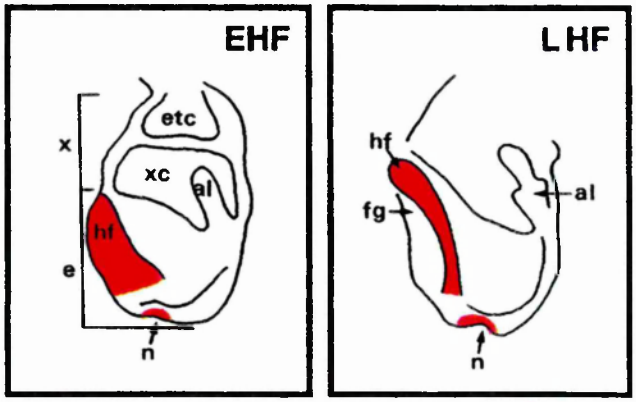

APPENDIX II

FIGURE A *MSX1* AND *PAX-3* mRNA LOCALISATION

Figures A - E show Msx1 mRNA localisation

Whole mount in situ hybridisation was carried out on embryos with between 2 and 20 somites. **(A)** Dorsal view of a flattened 2-somite embryo. Signal is seen in the primitive streak and lateral mesoderm emerging from the streak and in the base of the allantois. Rostral of the node *Msx1* transcripts are confined to the lateral edge of the neural plate, this expression does not extend to the anterior of the embryo. The semicircle of staining seen towards the anterior is staining in the yolksac mesoderm. **(B)** Dorsal view of the hindbrain region of a 12-somite embryo. Expression is seen along the dorsal edge of the closing neural tube, with elevated levels in rhombomeres 3 and 5. **(C)** Dorsal view of the hindbrain region of a 20-somite embryo. The pattern of expression in the hindbrain neurectoderm is similar to that in the 12-somite embryo, but it is now apparent that *Msx1* is also expressed in the neural crest adjacent to the midbrain and rhombomeres 1 and 4. *Msx1* is also expressed in the dorsal part of the otic vesicle. **(D)** Lateral view of a 17-somite embryo. Note *Msx1* expression in the dorsal neural tube along the full axis and expression in branchial arches 1 and 2. **(E)** Flat mount of the hindbrain region of a 20-somite embryo. The elevated expression in rhombomeres 3 and 5 is evident as is the more ventral limit of transcripts in these rhombomeres.

Figures F - J show Pax-3 mRNA localisation

(F) Dorsal view of a flattened 2-somite embryo. Rostral of the node transcripts are seen in the somites and in the lateral edge of the neural plate, this expression does not extend to the anterior of the embryo. *Pax-3* is also expressed at the junction of the primitive streak ectoderm and the surface ectoderm. **(G)** Dorsal view of the hindbrain region of a 12-somite embryo. Transcripts are seen at the dorsal edge of the hindbrain neurectoderm. The transcript level is lower in rhombomeres 5 and 6. *Pax-3* expression is also evident adjacent to rhombomeres 2 and 4. **(H)** Dorsal view of the hindbrain region of a 20-somite embryo. A similar pattern of transcript accumulation is seen in the hindbrain region to that detected in the 12-somite embryo, however, rostral of rhombomere 1 there is a patch of neurectoderm which does not contain *Pax-3* transcripts. **(I)** Lateral view of a 17-somite embryo. Pax-3 transcripts essentially extend along the dorsal edge of all the neurectoderm, however the precise domain of expression varies along the axis. The decrease in expression rostral to rhombomere 1 is beginning to be evident. The expression adjacent to rhombomeres 2 and 4 and the decrease in transcript level in rhombomeres 5 and 6 can be seen. **(J)** Flat mount of the hindbrain region of a 20-somite embryo showing *Pax-3* expression. The domain of expression is broader than that shown for *Msx1* in (E). Scale bar 400 μm (D,I); 300 μm (B,C,G,H); 200 μm (A,F); 100 μm (E,J).

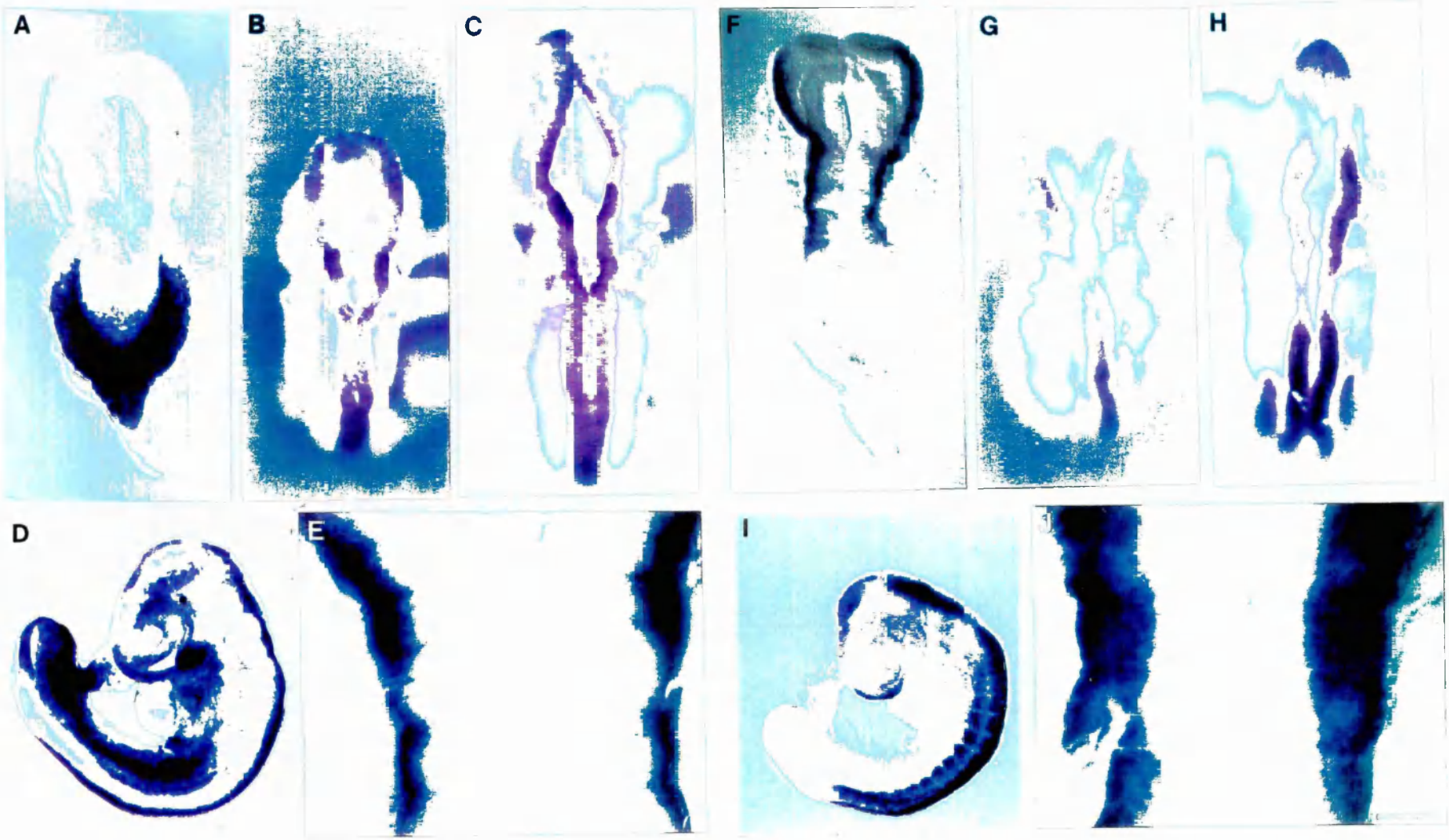
A
B
C
F
G
H
D
E
I
J

APPENDIX II

FIGURE B *AP-2* AND *Shh* mRNA LOCALISATION

Figures A - F show *AP-2* mRNA localisation

(A) Lateral view of an early allantoic bud stage embryo. *AP-2* appears to be expressed in the proximal epiblast. **(B)** Lateral view of an early headfold stage embryo. *AP-2* transcripts are localised to the surface ectoderm. **(C)** Dorsal view of a flattened 3-somite embryo. Transcripts are localised to the surface ectoderm and lateral neurectoderm. **(D)** Section through the hindbrain of a 5-somite embryo. *AP-2* is expressed in the surface ectoderm, the dorsal neurectoderm and the neural crest which is just beginning to emerge from the hindbrain at this stage of development. **(E)** Section through the hindbrain and forebrain of a 17-somite embryo. *AP-2* transcripts are seen in all of the surface ectoderm, and the neural crest adjacent to the hindbrain region. **(F)** Lateral view of a 14-somite embryo, showing widespread *AP-2* expression in both the surface ectoderm and the neural crest.

Figures G - J showing *Shh* mRNA localisation

(G) Dorsal view of a flattened 2-somite embryo. The node and notochord contain *Shh* transcripts. **(H)** Lateral view of an 8-somite embryo showing *Shh* expression. Expression continues in the node and notochord, and is now also initiated in the ventral midline of the midbrain. Expression is also seen in the hindgut and foregut pockets. **(I)** Flat mount of the hindbrain region of a 10-somite embryo, showing that *Shh* expression has spread to the hindbrain midline by this stage of development. **(J)** Lateral view of a 17-somite embryo after hybridisation to *Shh*. Expression is now seen in the floorplate along the length of the neural tube. Scale bar 500 μm (D); 400 μm (F,I); 300 μm (H); 200 μm (B,C,E,G); 100 μm (A,J).

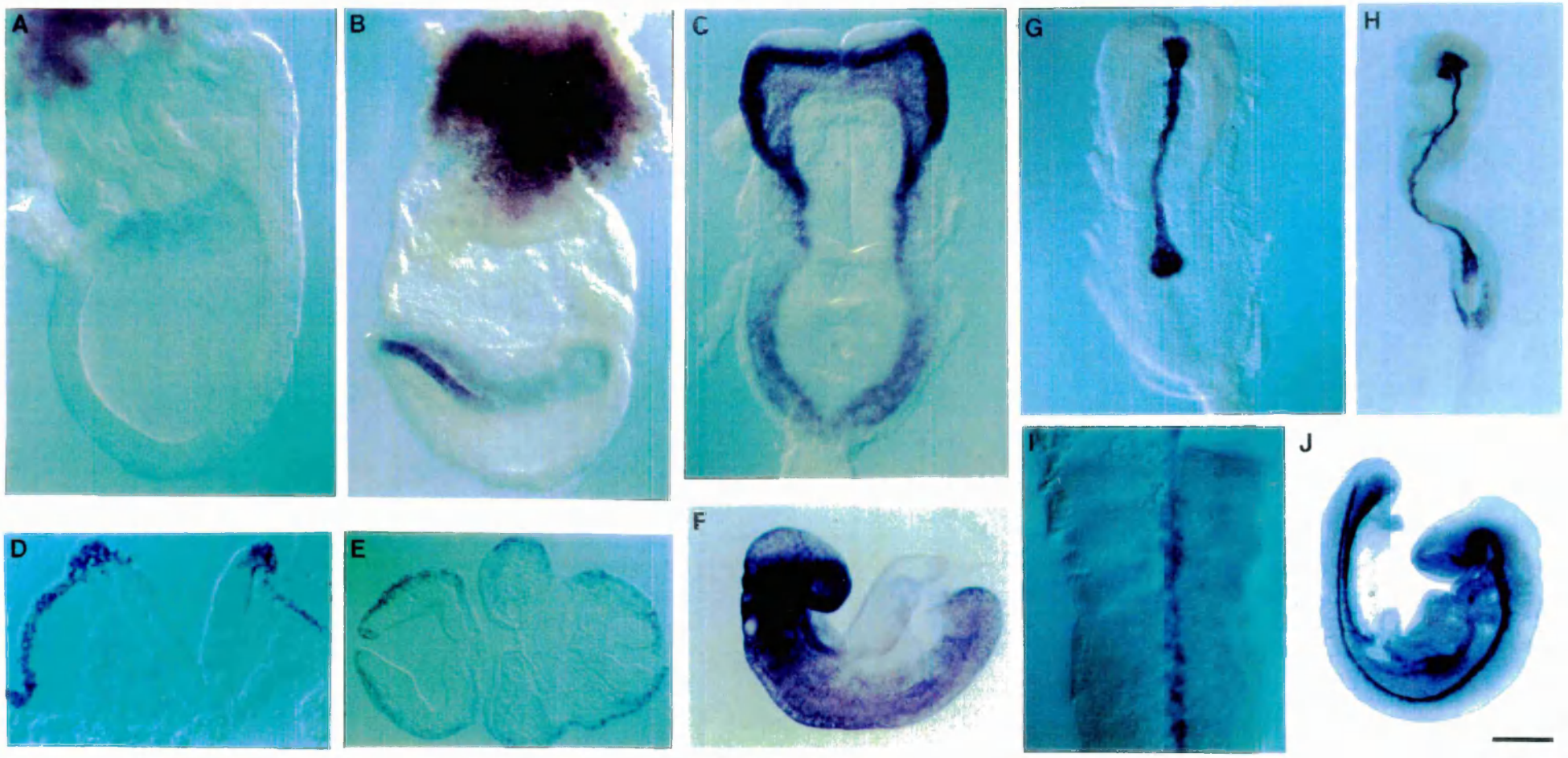
A
B
C
G
H
D
E
F
I
J